การสังเคราะห์ เอ็น-(พารา-อะมิโนเบนโซอิล)-1,2,3,4-เททระไฮโดรควิโนลีนและอนุพันธ์

นางสาวธนารัตน์ เกียรติสกล
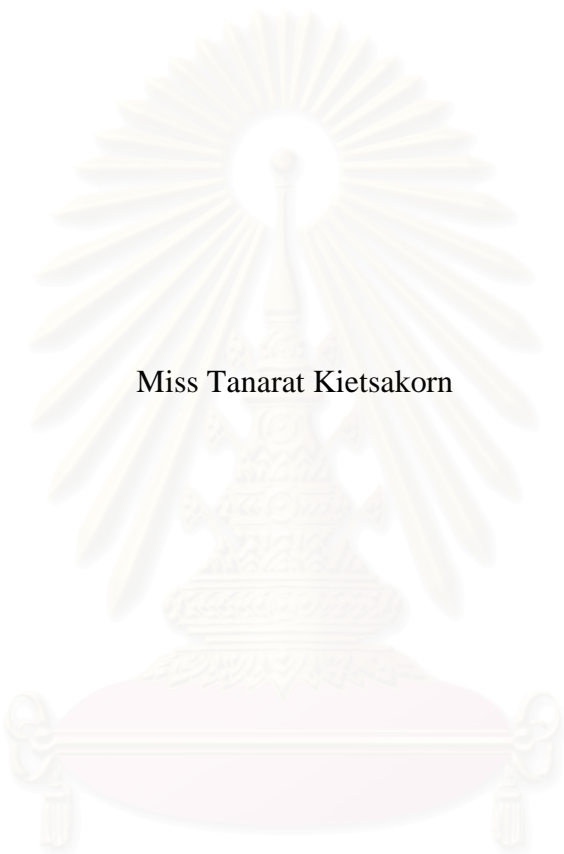
SYNTHESIS OF N-(*p*-AMINOBENZOYL)-1,2,3,4-TETRAHYDROQUINOLINE AND DERIVATIVES

Miss Tanarat Kietsakorn

A Thesis Submitted in Partial Fulfillment of the Requirements

for the Degree of Master of Pharmacy in Pharmaceutical Chemistry

Department of Pharmaceutical Chemistry

Faculty of Pharmaceutical Science

Chulalongkorn University

Academic Year 2000

Thesis Title   Synthesis of N-(*p*-aminobenzoyl)-1,2,3,4-tetrahydroquinoline and derivatives

By   Miss Tanarat Kietsakorn

Field of study   Pharmaceutical Chemistry

Thesis Advisor   Assistant Professor Chamnan Patarapanich, Ph.D.

Accepted by the Faculty of Pharmaceutical Science, Chulalongkorn University in Partial Fulfillment of the Requirements for the Master's Degree

…………………………………………...Dean of Faculty of
Pharmaceutical Science
(Associate Professor Sunibhond Pummangura, Ph.D.)

THESIS COMMITTEE

……………………………………………Chairman
(Associate Professor Phensri Thongnopnua, Ph.D.)

………………………………………….………Thesis Advisor
(Assistant Professor Chamnan Patarapanich, Ph.D.)

………………………………………….Member
(Associate Professor Boonardt Saisorn, M.Sc. in Pharm)

………………………………………………….Member
(Associate Professor Boonyong Tantisira, Ph.D.)

………………………………………………….Member
(Assistant Professor Wallee Vanichseni, M.Phil.)

นางสาวธนารัตน์ เกียรติสกล : การสังเคราะห์ เอ็น-(พารา-อะมิโนเบนโซอิล)-1,2,3,4-เททระไฮโดรควิโนลีนและอนุพันธ์. (SYNTHESIS OF N-(*p*-AMINOBENZOYL)-1,2,3,4-TETRAHYDROQUINOLINE AND DERIVATIVES) อ. ที่ปรึกษา : ผศ.ดร.ชำนาญ ภัตรพานิช, 296 หน้า. ISBN 974-13-0095-6.

การวิจัยครั้งนี้เป็นการศึกษาและพัฒนาปฏิกิริยาเคมีที่ใช้ในกระบวนการสังเคราะห์ เอ็น-(พารา-อะมิโนเบนโซอิล)-1,2,3,4-เททระไฮโดรควิโนลีนและอนุพันธ์ ซึ่งเป็นสารประกอบอินทรีย์กลุ่มใหม่ที่คาดว่าจะมีฤทธิ์ต้านอาการชัก สารประกอบกลุ่มนี้ถูกออกแบบขึ้นมาโดยอาศัยอะเมลโทไลด์ เป็นสารต้นแบบ

สารประกอบแปดตัวในกลุ่มของเอ็น-(พารา-อะมิโนเบนโซอิล)-1,2,3,4-เททระไฮโดร-ควิโนลีนและอนุพันธ์ (CU-17-02, CU-17-04, CU-17-06, CU-17-08, CU-17-10, CU-17-12, CU-17-14 และ CU-17-16) ถูกสังเคราะห์ขึ้นมาด้วยขั้นตอนการสังเคราะห์ดังต่อไปนี้ ขั้นตอนแรกเป็นการสังเคราะห์วงควิโนลีนจากปฏิกิริยาสครับดัดแปลง รีดิวซ์สารประกอบควิโนลีนด้วยโซเดียมโบโรไฮไดรด์และนิกเกิลคลอไรด์ ให้เป็นสารประกอบ1,2,3,4-เททระไฮโดรควิโนลีนชนิดที่มีโครงสร้างสอดคล้องกัน ขั้นตอนต่อมานำสารประกอบ1,2,3,4-เททระไฮโดรควิโนลีนมาทำปฏิกิริยาเอ็นเอซิเลชันกับสารประกอบพารา-ไนโตรเบนโซอิลคลอไรด์ แล้วจึงนำผลิตผลที่เกิดขึ้นมาทำปฏิกิริยาคะตะไลติกไฮโดรจีเนชันที่มีการใช้สารเร่งปฏิกิริยาให้เป็นสารประกอบเป้าหมายที่ต้องการคือเอ็น-(พารา-อะมิโนเบนโซอิล)-1,2,3,4-เททระไฮโดรควิโนลีนและอนุพันธ์

พิสูจน์เอกลักษณ์ของสารที่สังเคราะห์ได้โดยเทคนิคทาง อินฟราเรดสเปกโตรเมทรี, แมสสเปกโตรเมทรี, นิวเคลียร์แมกเนติกเรโซแนนซ์สเปกโตรเมทรี และการวิเคราะห์องค์ประกอบธาตุ

ภาควิชา	เภสัชเคมี	ลายมือชื่อนิสิต	
สาขาวิชา	เภสัชเคมี	ลายมือชื่ออาจารย์ที่ปรึกษา	
ปีการศึกษา	2543		

4176564433: MAJOR   PHARMACEUTICAL CHEMISTRY

KEY WORD: SYNTHESIS / N-(*p*-AMINOBENZOYL)-1,2,3,4-TETRAHYDROQUINOLINES

TANARAT KIETSAKORN : SYNTHESIS OF N-(*p*-AMINOBENZOYL)-1,2,3,4-
TETRAHYDROQUINOLINE AND DERIVATIVES

THESIS ADVISOR : ASSIST. PROF. CHAMNAN PATARAPANICH, Ph.D.,

296 pp. ISBN 974-13-0095-6.

The present investigation was to study and develop the synthetic routes of
N-(*p*-aminobenzoyl)-1,2,3,4-tetrahydroquinolines, the new series of organic
compounds, designed by using ameltolide as the lead agent. These rigid analogues of
ameltolide were expected to possess anticonvulsant activity.

Eight compounds in this new series (CU-17-02, CU-17-04, CU-17-06, CU-17-
08, CU-17-10, CU-17-12, CU-17-14 and CU-17-16) were successfully prepared as
followed: First, a number of substituted quinolines, synthesized by modified Skraup
reaction, were reduced to their corresponding 1,2,3,4-tetrahydroquinolines by using
sodium-borohydride nickelous chloride system. Then, N-acylation of the resulting
1,2,3,4-tetrahydroquinolines with *p*-nitrobenzoyl chloride followed by catalytic
hydrogenation yield the target compounds, N-(*p*-aminobenzoyl)-1,2,3,4-
tetrahydroquinolines.

The structures of the synthesized compounds were confirmed by infrared
spectrometry, mass spectrometry, nuclear magnetic resonance spectrometry and
elemental analysis techniques.

Department   Pharmaceutical Chemistry   Student's signature
Field of study Pharmaceutical Chemistry   Advisor's signature
Academic year 2000

ACKNOWLEDGEMENTS

LIST OF CONTENTS

<div align="right">Page</div>

LIST OF TABLES

LIST OF FIGURES

Page

LIST OF ABBREVIATIONS

%	percent
ν	stretching vibration (for IR spectra)
ν_{as}	asymmetrical stretching (for IR spectra)
ν_s	symmetrical stretching (for IR spectra)
δ	in-plane bending (for IR spectra);
	chemical shift (for NMR spectra)
μmol	micromole
AEDs	antiepileptic drugs
AMPA	α-amino-3-hydroxy-5-methyl-4-isoxazole-propionic acid
aq.	aqueous
ATPase	adenosine triphosphatase
BIC	bicuculline
BZD	benzodiazepine
°C	degree celsius
^{13}C-NMR	carbon-13 nuclear magnetic resonance
CBZ	carbamazepine
CHN analysis	elemental analysis
cm^{-1}	reciprocal centimeter (for IR spectra)
CNS	central nervous system
conc.	concentrated
d	doublet (for NMR spectra)
dd	doublet of doublet (for NMR spectra)
DEPT-135	Distortionless Enhancement by Polarization Transfer
EAAs	excitatory amino acids

ED_{50}	dose required to produce the desired endpoint in 50 % of animals
ED_{97}	dose required to produce anti-MES activity in 97 % of animals
EIMS	electron impact mass spectrum
ESM	ethosuximide
ev	electron volt
FBM	felbamate
g	gram
GABA	γ-aminobutyric acid
GABA-T	GABA aminotransferase
GBP	gabapentin
Glu	glutamate
Gly	glycine
^{1}H-NMR	proton nuclear magnetic resonance
HD_{50}	dose at which 50% of animals lost righting reflex
HH COSY	Correlated Spectroscopy: HH coupling
HMBC	^{1}H-detected Heteronuclear Multiple Bond Connectivity
HMQC	Heteronuclear Multiple Quantum Correlation Spectroscopy
hr	hour
Hz	hertz
ILAE	the International League Against Epilepsy
i.p.	intraperitoneal administration
IR	infrared spectrometry
iv.	intravenous administration
J	coupling constant (for NMR spectra)
kg	kilogram
LD_{50}	dose that caused death in 50 % of animals

LTG	lamotrigine
m	multiplet (for NMR spectra)
M^+	molecular ion
MES	maximal electroshock seizure
mg	milligram
MHz	megahertz
min	minute
ml	milliliter
mmol	millimole
m.p.	melting point
m/z	mass per charge ratio
NA	not appicable
NIH	the Epilepsy Branch of the National Institutes of Health
NMDA	*N*-methyl-D-aspartate
NMR	nuclear magnetic resonance
oop	out-of-plane vibration (for IR spectra)
PB	phenobarbital
Pd/C	palladium on activated charcoal
PHT	phenytoin
PI	protective index (TD_{50}/ED_{50})
PIC	picrotoxin
pKa	ionization constant
ppm	part (s) per million
PTZ	pentylenetetrazol
RT	room temperature
s	singlet (for NMR spectra)
sc.	subcutaneous administration

SSA	succinic acid semialdehyde
Strych	strychnine
t	triplet (for NMR spectra)
TD_3	dose eliciting evidence of minimal neurologic toxicity in 3 % of animals
TD_{50}	dose eliciting evidence of minimal neurotoxicity in 50 % of animals
TGB	tiagabine
TPM	topiramate
VGB	vigabatrine
VGSC	voltage-dependent Na^+ channel
VPA	valproate
w/v	weight by volume

CHAPTER I

INTRODUCTION

Epilepsy has been defined as a condition characterized by recurrent unprovoked seizures. A seizure is the result of transient dysfunction of part or all of the brain due to excessive discharge of a hyperexcitable population of neurons, causing sudden and transitory phenomena of motor, sensory, autonomic or psychic nature. (Kadir and Chadwick, 1999)

Epilepsy is a common chronic neurological condition. The incidence (number of new cases given population per year) has been estimated of between 2-8 per 10,000 persons. The incidence is higher in the first two decades of life, but fall over the next few decades, only to increase again in late life that due mainly to cardiovascular diseases. Most studies of the prevalence of active epilepsy (the number of cases in the population of any given times) have estimated figures between 4 and 8 per 1,000 and a rate of 5 per 1000 is commonly quoted. (Dhillon and Sander, 1999)

Up to 5% of people will suffer at least one seizure in their lifetime. However, the prevalence of active epilepsy is low, and most patients who develop seizures have a very good prognosis. About 70 to 80% of all people developing epilepsy will eventually become seizure-free, and about half will successfully withdraw their medication. Once a substantial period of remission has been achieved, the risk of further seizures is greatly reduced. A minority of patients (20 to 30%) will develop chronic epilepsy, and in such cases, treatment is more difficult. For chronic patients, less than 5% will be unable to live in the community or will depend on others for their day-to-day needs.

It seems to be a small but definite increase in mortality in patients suffering from epilepsy, especially amongst younger patients and those with severe epilepsy. Most studies have given overall standardized mortality ratios between two and three times higher than that of the general population. Common causes of death in people with epilepsy include accidents (e.g., drowning, head injury, traffic accidents), status epilepticus, tumors, cerebrovascular diseases, pneumonia and suicide. Sudden unexpected death, an entity that remains unexplained, is common, particularly in the young.

The International League Against Epilepsy (ILAE) has proposed two major schemes for classification of seizures and epilepsies: the International Classification of Epileptic Seizures and the International Classification of the Epilepsies and Epilepsy Syndromes. (Adams, Victor and Ropper, 1997; Graves and Garnett, 1999; Kadir and Chadwick, 1999)

The International Classification of Epileptic Seizures combines the clinical description with certain seizures. Seizures are divided into two main groups according to the aura of the brain in which the abnormal discharge originates. If it involves initial activation of both hemispheres of the brain simultaneously, the seizures are termed generalized. If a discharge starts in a localized aura of the Brain, they are termed partial or focal seizure (Table 1).

Partial seizures are classified as simple when consciousness is undisturbed. The symptoms (aura) often experienced prior to a generalized tonic-clonic seizure may be a simple partial seizure that secondarily generalized. Partial seizure with a loss or alteration of consciousness is described as complex partial. With complex partial seizures, the patient may have automatism, periods of memory loss, or

aberrations of behavior. A partial seizure that becomes generalized is referred to as a secondarily generalized seizure.

Generalized seizures are of two types-convulsive and nonconvulsive. The common convulsive type is the tonic-clonic (grand mal) seizure. Less common is a purely tonic, or clonic generalized. The classic nonconvulsive generalized seizure is the brief lapse of consciousness or absence (petit mal); included also under this heading are minor motor phenomena such as brief myoclonic or atonic.

The International Classification of Epilepsies and Epilepsy Syndromes adds components such as age of onset, intellectual development, findings on neurologic examination, and results of neuroimaging studies to more fully define epilepsy syndromes (Table 2). Syndromes can include one or many different seizure types (e.g., Lennox Gastaut syndrome). The syndromic approach includes seizure type and possible etiologic classifications (idiopathic, symptomatic, or unknown). Idiopathic describes syndromes that are presumably genetic but also those in which no underlying etiology is documented or suspected. A family history of seizures is commonly present, and neurologic function is essentially normal except for the occurrence of seizures. Symptomatic cases involve evidence of brain damage or a known underlying cause. A cryptogenic syndrome is assumed to be symptomatic of an underlying condition that cannot be documented. Unknown or undetermined is used when no cause can be identified. This syndromic classification is more important for prognostic determinations than a classification based simply on seizure type. The syndrome classification scheme requires more information and, in return, provides a more powerful tool for comprehensive clinical management. A patient's epilepsy is classified based on seizure type (generalized versus partial) and syndromic type (idiopathic, symptomatic, cryptogenic).

Table 1. International classification of epileptic seizures

I. Partial seizures (seizures begin locally)

    A. Simple (without impairment of consciousness)

        1. With motor symptoms

        2. With special sensory or somatosensory symptoms

        3. With psychic symptoms

    B. Complex (with impairment of consciousness)

        1. Simple partial onset followed by impairment of consciousness-with or without automatisms

        2. Impaired consciousness at onset-with or without automatisms

    C. Secondarily generalized (partial onset evolving to generalized tonic-clonic seizures)

II. Generalized seizures (bilaterally symmetrical and without local onset)

    A. Absence

    B. Myoclonic

    C. Clonic

    D. Tonic

    E. Tonic-clonic

    F. Atonic

    G. Infantile spasms

III. Unclassified seizures

IV Status epilepticus

Table 2. International classification of epilepsies and epilepsy syndromes.

_____

I.   Localization-related (focal, partial) epilepsies and syndromes

   A. Idiopathic (with age-related onset)

      1. Benign childhood epilepsy with centro-temporal spike

      2. Childhood epilepsy with occipital paroxysms

      3. Primary reading epilepsy

   B. Symptomatic

      1. Chronic progressive epilepsia partialis continua of childhood

      2. Syndromes characterized by seizures with specific modes of precipitation

   C. Cryptogenic

II. Generalized epilepsies and syndromes

   A. Idiopathic

      1. Benign neonatal familial convulsions

      2. Benign neonatal convulsions

      3. Benign myoclonic epilepsy in infancy

      4. Childhood absence epilepsy (pyknolepsy)

      5. Juvenile absence epilepsy

      6. Juvenile myoclonic epilepsy

      7. Epilepsy with grand mal (GTCS) seizures on awakening

      8. Other generalized idiopathic epilepsies not defined above

      9. Epilepsies with seizures precipitated by specific modes of activation

   B. Cryptogenic or symptomatic

      1. West syndrome

      2. Lennox-Gastaut syndrome

Table 2. (continued) International classification of epilepsies and epilepsy syndromes.

      3. Epilepsy with myoclonic-astatic seizures

      4. Epilepsy with myoclonic absence

   C. Symtomatic

      1. Nonspecific etiology

         a. Early myoclonic encephalopathy

         b. Early infantile epileptic encephalopathy

         c. Other symptomatic generalized epilepsies not defined above

      2. Specific syndromes

III. Epilepsies and syndromes undetermined whether focal or generalized

   A. With both generalized and focal seizures

      1. Neonatal seizures

      2. Severe myoclonic epilepsy in infancy

      3. Epilepsy with continuous spike-waves during slow wave sleep

      4. Acquired epileptic aphasia

      5. Other undetermined epilepsies not defined above

   B. Without unequivocal generalized of focal features

IV. Special syndromes

   A. Situation-related seizures

      1. Febrile convulsions

      2. Isolated seizures or isolated status epilepticus

      3. Seizure occurring only when there is an acute metabolic or toxic event

The treatment of epilepsy usually involves long-term treatment that may represent a dramatic change in the patient's life. The aim of the treatment is to prevent the recurrence of seizures with the minimum effective dose of an appropriate antiepileptic drug, resulting in improvement in the quality of life of patients. Of course, the ultimate aim of treatment will be no seizures and no drugs. Unfortunately, this may not be readily achievable for many patients with chronic epilepsy. (Kadir and Chadwich, 1999)

Antiepileptic drug therapy is the mainstay of epilepsy treatment. Today, there are numerous antiepileptic drugs (AEDs) including established AEDs (e.g., phenytoin (I), carbamazepine (II), clonazepam (III), ethosuximide (IV), phenobarbital (V), sodium valproate (VI)) and dimethadione (VII)) and new AEDs (e.g., felbamate (VIII), gabapentin (IX), lamotrigine (X), oxcarbazepine (XI), tiagabine (XII), topiramate (XIII), vigabatrin (XIV) and zonisamide (XV)) that have been launched since 1989. It is important to select an appropriate AED for the individual patient. The choice of antiepileptic drug should be based on the seizure classification, the age and sex of the patient, concurrent medical conditions, potential adverse effects, and the pharmacokinetic features of each drug. Table 3 gives the main indications for the AEDs currently available. (Dhillon and Sander, 1999)

Although, the older established AEDs are still widely prescribed, there is a significant group of patients that is resistant to those available therapeutic agents, or suffer from a range of side effects. New AEDs seem to show improved efficacy and side-effect profiles, but patients with intractable epilepsy remain untreated. There is clearly a need for improved medications; therefore, an enormous effort has been exerted towards this goal over the last several years.

Table 3. AEDs for different seizure types

Seizure type	First-line treatment	Second-line treatment
Partial seizures		
Simple partial,	Carbamazepine	Vigabatrin
Complex partial,	Phenytoin	Phenobarbital
Secondarily generalized	Valproate	Gabapentin
	Lamotrigine	Topiramate
Generalized seizures		
Tonic-clonic,	Valproate	Vigabatrin
Tonic,	Carbamazepine	Phenobarbital
Clonic	Phenytoin	
	Lamotrigine	
Absence	Ethosuximide	Clonazepam
	Valproate	Lamotrigine
Atypical absences,	Valproate	Phenobarbital
Atonic	Clonazepam	Lamotrigine
	Clobazam	Carbamazepine
		Phenytoin
Myoclonic	Valproate	Phenobarbital
	Clonazepam	
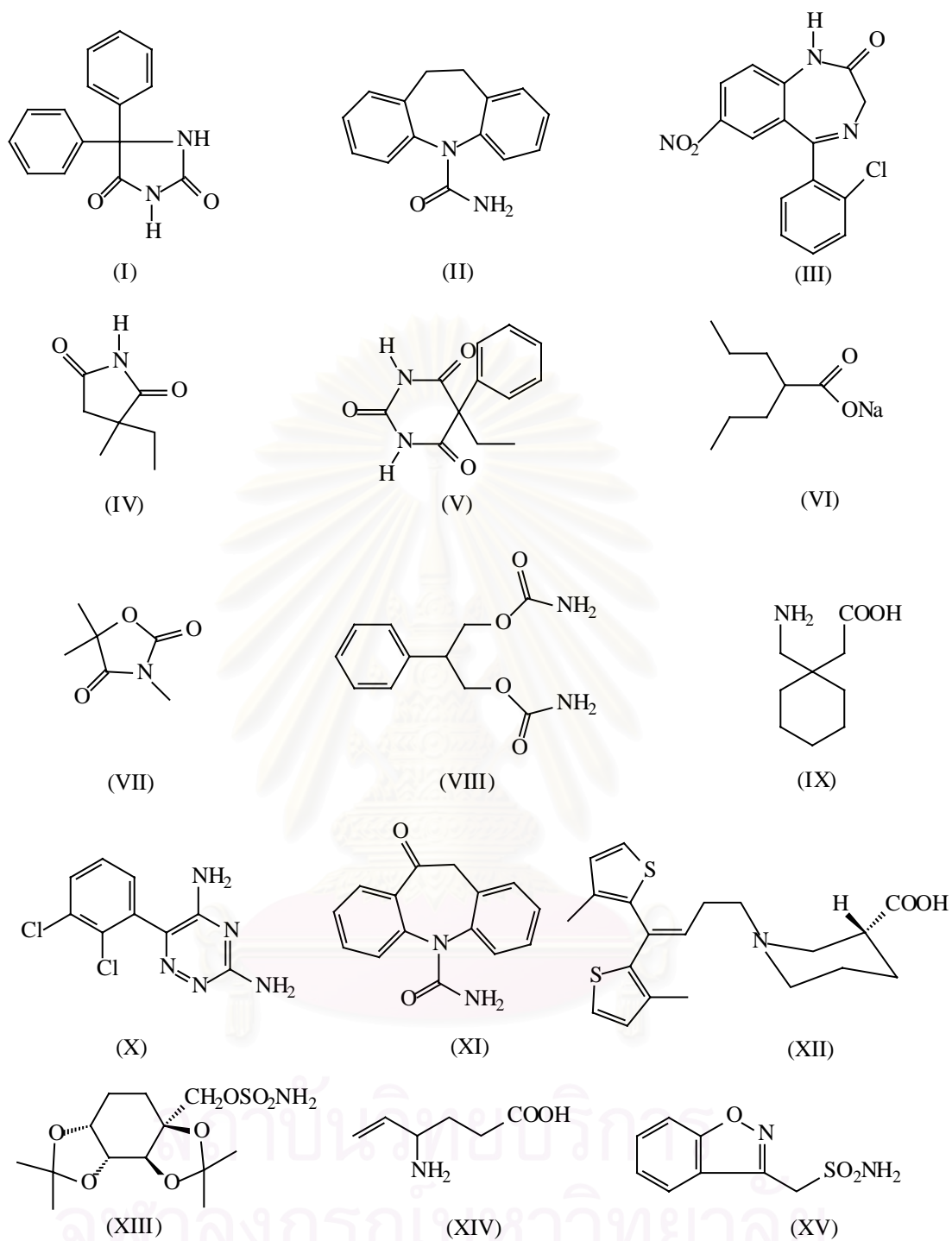
Figure 1. The chemical structures of some antiepileptic drugs (I-XV).
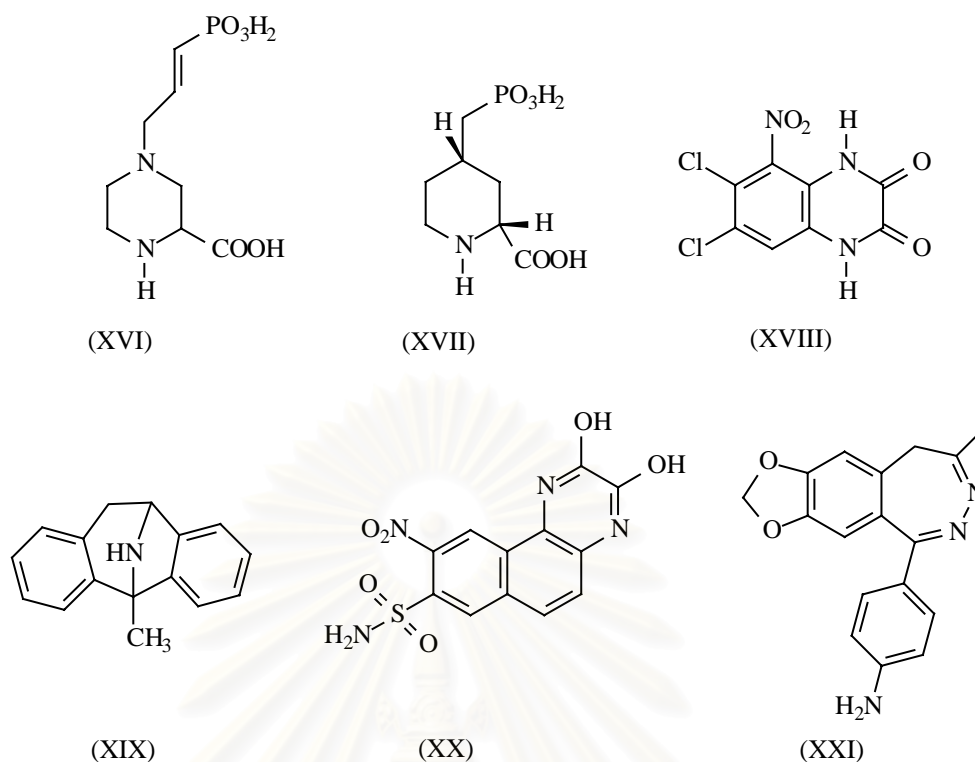
Figure 2. The chemical structures of some anticonvulsants (XVI-XXI).

Despite the fact that firstly detection of new AEDs was more or less by serendipity, so drug development moved on very slowly. In 1969, the Epilepsy Branch of the National Institutes of Health (NIH) established the first approach applied in the search for new AEDs in the US. NIH initiated the Drug Development Program, representing collaboration between academia and the pharmaceutical industry. By 1993, the collaboration had resulted in the screening of more than 15,000 compounds several of which have been developed and marketed as new AEDs. (Sabers and Gram, 1996)

A second approach, which has proved successful, is to undertake structural variation of known AEDs, modifying the chemical structure with the aim of improving efficacy and/or decrease toxicity. Well-established AEDs such as oxcarbazepine is the result of such an approach.

Finally, what has been termed rational drug development has emerged, base on the increased knowledge of basic pathophysiological events responsible for epilepsy, as well as better understanding of the basic mechanisms of drug activity.

Insights into mechanisms of seizures suggest that an abnormality of potassium conductance, a defect in the voltage-sensitive ion channel, or a deficiency in the membrane adenosine triphosphatase (ATPase) linked to ion transport may result in neuronal membrane instability and a seizure. Selected neurotransmitters (e.g., glutamate, aspartate, acetylcholine, norepinephrine, histamine, corticotropin-releasing factor, purines, peptides, cytokines, and steroid hormones) enhance the excitability and propagation. A deficiency of inhibitory neurotransmitters such as γ-aminobutyric acid (GABA) or an increase in excitatory neurotransmitters would promote abnormal neuronal activity. Normal neuronal activity also depends on an adequate supply of glucose, oxygen, sodium, potassium, chloride, calcium, and amino acids. Systemic pH is also a factor in precipitating seizures. The different kinds of epilepsies probably arise from different physiologic abnormalities. (Graves and Garnett, 1999)

Control of abnormal neuronal activity with AEDs is accomplished by elevating the threshold of neurons to electrical or chemical stimuli or by limiting the propagation of the seizure discharge from its origin. Raising the threshold most likely involves stabilization of neuronal membranes, whereas limiting the propagation involves depression of synaptic transmission and reduction of nerve conduction. The present understanding of the mechanisms by which AEDs exert therapeutic benefits may be summarized as follows:

a) By inhibiting excessive neuronal firing.

Neuronal activity depends on voltage-dependent ion channels, with Na^+, K^+, and Ca^{2+} channels determining the features of the action potential.

The sodium channels can exist in three conformational states: active, resting and inactivated. In general, after the neuronal cell membrane is depolarized, the permeability to sodium ion increases, with sodium ions entering the cells followed by a return to the normal state in a rate- and voltage-dependent manner. The established first choice AEDs – phenytoin and carbamazepine exert their effects by stabilizing the inactive forms of the voltage-dependent Na^+ channel (VGSC) and retarding its rate of recovery from inactivation. More over, high concentrations of valproate can also prolong inactivation of Na^+ channels. Many of the newer drugs, including felbamate, gabapentin, topiramate and lamotrigine exhibit significant inhibitory activity at VGSC in addition to other modes of action (Figure 3 and 5). (Edafiogho and Scott, 1996; McNamara, 1996; Meldrum 1996; White, 1997; Cosford, McDonald and Schweiger, 1998)

Recent evidence points to a significant role for neuronal voltage-gate calcium channels as molecular targets for the treatment of epilepsy. Several AEDs including valproate, ethosuximide, dimethadione and zonisamide are antagonists of T-type calcium channel current (Figure 4). Lamotrigine has recently been shown to inhibit N-type. (James, 1996; Cosford et al., 1998)

A potentiation of K^+-mediated currents has often been considered as a mechanism of AED action, but no antiepileptic effect of any established AEDs can confidently be attributed to this mechanism. (Meldrum, 1996)
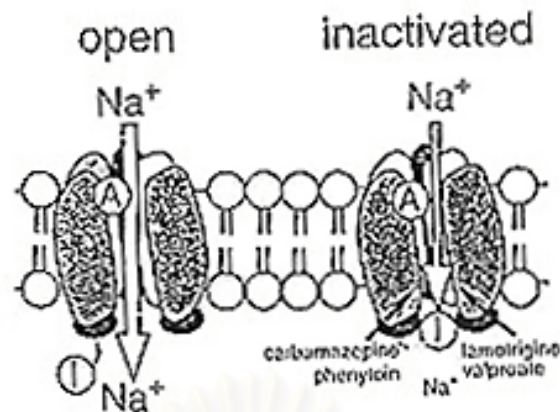
Figure 3. Antiseizure drug-enhanced Na$^+$ channel inactivation.
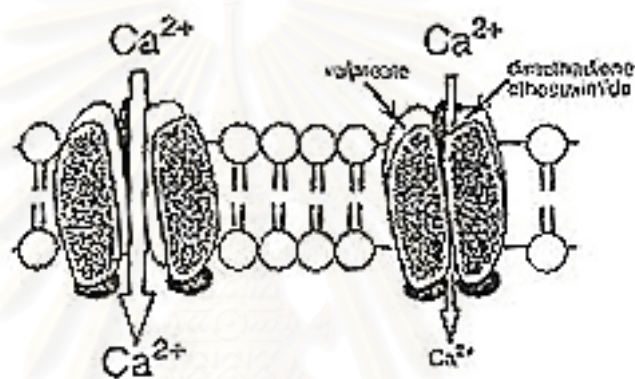
Figure 4. Antiseizure drug-induced reduction of current through T-type
Ca^{2+} channels.

b) By inhibiting excitatory mechanisms.

The acidic amino acids glutamate and aspartate are thought to be the major fast excitatory neurotransmitters in the mammalian central nervous system (CNS). It is believed that there are five subtypes of receptors for the excitatory amino acids (EAAs). The three major subtypes of EAA receptor that have been identified are classified as *N*-methyl-D-aspartate (NMDA), α-amino-3-hydroxy-5-methyl-4-isoxazole-propionic acid (AMPA), and kainate receptors. The AMPA and kainate receptors are usually referred to as the non-NMDA receptors for EAAs. (Edafiogho and Scott, 1996)

At the excitatory synapse, once released from the presynaptic terminal, glutamate can bind to both NMDA and non-NMDA receptors. Glycine is required as a co-agonist at the NMDA receptor, which is coupled to an associated ion channel permeable to Na^+, K^+ and Ca^+ (Figure 5). (White, 1997)

The NMDA receptor complex possesses multiple modulatory sites that are targeted by several new generation-AEDs. Drugs can decrease NMDA function competitively by binding to the NMDA receptor (e.g., D-CPPene (XVI) or CGS-19755 (XVII)) or the strychnine-insensitive glycine receptor (e.g., ACEA 1021 (XVIII) and felbamate) or noncompetitively by binding to a site within the open channel (e.g., dizocipine (XIX), felbamate).

Glutamate can also activate an ion channel coupled to the non-NMDA AMPA/Kainate receptor that is permeable to Na^+ and K^+. Activation of the non-NMDA receptor by glutamate provides sufficient depolarization to relieve the Mg^{2+}-dependent block of the NMDA receptor. Drug can block non-NMDA responses competitively (e.g., NBQX (XX)) or noncompetitively (GYKI 52466 (XXI)). Kainate-evoked currents can also be blocked by topiramate.

c) **By potentiating inhibitory mechanisms.**

The steps in the synaptic action of GABA which are possible sites of drug intervention include stimulation of GABA release, inhibition of GABA reuptake, reduction of the breakdown of GABA, and modulation of post-synaptic GABA receptor. GABA receptors are comprised of $GABA_A$ receptor and the metabotropic $GABA_B$ receptor. (Cosford, McDonald and Schweiger, 1998)

The GABA$_A$ receptor and its associated allosteric binding sites are coupled to a chloride-permeable ion channel. AEDs can enhance GABA at the postsynaptic receptor by increasing channel opening and burst frequency (e.g., benzodiazepines (such as clonazepam) and topiramate) or by increasing channel open and burst duration (e.g., phenobarbital). AEDs can also enhance GABA-mediated neurotransmission by blocking neuronal and glial reuptake of synaptically released GABA (e.g., tiagabine). Vigabatrine increases GABA levels within neuronal terminals and surrounding glial cells by irreversibly inhibiting GABA aminotransferase (GABA-T), which metabolizes GABA to succinic acid semialdehyde (SSA). Gabapentin has been shown to increase GABA levels within the occipital cortex of patients with epilepsy (Figure 6). (White, 1997)
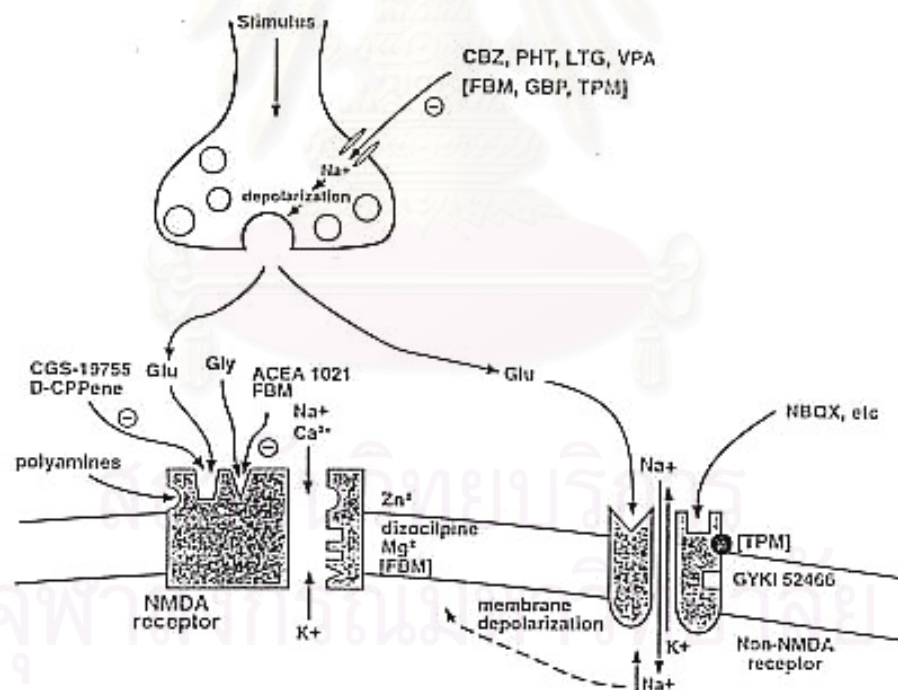
Figure 5. Proposed mechanisms of action of some AEDs mediated by glutamate at the excitatory synapse. (CBZ, carbamazepine; FBM, felbamate; GBP, gabapentin; Glu, glutamate; Gly, glycine; LTG, lamotrigine; PHT, phenytoin; TPM, topiramate; VPA, valproate)
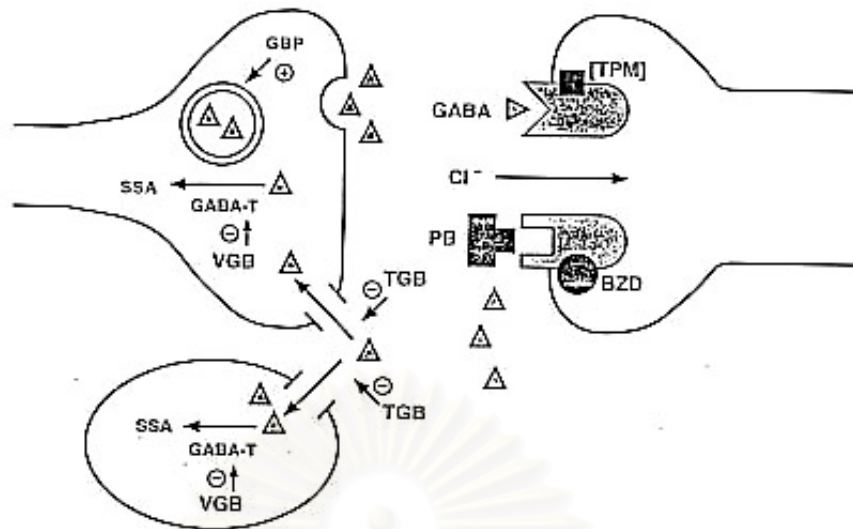
Figure 6. Proposed mechanisms of action of some AEDs at the $GABA_A$ inhibitory

synapse. (BZD, benzodiazepine; GABA, γ-aminobutyric acid; GABA-T;

GABA aminotransferase; GBP, gabapentin; PB, phenobarbital; TGB,

tiagabine; TPM, topiramate; SSA, succinic acid semialdehyde; VGB,

vigabatrine;)

The improved understanding of the molecular mechanism lead to discussion of

the concepts of drug treatment and drug discovery. Monotherapy (one medication)

has been prefered to polytherapy (multiple medications) in the treatment of epilepsy

for many years since fewer side effects, fewer drug interations, lower medication

costs, and better compliance are expected to present when monotherapy is utilized.

Polytherapy will be instituted when the patient cannot be controlled by a single drug.

However, with the known mode of action and a very favorable toxicity profiles of

many new drugs over the old AEDs, a novel concept of "rational polytherapy" have

emerged as an alternative. This concept is based on the assumption that combining

some AEDs may result in supra additive (synergistic efficacy) and infra additive

(antagonistic) toxicity, resulting in an enhanced efficacy and toxicity profile.

However it is important to examine the benefits of this combination therapy. When

polytherapy is used, it should satisfactorily embrace the following principles. Firstly,

it is best to combine antiepileptic drugs with different mechanism of action than to prescribe combination those have similar mechanism of action. Second, it is best to select antiepileptic drugs with relatively little potential for drug-drug interaction. Third, patients treated with polytherapy demand more intensive monitoring, both clinically and possibly with antiepileptic drug levels. (Sabers and Gram, 1996; Kadir and Chadwich, 1999)

In AEDs development, general researches focus on searching a new drug with less toxic and known mechanism of action. According to the concept of monotherapy, AEDs with multiple modes of action are required to treat various type of seizures. On the other hand, with the concept of rational polytherapy, and advanced knowledge in mechanism of action at molecular level, there is a high possibility that AEDs with highly selective mechanism of action will be developed. (Cosford, et al., 1998)

Representing a promising anticonvulsant agent, ameltolide (4-amino-*N*-(2,6-dimethylphenyl)benzamide, LY201116, ADD75073, XXII) is one of the most potent and selective compound in the series of 4-aminobenzamides which inhibits maximal electroshock-induced seizure (MES), but ineffective against a variety of chemically induced seizures. Since this anticonvulsant profile similar to those of phenytoin, ameltolide is as interesting as a new lead compound that may replace phenytoin, which has drawn back due to its side effect. (Clark et al., 1985)
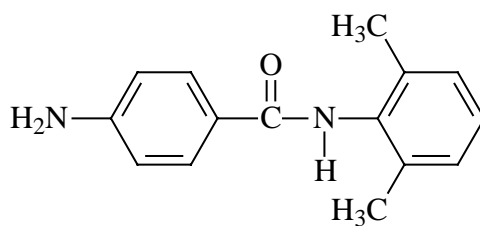
(XXII)

Initial results indicated that ameltolide possesses greater anticonvulsant activity and a higher protective index than phenytoin. In addition, it does not increase hexobarbital-induced sleeping time. (Clark, 1988) Unfortunately, ameltolide was rapidly metabolically inactivated by N-acetylation at N-terminus and subsequent hydroxylation of one of the methyl substituent. However, following the pioneering discovery of ameltolide, it has become one of a fruitful compound for designing of several new and potent anticonvulsants. (Robertson et al., 1991)

More than one conformations of ameltolide, resulted from rotation of single bond, were detected by crystallographic and molecular modeling studies. (Duke and Codding, 1992) These studies also reported a high barrier to rotation about Ph-(C=O) single bond but a low barrier for rotation of (C=O)-NH-Ph single bonds in a series of 4-amino-*N*-phenylbenzamides. Since, there must be only one conformation fitting to the binding site, design of a constrained analogue of the active conformer should lead to anticonvulsant with high activity.

In 1994, N-(*p*-aminobenzoyl)-1,2,3,4-tetrahydro-4,8-dimethylquinoline (XXIII) was firstly synthesized by Sathit Niratisai as the rigid analogue of ameltolide (Sathit Niratisai, 1994). The preliminary result indicated that it exhibited anticonvulsant activity against MES test. However, its synthetic approaches are complicate with several steps.
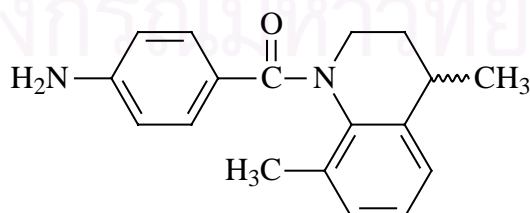
(XXIII)

To extend the structure activity relationship on N-(*p*-aminobenzoyl)-1,2,3,4-tetrahydroquinoline pharmacophore and to improve the synthetic procedures, herein,

N-(*p*-aminobenzoyl)-1,2,3,4-tetrahydroquinoline (CU-17-02) and derivatives with substituent on 1,2,3,4-tetrahydroquinoline ring were synthesized by simpler methods, and expected to possess anticonvulsant activity. Certainly, the introduction of methyl group along the variable positions of 1,2,3,4-tetrahydroquinoline nucleus especially at the piperidine ring and C-8 (see Table 4) will affect the conformational orientation of the target compounds. These data may lead to an understanding of an appropriate conformational structure of this series for target binding site in the future study. In addition, steric hindrance in some compounds may affect the metabolic hydroxylation, which may in turn change the potency or duration of anticonvulsant activity. The chemical structures of target compounds are illustrated in Table 4.

Table 4. Structures of N-(*p*-aminobenzoyl)-1,2,3,4-tetrahydroquinolines to be synthesized
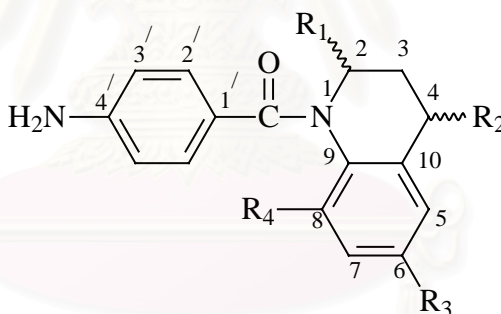
Compounds	Substituent			
	R_1	R_2	R_3	R_4
CU-17-02 (4a)	H	H	H	H
CU-17-04 (4b)	CH_3	H	H	H
CU-17-06 (4c)	H	CH_3	H	H
CU-17-08 (4d)	H	H	H	CH_3
CU-17-10 (4e)	CH_3	H	F	H
CU-17-12 (4f)	CH_3	H	H	CH_3
CU-17-14 (4g)	H	CH_3	H	CH_3
CU-17-16 (4h)	H	H	H	OMe

The synthetic approach for all compounds is shown in Figure 7.

1f $R_1 = R_4 = Me$
1g $R_2 = R_4 = Me$
1h $R_4 = OMe$

2b $R_1 = Me$
2c $R_2 = Me$
2d $R_4 = Me$
2e $R_1 = Me, R_3 = F$
2f $R_1 = R_4 = Me$
2g $R_2 = R_4 = Me$
2h $R_4 = OMe$

3a Unsubstituted
3b $R_1 = Me$
3c $R_2 = Me$
3d $R_4 = Me$
3e $R_1 = Me, R_3 = F$
3f $R_1 = R_4 = Me$
3g $R_2 = R_4 = Me$
3h $R_4 = OMe$

4a Unsubstituted
4b $R_1 = Me$
4c $R_2 = Me$
4d $R_4 = Me$
4e $R_1 = Me, R_3 = F$
4f $R_1 = R_4 = Me$
4g $R_2 = R_4 = Me$
4h $R_4 = OMe$
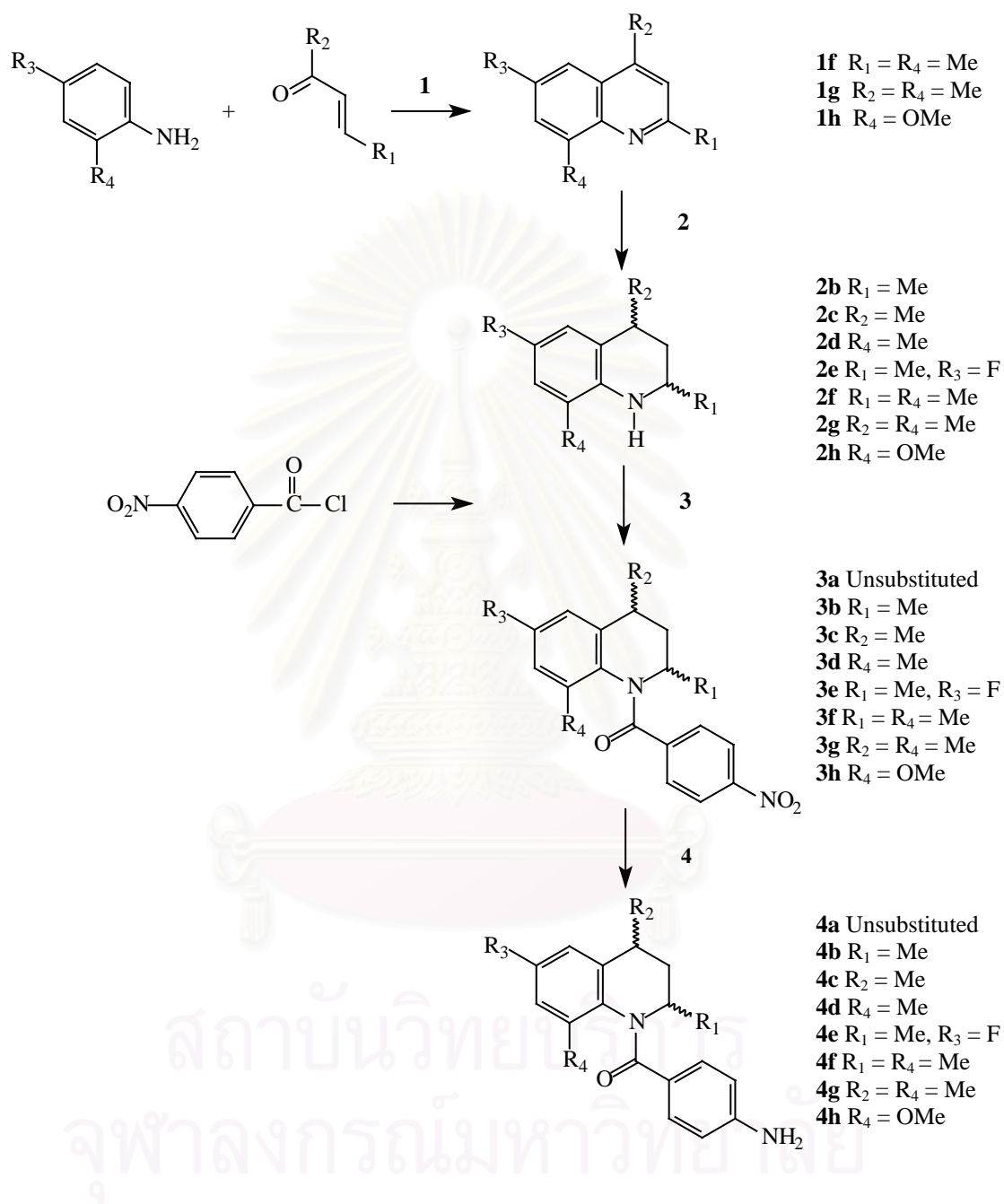
Figure 7. Synthesis of N-(*p*-aminobenzoyl)-1,2,3,4-tetrahydroquinolines (4a - 4h).
1: conc. HCl, 2,3-dichloro-1,4-napthoquinone, EtOH, reflux; **2**: NaBH$_4$,
NiCl$_2$.6H$_2$O, MeOH; **3**: *p*-nitrobenzoyl chloride, K$_2$CO$_3$, THF, reflux,
70 °C; **4**: H$_2$, 10% Pd/C, CH$_2$Cl$_2$

In this chapter, the historical aspects of ameltolide, a prototype of the target compounds (N-(*p*-aminobenzoyl)-1,2,3,4-tetrahydroquinoline derivatives) reported herein, are reviewed. Futhermore, the general synthetic methods that might be used to prepared N-(*p*-aminobenzoyl)-1,2,3,4-tetrahydroquinolines and their intermediates are also reported.

Molecular modification of 4-aminobenzamides

In 1984, Clark and co-workers firstly reported anticonvulsant activity of several 4-aminobenzamides. Some of them produced a high level of protection against seizures in animal models induced by maximal electroshock (MES) (Clark et al., 1994). The advance studies on the relationship between 4-aminobenzamide structure and anticonvulsant effects led to the conclusion of features required for optimum activity (Figure 8).

2. On benzamide phenyl ring, an amino substituent is required; the potency of *p*-NH$_2$ > m-NH$_2$ > o-NH$_2$

1. On amide nitrogen, cyclic substituent, such as a cyclohexyl or a phenyl ring are the best.

4. Insertion of methylene group led to loss of activity.

3. On anilide phenyl ring, the ortho methyl groups are prefered for great activity; introduction of amino group decrease potency after i.p. in mice, but enhance potency after oral in rats.

Figure 8. 4-Aminobenzamide structure activity relationship summary.

1. For the amide nitrogen atom, the introduction of an alkyl or aryl substituent onto this position confers MES activity while the unsubstituted 4-aminobenzamide (XXIV) is MES-inactive. Also a cyclic substituent, such as a cyclohexyl or a phenyl ring, yields greater MES potency than does a noncyclic anologue such as a saturated n-hexyl chain. (Clark et al., 1984)

(XXIV)
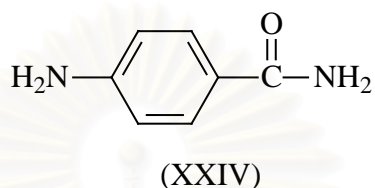
2. For the benzamide phenyl ring, an amino substituent is required for optimal MES activity, and drug potency, following the order of para > meta > ortho to the amino position. This order suggests that the substituent is not acting purely via electronic effects, but that the amino group must occupy a particular position with response to the remainder of the molecule. Moreover, a primary amino group is preferred; methylation at the nitrogen reduces MES activity, and N-acetylation destroys the anticonvulsant activity. (Clark, Lin and Sansom, 1986; Robertson et al., 1991)

3. For the anilide phenyl ring, the MES activity of 4-amino-*N*-phenyl-benzamide (XXVa), is increased by the addition of an *o*-methyl substituent on the phenyl ring (XXVb); the addition of a second *o*-methyl group (XXVh, known as ameltolide) yields an even more MES-potent anticonvulsant. The superior activity of XXVh is not simply a result of two methyl substituens, being present, but is closely related to the positions of these groups on the phenyl ring. This phenomena can be observed by comparing MES activity for these benzamides; the order of activity is XXVg < XXVf ≈ XXVj < XXVa ≈ XXVc ≈ XXVd ≈ XXVe ≈ XXVi ≤ XXVb < XXVh (Table 5). (Clark et al., 1985)

Table 5. Anticonvulsant activity of 4-amino-*N*-phenylbenzamides
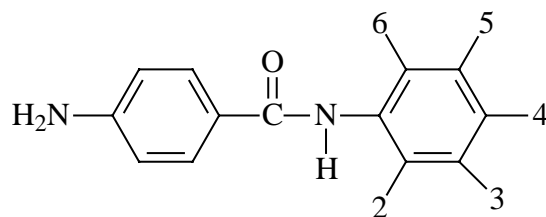
(XXV) (a-j)

compounds	Substituent position					MES[a]	
	2	3	4	5	6	30 min	4 hr
XXVa	H	H	H	H	H	++++	++
XXVb	CH$_3$	H	H	H	H	++++	+++
XXVc	H	CH$_3$	H	H	H	+++	++
XXVd	H	H	CH$_3$	H	H	+++	+++
XXVe	CH$_3$	CH$_3$	H	H	H	++++	++
XXVf	CH$_3$	H	CH$_3$	H	H	++	+
XXVg	CH$_3$	H	H	CH$_3$	H	++	-
XXVh	CH$_3$	H	H	H	CH$_3$	++++	++++
XXVi	H	CH$_3$	CH$_3$	H	H	+++	+++
XXVj	H	CH$_3$	H	CH$_3$	H	++	+

[a] ++++, +++, ++ and + signify activity at 30, 100, 300, and 600 mg/kg, respectively; - denotes no activity observed at 600 mg/kg.

The introduction of a second amino group on the substituted phenyl ring (e.g. 4-amino-(2-methyl-4-aminophenyl)benzamide, XXVI) decrease the anticonvulsant potency after intraperitoneal administration to mice; in contrast, it enhances the

activity after oral administration to rats, probably due to pharmacokinetic factors. (Kanyonyo, Poupaert and Lambert, 1998)

$$H_2N - \text{(C}_6\text{H}_4\text{)} - \overset{\overset{\displaystyle O}{\|}}{C} - \overset{\overset{\displaystyle }{}}{\underset{\overset{\displaystyle |}{H}}{N}} - \text{(C}_6\text{H}_3, \text{CH}_3) - NH_2$$

H$_3$C

(XXVI)
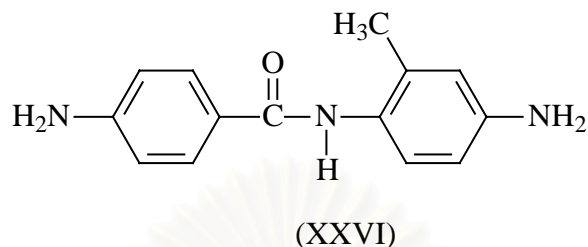
4. Insertion of a methylene group between the anilide carbonyl group and the adjacent phenyl group results in a distinct loss of MES activity that might due to the effect of different electronic and conformational factors. (Clark and Davenport, 1987)

Pharmacology (Clark, 1988; Leander, 1992; Leander et al., 1992)

Ameltolide was a potent and selective anticonvulsant in the MES test (anti-MES activity: ED_{50} = 2.6 mg/kg, i.p. in mice; ED_{50} = 3.9 mg/kg, orally in mice; ED_{50} = 32.5 mg/kg, orally in rats). It was unable to antagonize any of the standard chemically induced seizures (pentylenetetrazole, picrotoxin, bicuculline and strychnine). Such a profile of activity has been described as "preventing seizure spread" rather than "raising seizure threshold". This anticonvulsant profile of ameltolide is similar to that of phenytoin. The anticonvulsant effect in the MES test occurs at dose significantly lower than those that produce neurologic impairment (rotorod test: TD_{50} = 15 mg/kg, i.p. in mice; 38.3 mg/kg, orally in mice; 458.9 mg/kg, orally in rats), and well beyond those that impair the righting reflex (HD_{50} = 43.8 mg/kg, i.p. in mice) or produce lethality (LD_{50} = 160.8 mg/kg, i.p. in mice).

By considering the values of ED_{50}, TD_{50}/ED_{50}, LD_{50}/HD_{50}, LD_{50}/TD_{50} and TD_3/ED_{97}, the anticonvulsant activity and neurotoxicity of ameltolide compare favorably with those of prototype anticonvulsants in the same assays (Table 6-9). Ameltolide produces no sign of tolerance with daily administration, and does not interact with the hypnotic effects of hexobarbital after either acute or chronic administration. All of these results suggest that ameltolide will be an effective anticonvulsant in humans and support development of the compound for the treatment of epilepsy.

Metabolism, Disposition, and Pharmacokinetics of ameltolide (Potts, Gabriel and Parli, 1989; Roberson et al., 1991; Leander et al., 1992)

The metabolism, disposition, and pharmacokinetics of ameltolide have been studied in rats. ^{14}C-ameltolide was well absorbed (~94%) from the gastrointestinal tract following oral administration. Of the dose administered, 64.5% was excreted in the urine and 29% in the bile with the majority being excreted during the first 24 hr. Peak plasma levels of ameltolide were observed at 0.75 hr, whereas peak plasma concentrations of radioactivity were seen at 2 hr after dosing. Maximum levels of radioactivity were observed at 2 hr in all of the tissues studied. The elimination of radioactivity from the tissues was monophasic with a mean half-life of 3.4 hr. Biotransformation of ameltolide in rats was investigated by quantitating and isolating metabolites from urine and plasma. The major route of metabolism was N-acetylation to form 4-(acetylamino)-*N*-(2,6-dimethylphenyl)benzaminde (LY201979, XXVII), and then subsequent hydroxylation to form 4-(acetylamino)-*N*-(2-hydroxymethyl-6-methylphenyl)benzamide (LY272546, XXVIII). Two hours after oral dosing with ^{14}C-ameltolide, XXVII and XXVIII comprised 92% of the total radioactivity in the

plasma. The major urinary metabolite, accounting for 63% of the radioactivity in the urine, was XXVIII.

Pharmacological studies demonstrated that N-acetylation followed by hydroxylation of one of the benzylic methyl groups result in virtually complete metabolic inactivation of ameltolide. XXVII can be metabolized back to ameltolide in a variety of species whereas XXVIII cannot be converted back to its parent compound (Figure 9).
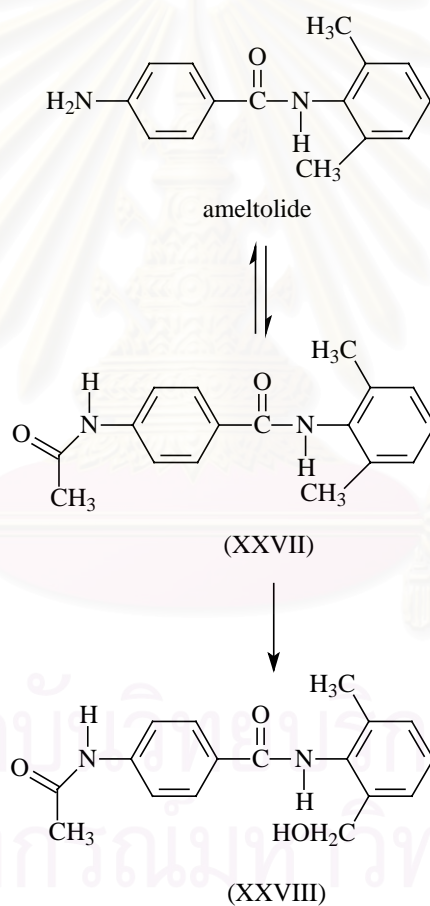
Figure 9. The major route of metabolism of ameltolide in rats, detected in plasma and urine.

Table 6. Minimal neurotoxicity and anticonvulsant potency of intraperitoneally administered ameltolide and some prototype antiepileptic drugs in mice

Substance	Time of Test[a] (hr)	Rotorod TD_{50} (mg/kg)	ED_{50} (mg/kg) and PI				
			MES	sc. PTZ	sc. BIC	sc. PIC	sc. Strych
Ameltolide	½, ½	15.0	[5.8] 2.6	[<0.75]	[<0.75]	[<0.5]	[<0.75]
PHT	2, 2	65.5	[6.89] 9.5	[<0.22]	[<0.65]	[<0.65]	maximum protection at 55-108
PB	½, 1	69.0	[3.17] 21.8	[5.24] 13.2	[1.83] 37.7	[2.51] 27.5	-
ESM	½, ½	441	[<0.44]	[3.38] 130	[0.96] 459	[1.82] 243	-
VPA	¼, ¼	426	[1.57] 272	[2.87] 149	[1.18] 360	[1.10] 387	[1.45] 293

PHT, phenytoin; PB, phenobarbital; ESM, ethosuximide; VPA, valproate; TD_{50}, dose eliciting evidence of minimal neurotoxicity in 50% of animals; ED_{50}, dose required to produce the desired endpoint in 50% of animals; MES, maximal electroshock seizure; sc. PTZ, subcutaneous pentylenetetrazol; sc. BIC, sc. bicuculline; sc. PIC, sc. picrotoxin; sc. Strych, sc. strychine; Protective index (PI = TD_{50}/ED_{50}) in [].

[a] First number, TD_{50}; second number, ED_{50}

Table 7. Minimal neurotoxicity and anticonvulsant potency of orally administered ameltolide and some prototype antiepileptic drugs in mice and rats

Time of test [a](hr)			TD_{50} (mg/kg)		MES ED_{50} (mg/kg)		sc. PTZ ED_{50} (mg/kg)	
Substance	Mice	Rats	Mice	Rats	Mice	Rats	Mice	Rats
ameltolide	½, 1	2,1	38.3	458.9	[9.8] 3.9	[14.1] 32.5	[<0.5]	[<0.9]
PHT	2, 2	½, 4	86.7	No ataxia up to 3,000	[9.59] 9.04	[>100] 29.8	[<0.29]	NA
PB	2, 2	½, 5	96.8	61.1	[4.82] 20.1	[6.68] 9.14	[7.69] 12.6	[5.29] 11.6
ESM	1, ½	2, 2	879	1,012	[<0.44]	[<0.84]	[4.56] 193	[18.8] 54
VPA	2,1	1, ½	1,264	280	[1.90] 665	[0.57] 490	[3.26] 388	[1.56] 180

PHT, phenytoin; PB, phenobarbital; ESM, ethosuximide; VPA, valproate; TD_{50}, dose eliciting evidence of minimal neurotoxicity in 50% of animals; ED_{50}, dose required to produce the desired endpoint in 50% of animals; MES, maximal electroshock seizure; sc. PTZ, subcutaneous pentylenetetrazol; Protective index (PI = TD_{50}/ED_{50}) in []; NA, not appicable

[a] Toxicity, MES and sc. PTZ, respectively.

Table 8. Quantitative toxicity profile of intraperitoneally administered ameltolide and some prototype antiepileptic drugs in mice

Substance	Time of test [a] (hr)	Dose (mg/kg)		
		Lethality (LD_{50})	Righting reflex (HD_{50})	Rotorod (TD_{50})
ameltolide	24, ½, ½	160.8	[3.67] 43.8	[10.71] 15.0
PHT	24, 12, 2	230	[1.29] 178	[3.51] 65.5
PB	24, 1, ½	265	[1.95] 135	[3.84] 69.0
ESM	24, ½, ½	1,752	[2.06] 851	[3.98] 441
VPA	24, ¼, ¼	1,105	[1.25] 886	[2.59] 426

PHT, phenytoin; PB, phenobarbital; ESM, ethosuximide; VPA, valproate; LD_{50}, dose that caused death in 50% of animals; HD_{50}, dose at which 50% of animals lost righting reflex; TD_{50}, dose eliciting evidence of minimal neurotoxicity in 50% of animals. Ratio LD_{50}/HD_{50} or LD_{50}/TD_{50} in [].

[a] Lethality, righting reflex, and rotorod, respectively.

Table 9. Safety ratios (TD_3/ED_{97}) of ameltolide, PHT, PB, and VPA

Substance	Spices and route of administration	Parameter		
		TD_3 (mg/kg)	MES ED_{97} (mg/kg)	Ratio
ameltolide	Mice, i.p.	9.8	6.0	1.6
	Mice, oral	23	9.1	2.5
	Rats, oral	230	47	4.9
PHT	Mice, i.p.	49	13.5	3.6
	Mice, oral	185	62	3.4
	Rats, oral	NA	95	-
PB	Mice, i.p.	59	29	2.0
	Mice, oral	58	46	1.3
	Rats, oral	14	26	0.5
VPA	Mice, i.p.	345	380	0.9
	Mice, oral	500	850	0.6
	Rats, oral	115	1800	0.1

PHT, phenytoin; PB, phenobarbital; ESM, ethosuximide; VPA, valproate; NA, not applicable.

[a] Ratios < 1 indicate that 97% protection is obtained only with some minimal neurotoxicity.

[b] TD_3, dose eliciting evidence of minimal neurologic toxicity in 3% of animals; ED_{97}, dose required to produce anti-MES activity in 97% of animals.

The elimination of ameltolide from the systemic circulation following iv. administration to rats was monophasic, with a terminal half-life of 9.4 min. The volume of distribution was 911 ml/kg. The plasma clearance value (66.9 ml/min/kg) is approximately equal to hepatic blood flow (66.2 – 78.1 ml/min/kg) . This result would suggest a large first-pass metabolism in the liver, which would explain the apparent discrepancy between the complete oral absorption of ameltolide and its low systemic bioavailability.

Mechanism of action of ameltolide. (Vamecq et al., 1998)

Up to now, the mechanism of action of ameltolide is still not clear. However it is expected to exert anticonvulsant activity by blocking sodium channels according to its phenytoin-like profile, selective to MES test. This hypothesis was supported by the experiment of Vamecq's team that reported a correlation between interaction with the neuronal voltage-dependent sodium channel and anticonvulsant activity of ameltolide in the MES test.

Analogues of ameltolide

1. **LY201409 (4-Amino-*N*-(2,6-dimethylphenyl)-3,5-dimethylbenzamide, XXIX)**
(Robertson et al., 1987, 1988)
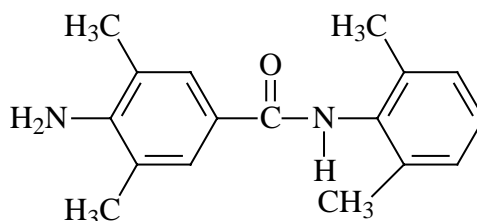
(XXIX)

In an attempt to preclude metabolic N-acetylation sterically, LY201409 was synthesized and evaluated for anticonvulsant activity. This structural modification successfully altered the metabolic pathway while that of compound with one methyl group ortho to the 4-amino substituent was converted to its parent compound. LY201409 displayed potent anticonvulsant activity in both mice and rats (anti-MES activity: $ED_{50} = 10.5$ mg/kg, i.p. in mice; $ED_{50} = 16.2$ mg/kg, orally in mice; $ED_{50} = 4.2$ mg/kg, orally in rats). However, its ability to potentiate hexobarbital-induced sleeping time in mice diminishes its attractiveness as a drug candidate.

2. 4-Amino-*N*-phenylphthalimide Derivatives (Bailleux et al., 1994, 1995; Poupaert et al., 1995; Vamecq et al., 2000)

Thalidomide   Ameltolide

Design

4-Amino-*N*-phenylphthalimides
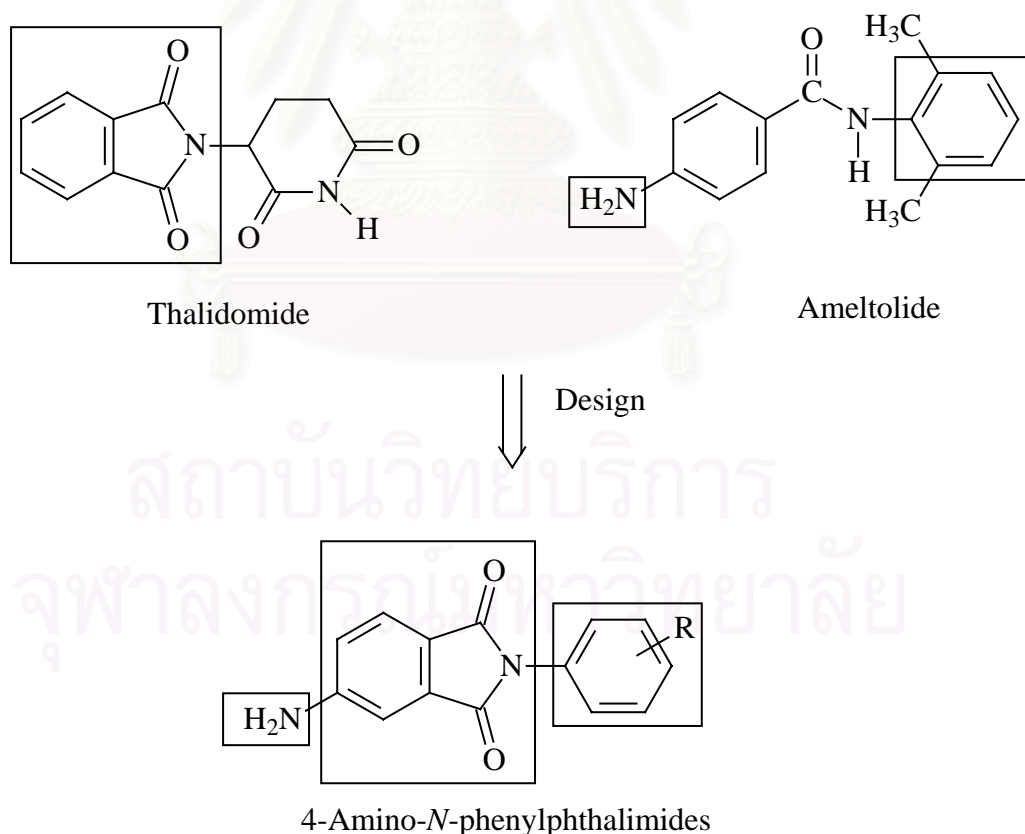
Figure 10. Design of 4-amino-*N*-phenylphthalimides.

The discovery of a potent anticonvulsant series of 4-amino-*N*-phenylphthalimides was one of the successive works using ameltolide as lead agent. They were designed from the models of ameltolide and thalidomide (Figure 10), and shown to possess similar anticonvulsant properties to those of ameltolide, also associating with a phenytoin-like profile.

After intraperitoneal administration, none of them were more active than ameltolide even if some of them showed significantly higher protective indexes (PI, i.e. the ratio of TD_{50}/ED_{50}) were found. After oral administration, many compounds were superior to ameltolide. One of the most active compound in this family was the ADD213063 (XXX, 4-amino-*N*-(2,6-dimethylphenyl)phthalimide). It was effective anticonvulsant mainly in the MES test (anti-MES activity: ED_{50} = 49.5 μmol/kg, i.p. in mice; ED_{50} = 33.4 μmol/kg, orally in mice; ED_{50} = 25.2 μmol/kg, orally in rats). With its interesting anticonvulsant pattern, it may be new lead as potential anticonvulsant for the future development.
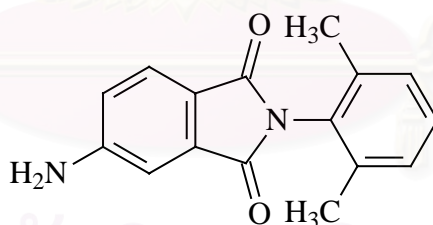
XXX

General methods concerning to the preparation of N-(*p*-aminobenzoyl)-1,2,3,4-tetrahydroquinoline derivatives.

In this section, the general synthetic procedures that may be used to prepare a series of N-(*p*-aminobenzoyl)-1,2,3,4-tetrahydroquinolines and its intermediates are reviewed, including synthesis of quinolines, 1,2,3,4-tetrahydroquinolines, amide compounds, and reduction of nitro compounds to amines.

Synthesis of Quinolines. (Furniss et al., 1991; Song, Mertzman and Hughes, 1993; Joule, Mills and Smith, 1995)

Many excellent syntheses have been developed for obtaining quinolines. Three of more generally important procedures are summarized:

a) The Combes synthesis
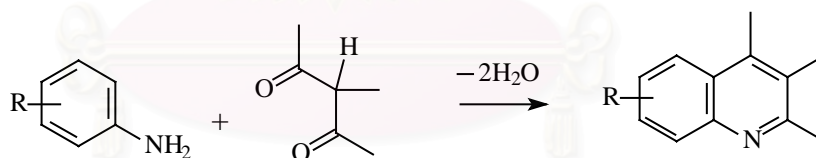
Condensation of a 1,3-dicarbonyl compound with an arylamine gives a high yield of a β-amino-enone, which can then be cyclised with concentrated acid. The cyclisation step may be an electrophilic substitution by the *o*-protonated amino-enone, as shown, followed by loss of water to give the aromatic quinoline.
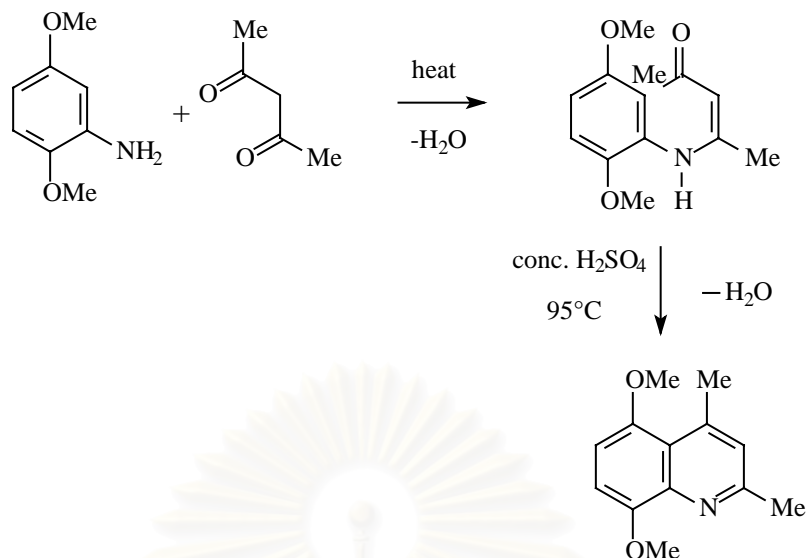
b) The Skraup synthesis
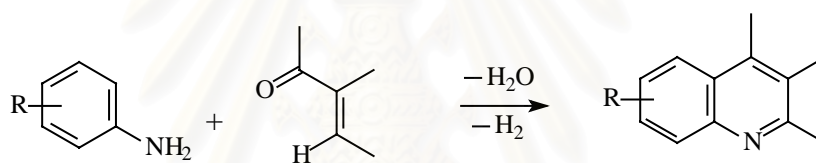
The Skraup reaction is the great general utility and has been applied to many aromtic amines. In this extraordinary reaction, quinoline is produced when aniline, concentrated sulfuric acid, glycerol and a mild oxidizing agent are heated together. The reaction has been shown to proceed by dehydration of the glycerol to acrolein to which aniline then adds in a conjugate fashion. Acid-catalyst cyclisation produces a 1,2-dihydroquinoline finally dehydrogenated by the oxidising agent; the corresponding nitrobenzene or arsenic acid has been used classically though with the inclusion of a little sodium iodide; the sulfuric acid can serve as oxidant.

conc. H₂SO₄
PhNO₂/130°C

−H₂O

[O]

85%
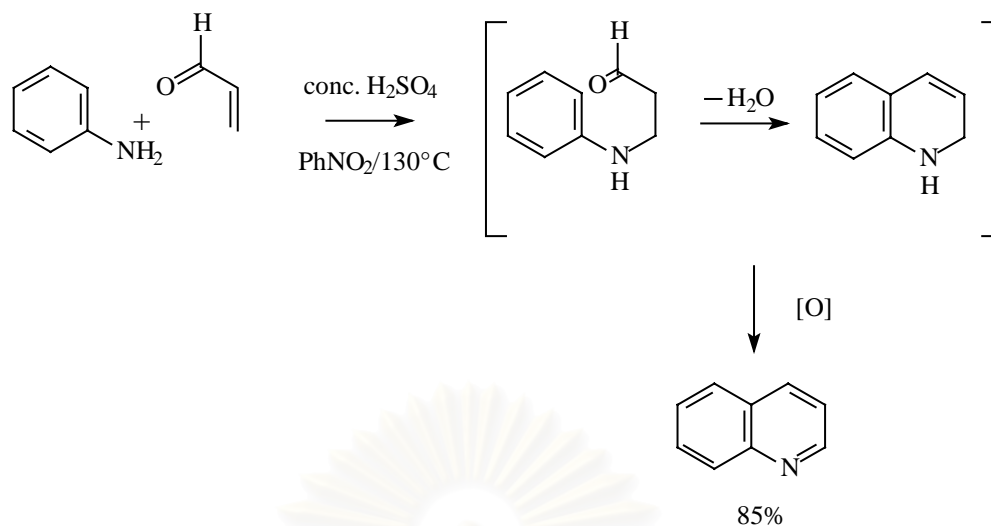
Skraup syntheses sometimes become very vigorous and extreme; care must be taken to control their potential violence; performing the Michael adduct and using an alternative oxidant (e.g., *p*-chloranil, 2,3-dichloro-1,4-napthoquinone) has been shown to be advantageous in terms of yield and as a better means for controlling the reaction.

c) **The Friedlander synthesis**

−2H₂O
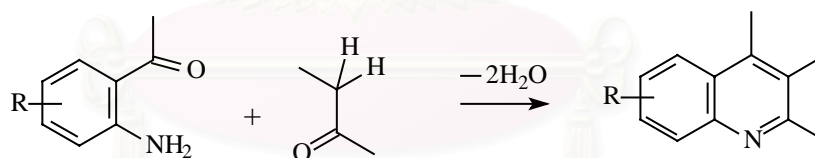
o-Acylanilines condense with a ketone or aldehyde (which must contain an α-methyl group) by base or acid catalysis to yield quinolines. The orientation of condensation depends on the orientation of enolate or enol formation.

aq. KOH
EtOH/0°C

71%

conc. H₂SO₄
AcOH/heat

88%

Synthesis of 1,2,3,4- tetrahydroquinolines
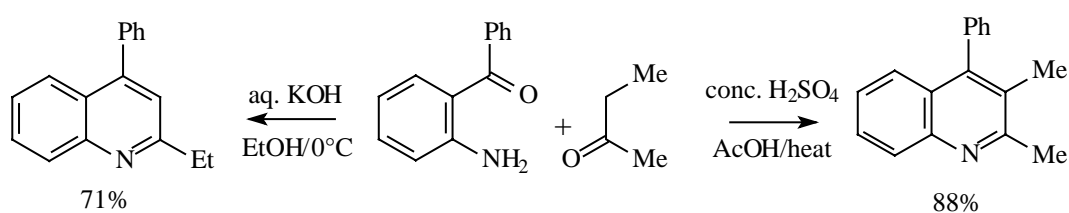
quinoline   1,2,3,4-tetrahydroquinoline
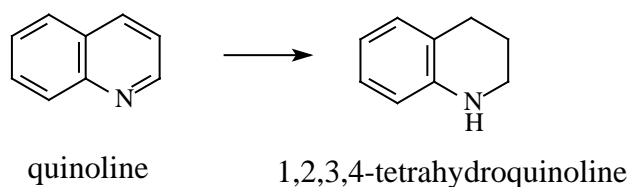
Selective reduction of pyriding rings in quinolines can be achieved by two general ways:

a) By catalytic hydrogenation

Traditionally, hydrogenation of quinolines over platinum oxide or platinum in methanol at room temperature and room pressure gives a high yield of 1,2,3,4-tetrahydroquinolines. For example, hydrogenation of quinoline in methanol by using PtO_2 as catalyst stop cleanly at the tetrahydro stage (97.5%); however, reaction time were rather long (35 hr); after 20 hr, only 70% of starting material had reacted. (Vierhapper and Eliel, 1975)

b) By chemical reduction

Sodium borohydride-nickelous chloride system exhibits strong reducing activity. Quinoline, 2-methylquinoline and 4-methylquinoline were reduced with this system to give the corresponding 1,2,3,4-tetrahydro derivatives (93.5%, 82.8% and 83.0%, respectively). (Nose and Kudo, 1984)

Synthesis of amides (March, 1968; Morrison and Boyd, 1987; Carey and Sunberg, 1993, Bruice, 1995)

    a) **The synthesis of amides from acids.**

In the industry, amides are often prepared by heating an acid with an amine. Because an acid has a lower pKa than a protonated amine, the acid immediately donates a proton to the amine when the two compounds are mixed. The protonated amine is not nucleophile, so it cannot attack the carbonyl carbon and therefore this salt is the final product of the reaction. However, removal of water from an ammonium salt by using high temperature will produce the corresponding amide.

$$RCOOH \ + \ R'NH_2 \ \longrightarrow \ RCOOH_3N^+R' \ \xrightarrow{\text{heat}} \ RCONHR' \ + \ H_2O$$

    b) **The synthesis of amides from acyl halides.**

The treatment of acyl halides with amines is a very general reaction for the preparation of amides. Acyl chlorides are highly reactive acylating agents and react very rapidly with amines. The reaction of an acyl chloride with ammonia or with a primary or secondary amine or arylamine produces an amide, H^+ and Cl^-. The H^+ generated in the reaction will protonate unreacted ammonia or unreacted amine; because these protonated compounds are not nucleophiles, they cannot react with the acyl chloride. The reaction, therefore, must be carried out with twice as much ammonia as acyl chloride or else there will be only enough amine to react with half of the acyl halides. In some cases aqueous alkali is added to combine with the liberated HCl.

$$RCOCl \ + \ 2NH_3 \ \longrightarrow \ RCONH_2 \ + \ NH_4Cl$$

c) The synthesis of amides from acid anhydride.

Acid anhydrides react with amines to form amides by the same reaction as that of acyl chlorides, but a little more slowly. Two equivalents of an amine or 1 equivalent of an amine with 1 equivalent of pyridine must be employed in the reaction of an amine with an anhydride so that sufficient amine is presented to react with the proton produced in the reaction.

$$R'COOCOR \ + \ 2NH_3 \ \longrightarrow \ RCONH_2 \ + \ R'COONH_4$$

d) The synthesis of amides from esters.

Esters react with amines to form amides. Comparatively, the aminolysis (reaction of a compound with an amine) of an ester requires only one equivalent of amine, unlike the aminolysis of an acyl halide or an acid anhydride, which requires two equivalents. This is because the leaving group of an ester (RO^-) is more basic than the amine nucleophile (RNH_2), so the alkoxide ion rather than the amine picks up the proton produced during the course of the reaction.

$$RCOOR' \ + \ NH_3 \ \longrightarrow \ RCONH_2 \ + \ R'OH$$

e) The synthesis of amides from nitrile

Nitriles are hydrolyzed to amides. The reaction requires either H^+ or HO^- as a catalyst.

$$RCN \ + \ H_2O \ \longrightarrow \ RCONH_2$$
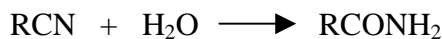
Reactions particularly applicable to aromatic nitriles involve the use of an aqueous solution of sodium hydroxide containing hydrogen peroxide, but alkyl cyanides do not always give good results.

Reduction of nitro compounds to amines. (March, 1968; Morrison and Boyd, 1987)

$$RNO_2 \ \longrightarrow \ RNH_2$$

Like many organic compounds, a nitro compound can be reduced to an amine in two general ways:

a) By catalytic hydrogenation.

Hydrogenation of a nitro compound to an amine takes place smoothly when a solution of the nitro compound is shaken with finely divided palladium, platinum or nickel under hydrogen gas. Palladium is the most common hydrogenation catalyst for both aromatic and aliphatic nitro compounds. This method cannot be used when the molecule also contains some other easily hydrogenated group, such as a carbon-carbon double bond.

b) By chemical reduction.

Adding hydrochloric acid to a mixture of the nitro compound and a metal, usually granulated tin most often carries out chemical reduction in the laboratory. In the acidic solution, the amine is obtained as its salt; the free amine is liberated by

addition of base, and is steam-distillated from the reaction mixture. The crude amine is generally contaminated with some unreduced nitro compound, from which it can be separated by taking advantage of the basic properties of the amine; the amine is soluble in aqueous mineral acid, and the nitro compound is not.

CHAPTER III

EXPERIMENTS

Instruments

1. Melting Point Apparatus: Buchi Capillary Melting Point Apparatus

2. CHNS/O Analyser: Perkin Elmer PE 2400 Series II

3. Infrared Spectrophotometer: Perkin Elmer Model 2000

4. Nuclear Magnetic Resonance Spectrometer

   : Bruker Spectrospin 300 (300 MHz)

   : Jeol JNM-A 500 (500 MHz)

5. Mass Spectrometer: Platform II

Chemicals

Acrolein (Merck)

o-Anisidine (Fluka)

Crotonaldehyde (Merck)

2,3-Dichloro-1,4-napthoquinone (Fluka)

6-Fluoro-2-methylquinoline (TCI)

Hydrochloric acid concentrated (Merck)

Lepidine (4-Methylquinoline, Fluka)

8- Methylquinoline (TCI)

Methyl vinyl ketone (TCI)

Nickel chloride hexahydrate (Fluka)

10% Palladium on activated charcoal (Merck)

Potassium carbonate (Merck)

Quinaldine (2-Methylquinoline, Fluka)

Sodium borohydride (Fluka)

Sodium hydroxide (BHD)

Sodium sulfate, anhydrous (Merck)

Tetrahydrofuran (Merck)

1,2,3,4-Tetrahydroquinoline (Fluka)

o-Toluidine hydrochloride (Fluka)

Zinc chloride (Merck)

All solvents used were laboratory grade and were redistilled prior to use.

General Procedures for the Synthesis of Quinoline Derivatives (1f - 1h)

To the substituted aniline in a two-neck round bottom flask, concentrated hydrochloric acid was added. Then, 2,3-dichloro-1,4-napthoquinone was added to the flask along with absolute ethanol to wash the solid down into the flask. This mixture was stirred and heated to reflux. Then a solution of α,β-unsaturated carbonyl compound in absolute ethanol was added to the refluxing solution. After the addition was complete, the mixture was allowed to reflux for another 20 minutes and a solution of zinc chloride dissolved in THF was added in several portions. Reflux the mixture for another 20 minutes, and was then allowed to cool slowly and stand for 1 hour. The solid was then collected by filtration, washed with THF and ether to give the corresponding quinoline.HCl.1/2 zinc chloride complex. Quinoline derivatives (1f, 1g and 1h) obtained from their corresponding zinc chloride complex by acid-base extraction. The conditions for synthesis of 1g - 1h are listed in Table 10.

Table 10. Details of reagents used in the synthesis of substituted quinolines (1f - 1h; as the ZnCl$_2$ complex)

Substituted Aniline	α,β-Unsaturated Carbonyl Compound	conc. HCl	2,3-Dichloro-1,4-napthoquinone	EtOH	ZnCl$_2$	THF	Product; Substituted Quinoline.HCl. 1/2 ZnCl$_2$ (yield)
o-toluidine.HCl 2.888 g (20 mmol)	crotonaldehyde 1.690 g (24 mmol)	4 ml (40 mmol)	4.574 g (20 mmol)	30 ml	2.759 g (20 mmol)	40 ml	1f.HCl.1/2 ZnCl$_2$ 4.088 g (77.6 %)
o-toluidine.HCl 2.875 g (20 mmol)	methyl vinyl ketone 1.684 g (24 mmol)	4 ml (40 mmol)	4.572 g (20 mmol)	30 ml	2.794 g (20 mmol)	40 ml	1g.HCl.1/2 ZnCl$_2$ 3.438 g (65.6 %)
o-anisidine 6.179 g (50 mmol)	acrolein 3.730 g (66 mmol)	15 ml (150 mmol)	11.394 g (50 mmol)	75 ml	6.931 g (51 mmol)	100 ml	1h.HCl.1/2 ZnCl$_2$ 6.621 g (50.0 %)

2,8-Dimethylquinoline (1f)

: 2,8-dimethylquinoline.HCl.1/2 ZnCl$_2$

Description	:	Brownish solid
% Yield	:	77.6 %

: 2,8-dimethylquinoline

Description	:	Yellowish liquid

IR	:	3044 cm^{-1}	(ν C-H, aromatic)
(Neat, NaCl cell)		2955 - 2920 cm^{-1}	(ν C-H, aliphatic)
		1616 - 1426 cm^{-1}	(ν C=C, C=N, aromatic)
		831 - 760 cm^{-1}	(δ C-H, out-of -plane, aromatic)
		(Figure 11)	

^{1}H-NMR	:	2.70, 2.83 ppm	(6H, 2-CH$_3$ + 8-CH$_3$)
(CDCl$_3$)		7.20 - 8.00 ppm	(5H, aromatic)
		(Figure 12-13)	

4,8-dimethylquinoline (1g)

: 4,8-dimethylquinoline.HCl.1/2 ZnCl$_2$

Description	:	Brownish solid
% Yield	:	65.6 %

: 4,8-dimethylquinoline

Description	:	White solid

m.p.	:	53-55 °C	

IR	:	3074 - 3034 cm^{-1}	(ν C-H, aromatic)
(KBr)		2966 - 2918 cm^{-1}	(ν C-H, aliphatic)
		1594 - 1436 cm^{-1}	(ν C=C, C=N, aromatic)
		845 - 770 cm^{-1}	(δ C-H, out-of -plane, aromatic)
		(Figure 14)	

^{1}H-NMR	:	2.62, 2.90 ppm	(6H, 4-CH$_3$ + 8-CH$_3$)
(CDCl$_3$)		7.17 - 8.80 ppm	(5H, aromatic)
		(Figure 15-16)	

8-methoxyquinoline (1h)

: 8-methoxyquinoline.HCl.1/2 ZnCl$_2$

Description	:	Brownish solid
% Yield	:	50.0 %

: 8-methoxyquinoline

Description	:	Yellowish liquid

IR	:	3055 - 3011 cm^{-1}	(ν C-H, aromatic)
(Neat, NaCl cell)		2945 - 2839 cm^{-1}	(ν C-H, aliphatic)
		1617 - 1474 cm^{-1}	(ν C=C, C=N, aromatic)
		823 - 713 cm^{-1}	(δ C-H, out-of -plane, aromatic)
		(Figure 17)	

¹H-NMR	:	4.10 ppm	(s, 3H, 8-OCH₃)
(CDCl₃)		7.07 - 8.98 ppm	(6H, aromatic)
		(Figure 18-19)	

General Procedures for the Synthesis of 1,2,3,4-Tetrahydroquinoline Derivatives (2b - 2h)

Quinoline derivative and NiCl₂.6H₂O were dissolved in methanol, and NaBH₄ was added in portions with stirring under cooling for 30 min. Then the stirring was continued for 30 min at room temperature. The reaction mixture was filtered. The filtrate was concentrated, and the resulting residue was dissolved in 10% HCl. The acidic solution was basified by the addition of concentrated ammonium hydroxide and extracted with chloroform. The extract was dried over anhydrous sodium sulfate. The chloroform was evaporated off to give the corresponding 1,2,3,4-tetrahydroquinoline derivative. The conditions for synthesis of 2b - 2h are listed in Table 11.

Table 11. Details of reagents used in the synthesis of 1,2,3,4-tetrahydroquinoline derivatives (2b – 2h) by using NaBH$_4$-NiCl$_2$ system

Substituted Quinline (A)	NiCl$_2$.6H$_2$O (B)	NaBH$_4$ (C)	MeOH	Ratio (mmol) A : B : C	Product; 1,2,3,4 -Tetrahydroquinoline Derivative (yield)
2-methylquinoline 1.455 g (10 mmol)	0.422 g (2 mmol)	1.517 g (40 mmol)	30 ml	1 : 0.2 : 4	2b 1.338 g (89.4 %)
4-methylquinoline 1.442 g (10 mmol)	2.380 g (10 mmol)	3.786 g (100 mmol)	30 ml	1 : 1 : 10	2c 1.322 g (89.2 %)
8-methylquinoline 2.370 g (16 mmol)	1.798 g (8 mmol)	2.273 g (60 mmol)	50 ml	1 : 0.5 : 3.8	2d 2.382 g (97.8 %)
6-fluoro-2-methylquinoline 1.613 g (10 mmol)	0.422 g (2 mmol)	1.524 g (40 mmol)	30 ml	1 : 0.2 : 4	2e; 0.978 g (59.1 %) 2b; 0.492 g (33.4 %)

Table 11. (continued) Details of reagents used in the synthesis of 1,2,3,4-tetrahydroquinoline derivatives (2b – 2h) by using $NaBH_4$-$NiCl_2$ system

Substituted Quinline (A)	$NiCl_2.6H_2O$ (B)	$NaBH_4$ (C)	MeOH	Ratio (mmol) A : B : C	Product; 1,2,3,4 -Tetrahydroquinoline Derivative (yield)
1f (2,8-dimethylquinoline) 1.312 g (8 mmol)	1.987 g (8 mmol)	3.178 g (84 mmol)	30 ml	1 : 1 : 10	2f 1.201 g (89.2 %)
1g (4,8-dimethylquinoline) 0.842 g (5 mmol)	2.552 g (11 mmol)	5.090 g (134 mmol)	16 ml	1 : 2 : 27	2g 0.718 g (83.1 %)
1h (8-methoxyquinoline) 2.297 g (14 mmol)	3.446 g (14 mmol)	5.462 g (144 mmol)	40 ml	1 : 1 : 10	2h 2.061 g (87.5 %)

1,2,3,4-Tetrahydro-2-methylquinoline (2b)

Description	:	Yellowish liquid	
% Yield	:	89.4 %	

IR	:	3394 cm^{-1}	(ν N-H)
(Neat, NaCl cell)		3054 - 3015 cm^{-1}	(ν C-H, aromatic)
		2963 - 2844 cm^{-1}	(ν C-H, aliphatic)
		1609 - 1584 cm^{-1}	(ν C=C, aromatic; δ N-H)
		746, 716 cm^{-1}	(δ C-H, out-of -plane, aromatic)
		(Figure 20)	

^{1}H-NMR	:	1.20 ppm	(d, J = 6.3 Hz, 3H, 2-CH$_3$)
(CDCl$_3$)		1.60 ppm	(m, 1H, H-3)
		1.90 ppm	(m, 1H, H-3)
		2.78 ppm	(m, 2H, H-4)
		3.40 ppm	(m, 1H, H-2)
		6.43 - 7.02 ppm	(4H, aromatic)
		(Figure 21-22)	

1,2,3,4-Tetrahydro-4-methylquinoline (2c)

Description	:	Yellowish liquid	
% Yield	:	89.2 %	

IR	:	3407 cm^{-1}	(ν N-H)
(Neat, NaCl cell)		3052 - 3016 cm^{-1}	(ν C-H, aromatic)

		2956 - 2864 cm^{-1}	(ν C-H, aliphatic)
		1607 - 1583 cm^{-1}	(ν C=C, aromatic; δ N-H)
		746 cm^{-1}	(δ C-H, out-of -plane, aromatic)
		(Figure 23)	

^{1}H-NMR	:	1.27 ppm	(dd, J = 7.0, 2.7 Hz, 3H, 4-CH$_3$)
(CDCl$_3$)		1.65 ppm	(m, 1H, H-3)
		1.95 ppm	(m, 1H, H-3)
		2.89 ppm	(m, 1H, H-4)
		3.25 ppm	(m, 2H, H-2)
		3.64 ppm	(s, broad, 1H, NH)
		6.40 - 7.07 ppm	(4H, aromatic)
		(Figure 24-25)	

1,2,3,4-Tetrahydro-8-methylquinoline (2d)

Description	:	Yellowish liquid	
% Yield	:	97.8 %	

IR	:	3426 cm^{-1}	(ν N-H)
(Neat, NaCl cell)		3044 - 3011 cm^{-1}	(ν C-H, aromatic)
		2927 - 2841 cm^{-1}	(ν C-H, aliphatic)
		1599 cm^{-1}	(ν C=C, aromatic; δ N-H)
		757, 734 cm^{-1}	(δ C-H, out-of -plane, aromatic)
		(Figure 26)	

^{1}H-NMR	:	1.91 ppm	(m, 2H, H-3)

(CDCl$_3$)	2.04 ppm	(s, 3H, 8-CH$_3$)
	2.76 ppm	(t, J = 6.3 Hz, 2H, H-4)
	3.33 ppm	(t, J = 5.4 Hz, 2H, H-2)
	3.45 ppm	(s, broad, 1H, NH)
	6.49 - 6.89 ppm	(3H, aromatic)
	(Figure 27-28)	

1,2,3,4-Tetrahydro-6-fluoro-2-methylquinoline (2e)

1,2,3,4-tetrahydro-6-fluoro-2-methylquinoline

| Description | : | Yellowish liquid |
| % Yield | : | 59.1 % |

1,2,3,4-tetrahydro-2-methylquinoline

| Description | : | Yellowish liquid |
| % Yield | : | 33.4 % |

Spectroscopic data for 1,2,3,4-tetrahydro-6-fluoro-2-methylquinoline:

IR	:	3401 cm^{-1}	(ν N-H)
(Neat, NaCl cell)		3033 cm^{-1}	(ν C-H, aromatic)
		2965 - 2848 cm^{-1}	(ν C-H, aliphatic)
		1610 cm^{-1}	(ν C=C, aromatic; δ N-H)
		895 - 722 cm^{-1}	(δ C-H, out-of -plane, aromatic)
		(Figure 29)	

| ^{1}H-NMR | : | 1.20 ppm | (d, J = 6.3 Hz, 3H, 2-CH$_3$) |
| (CDCl$_3$) | | 1.57 ppm | (m, 1H, H-3) |

1.92 ppm	(m, 1H, H-3)
2.60-2.90 ppm	(m, 3H, H-4 + NH)
3.35 ppm	(m, 1H, H-2)
6.35 - 6.75 ppm	(3H, aromatic)
(Figure 30-31)	

1,2,3,4-Tetrahydro-2,8-dimethylquinoline (2f)

| Description | : | Yellowish liquid |
| % Yield | : | 89.2 % |

IR	:	3419 cm^{-1}	(ν N-H)
(Neat, NaCl cell)		3045 - 3010 cm^{-1}	(ν C-H, aromatic)
		2963 - 2847 cm^{-1}	(ν C-H, aliphatic)
		1600 cm^{-1}	(ν C=C, aromatic; δ N-H)
		756, 733 cm^{-1}	(δ C-H, out-of -plane, aromatic)
		(Figure 32)	

^{1}H-NMR	:	1.25 ppm	(d, J = 6.2 Hz, 3H, 2-CH$_3$)
(CDCl$_3$)		1.58 ppm	(m, 1H, H-3)
		1.92 ppm	(m, 1H, H-3)
		2.08 ppm	(s, 3H, 8-CH$_3$)
		2.80 ppm	(m, 2H, H-4)
		3.35 - 3.50 ppm	(m, 2H, H-2 + NH)
		6.54 ppm	(t, J = 7.4 Hz, 1H, H-6)
		6.80 - 6.92 ppm	(2H, H-5 + H-7)
		(Figure 33-34)	

1,2,3,4-Tetrahydro-4,8-dimethylquinoline (2g)

Description	:	Yellowish liquid	
% Yield	:	83.1 %	

IR	:	3429 cm^{-1}	(v N-H)
(Neat, NaCl cell)		3049 cm^{-1}	(v C-H, aromatic)
		2958 - 2855 cm^{-1}	(v C-H, aliphatic)
		1600 cm^{-1}	(v C=C, aromatic; δ N-H)
		769, 742 cm^{-1}	(δ C-H, out-of -plane, aromatic)
		(Figure 35)	

^{1}H-NMR	:	1.29 ppm	(d, J = 7.1 Hz, 3H, 4-CH$_3$)
(CDCl$_3$)		1.70 ppm	(m, 1H, H-3)
		1.98 ppm	(m, 1H, H-3)
		2.08 ppm	(s, 3H, 8-CH$_3$)
		2.94 ppm	(m, 1H, H-4)
		3.37 ppm	(m, 2H, H-2)
		6.58 ppm	(dd, J = 7.4, 7.5 Hz, 1H, H-6)
		6.85 - 7.00 ppm	(2H, H-5 + H-7)
		(Figure 36-37)	

1,2,3,4-Tetrahydro-8-methoxyquinoline (2h)

Description	:	Yellowish liquid	
% Yield	:	87.5 %	

IR	:	3424 cm^{-1}	(ν N-H)
(Neat, NaCl cell)		3069 - 3044 cm^{-1}	(ν C-H, aromatic)
		2932 - 2835 cm^{-1}	(ν C-H, aliphatic)
		1611, 1588 cm^{-1}	(ν C=C, aromatic; δ N-H)
		759, 728 cm^{-1}	(δ C-H, out-of -plane, aromatic)
		(Figure 38)	

^{1}H-NMR	:	1.95 ppm	(m, 2H, H-3)
(CDCl$_3$)		2.77 ppm	(t, J = 6.4 Hz, 2H, H-4)
		3.33 ppm	(dd, J = 5.5, 5.4 Hz, 2H, H-2)
		3.84 ppm	(s, 3H, 8-OCH$_3$)
		6.52 - 6.68 ppm	(m, 3H, aromatic)
		(Figure 39-40)	

General Procedures for the Synthesis of N-(*p*-Nitrobenzoyl)-1,2,3,4-tetrahydroquinoline Derivatives.

p-Nitrobenzoyl chloride in THF was added portionwise to the mixture of 1,2,3,4-tetrahydroquinoline derivative, THF and potassium carbonate. Then the resulting mixture was refluxed. The reaction mixture was then cooled to room temperature, poured into water, and extracted with chloroform. The extracts were combined, washed with 5% w/v of sodium hydroxide or 5% w/v of hydrochloric acid to remove excess *p*-nitrobenzoyl chloride or 1,2,3,4-tetrahydroquinoline derivative. Then, the extract was washed with water and brine, dried over anhydrous sodium sulfate and concentrated. The resulting residue was purified by recrystallization from ethanol. The conditions for synthesis of 3a - 3h are listed in Table 12.

Table 12. Details of reagents used in the synthesis of N-(*p*-nitrobenzoyl)-1,2,3,4-tetrahydroquinoline derivatives (3a - 3h)

1,2,3,4-Tetrahydroquinoline Derivative	*p*-Nitrobenzoyl Chloride	K_2CO_3	THF	Refluxing Time	Product; N-(*p*-Nitrobenzoyl)-1,2,3,4-tetrahydroquinoline Derivative (yield)
1,2,3,4-tetrahydroquinoline 1.343 g (10 mmol)	2.229 g (12 mmol)	1.681 g (10 mmol)	20 ml	1 hr	3a (CU17-01) 2.512 g (88.2 %)
2b (1,2,3,4-tetrahydro-2-methylquinoline) 0.736 g (5 mmol)	1.300 g (7 mmol)	0.834 g (5 mmol)	10 ml	1 hr	3b (CU17-03) 1.170 g (79.0 %)
2c (1,2,3,4-tetrahydro-4-methylquinoline) 0.734 g (5 mmol)	1.303 g (7 mmol)	1.656 g (10 mmol)	10 ml	1 hr	3c (CU17-05) 1.225 g (82.9 %)
2d (1,2,3,4-tetrahydro-8-methylquinoline) 2.224 g (15 mmol)	1.866 g (10 mmol)	2.479 g (15 mmol)	40 ml	5 hr	3d (CU17-07) 2.296 g (77.0 %)
2e (1,2,3,4-tetrahydro-6-fluoro-2-methylquinoline) 0.336 g (2 mmol)	0.558 g (3 mmol)	0.338 g (2 mmol)	8 ml	1 hr	3e (CU17-09) 0.547 g (85.6 %)

Table 12. (continued) Details of reagents used in the synthesis of N-(*p*-nitrobenzoyl)-1,2,3,4-tetrahydroquinoline derivatives (3a - 3h)

1,2,3,4-Tetrahydroquinoline Derivative	*p*-Nitrobenzoyl Chloride	K_2CO_3	THF	Refluxing Time	Product; N-(*p*-Nitrobenzoyl)-1,2,3,4-tetrahydroquinoline Derivative (yield)
2f (1,2,3,4-tetrahydro-2,8-dimethylquinoline) 1.201 g (7 mmol)	0.931 g (5 mmol)	1.238 g (8 mmol)	20 ml	5 hr	3f (CU17-11) 1.187 g (76.2 %)
2g (1,2,3,4-tetrahydro-4,8-dimethylquinoline) 0.718 g (4 mmol)	0.560 g (3 mmol)	0.736 g (4 mmol)	10 ml	10 hr	3g (CU17-13) 0.778 g (83.1 %)
2h (1,2,3,4-tetrahydro-8-methoxyquinoline) 1.735 g (11 mmol)	1.300 g (7 mmol)	1.654 g (10 mmol)	20 ml	7 hr	3h (CU17-15) 1.733 g (79.2 %)

N-(*p*-Nitrobenzoyl)-1,2,3,4-tetrahydroquinoline (3a, CU-17-01)

Description	:	Yellowish solid
% Yield	:	88.2 %
m.p.	:	99-100 °C

Anal.calcd. for $C_{16}H_{14}N_2O_3$: C, 68.075; H, 4.998; N, 9.923

Found   : C, 68.062; H, 5.102; N, 9.933

IR	:	3113 - 3026 cm^{-1}	(ν C-H, aromatic)
(KBr)		2964 - 2843 cm^{-1}	(ν C-H, aliphatic)
		1649 cm^{-1}	(ν C=O, amide)
		1599 cm^{-1}	(ν C=C, aromatic)
		1520 cm^{-1}	(ν_{as} N-O)
		1489 - 1386 cm^{-1}	(δ C-H, aliphatic; ν C=C, aromatic)
		1344 cm^{-1}	(ν_s N-O)
		856 - 711 cm^{-1}	(δ C-H, out-of -plane, aromatic; ν C-N, Ar-NO$_2$)
		(Figure 41)	

^{1}H-NMR	:	2.09 ppm	(m, 2H, H-3)
(CDCl$_3$)		2.86 ppm	(dd, J = 6.6, 6.5 Hz, 2H, H-4)
		3.93 ppm	(t, J = 6.6 Hz, 2H, H-2)
		6.57 ppm	(d, J = 5.9 Hz, 1H, H-8)
		6.86 ppm	(t, J = 7.5 Hz, 1H, H-7)
		7.04 ppm	(dd, J = 7.2, 7.3 Hz, 1H, H-6)

	7.18 ppm	(d, J = 7.4 Hz, 1H, H-5)
	7.48 ppm	(d, J = 8.7 Hz, 2H, H-2$^/$)
	8.11 ppm	(d, J = 8.6 Hz, 2H, H-3$^/$)
	(Figure 42-43)	

^{13}C-NMR	:	24.00 ppm	(C-3)
(CDCl$_3$)		26.88 ppm	(C-4)
		44.33 ppm	(C-2)
		123.31 - 148.45 ppm	(aromatic C)
		167.72 ppm	(C=O)
		(Figure 44)	

EIMS	:	282 (58.65 %), 150 (100.00 %), 104 (72.93 %), 76
		(48.87%)
		(Figure 45)

N-(*p*-Nitrobenzoyl)-1,2,3,4-tetrahydro-2-methylquinoline (3b, CU-17-03)

Description	:	Yellowish solid
% Yield	:	79.0 %
m.p.	:	140-141 °C

Anal.calcd. for C$_{17}$H$_{16}$N$_2$O$_3$: C, 68.906; H, 5.442; N, 9.454

Found   : C, 68.925; H, 5.500; N, 9.505

IR	:	3102 - 3030 cm^{-1}	(ν C-H, aromatic)
(KBr)		2973 - 2850 cm^{-1}	(ν C-H, aliphatic)

		1645 cm^{-1}	(ν C=O, amide)
		1601 cm^{-1}	(ν C=C, aromatic)
		1524 cm^{-1}	(ν_{as} N-O)
		1490 - 1386 cm^{-1}	(δ C-H, aliphatic; ν C=C, aromatic)
		1342 cm^{-1}	(ν_s N-O)
		861 - 713 cm^{-1}	(δ C-H, out-of -plane, aromatic; ν C-N, Ar-NO$_2$)
		(Figure 46)	
^{1}H-NMR	:	1.27 ppm	(d, J = 6.5 Hz, 3H, 2-CH$_3$)
(CDCl$_3$)		1.52 ppm	(m, 1H, H-3)
		2.49 ppm	(m, 1H, H-3)
		2.77 ppm	(m, 2H, H-4)
		4.86 ppm	(m, 1H, H-2)
		6.48 ppm	(d, J = 6.2 Hz, 1H, H-8)
		6.86 ppm	(dd, J = 7.5, 7.6 Hz, 1H, H-7)
		7.06 ppm	(dd, J = 7.4, 7.5 Hz, 1H, H-6)
		7.20 ppm	(d, J = 7.4 Hz, 1H, H-5)
		7.40 ppm	(d, J = 8.6 Hz, 2H, H-2$^{/}$)
		8.07 ppm	(d, J = 8.6 Hz, 2H, H-3$^{/}$)
		(Figure 47-48)	
^{13}C-NMR	:	19.82 ppm	(2-CH$_3$)
(CDCl$_3$)		25.84 ppm	(C-4)
		32.28 ppm	(C-3)
		49.81 ppm	(C-2)

123.15 - 148.28 ppm (aromatic C)

167.30 ppm (C=O)

(Figure 49)

EIMS : 296 (76.47 %), 281 (34.51 %), 150 (100.00 %), 146

(31.37 %), 104 (98.43 %), 92 (52.55 %), 76 (86.27 %)

(Figure 50)

N-(*p*-Nitrobenzoyl)-1,2,3,4-tetrahydro-4-methylquinoline (3c, CU-17-05)

Description : Yellowish solid

% Yield : 82.9 %

m.p. : 132-134 °C

Anal.calcd. for $C_{17}H_{16}N_2O_3$: C, 68.906; H, 5.442; N, 9.454

Found : C, 69.047; H, 5.414; N, 9.446

IR : 3109 - 3070 cm^{-1} (ν C-H, aromatic)

(KBr) 2963 - 2855 cm^{-1} (ν C-H, aliphatic)

1646 cm^{-1} (ν C=O, amide)

1602 cm^{-1} (ν C=C, aromatic)

1523 cm^{-1} (ν_{as} N-O)

1490 - 1380 cm^{-1} (δ C-H, aliphatic; ν C=C,

aromatic)

1344 cm^{-1} (ν_s N-O)

863 - 712 cm^{-1} (δ C-H, out-of -plane, aromatic;

ν C-N, Ar-NO$_2$)

(Figure 51)

^{1}H-NMR	:	1.44 ppm	(d, J = 6.9 Hz, 3H, 4-CH$_3$)
(CDCl$_3$)		1.70 ppm	(m, 1H, H-3)
		2.25 ppm	(m, 1H, H-3)
		2.98 ppm	(m, 1H, H-4)
		3.87 ppm	(m, 1H, H-2)
		4.03 ppm	(m, 1H, H-2)
		6.54 ppm	(s, broad, 1H, H-8)
		6.86 ppm	(dd, J = 7.5, 7.6 Hz, 1H, H-7)
		7.09 ppm	(dd, J = 7.5, 7.7 Hz, 1H, H-6)
		7.27 ppm	(d, J = 7.5 Hz, 1H, H-5)
		7.48 ppm	(d, J = 8.6 Hz, 2H, H-2$^/$)
		8.11 ppm	(d, J = 8.6 Hz, 2H, H-3$^/$)

(Figure 52-53)

^{13}C-NMR	:	19.45 ppm	(4-CH$_3$)
(CDCl$_3$)		30.98 ppm	(C-4)
		32.07 ppm	(C-3)
		43.23 ppm	(C-2)
		123.32 – 148.36 ppm	(aromatic C)
		167.64 ppm	(C=O)

(Figure 54)

EIMS	:	296 (65.77 %), 281 (6.48 %), 150 (100.00 %), 104
		(72.07 %), 92 (38.51 %), 76 (41.44 %)

(Figure 55)

N-(*p*-Nitrobenzoyl)-1,2,3,4-tetrahydro-8-methylquinoline (3d, CU-17-07)

Description	:	Yellowish solid
% Yield	:	77.0 %
m.p.	:	113-114 °C

Anal.calcd. for $C_{17}H_{16}N_2O_3$: C, 68.906; H, 5.442; N, 9.454

Found : C, 68.979; H, 5.406; N, 9.496

IR	:	3109 - 3051 cm^{-1}	(ν C-H, aromatic)
(KBr)		2960 - 2860 cm^{-1}	(ν C-H, aliphatic)
		1640 cm^{-1}	(ν C=O, amide)
		1603 cm^{-1}	(ν C=C, aromatic)
		1525 cm^{-1}	(ν_{as} N-O)
		1470 - 1384 cm^{-1}	(δ C-H, aliphatic; ν C=C, aromatic)
		1348 cm^{-1}	(ν_s N-O)
		866 - 706 cm^{-1}	(δ C-H, out-of -plane, aromatic; ν C-N, Ar-NO$_2$)
		(Figure 56)	

^{1}H-NMR	:	Assignment for only major conformer:	
(CDCl$_3$)		1.72 ppm	(s, 3H, 8-CH$_3$)
		1.79 ppm	(m, 1H, H-3)
		2.42 ppm	(m, 1H, H-3)
		2.80 ppm	(m, 2H, H-4)
		3.22 ppm	(m, 1H, H-2)

	4.75 ppm	(m, 1H, H-2)
	6.83 ppm	(d, J = 6.8 Hz, 1H, H-7)
	7.02 - 7.18 ppm	(m, 2H, H-5 + H-6)
	7.37 ppm	(d, J = 8.6 Hz, 2H, H-2$^/$)
	8.00 ppm	(d, J = 8.5 Hz, 2H, H-3$^/$)
	(Figure 57-58)	

^{13}C-NMR : Assignment for only major conformer:

(CDCl$_3$)   18.51 - 48.25 ppm   (aliphatic C)

123.05 - 148.64 ppm (aromatic C)

167.42 ppm   (C=O)

(Figure59)

EIMS   :   296 (17.31 %), 281 (3.14 %), 150 (78.85 %), 146 (68.27
%), 104 (100.00 %), 92 (41.11 %), 76 (79.81 %)
(Figure 60)

N-(*p*-Nitrobenzoyl)-1,2,3,4-tetrahydro-6-fluoro-2-methylquinoline (3e, CU-17-09)

Description   :   Yellowish solid

% Yield   :   85.6 %

m.p.   :   139-140 °C

Anal.calcd. for C$_{17}$H$_{15}$N$_2$O$_3$F : C, 64.962; H, 4.810; N, 8.912

Found   : C, 64.994; H, 4.784; N, 8.929

IR   :   3110 - 3048 cm^{-1} (ν C-H, aromatic)

(KBr)   2969 - 2873 cm^{-1} (ν C-H, aliphatic)

	1638 cm^{-1}	(ν C=O, amide)
	1600 cm^{-1}	(ν C=C, aromatic)
	1520 cm^{-1}	(ν_{as} N-O)
	1493 - 1392 cm^{-1}	(δ C-H, aliphatic; ν C=C, aromatic)
	1344 cm^{-1}	(ν_s N-O)
	863 - 725 cm^{-1}	(δ C-H, out-of -plane, aromatic; ν C-N, Ar-NO$_2$)
	(Figure 61)	

^{1}H-NMR	:	1.25 ppm	(d, J = 6.4 Hz, 3H, 2-CH$_3$)
(CDCl$_3$)		1.52 ppm	(m, 1H, H-3)
		2.48 ppm	(m, 1H, H-3)
		2.76 ppm	(m, 2H, H-4)
		4.83 ppm	(broad, 1H, H-2)
		6.49 ppm	(s, broad, 1H, H-8)
		6.59 ppm	(dd, J = 6.6, 7.7 Hz, 1H, H-7)
		6.93 ppm	(dd, J = 8.4, 2.2 Hz, 1H, H-5)
		7.41 ppm	(d, J = 8.4 Hz, 2H, H-2$^/$)
		8.11 ppm	(d, J = 8.5 Hz, 2H, H-3$^/$)
		(Figure 62-63)	

^{13}C-NMR	:	19.65 ppm	(2-CH$_3$)
(CDCl$_3$)		25.95 ppm	(C-4)
		31.85 ppm	(C-3)
		49.74 ppm	(C-2)
		113.06 - 161.88 ppm	(aromatic C)

167.18 ppm   (C=O)

(Figure 64)

EIMS   :   314 (14.57 %), 299 (3.06 %), 150 (100.00 %), 104

(98.26 %), 92 (41.52 %), 76 (75.65 %)

(Figure 65)

N-(*p*-Nitrobenzoyl)-1,2,3,4-tetrahydro-2,8-dimethylquinoline (3f, CU-17-11)

Description   :   Yellowish solid

% Yield   :   76.2 %

m.p.   :   134-135 °C

Anal.calcd. for $C_{18}H_{18}N_2O_3$: C, 69.662; H, 5.846; N, 9.026

Found   : C, 69.723; H, 5.831; N, 9.037

IR   :   3108 - 3048 cm^{-1} (ν C-H, aromatic)

(KBr)   2983 - 2872 cm^{-1} (ν C-H, aliphatic)

1636 cm^{-1} (ν C=O, amide)

1600 cm^{-1} (ν C=C, aromatic)

1525 cm^{-1} (ν_{as} N-O)

1472 - 1391 cm^{-1} (δ C-H, aliphatic; ν C=C,

aromatic)

1341 cm^{-1} (ν_s N-O)

871 - 708 cm^{-1} (δ C-H, out-of -plane, aromatic;

ν C-N, Ar-NO$_2$)

(Figure 66)

^{1}H-NMR	:	Assignment for only major conformer:	
(CDCl$_3$)		1.21 ppm	(d, J = 6.5 Hz, 3H, 2-CH$_3$)
		1.23 ppm	(m, 1H, H-3)
		1.74 ppm	(s, 3H, 8-CH$_3$)
		2.64 ppm	(m, 3H, H-3 + H-4)
		5.00 ppm	(m, 1H, H-2)
		6.82 ppm	(1H, H-7)
		7.04 - 7.19 ppm	(m, 2H, H-5 + H-6)
		7.34 ppm	(d, J = 8.7 Hz, 2H, H-2$^/$)
		7.98 ppm	(d, J = 8.7 Hz, 2H, H-3$^/$)
		(Figure 67-68)	

^{13}C-NMR	:	Assignment for only major conformer:	
(CDCl$_3$)		17.61 ppm	(8-CH$_3$)
		20.93 ppm	(2-CH$_3$)
		27.52 ppm	(C-4)
		33.79 ppm	(C-3)
		50.32 ppm	(C-2)
		122.55 - 148.34 ppm	(aromatic C)
		166.76 ppm	(C=O)
		(Figure 69)	

EIMS	:	310 (45.95 %), 295 (24.77 %), 160 (65.77 %), 150
		(100.00 %), 104 (59.46 %), 92 (18.69 %), 76 (30.18 %)
		(Figure 70)

N-(*p*-Nitrobenzoyl)-1,2,3,4-tetrahydro-4,8-dimethylquinoline (3g, CU-17-13)

Description	:	Yellowish solid
% Yield	:	83.1 %
m.p.	:	141-142 °C

Anal.calcd. for $C_{18}H_{18}N_2O_3$: C, 69.662; H, 5.846; N, 9.026

Found   : C, 69.702; H, 5.576; N, 9.010

IR	:	3107 - 3045 cm^{-1}	(ν C-H, aromatic)
(KBr)		2960 - 2859 cm^{-1}	(ν C-H, aliphatic)
		1649 cm^{-1}	(ν C=O, amide)
		1601 cm^{-1}	(ν C=C, aromatic)
		1517 cm^{-1}	(ν_{as} N-O)
		1478 - 1385 cm^{-1}	(δ C-H, aliphatic; ν C=C, aromatic)
		1344 cm^{-1}	(ν_s N-O)
		861 - 712 cm^{-1}	(δ C-H, out-of -plane, aromatic; ν C-N, Ar-NO$_2$)
		(Figure 71)	

^{1}H-NMR	:	Assignment for only major conformer:	
(CDCl$_3$)		1.45 ppm	(d, J = 6.8 Hz, 3H, 4-CH$_3$)
		1.75 ppm	(s, 3H, 8-CH$_3$)
		2.07 ppm	(m, 1H, H-3)
		2.39 ppm	(m, 1H, H-3)
		2.84 ppm	(m, 1H, H-4)

3.24 ppm		(m, 1H, H-2)
4.74 ppm		(m, 1H, H-2)
6.85 ppm		(d, J = 6.8 Hz, 1H, H-7)
7.10 - 7.23 ppm		(m, 2H, H-5 + H-6)
7.35 ppm		(d, J = 8.7 Hz, 2H, H-2$^{/}$)
7.99 ppm		(d, J = 8.5 Hz, 2H, H-3$^{/}$)
(Figure 72-73)		

^{13}C-NMR	:	Assignment for only major conformer:
(CDCl$_3$)		17.02 - 42.43 ppm (aliphatic C)
		121.75 – 148.40 ppm (aromatic C)
		167.15 ppm (C=O)
		(Figure 74)

EIMS	:	310 (56.30 %), 295 (13.45 %), 160 (100.00 %), 150 (78.99 %), 104 (56.30 %), 92 (16.81 %), 76 (30.25 %) (Figure 75)

N-(*p*-Nitrobenzoyl)-1,2,3,4-tetrahydro-8-methoxyquinoline (3h, CU-17-15)

Description	:	Yellowish solid
% Yield	:	79.2 %
m.p.	:	156-157 °C

Anal.calcd. for C$_{17}$H$_{16}$N$_2$O$_4$: C, 65.376; H, 5.163; N, 8.969

Found   : C, 65.460; H, 5.128; N, 8.979

IR	:	3106 - 3031 cm^{-1}	(ν C-H, aromatic)
(KBr)		2971 - 2841 cm^{-1}	(ν C-H, aliphatic)
		1644 cm^{-1}	(ν C=O, amide)
		1605 cm^{-1}	(ν C=C, aromatic)
		1523 cm^{-1}	(ν_{as} N-O)
		1483 - 1385 cm^{-1}	(δ C-H, aliphatic; ν C=C, aromatic)
		1347 cm^{-1}	(ν_s N-O)
		864 - 708 cm^{-1}	(δ C-H, out-of -plane, aromatic; ν C-N, Ar-NO$_2$)
		(Figure 76)	

^{1}H-NMR	:	1.80 ppm	(m, 1H, H-3)
(CDCl$_3$)		2.36 ppm	(m, 1H, H-3)
		2.79 ppm	(m, 2H, H-4)
		3.24 ppm	(s, 3H, 8-OCH$_3$)
		3.36 ppm	(m, 1H, H-2)
		4.47 ppm	(m, 1H, H-2)
		6.46 ppm	(d, J = 8.2 Hz, 1H, H-7)
		6.85 ppm	(d, J = 7.5 Hz, 1H, H-5)
		7.06 ppm	(dd, J = 8.0, 7.9 Hz, 1H, H-6)
		7.44 ppm	(d, J = 8.6 Hz, 2H, H-2$^/$)
		8.03 ppm	(d, J = 8.7 Hz, 2H, H-3$^/$)
		(Figure 77-78)	

^{13}C-NMR	:	24.55 ppm	(C-3)
(CDCl$_3$)		26.85 ppm	(C-4)

43.19 ppm	(C-2)
54.40 ppm	(8-OCH$_3$)
109.77 - 151.20 ppm	(aromatic C)
168.42 ppm	(C=O)
(Figure 79)	

General Procedures for the Synthesis of N-(*p*-Aminobenzoyl)-1,2,3,4-tetrahydroquinoline Derivatives.

A solution of N-(*p*-nitrobenzoyl)-1,2,3,4-tetrahydroquinoline derivative in dichloromethane was added to a Parr hydrogenation bottle along with 10 % palladium on activated charcoal and subjected to low-pressure hydrogenation for 3 hr. The bottle was then removed, and the contents were filtered. The filtrate was concentrated, and the resulting residue was purified by recrystallization from chloroform-hexane mixture to give the corresponding N-(*p*-aminobenzoyl)-1,2,3,4-tetrahydroquinoline derivative. The conditions for synthesis of 4a - 4h are listed in Table 13.

Table 13. Details of reagents used in the synthesis of N-(*p*-aminobenzoyl)-1,2,3,4-tetrahydroquinoline derivatives (4a - 4h)

N-(*p*-Nitrobenzoyl)-1,2,3,4-tetrahydroquinoline Derivative (D)	10 % Pd/C (E)	CH_2Cl_2	Ratio of D (mmol) : E (g)	Product; N-(*p*-Aminobenzoyl)-1,2,3,4-tetrahydroquinoline Derivative (yield)
3a (CU1701; N-(*p*-nitrobenzoyl)-1,2,3,4-tetrahydroquinoline) 1.412 g (5 mmol)	0.062 g	20 ml	1 : 0.012	4a (CU1702) 1.103 g (87.4 %)
3b (CU1703; N-(*p*-nitrobenzoyl)-1,2,3,4-tetrahydro-2-methylquinoline) 0.745 g (2.5 mmol)	0.060 g	10 ml	1 : 0.024	4b (CU1704) 0.493 g (73.6 %)
3c (CU1705; N-(*p*-nitrobenzoyl)-1,2,3,4-tetrahydro-4-methylquinoline) 0.731 g (2.5 mmol)	0.030 g	10 ml	1 : 0.012	4c (CU1706) 0.460 g (70.0 %)
3d (CU1707; N-(*p*-nitrobenzoyl)-1,2,3,4-tetrahydro-8-methylquinoline) 0.885 g (3 mmol)	0.182 g	20 ml	1 : 0.061	4d (CU1708) 0.572 g (71.9 %)
3e (CU1709; N-(*p*-nitrobenzoyl)-1,2,3,4-tetrahydro-6-fluoro-2-methylquinoline) 0.628 g (2 mmol)	0.048 g	8 ml	1 : 0.024	4e (CU1710) 0.401 g (70.6 %)

Table 13. (continued) Details of reagents used in the synthesis of N-(*p*-aminobenzoyl)-1,2,3,4-tetrahydroquinoline derivatives (4a - 4h)

N-(*p*-Nitrobenzoyl)-1,2,3,4-tetrahydroquinoline Derivative (D)	10 % Pd/C (E)	CH_2Cl_2	Ratio of D (mmol) : E (g)	Product; N-(*p*-Aminobenzoyl)-1,2,3,4-tetrahydroquinoline Derivative (yield)
3f (CU1711; N-(*p*-nitrobenzoyl)-1,2,3,4-tetrahydro-2,8-dimethylquinoline) 0.838 g (2.7 mmol)	0.154 g	20 ml	1 : 0.057	4f (CU1712) 0.513 g (67.8 %)
3g (CU1713; N-(*p*-nitrobenzoyl)-1,2,3,4-tetrahydro-4,8-dimethylquinoline) 0.759 g (2.4 mmol)	0.148 g	10 ml	1 : 0.062	4g (CU1714) 0.500 g (72.9 %)
3h (CU1715; N-(*p*-nitrobenzoyl)-1,2,3,4-tetrahydro-8-methoxyquinoline) 0.785 g (2.5 mmol)	0.152 g	20 ml	1 : 0.061	4h (CU1716) 0.561 g (79.0 %)

N-(*p*-Aminobenzoyl)-1,2,3,4-tetrahydroquinoline (4a, CU-17-02)

Description	:	White solid
% Yield	:	87.4 %
m.p.	:	211-212 °C.

Anal.calcd. for $C_{16}H_{16}N_2O$: C, 76.165; H, 6.391; N, 11.103

Found   : C, 76.150; H, 6.312; N, 11.040

IR	:	3462 cm^{-1}	(ν_{as} N-H, Ar-NH$_2$)
(KBr)		3337 cm^{-1}	(ν_s N-H, Ar-NH$_2$)
		3221 cm^{-1}	(overtone of δ-NH$_2$)
		3055 - 3026 cm^{-1}	(ν C-H, aromatic)
		2946 - 2886 cm^{-1}	(ν C-H, aliphatic)
		1637 - 1594 cm^{-1}	(ν C=O, amide; δ-NH$_2$; ν C=C, aromatic)
		841 - 760 cm^{-1}	(δ C-H, out-of -plane, aromatic)
		(Figure 80)	

^{1}H-NMR	:	2.03 ppm	(m, 2H, H-3)
(CDCl$_3$)		2.82 ppm	(t, J = 6.6 Hz, 2H, H-4)
		3.88 ppm	(4H, H-2 + 4$'$-NH$_2$)
		6.50 ppm	(d, J = 8.4 Hz, 2H, H-3$'$)
		6.74 ppm	(d, J = 8.0 Hz, 1H, H-8)
		6.88 ppm	(dd, J = 7.3, 7.8 Hz, 1H, H-7)
		6.97 ppm	(dd, J = 7.3, 7.2 Hz, 1H, H-6)
		7.13 ppm	(d, J = 7.4 Hz, 1H, H-5)

		7.20 ppm	(d, J = 8.4 Hz, 2H, H-2$'$)
		(Figure 81-82)	

^{13}C-NMR	:	24.25 ppm	(C-3)
(CDCl$_3$)		26.99 ppm	(C-4)
		44.44 ppm	(C-2)
		113.81 ppm	(C-3$'$)
		124.01 ppm	(C-6)
		125.35, 125.69 ppm	(C-7 + C-8)
		125.61 ppm	(C-1$'$)
		128.22 ppm	(C-5)
		130.86 ppm	(C-2$'$)
		131.29 ppm	(C-10)
		140.23 ppm	(C-9)
		148.54 ppm	(C-4$'$)
		170.36 ppm	(C=O)
		(Figure 83)	

Other NMR	:	DEPT135	See Figure 84
Analyses		HH COSY	See Figure 85-86
		HMQC	See Figure 87-88
		HMBC	See Figure 89-91

EIMS	:	252 (66.27 %), 120 (100.00 %), 92 (76.47 %), 65 (70.98%)
		(Figure 92)

N-(*p*-Aminobenzoyl)-1,2,3,4-tetrahydro-2-methylquinoline (4b, CU-17-04)

Description	:	White solid
% Yield	:	73.6 %
m.p.	:	214-216 °C.

Anal.calcd. for $C_{17}H_{18}N_2O$: C, 76.663; H, 6.812; N, 10.518

Found   : C, 76.560; H, 6.806; N, 10.445

IR	:	3465 cm^{-1}	(ν_{as} N-H, Ar-NH$_2$)
(KBr)		3355 cm^{-1}	(ν_s N-H, Ar-NH$_2$)
		3210 cm^{-1}	(overtone of δ-NH$_2$)
		3041 - 3015 cm^{-1}	(ν C-H, aromatic)
		2982 - 2841 cm^{-1}	(ν C-H, aliphatic)
		1625 - 1595 cm^{-1}	(ν C=O, amide; δ-NH$_2$; ν C=C, aromatic)
		827 - 758 cm^{-1}	(δ C-H, out-of -plane, aromatic)
		(Figure 93)	

^{1}H-NMR	:	1.22 ppm	(d, J = 6.5 Hz, 3H, 2-CH$_3$)
(CDCl$_3$)		1.52 ppm	(m, 1H, H-3)
		2.41 ppm	(m, 1H, H-3)
		2.74 ppm	(dd, J = 6.8, 6.4 Hz, 2H, H-4)
		3.82 ppm	(s, broad, 2H, 4$^/$-NH$_2$)
		4.81 ppm	(m, 1H, H-2)
		6.46 ppm	(d, J = 8.5 Hz, 2H, H-3$^/$)
		6.63 ppm	(d, J = 7.9 Hz, 1H, H-8)

		6.88 ppm	(dd, J = 7.2, 7.6 Hz, 1H, H-7)
		6.99 ppm	(dd, J = 7.4, 7.3 Hz, 1H, H-6)
		7.11 ppm	(d, J = 8.6 Hz, 2H, H-2$'$)
		7.14 ppm	(1H, H-5)
		(Figure 94-95)	

^{13}C-NMR	:	19.71 ppm	(2-CH$_3$)
(CDCl$_3$)		25.49 ppm	(C-4)
		32.11 ppm	(C-3)
		49.16 ppm	(C-2)
		113.72 ppm	(C-3$'$)
		124.37 ppm	(C-6)
		125.84 ppm	(C-7)
		125.89 ppm	(C-1$'$)
		126.74 ppm	(C-8)
		127.47 ppm	(C-5)
		130.77 ppm	(C-2$'$)
		132.78 ppm	(C-10)
		138.70 ppm	(C-9)
		148.22 ppm	(C-4$'$)
		169.83 ppm	(C=O)
		(Figure 96)	

Other NMR	:	DEPT135	See Figure 97
Analyses		HH COSY	See Figure 98-99
		HMQC	See Figure 100-101
		HMBC	See Figure 102-104

EIMS   :   266 (81.18 %), 120 (100.00 %), 92 (97.65 %), 65 (86.27
                   %)

                   (Figure 105)

N-(*p*-Aminobenzoyl)-1,2,3,4-tetrahydro-4-methylquinoline (4c, CU-17-06)

Description   :   White solid

% Yield   :   70.0 %

 m.p.   :   192-193 °C.

Anal.calcd. for $C_{17}H_{18}N_2O$: C, 76.663; H, 6.812; N, 10.518

Found   : C, 76.299; H, 6.913; N, 10.488

IR   : 3437 cm^{-1} (ν_{as} N-H, Ar-NH$_2$)

(KBr) 3332 cm^{-1} (ν_s N-H, Ar-NH$_2$)

                 3224 cm^{-1} (overtone of δ-NH$_2$)

                 $3056 - 3034 \text{ cm}^{-1}$ (ν C-H, aromatic)

                 $2951 - 2872 \text{ cm}^{-1}$ (ν C-H, aliphatic)

                 $1623 - 1599 \text{ cm}^{-1}$ (ν C=O, amide; δ-NH$_2$; ν C=C,

                                                    aromatic)

                 $839 - 757 \text{ cm}^{-1}$ (δ C-H, out-of -plane, aromatic)

                 (Figure 106)

^{1}H-NMR   :   1.40 ppm   (d, J = 6.9 Hz, 3H, 4-CH$_3$)

(CDCl$_3$)   1.64 ppm   (m, 1H, H-3)

                 2.18 ppm   (m, 1H, H-3)

                 2.94 ppm   (m, 1H, H-4)

	3.92 ppm	(m, 4H, H-2 + 4$^{/}$-NH$_2$)
	6.48 ppm	(d, J = 8.4 Hz, 2H, H-3$^{/}$)
	6.71 ppm	(d, J = 7.9 Hz, 1H, H-8)
	6.89 ppm	(dd, J = 7.4, 7.5 Hz, 1H, H-7)
	7.02 ppm	(dd, J = 7.3, 7.2 Hz, 1H, H-6)
	7.18 ppm	(d, J = 8.6 Hz, 2H, H-2$^{/}$)
	7.21 ppm	(1H, H-5)
	(Figure 107-108)	

^{13}C-NMR	:	19.80 ppm	(4-CH$_3$)
(CDCl$_3$)		31.01 ppm	(C-4)
		32.46 ppm	(C-3)
		43.26 ppm	(C-2)
		113.78 ppm	(C-3$^{/}$)
		124.14 ppm	(C-6)
		125.45, 125.72 ppm	(C-7 + C-8)
		125.60 ppm	(C-1$^{/}$)
		126.08 ppm	(C-5)
		130.97 ppm	(C-2$^{/}$)
		136.12 ppm	(C-10)
		139.59 ppm	(C-9)
		148.46 ppm	(C-4$^{/}$)
		170.27 ppm	(C=O)
		(Figure 109)	

Other NMR	:	DEPT135	See Figure 110
Analyses		HH COSY	See Figure 111-112

HMQC	See Figure 113-114
HMBC	See Figure 115-117

EIMS   :   266 (32.14 %), 120 (100.00 %), 92 (31.75 %), 65 (21.92 %)

(Figure 118)

N-(*p*-Aminobenzoyl)-1,2,3,4-tetrahydro-8-methylquinoline (4d, CU-17-08)

Description	:	White solid
% Yield	:	71.9 %
m.p.	:	172-173 °C.

Anal.calcd. for $C_{17}H_{18}N_2O$: C, 76.663; H, 6.812; N, 10.518

Found   : C, 76.640; H, 6.796; N, 10.541

IR	:	3465 cm^{-1}	(ν_{as} N-H, Ar-NH$_2$)
(KBr)		3341 cm^{-1}	(ν_s N-H, Ar-NH$_2$)
		3221 cm^{-1}	(overtone of δ-NH$_2$)
		3060 - 3020 cm^{-1}	(ν C-H, aromatic)
		2948 - 2879 cm^{-1}	(ν C-H, aliphatic)
		1633 - 1596 cm^{-1}	(ν C=O, amide; δ-NH$_2$; ν C=C, aromatic)
		838 - 757 cm^{-1}	(δ C-H, out-of -plane, aromatic)

(Figure 119)

^{1}H-NMR	:	
room temperature	:	broad signals
(CDCl$_3$)		(Figure 120)
various temperature	:	room temperature, 15 °C, 0 °C, -15 °C, -30 °C
(CDCl$_3$)		(Figure 121-122)
-30 °C	:	Assignment for only major conformer:

(CDCl$_3$)	1.71 ppm	(m, 1H, H-3)
	1.74 ppm	(s, 3H, 8-CH$_3$)
	2.38 ppm	(m, 1H, H-3)
	2.78 ppm	(m, 2H, H-4)
	3.24 ppm	(m, 1H, H-2)
	3.93 ppm	(s, broad, 2H, 4$^/$-NH$_2$)
	4.62 ppm	(m, 1H, H-2)
	6.40 ppm	(d, J = 8.8 Hz, 2H, H-3$^/$)
	6.86 ppm	(d, J = 7.3 Hz, 1H, H-7)
	7.05 - 7.15 ppm	(m, 4H, H-5 + H-6 + H-2$^/$)
	(Figure 123-124)	

EIMS	:	266 (28.00 %), 120 (100.00 %), 92 (38.80 %), 65 (27.20 %)
		(Figure 125)

N-(*p*-Aminobenzoyl)-1,2,3,4-tetrahydro-6-fluoro-2-methylquinoline (4e, CU-17-10)

Description	:	White solid
% Yield	:	70.6 %

m.p.	:	210-211 °C.	

Anal.calcd. for $C_{17}H_{17}N_2OF$: C, 71.813; H, 6.026; N, 9.852

Found   : C, 71.833; H, 6.027; N, 9.847

IR	:	3469 cm^{-1}	(ν_{as} N-H, Ar-NH$_2$)
(KBr)		3331 cm^{-1}	(ν_s N-H, Ar-NH$_2$)
		3225 cm^{-1}	(overtone of δ-NH$_2$)
		3047 - 3011 cm^{-1}	(ν C-H, aromatic)
		2927 - 2872 cm^{-1}	(ν C-H, aliphatic)
		1614 - 1589 cm^{-1}	(ν C=O, amide; δ-NH$_2$; ν C=C, aromatic)
		842 - 760 cm^{-1}	(δ C-H, out-of -plane, aromatic)
		(Figure 126)	

^{1}H-NMR	:	1.21 ppm	(d, J = 6.5 Hz, 3H, 2-CH$_3$)
(CDCl$_3$)		1.51 ppm	(m, 1H, H-3)
		2.39 ppm	(m, 1H, H-3)
		2.72 ppm	(dd, J = 6.7, 6.5 Hz, 2H, H-4)
		3.87 ppm	(s, broad, 2H, 4$^/$-NH$_2$)
		4.80 ppm	(m, 1H, H-2)
		6.47 ppm	(d, J = 8.4 Hz, 2H, H-3$^/$)
		6.58 - 6.65 ppm	(m, 2H, H-7 + H-8)
		6.87 ppm	(d, J = 8.5 Hz, 1H, H-5)
		7.10 ppm	(d, J = 8.4 Hz, 2H, H-2$^/$)
		(Figure 127-128)	

^{13}C-NMR	:	19.55 ppm	(2-CH$_3$)
(CDCl$_3$)	:	25.62 ppm	(C-4)
		31.76 ppm	(C-3)
		49.10 ppm	(C-2)
		112.66, 112.96 ppm	(d, J = 22.6 Hz, C-7)
		113.76 ppm	(C-3$^/$)
		113.87, 114.16 ppm	(d, J = 22.4 Hz, C-5)
		125.52 ppm	(C-1$^/$)
		127.91, 128.02 ppm	(d, J = 8.4 Hz, C-8)
		130.65 ppm	(C-2$^/$)
		134.60 ppm	(C-9 + C-10)
		148.34 ppm	(C-4$^/$)
		157.93, 161.16 ppm	(d, J = 244.1 Hz, C-6)
		169.73	(C=O)
		(Figure 129-130)	

Other NMR	:	DEPT135	See Figure 131
Analyses		HH COSY	See Figure 132-133
		HMQC	See Figure 134-135
		HMBC	See Figure 136-138

EIMS	:	284 (26.48 %), 120 (100.00 %), 92 (41.90 %), 65 (31.62 %)
		(Figure 139)

N-(*p*-Aminobenzoyl)-1,2,3,4-tetrahydro-2,8-dimethylquinoline (4f, CU-17-12)

Description	:	White solid
% Yield	:	67.8 %
m.p.	:	184-185 °C.

Anal.calcd. for $C_{18}H_{20}N_2O$: C, 77.112; H, 7.190; N, 9.992

Found   : C, 77.119; H, 7.019; N, 9.967

IR	:	3467 cm^{-1}	(ν_{as} N-H, Ar-NH$_2$)
(KBr)		3340 cm^{-1}	(ν_s N-H, Ar-NH$_2$)
		3227 cm^{-1}	(overtone of δ-NH$_2$)
		3078 - 3036 cm^{-1}	(ν C-H, aromatic)
		2965 - 2862 cm^{-1}	(ν C-H, aliphatic)
		1605 - 1593 cm^{-1}	(ν C=O, amide; δ-NH$_2$; ν C=C, aromatic)
		840 - 759 cm^{-1}	(δ C-H, out-of -plane, aromatic)
		(Figure 140)	

^{1}H-NMR	:	1.17 ppm	(d, J = 6.4 Hz, 3H, 2-CH$_3$)
(CDCl$_3$)		1.22 ppm	(m, 1H, H-3)
		1.74 ppm	(s, 3H, 8-CH$_3$)
		2.48 - 2.65 ppm	(m, 3H, H-3 + H-4)
		3.81 ppm	(s, broad, 2H, 4$^/$-NH$_2$)
		4.92 ppm	(m, 1H, H-2)
		6.34 ppm	(d, J = 8.4 Hz, 2H, H-3$^/$)
		6.84 ppm	(d, J = 6.5 Hz, 1H, H-7)

		6.95 - 7.10 ppm	(m, 4H, H-5 + H-6 + H-2$'$)
		(Figure 141-142)	

^{13}C-NMR	:	17.74 ppm	(8-CH$_3$)
(CDCl$_3$)		21.25 ppm	(2-CH$_3$)
		27.48 ppm	(C-4)
		34.31 ppm	(C-3)
		49.76 ppm	(C-2)
		113.27 ppm	(C-3$'$)
		124.17 ppm	(C-5)
		125.75 ppm	(C-6)
		126.05 ppm	(C-1$'$)
		129.01 ppm	(C-7)
		130.34 ppm	(C-2$'$)
		133.68 ppm	(C-8)
		137.36 ppm	(C-10)
		138.16 ppm	(C-9)
		148.25 ppm	(C-4$'$)
		169.01 ppm	(C=O)
		(Figure 143)	

Other NMR	:	DEPT135	See Figure 144
Analyses		HH COSY	See Figure 145-146
		HMQC	See Figure 147-148
		HMBC	See Figure 149-151

EIMS   :   280 (25.20 %), 120 (100.00 %), 92 (35.08 %), 65 (24.50

                        %)

                        (Figure 152)

N-(*p*-Aminobenzoyl)-1,2,3,4-tetrahydro-4,8-dimethylquinoline (4g, CU-17-14)

Description   :   White solid

% Yield   :   72.9 %

 m.p.   :   170-171 °C.

Anal.calcd. for $C_{18}H_{20}N_2O$: C, 77.112; H, 7.190; N, 9.992

Found   : C, 77.185; H, 7.221; N, 9.999

IR   :   3459 cm^{-1} (ν_{as} N-H, Ar-NH$_2$)

(KBr)   3335 cm^{-1} (ν_s N-H, Ar-NH$_2$)

                    3220 cm^{-1} (overtone of δ-NH$_2$)

                    3063 - 3037 cm^{-1} (ν C-H, aromatic)

                    2959 - 2873 cm^{-1} (ν C-H, aliphatic)

                    1634 - 1596 cm^{-1} (ν C=O, amide; δ-NH$_2$; ν C=C,

                                                aromatic)

                    836 - 756 cm^{-1} (δ C-H, out-of -plane, aromatic)

                    (Figure 153)

^{1}H-NMR   :

room temperature   :   broad signals

(CDCl$_3$)   (Figure 154)

various temperature :   room temperature, 15 °C, 0 °C, -15 °C, -30 °C

(CDCl$_3$) (Figure 155-156)

-30 °C : Assignment for only major conformer:

(CDCl$_3$) 1.38 ppm (m, 1H, H-3)

1.45 ppm (d, J = 6.7 Hz, 3H, 4-CH$_3$)

1.74 ppm (s, 3H, 8-CH$_3$)

2.35 ppm (m, 1H, H-3)

2.82 ppm (m, 1H, H-4)

3.24 ppm (m, 1H, H-2)

3.93 ppm (s, broad, 2H, 4$^/$-NH$_2$)

4.62 ppm (m, 1H, H-2)

6.40 ppm (d, J = 8.5 Hz, 2H, H-3$^/$)

6.89 ppm (d, J = 7.0 Hz, 1H, H-7)

7.05 ppm (d, J = 8.5 Hz, 2H, H-2$^/$)

7.10 - 7.20 ppm (m, 2H, H-6 + H-5)

(Figure 157-158)

EIMS : 280 (71.37 %), 120 (100.00 %), 92 (79.61 %), 65 (72.55 %)

(Figure 159)

N-(*p*-Aminobenzoyl)-1,2,3,4-tetrahydro-8-methoxyquinoline (4h, CU-17-16)

Description : White solid

% Yield : 79.0 %

m.p. : 199-200 °C.

Anal.calcd. for C$_{17}$H$_{18}$N$_2$O$_2$: C, 72.319; H, 6.426; N, 9.922

Found   : C, 72.313; H, 6.528; N, 9.921

IR	:	3466 cm^{-1}	(ν_{as} N-H, Ar-NH$_2$)
(KBr)		3354 cm^{-1}	(ν_s N-H, Ar-NH$_2$)
		3225 cm^{-1}	(overtone of δ-NH$_2$)
		3084 - 3012 cm^{-1}	(ν C-H, aromatic)
		2962 - 2832 cm^{-1}	(ν C-H, aliphatic)
		1625 - 1597 cm^{-1}	(ν C=O, amide; δ-NH$_2$; ν C=C, aromatic)
		836 - 707 cm^{-1}	(δ C-H, out-of -plane, aromatic)
		(Figure 160)	

^{1}H-NMR	:	1.75 ppm	(s, broad, 1H, H-3)
(CDCl$_3$)		2.27 ppm	(s, broad, 1H, H-3)
		2.74 ppm	(broad, 2H, H-4)
		3.29 ppm	(s, 3H, 8-OCH$_3$)
		3.39 ppm	(s, broad, 1H, H-2)
		3.76 ppm	(s, broad, 2H, 4$^/$-NH$_2$)
		4.30 ppm	(s, broad, 1H, H-2)
		6.43 ppm	(d, J = 8.5 Hz, 2H, H-3$^/$)
		6.52 ppm	(d, J = 8.1 Hz, 1H, H-7)
		6.80 ppm	(d, J = 7.4 Hz, 1H, H-5)
		7.01 ppm	(t, J = 7.9 Hz, 1H, H-6)
		7.16 ppm	(d, J = 8.5 Hz, 2H, H-2$^/$)
		(Figure 161-162)	

^{13}C-NMR	:	25.01 ppm	(C-3)
(CDCl$_3$)		26.89 ppm	(C-4)
		43.50 ppm	(C-2)
		54.89 ppm	(8-OCH$_3$)
		109.98 ppm	(C-7)
		113.30 ppm	(C-3$^/$)
		119.75 ppm	(C-5)
		125.69 ppm	(C-6)
		127.06 ppm	(C-1$^/$)
		129.46 ppm	(C-2$^/$)
		130.01 ppm	(C-9)
		135.36 ppm	(C-10)
		148.03 ppm	(C-4$^/$)
		151.96 ppm	(C-8)
		170.87 ppm	(C=O)
		(Figure 163)	
Other NMR	:	DEPT135	See Figure 164
Analyses		HH COSY	See Figure 165-166
		HMQC	See Figure 167-168
		HMBC	See Figure 169-170
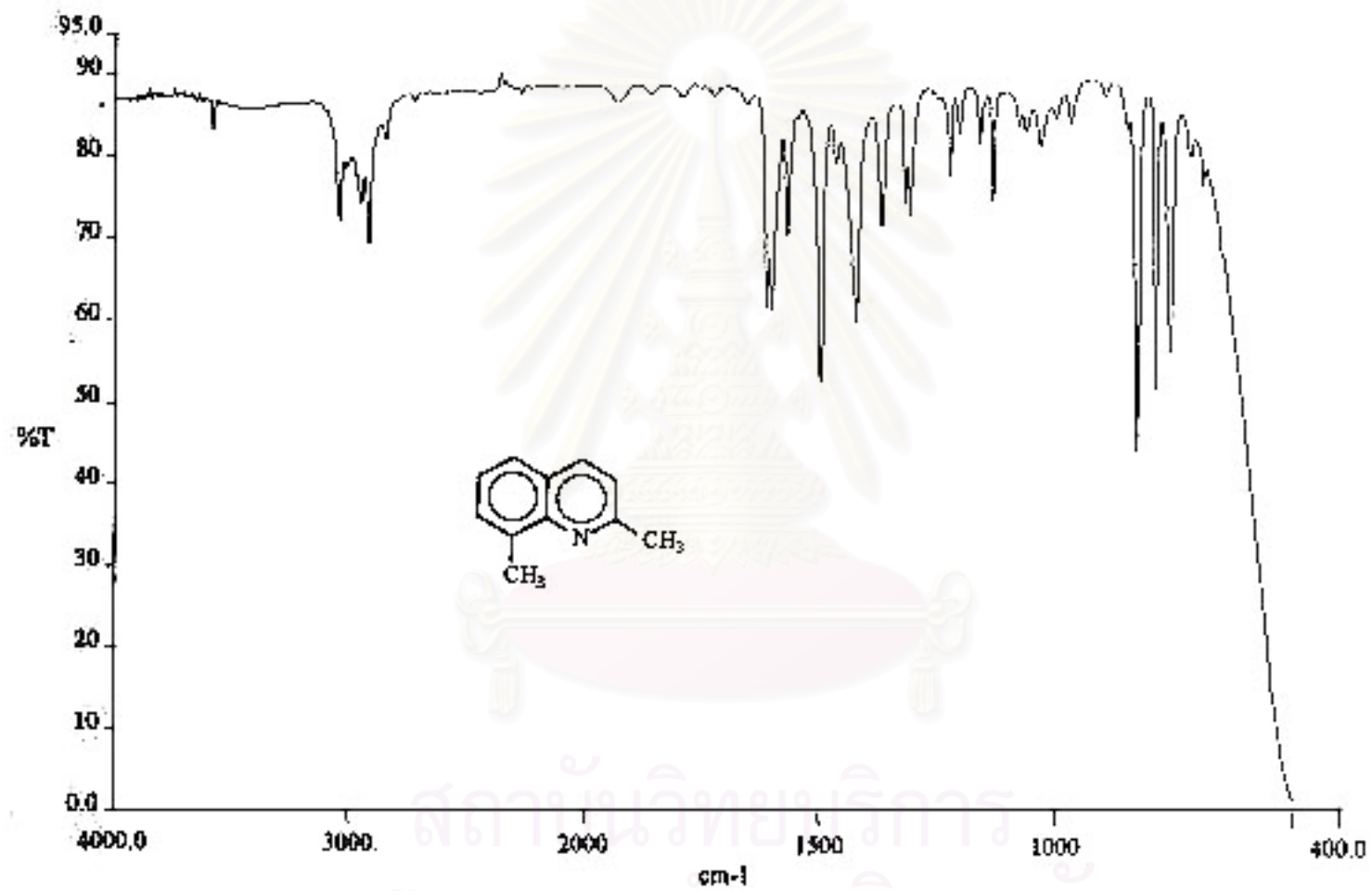
Figure 11. The IR spectrum (Neat, NaCl cell) of 2,8-dimethylquinoline (1f).
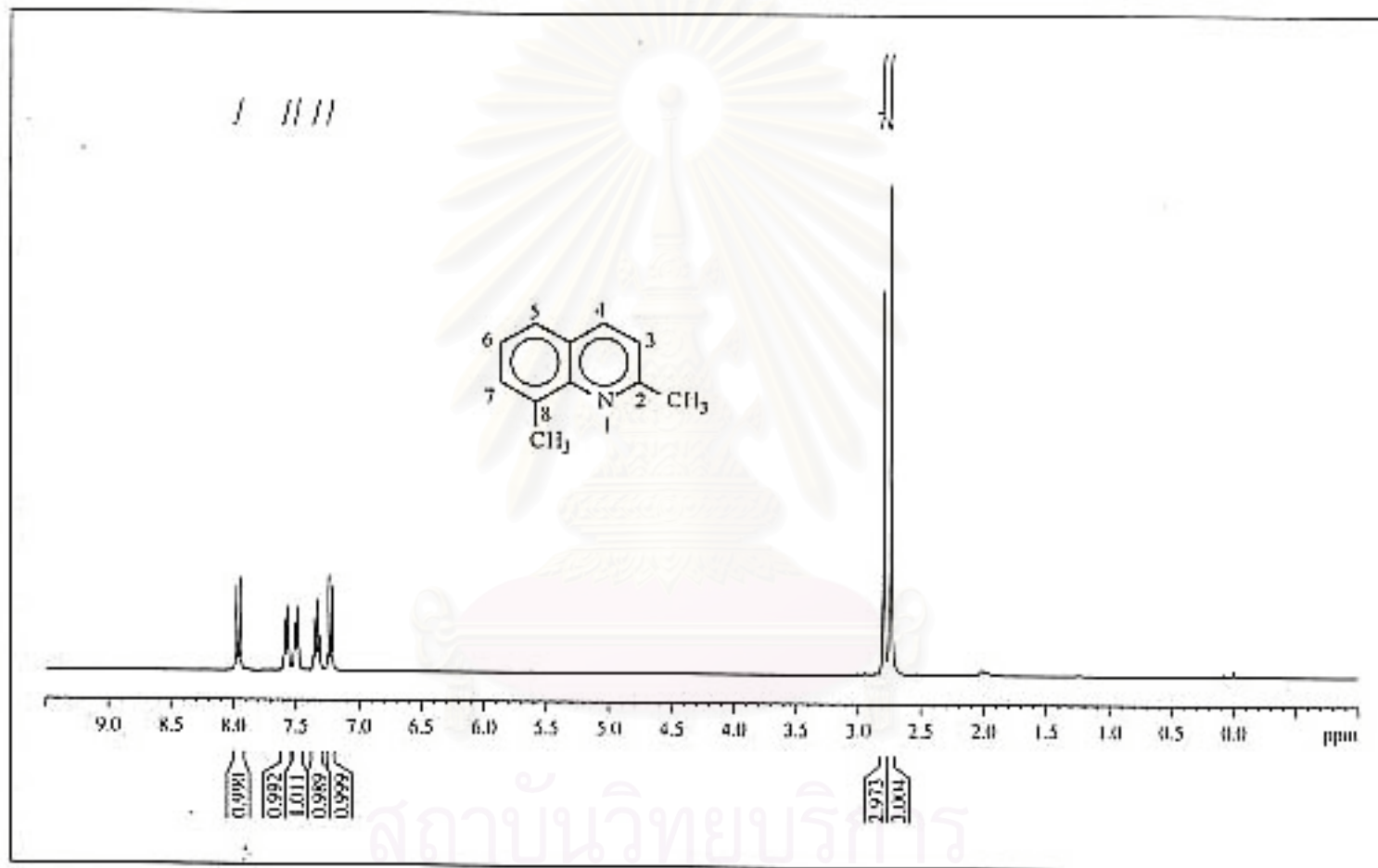
Figure 12. The 300 MHz ^{1}H-NMR spectrum of 2,8-dimethylquinoline (1f) in CDCl$_3$.
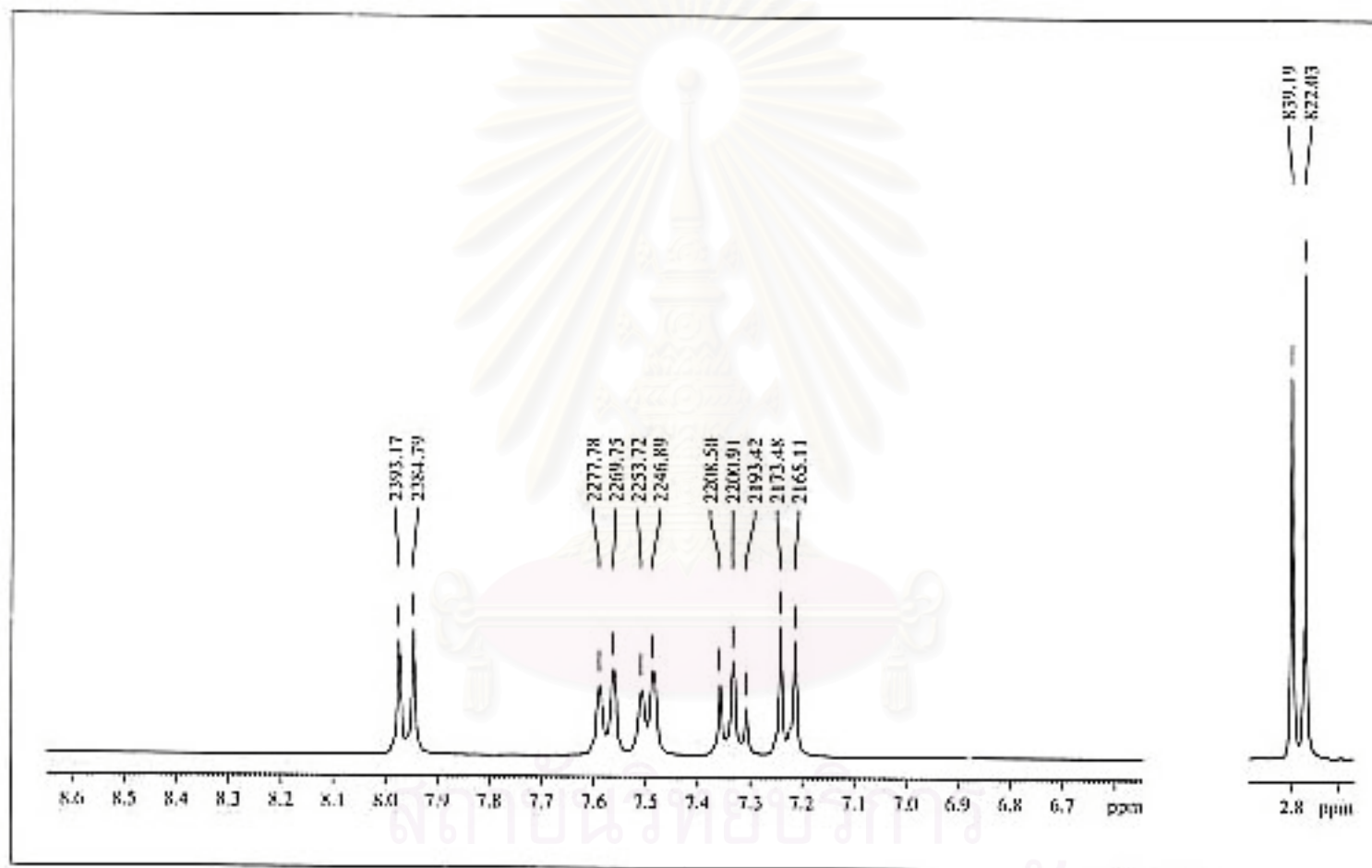
Figure 13. The 300 MHz 1H-NMR spectrum of 2,8-dimethylquinoline (1f) in CDCl$_3$. (Enlarged scale)
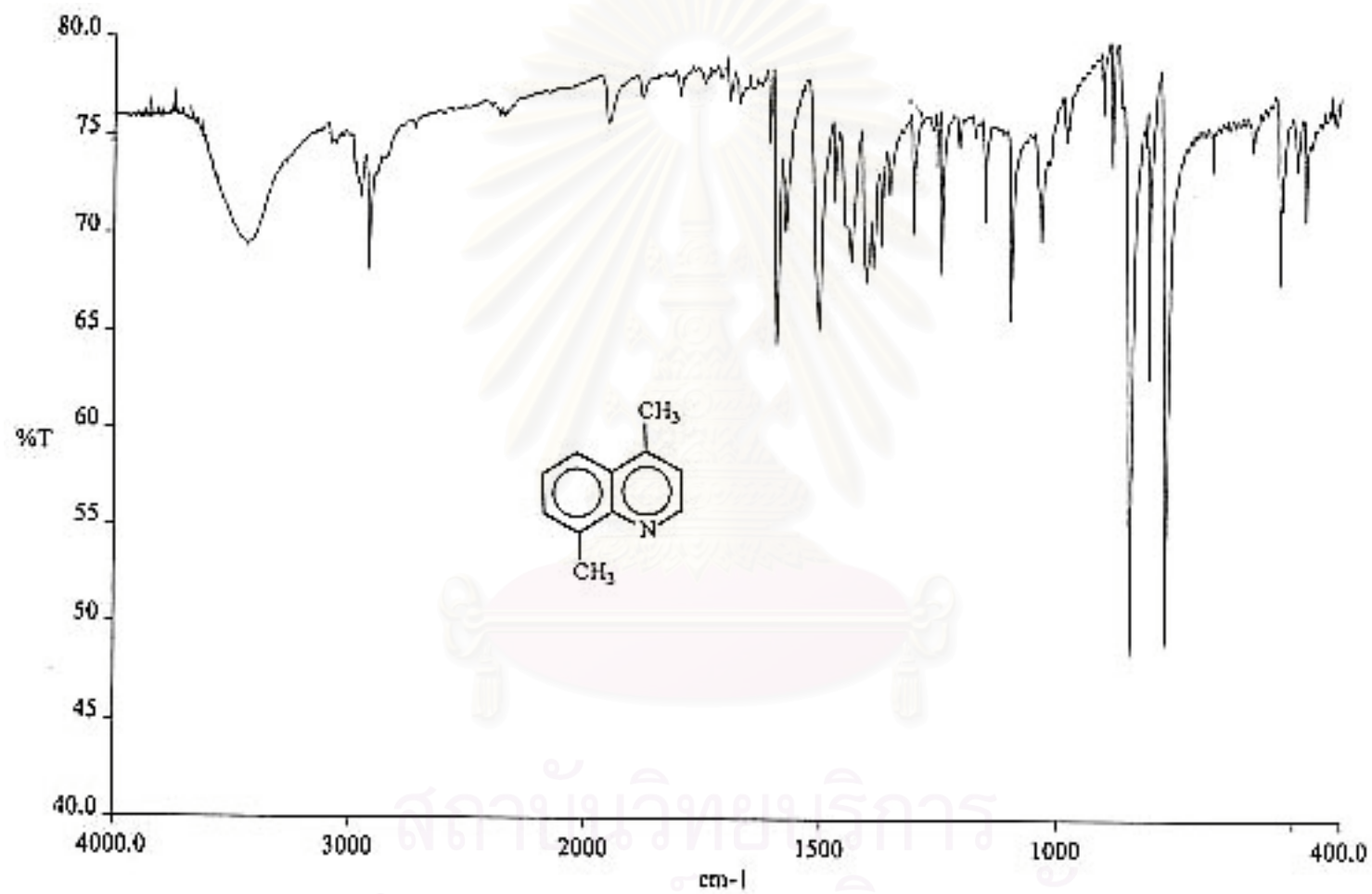
Figure 14. The IR spectrum (KBr) of 4,8-dimethylquinoline (1g).
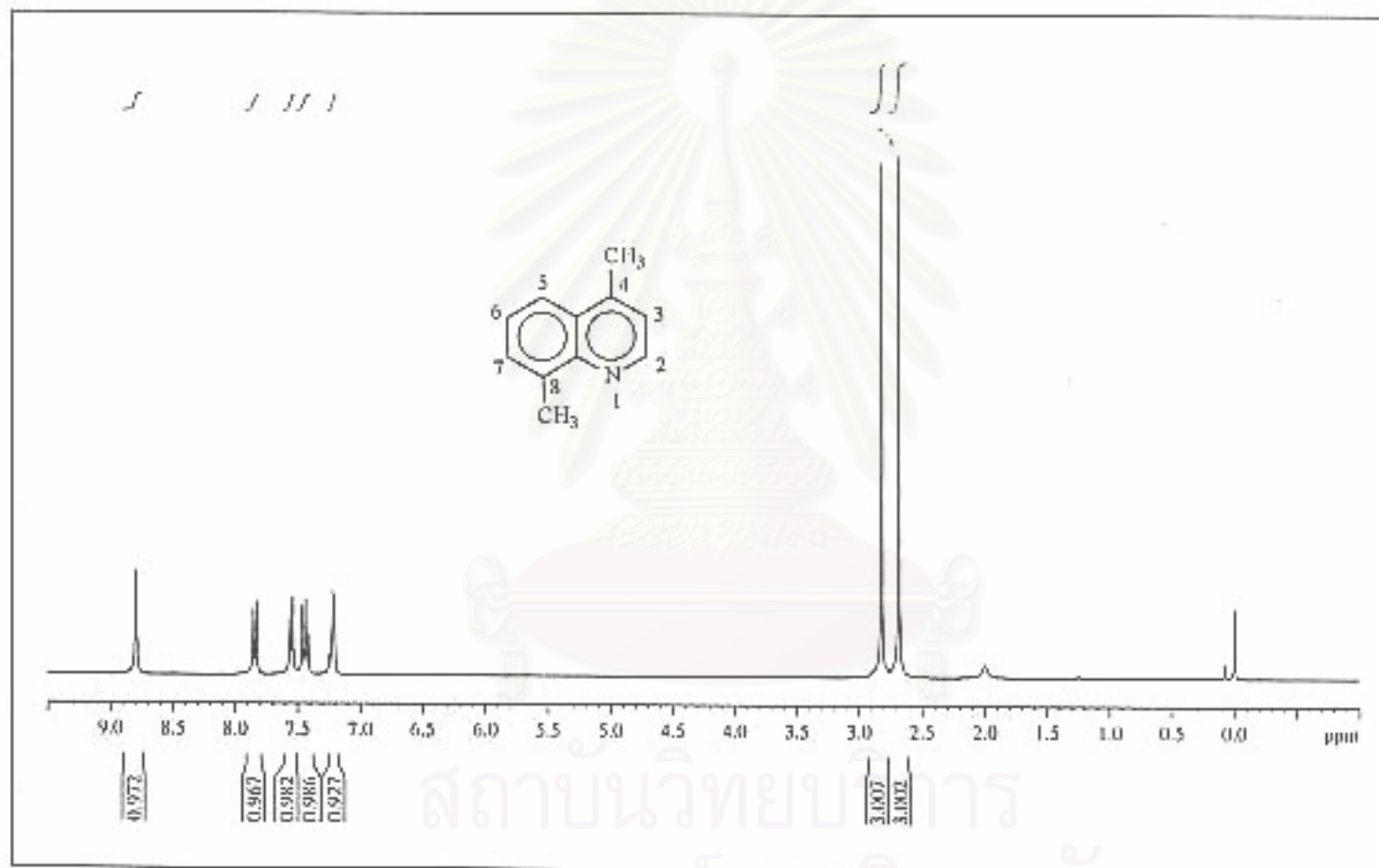
Figure 15. The 300 MHz 1H-NMR spectrum of 4,8-dimethylquinoline (1g) in CDCl₃.
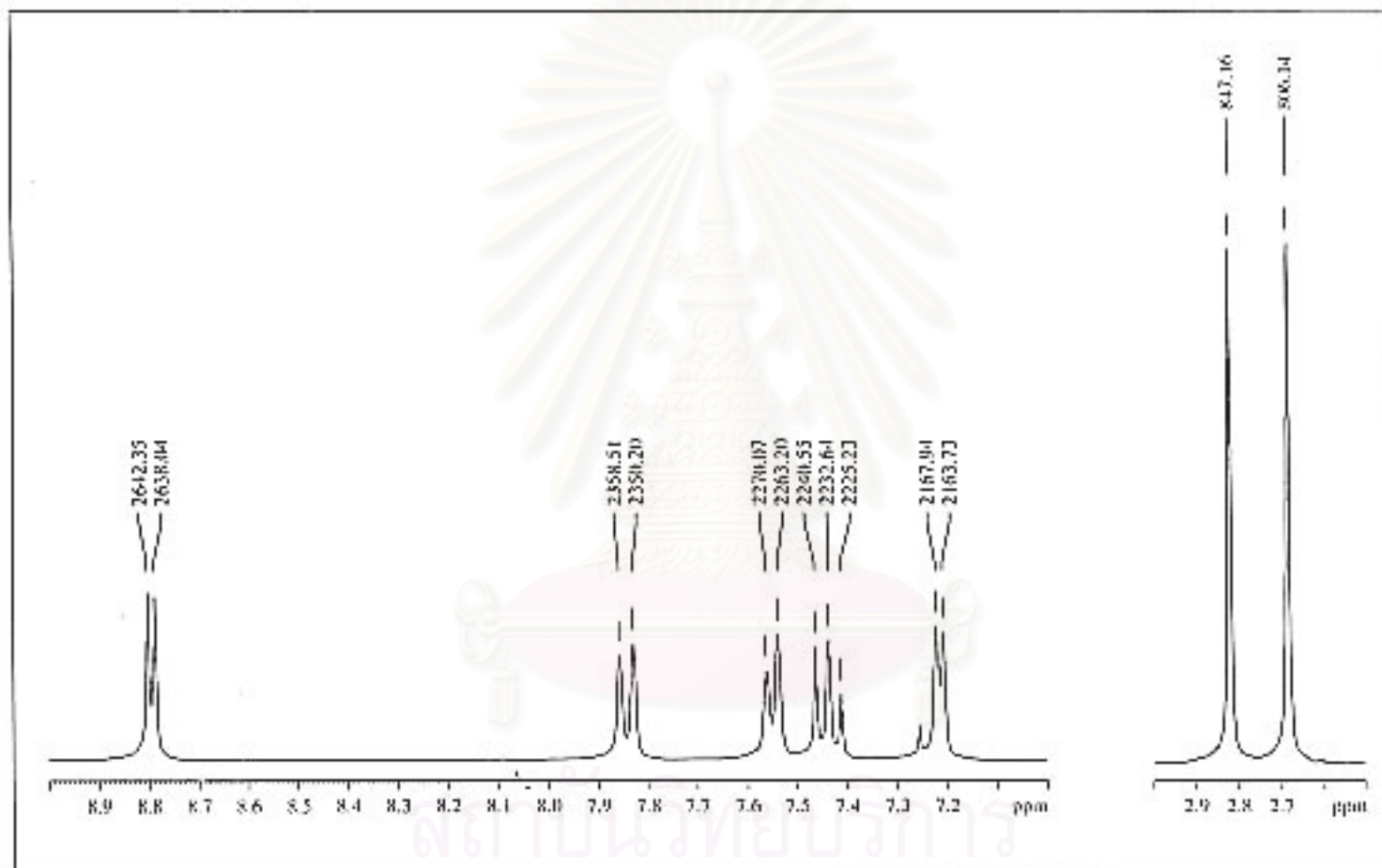
Figure 16. The 300 MHz 1H-NMR spectrum of 4,8-dimethylquinoline (1g) in CDCl₃. (Enlarged scale)
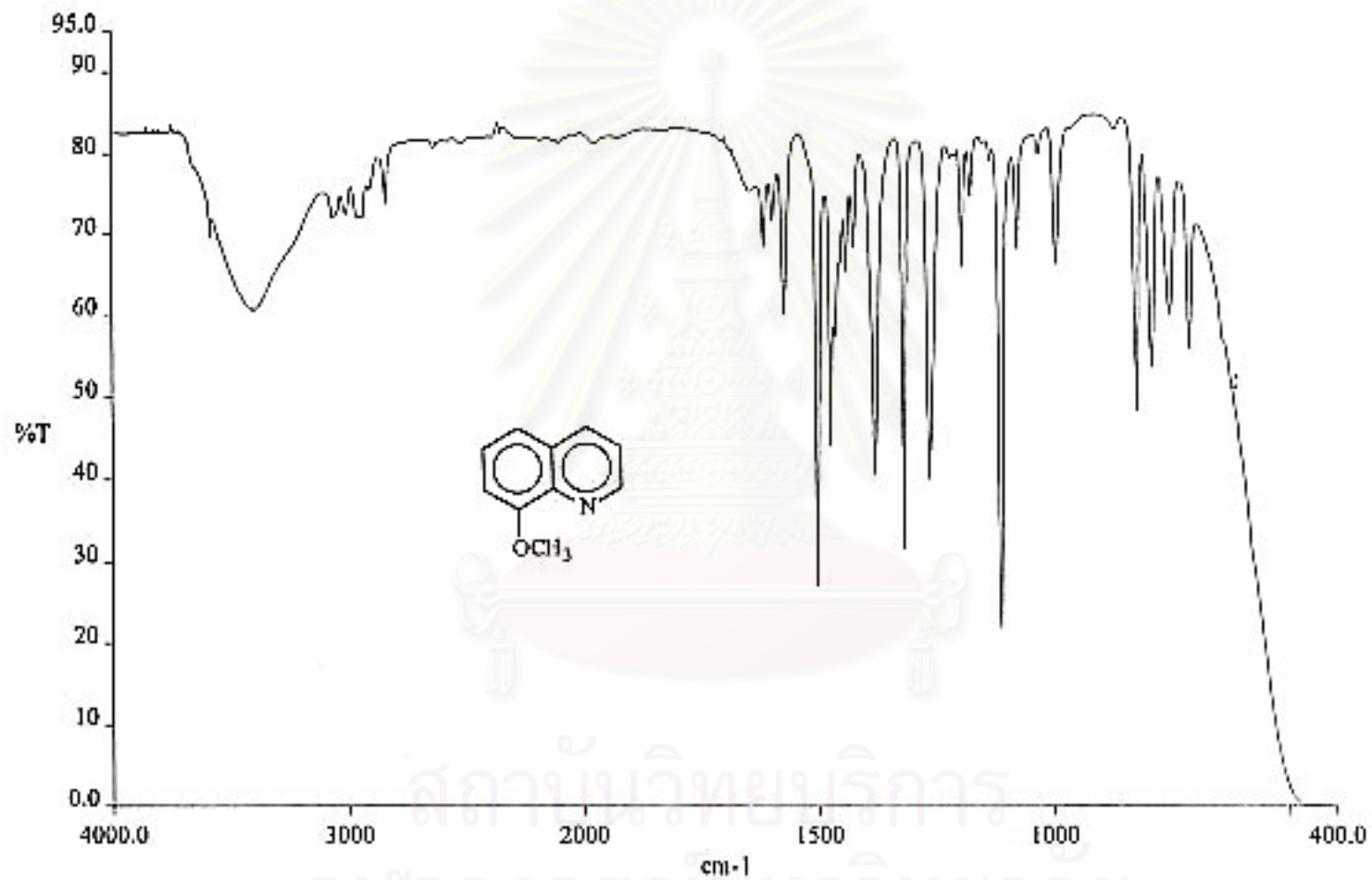
Figure 17. The IR spectrum (Neat, NaCl cell) of 8-methoxyquinoline (1h).
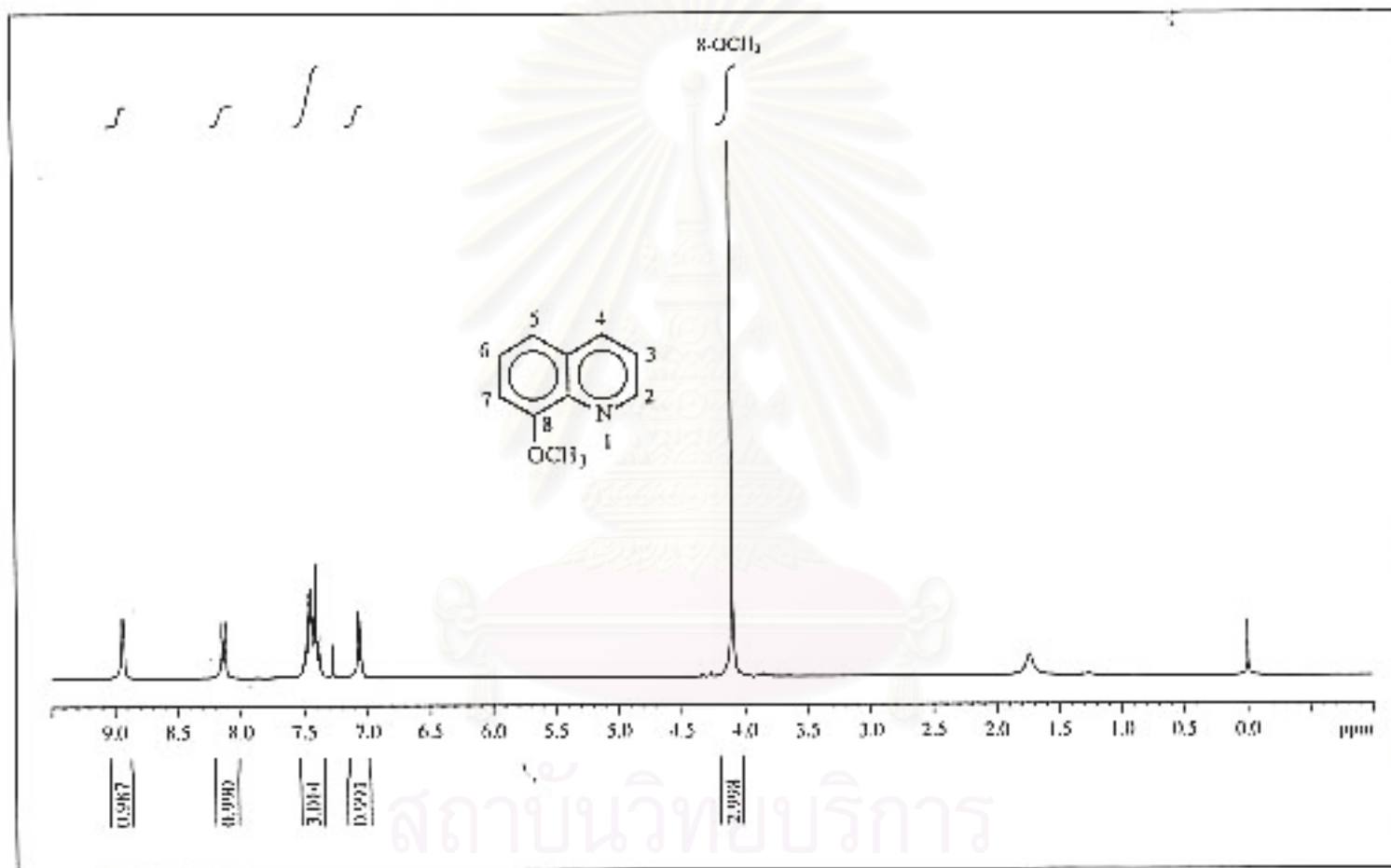
Figure 18. The 300 MHz 1H-NMR spectrum of 8-methoxyquinoline (1h) in CDCl₃.
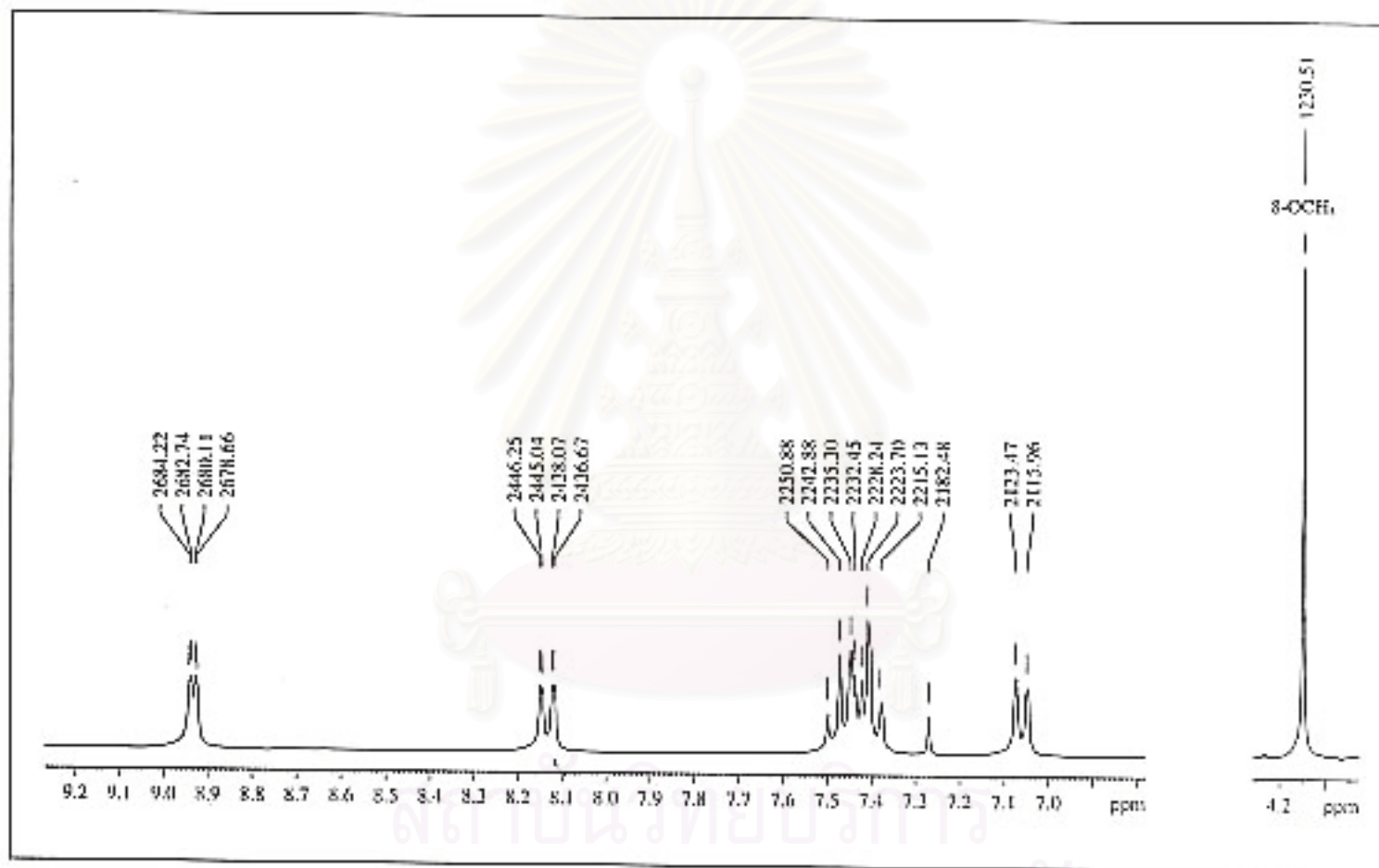
Figure 19. The 300 MHz 1H-NMR spectrum of 8-methoxyquinoline (1h) in CDCl₃. (Enlarged scale)
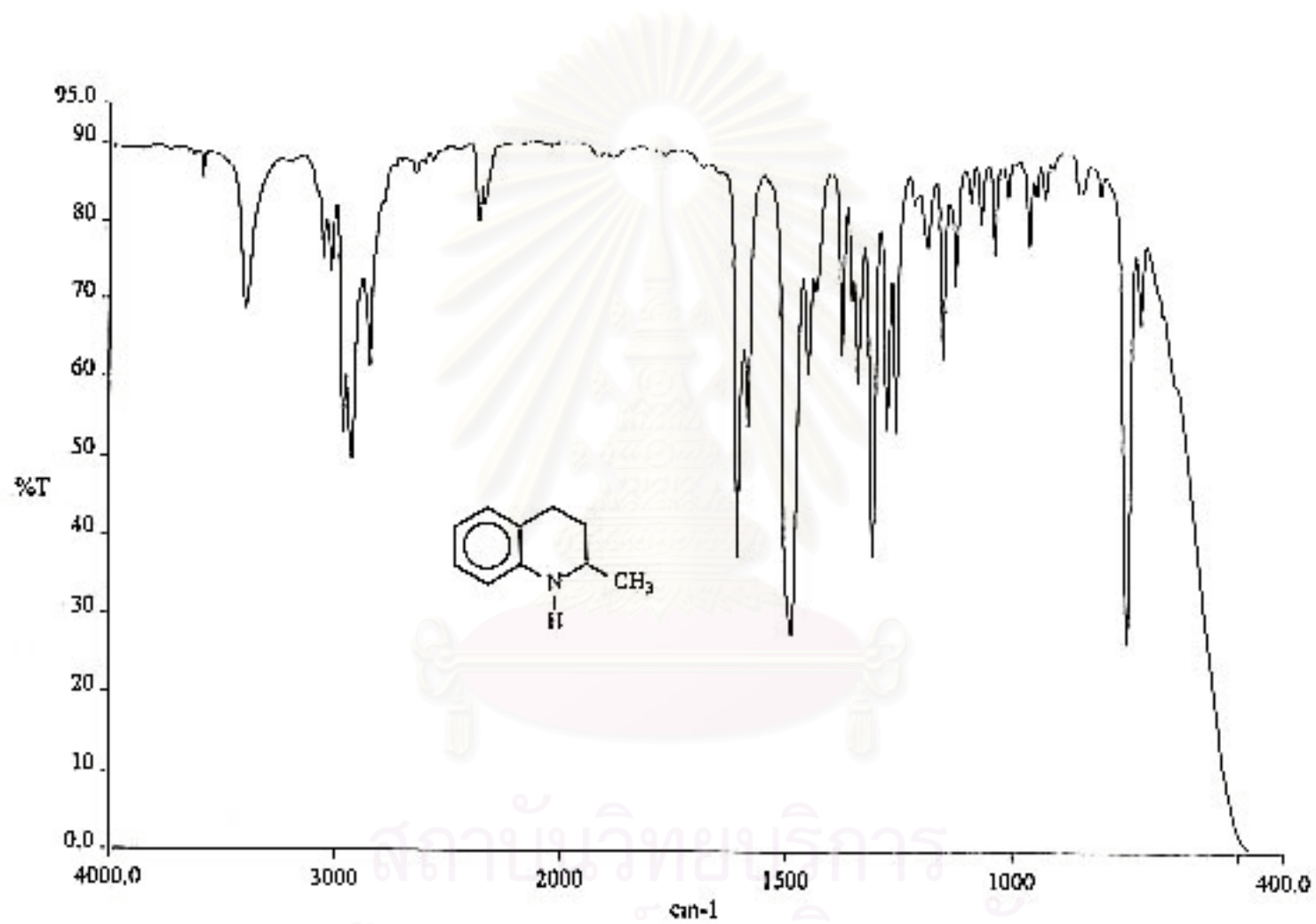
Figure 20. The IR spectrum (Neat, NaCl cell) of 1,2,3,4-tetrahydro-2-methylquinoline (2b).
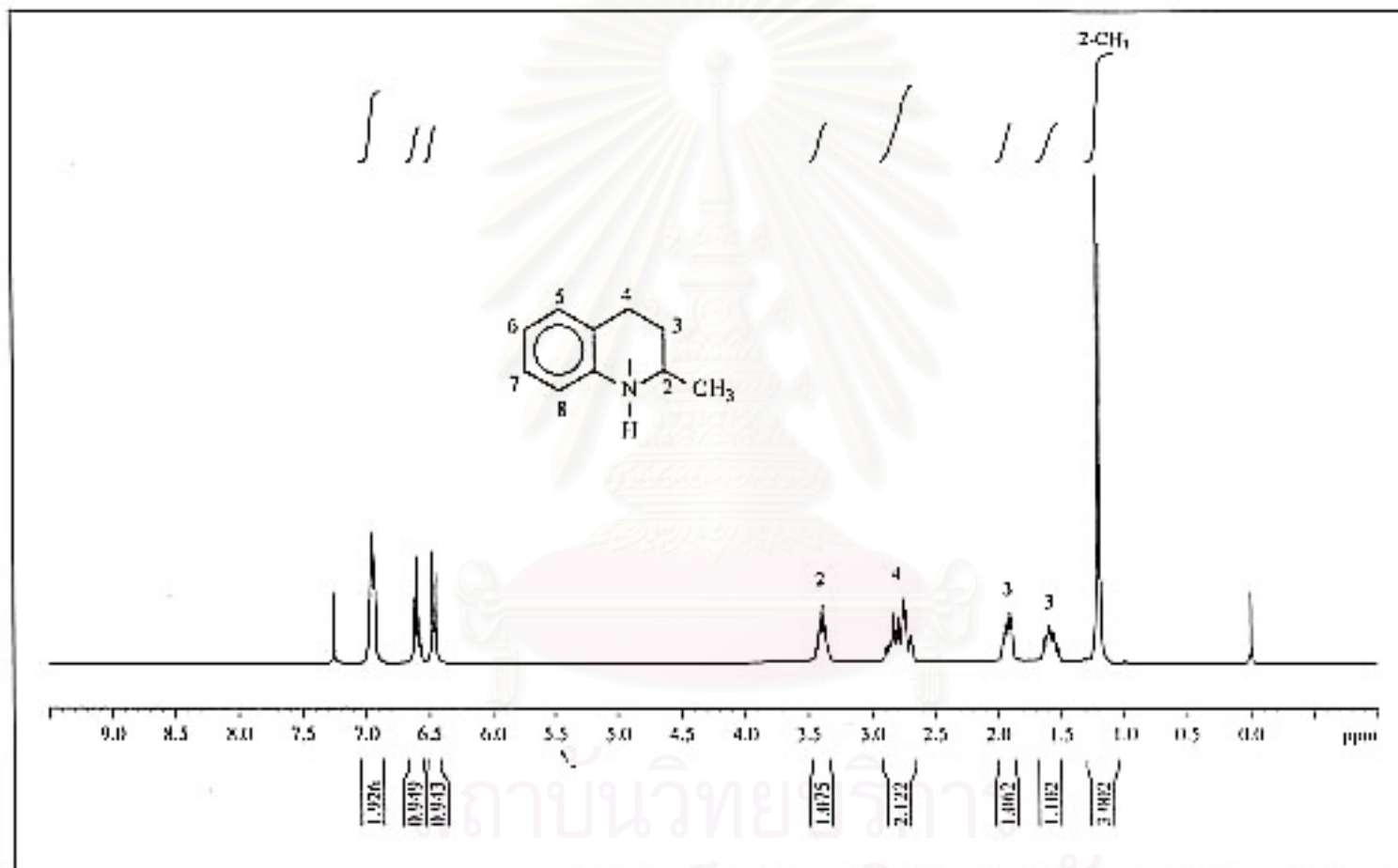
Figure 21. The 300 MHz 1H-NMR spectrum of 1,2,3,4-tetrahydro-2-methylquinoline (2b) in CDCl$_3$.
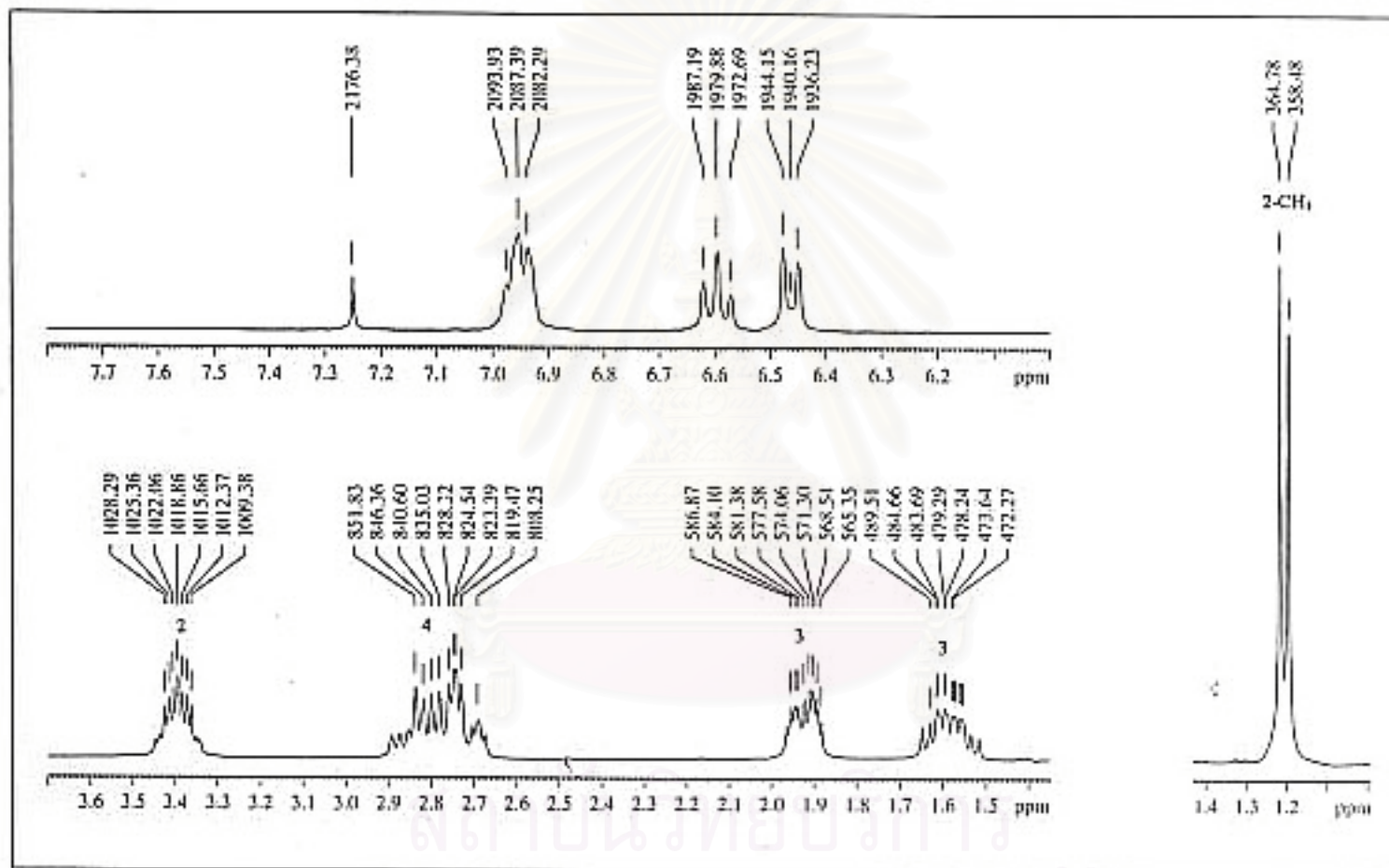
Figure 22. The 300 MHz 1H-NMR spectrum of 1,2,3,4-tetrahydro-2-methylquinoline (2b) in CDCl₃. (Enlarged scale)
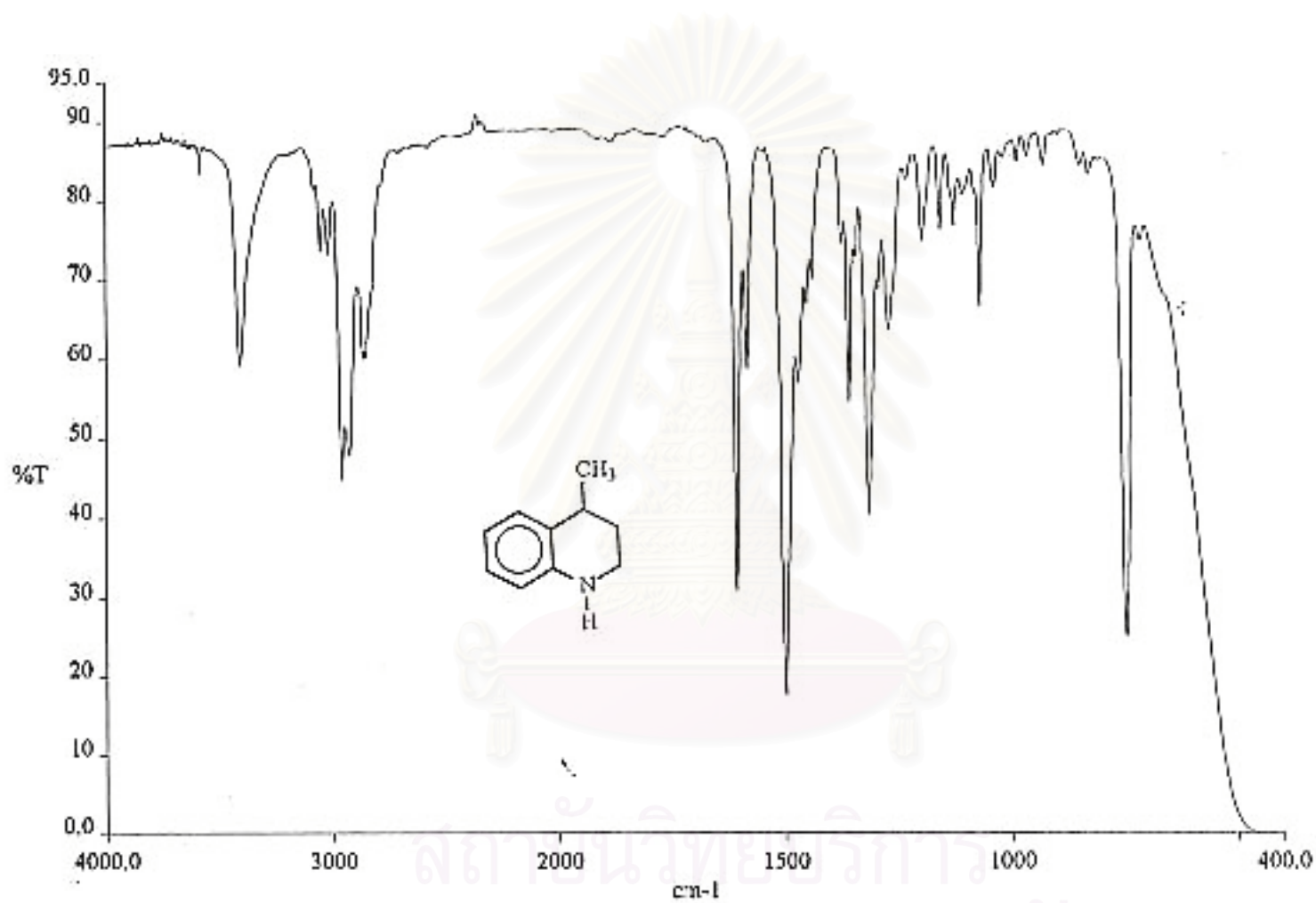
Figure 23. The IR spectrum (Neat, NaCl cell) of 1,2,3,4-tetrahydro-4-methylquinoline (2c).
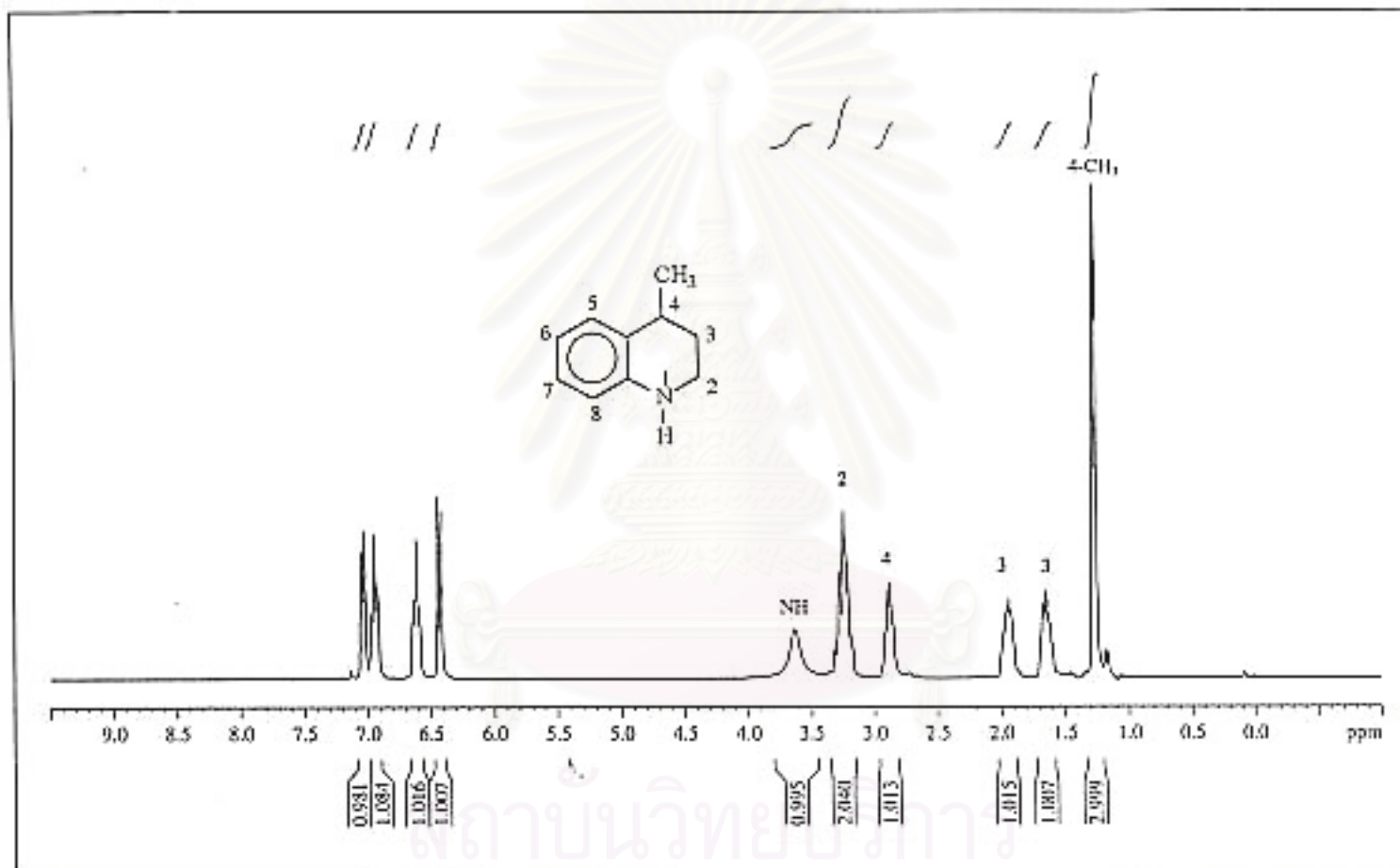
Figure 24. The 300 MHz 1H-NMR spectrum of 1,2,3,4-tetrahydro-4-methylquinoline (2c) in CDCl₃.
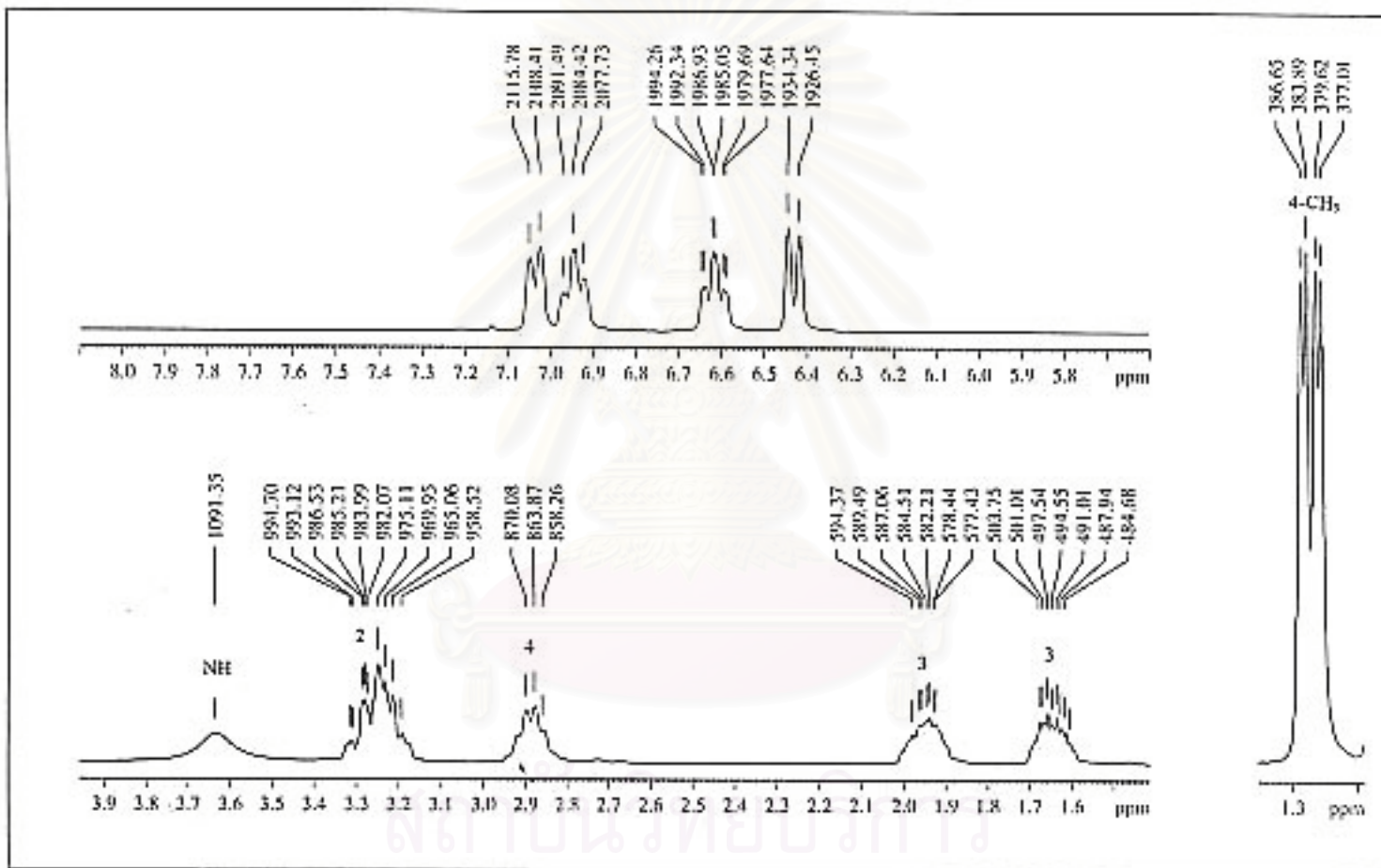
Figure 25. The 300 MHz 1H-NMR spectrum of 1,2,3,4-tetrahydro-4-methylquinoline (2c) in CDCl$_3$. (Enlarged scale)
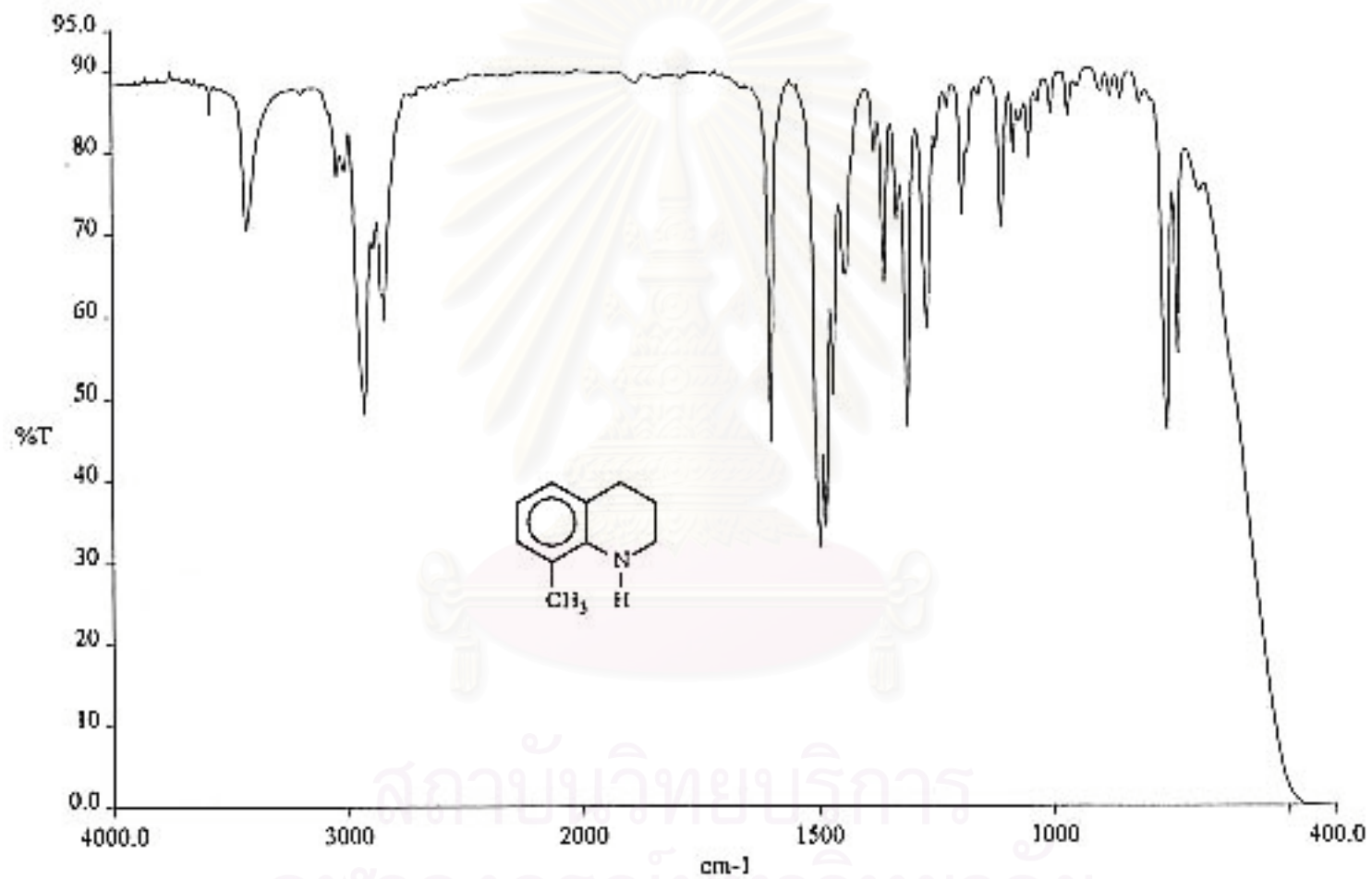
Figure 26. The IR spectrum (Neat, NaCl cell) of 1,2,3,4-tetrahydro-8-methylquinoline (2d).
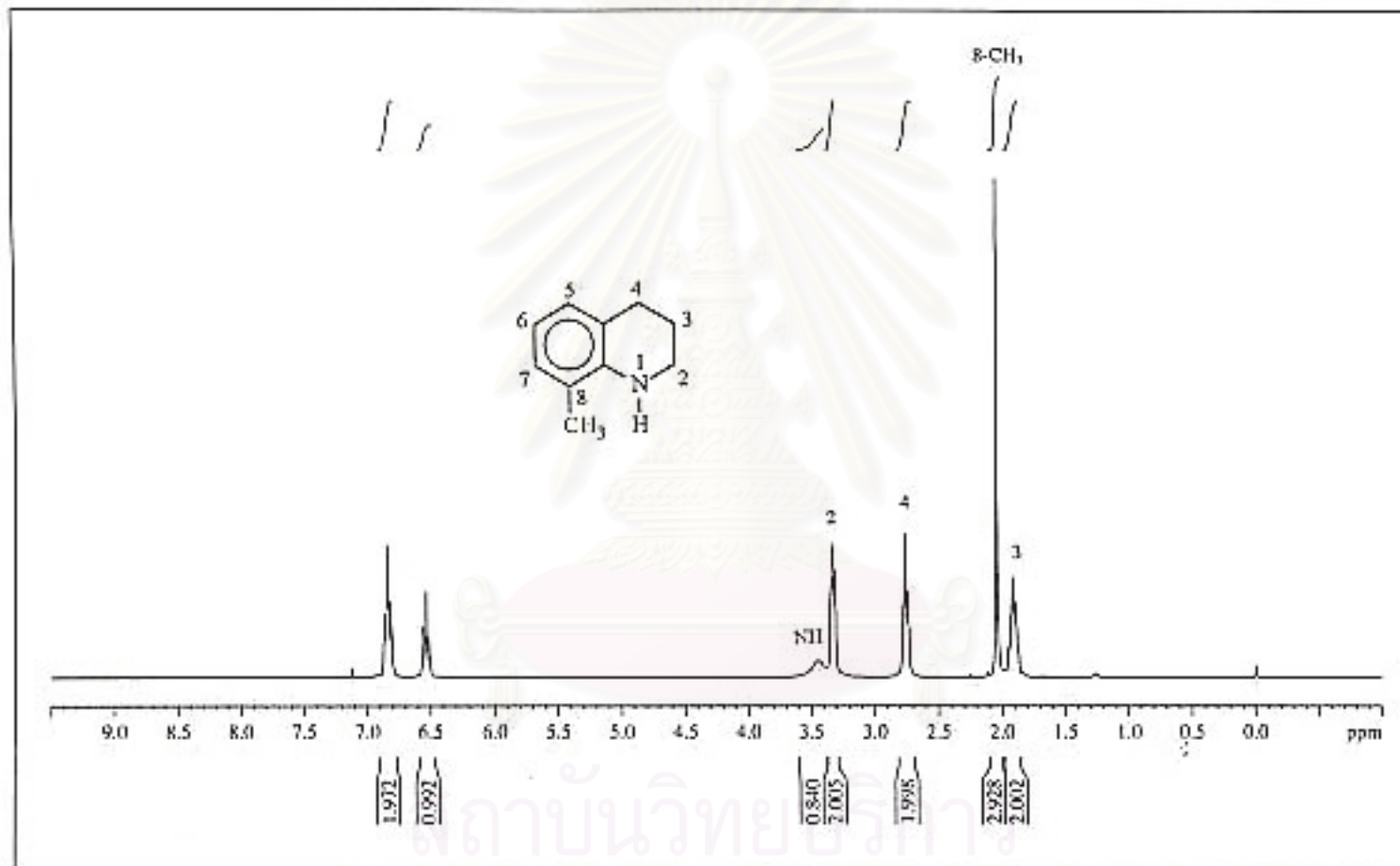
Figure 27. The 300 MHz 1H-NMR spectrum of 1,2,3,4-tetrahydro-8-methylquinoline (2d) in CDCl$_3$.
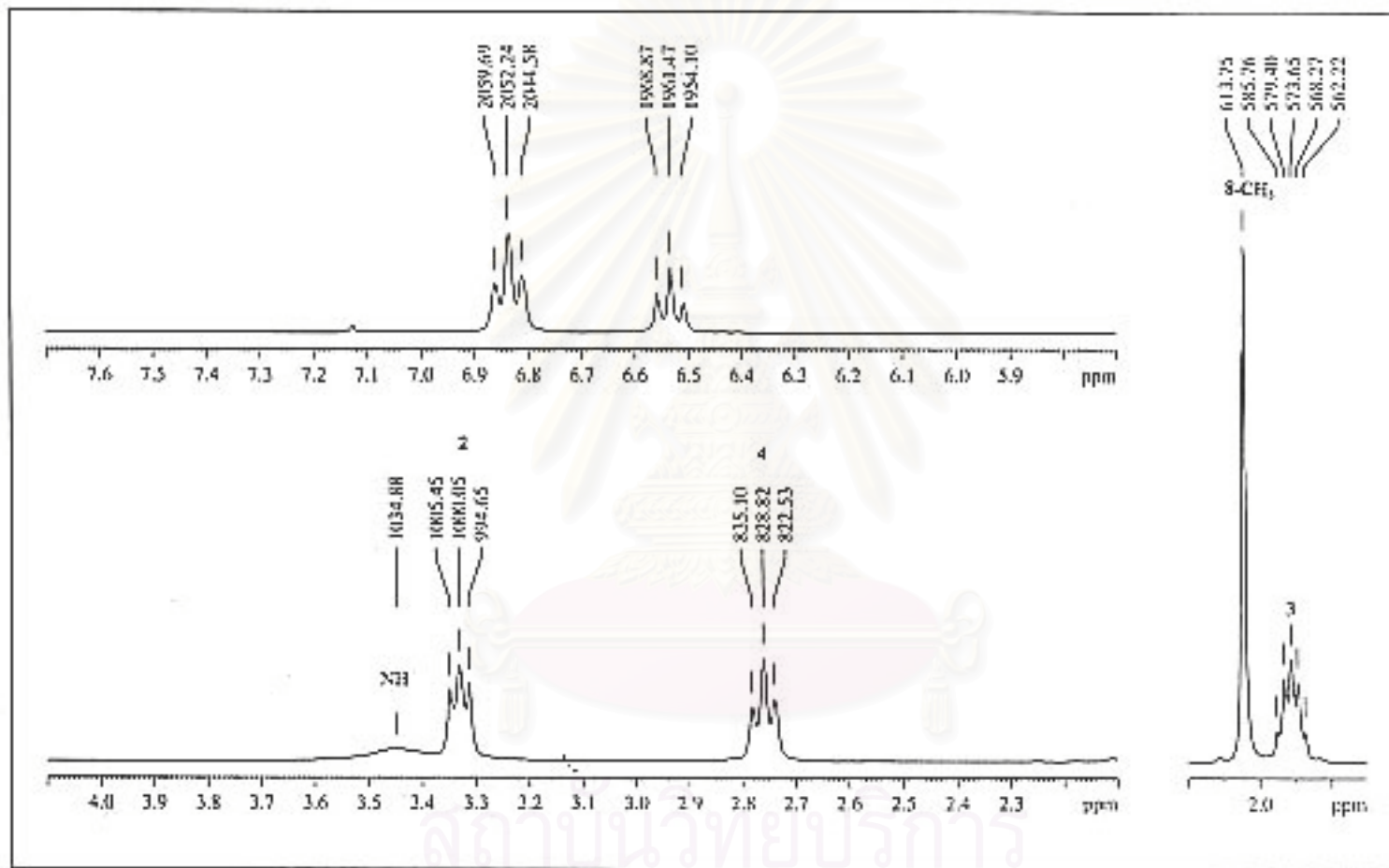
Figure 28. The 300 MHz 1H-NMR spectrum of 1,2,3,4-tetrahydro-8-methylquinoline (2d) in CDCl$_3$. (Enlarged scale)
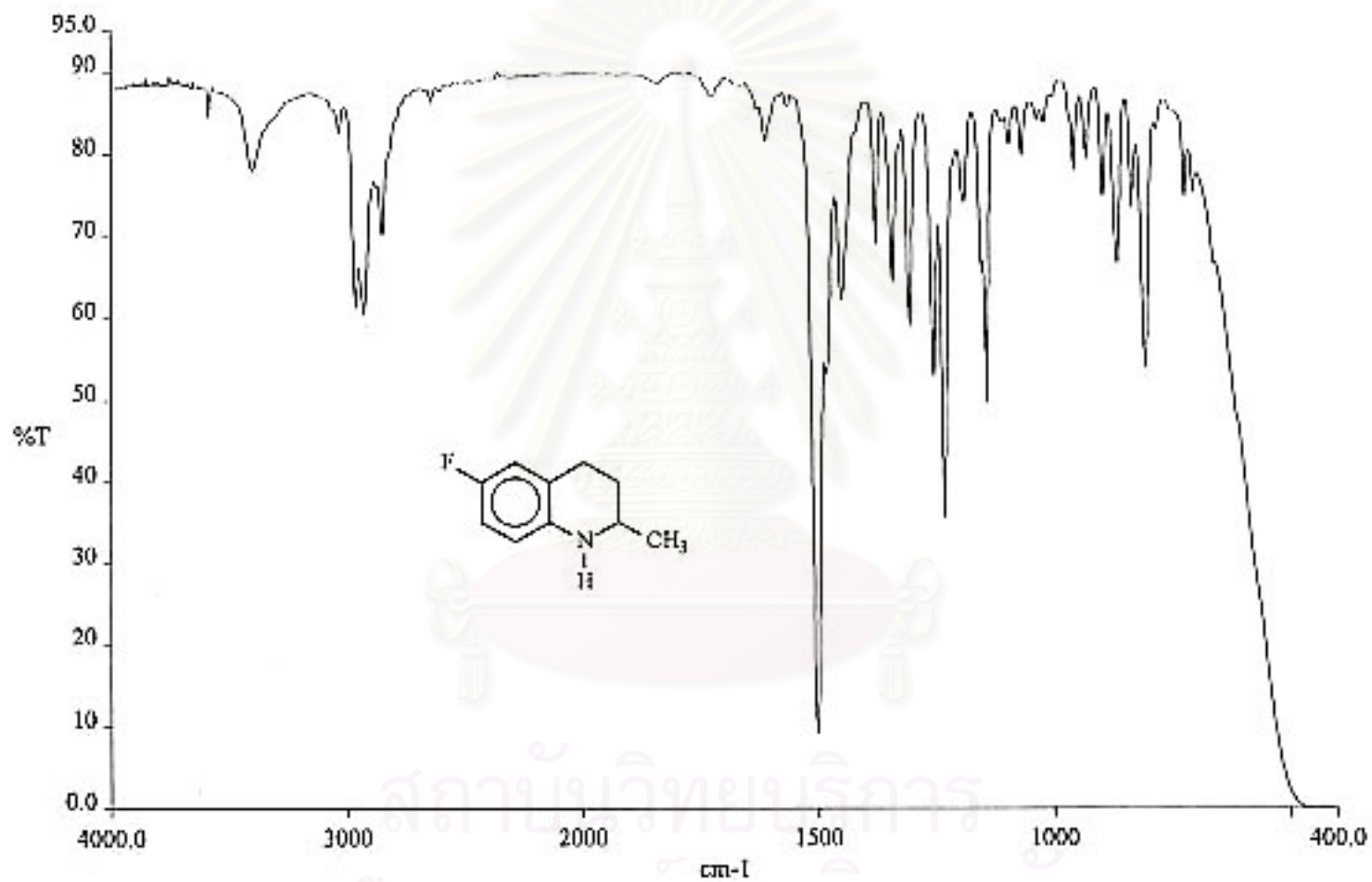
Figure 29. The IR spectrum (Neat, NaCl cell) of 1,2,3,4-tetrahydro-6-fluoro-2-methylquinoline (2e).
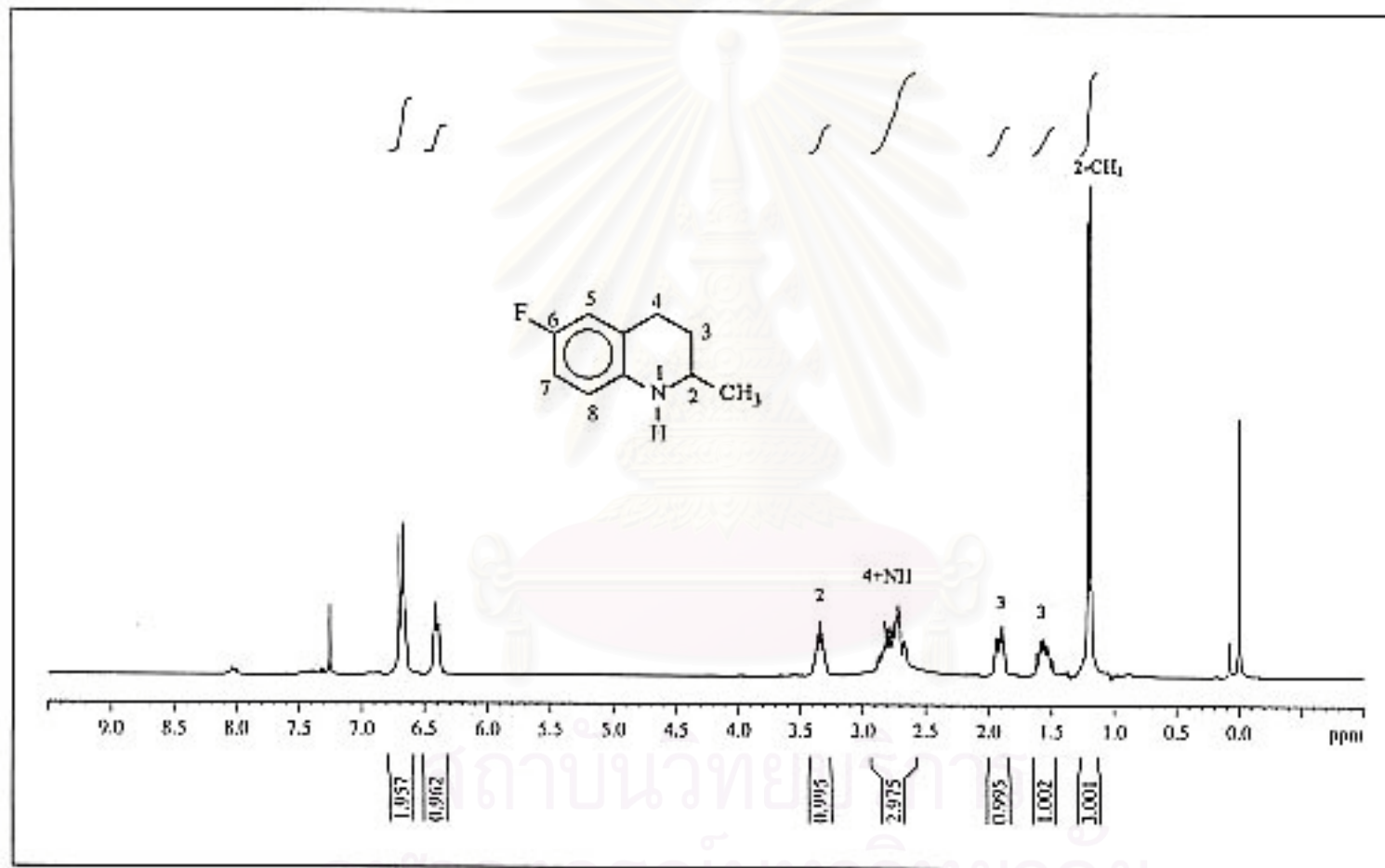
Figure 30. The 300 MHz 1H-NMR spectrum of 1,2,3,4-tetrahydro-6-fluoro-2-methylquinoline (2e) in CDCl₃.
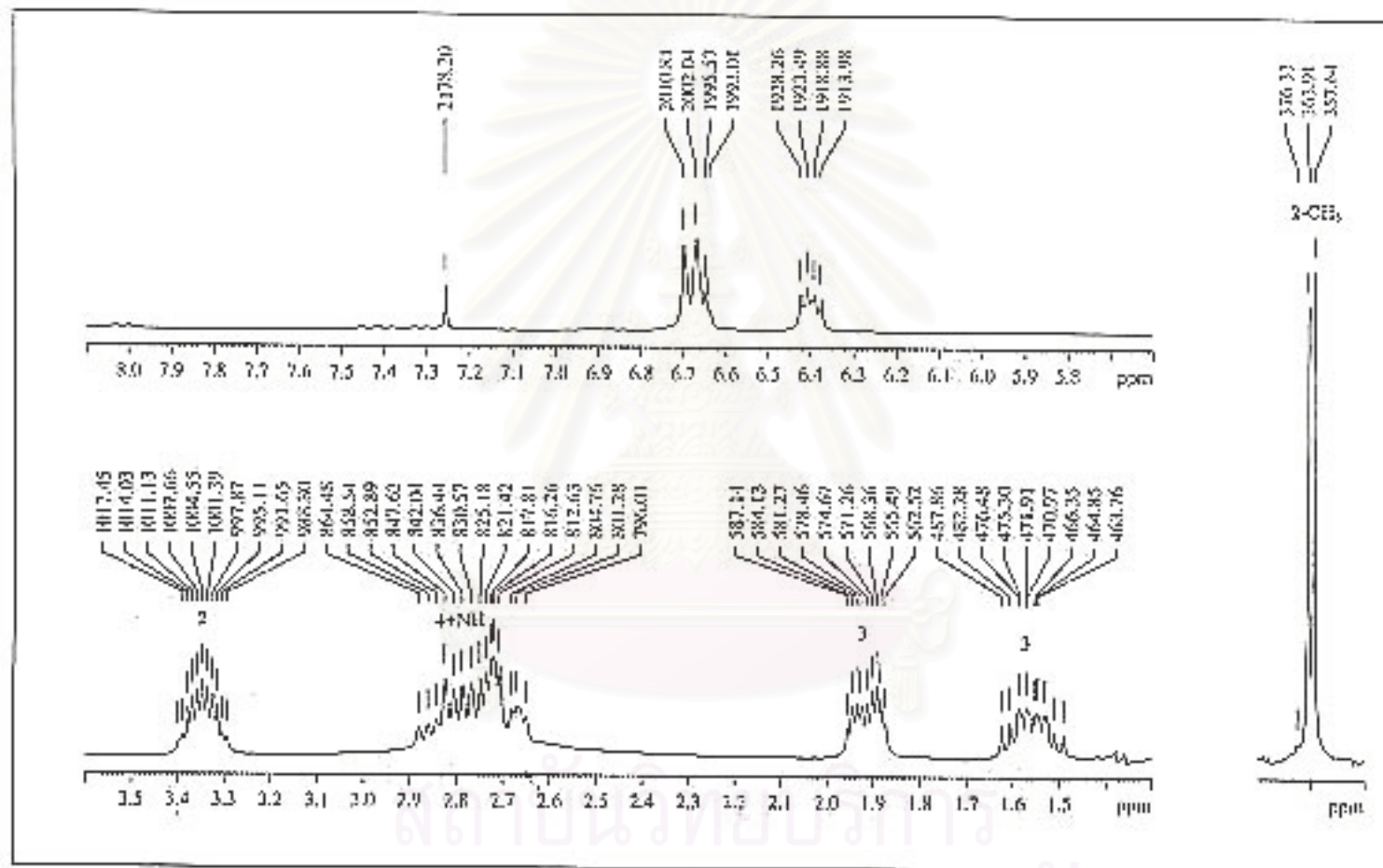
Figure 31. The 300 MHz 1H-NMR spectrum of 1,2,3,4-tetrahydro-6-fluoro-2-methylquinoline (2e) in CDCl$_3$. (Enlarged scale)
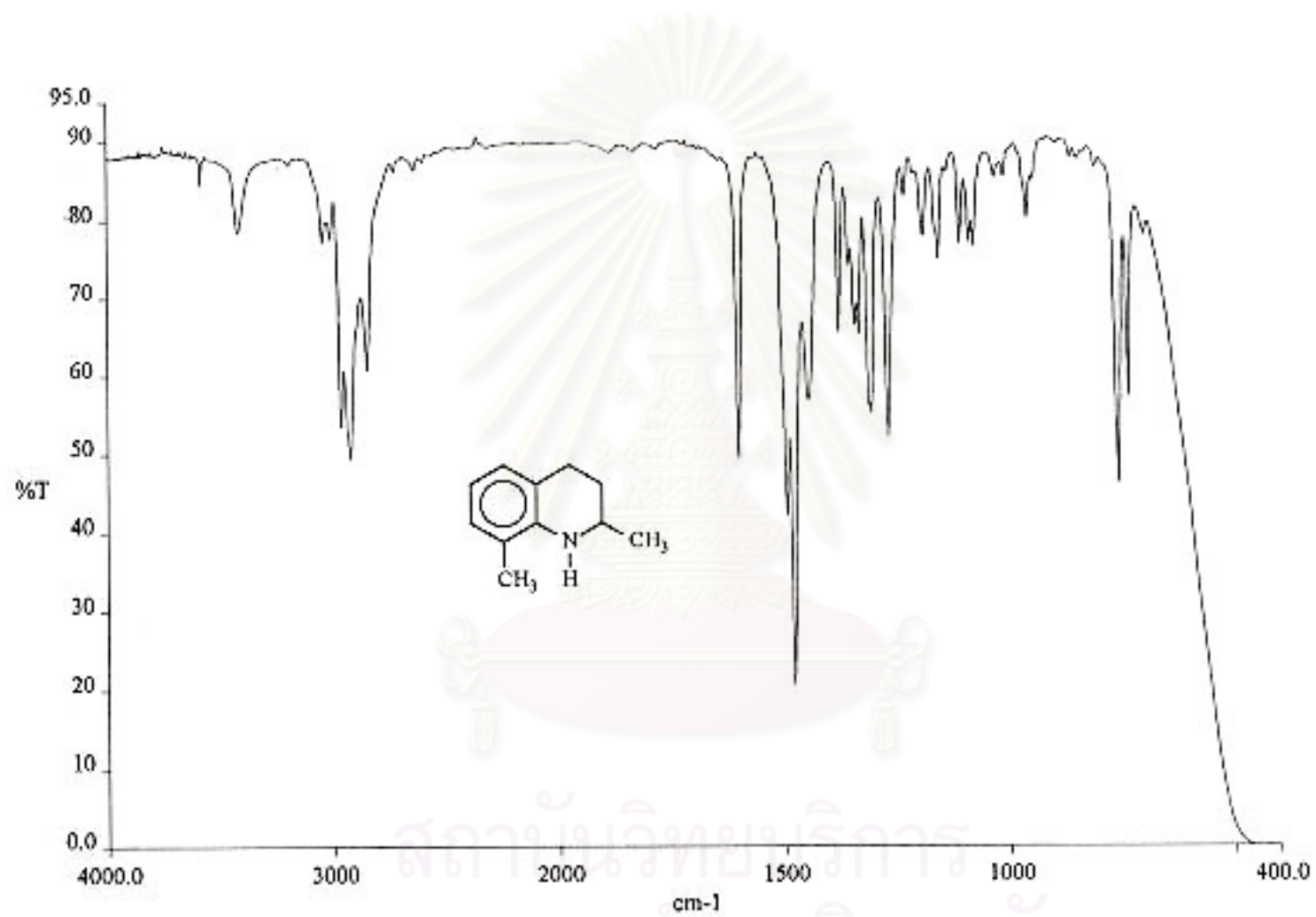
Figure 32. The IR spectrum (Neat, NaCl cell) of 1,2,3,4-tetrahydro-2,8-dimethylquinoline (2f).
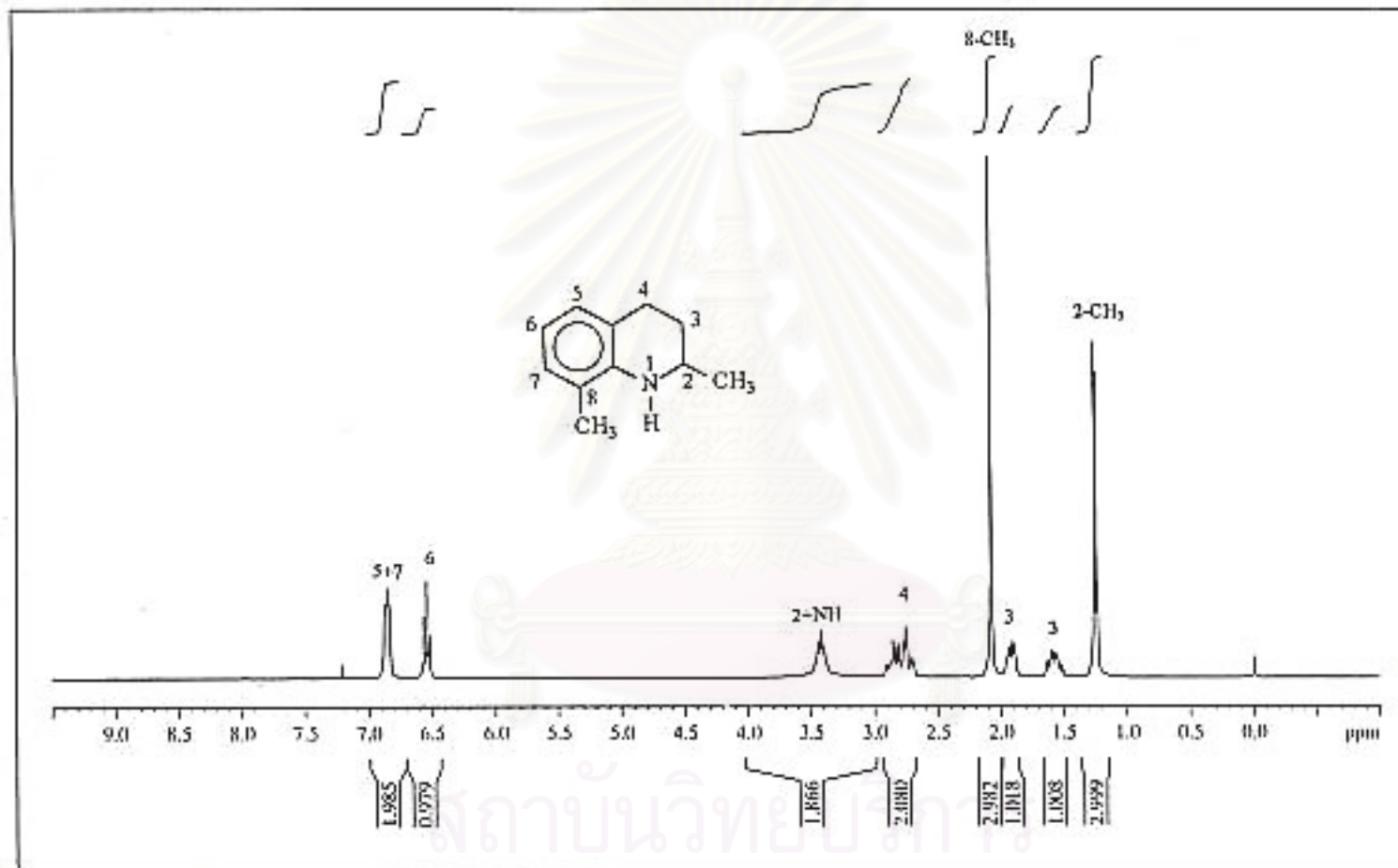
Figure 33. The 300 MHz 1H-NMR spectrum of 1,2,3,4-tetrahydro-2,8-dimethylquinoline (2f) in CDCl₃.
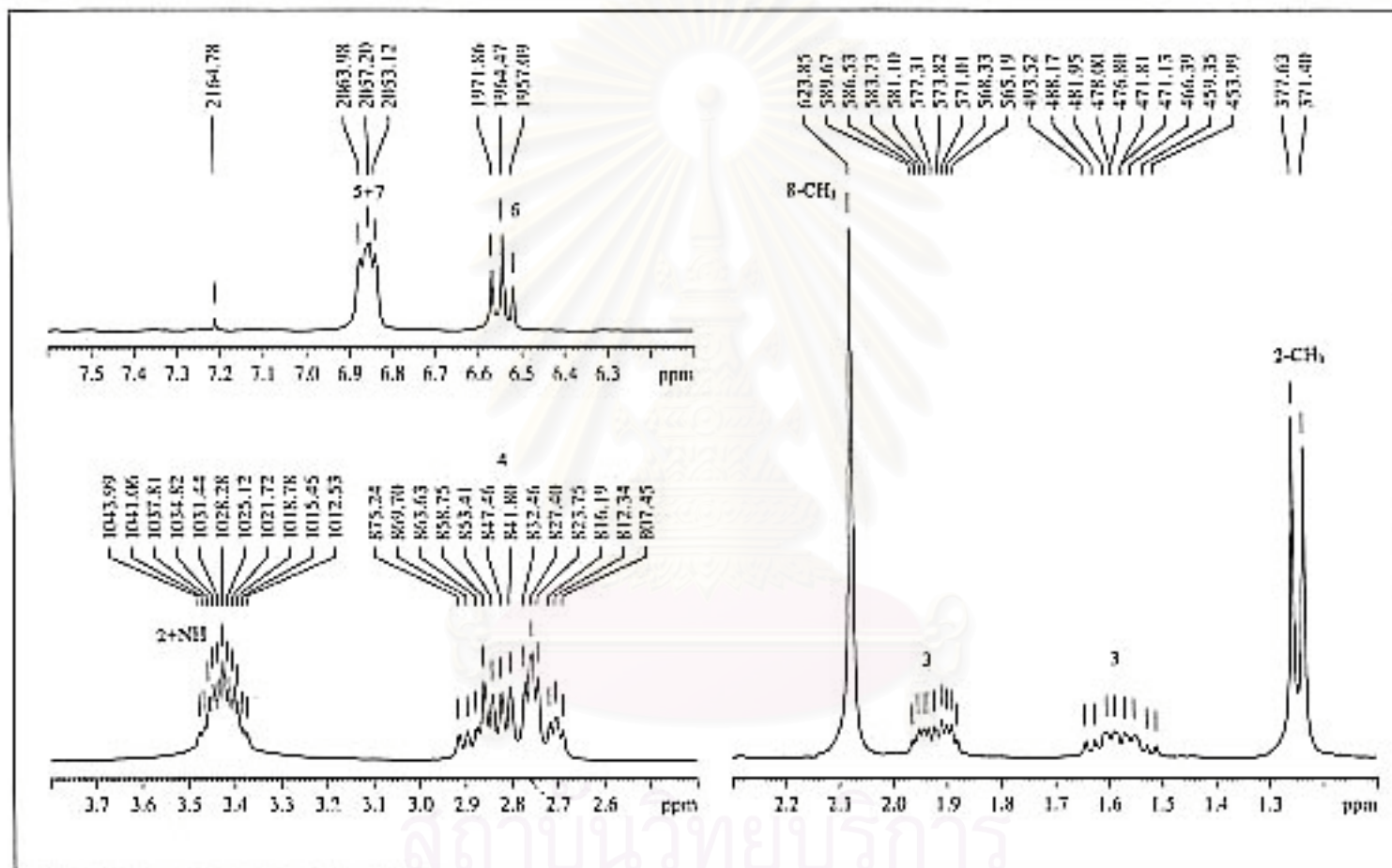
Figure 34. The 300 MHz 1H-NMR spectrum of 1,2,3,4-tetrahydro-2,8-dimethylquinoline (2f) in CDCl$_3$. (Enlarged scale)
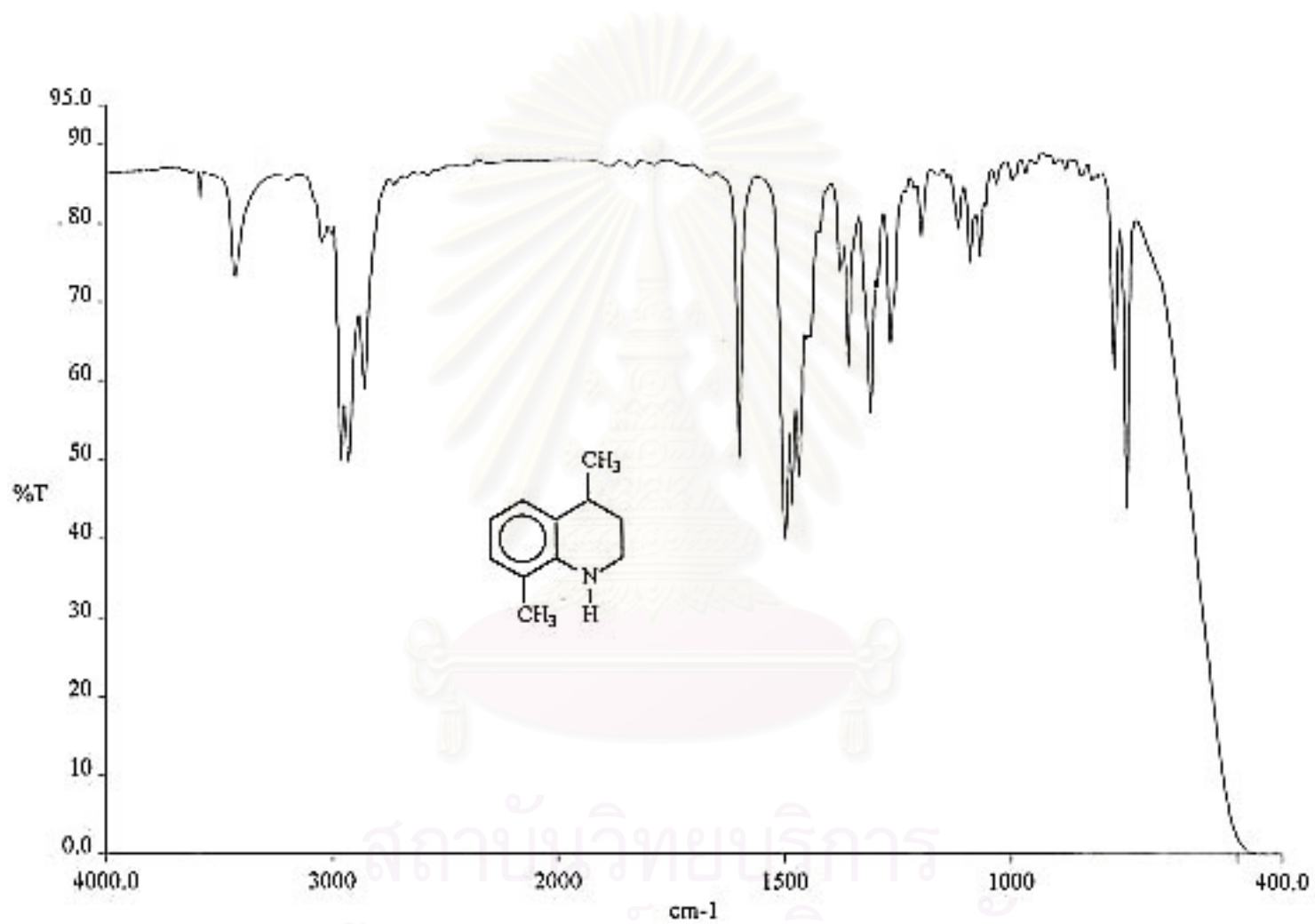
Figure 35. The IR spectrum (Neat, NaCl cell) of 1,2,3,4-tetrahydro-4,8-dimethylquinoline (2g).
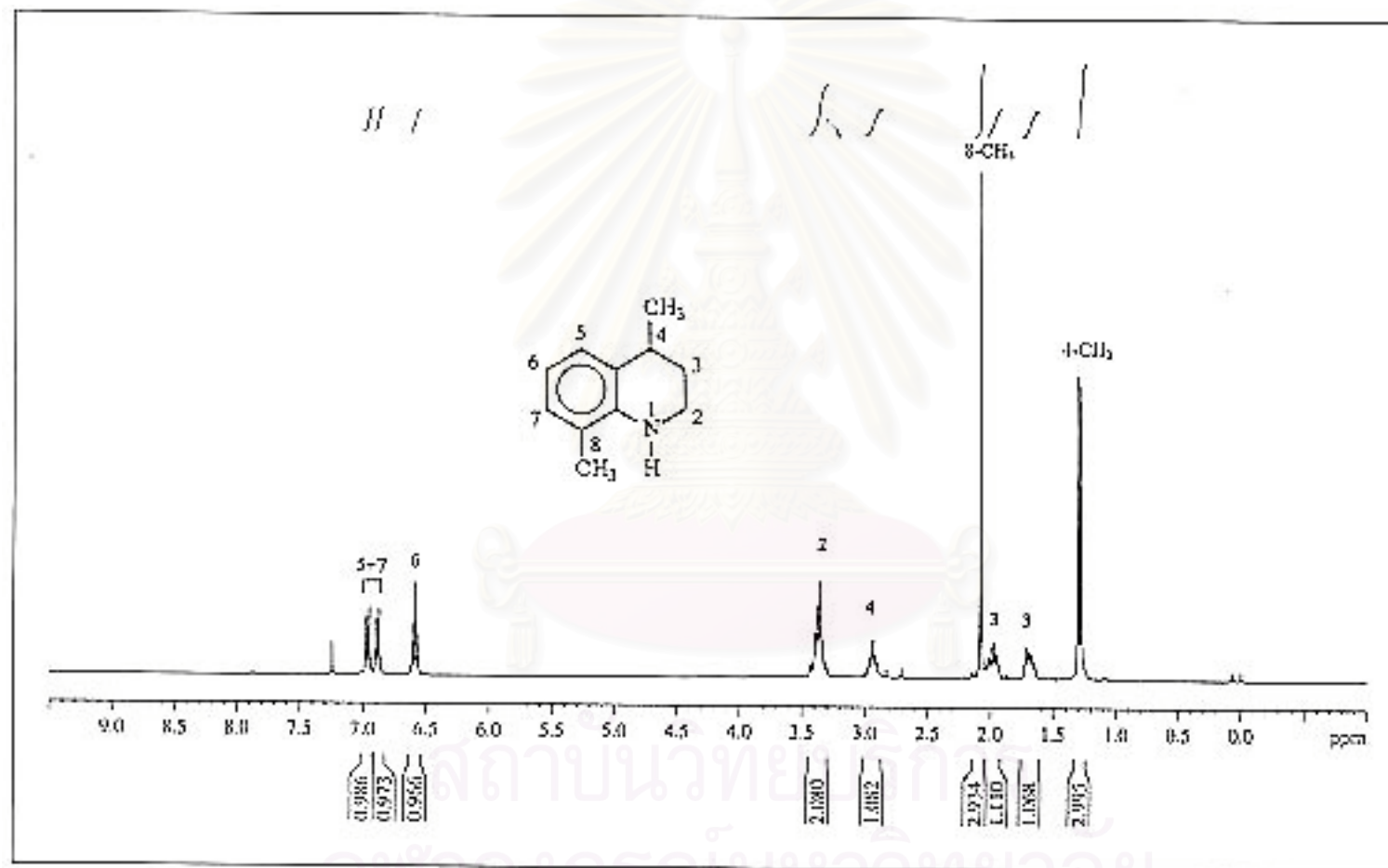
Figure 36. The 300 MHz 1H-NMR spectrum of 1,2,3,4-tetrahydro-4,8-dimethylquinoline (2g) in CDCl$_3$.
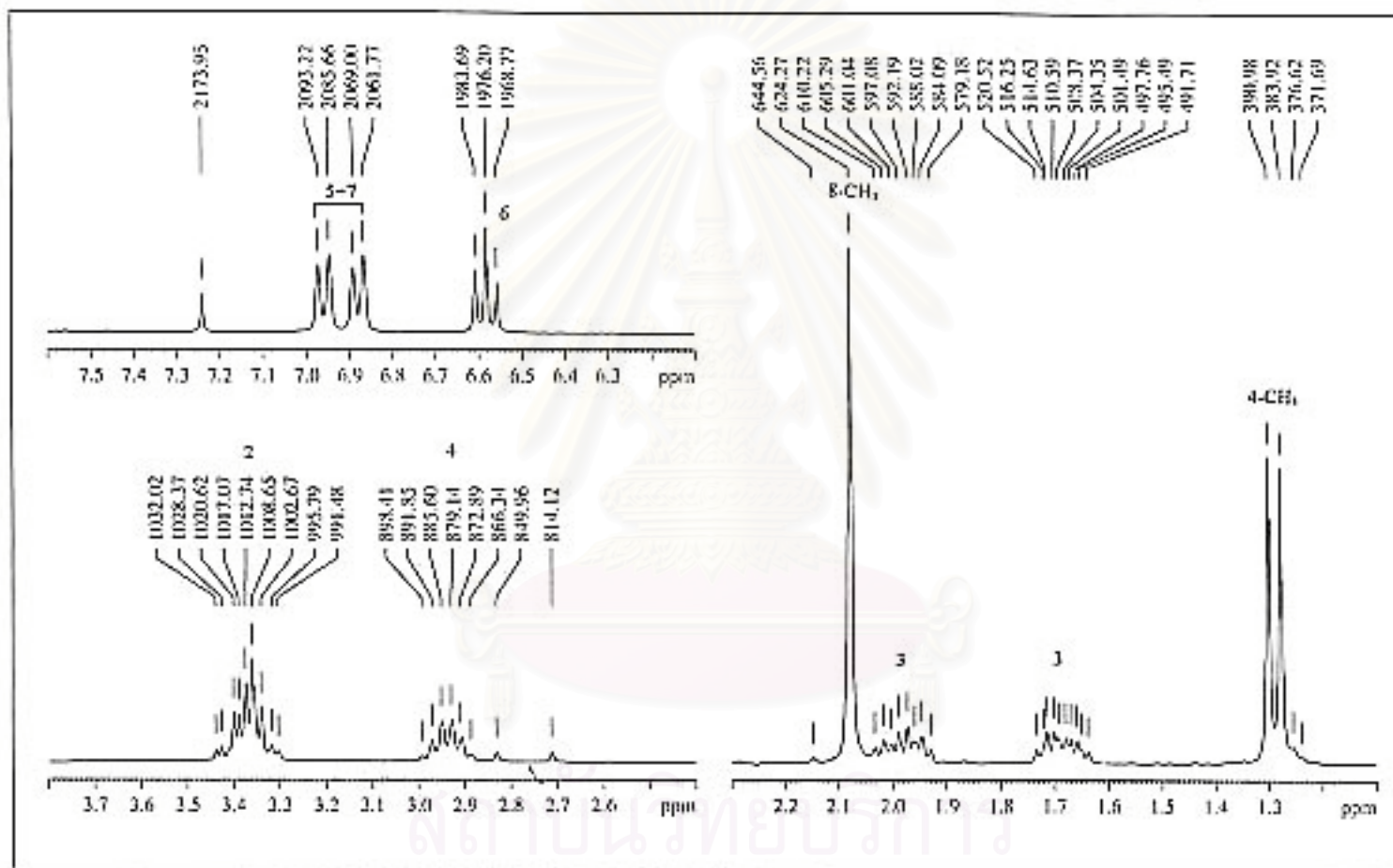
Figure 37. The 300 MHz 1H-NMR spectrum of 1,2,3,4-tetrahydro-4,8-dimethylquinoline (2g) in CDCl₃. (Enlarged scale)
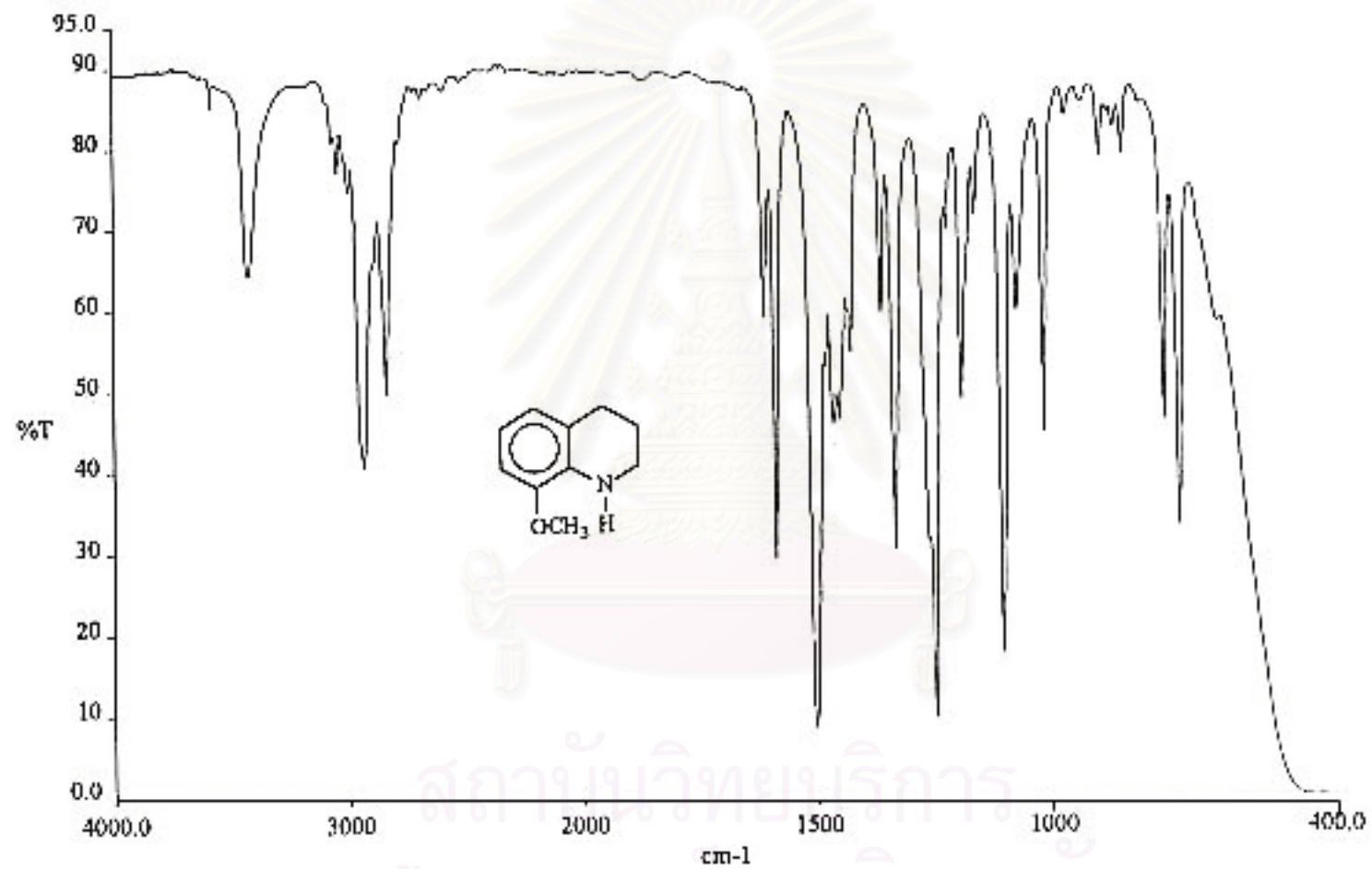
Figure 38. The IR spectrum (Neat, NaCl cell) of 1,2,3,4-tetrahydro-8-methoxyquinoline (2h).
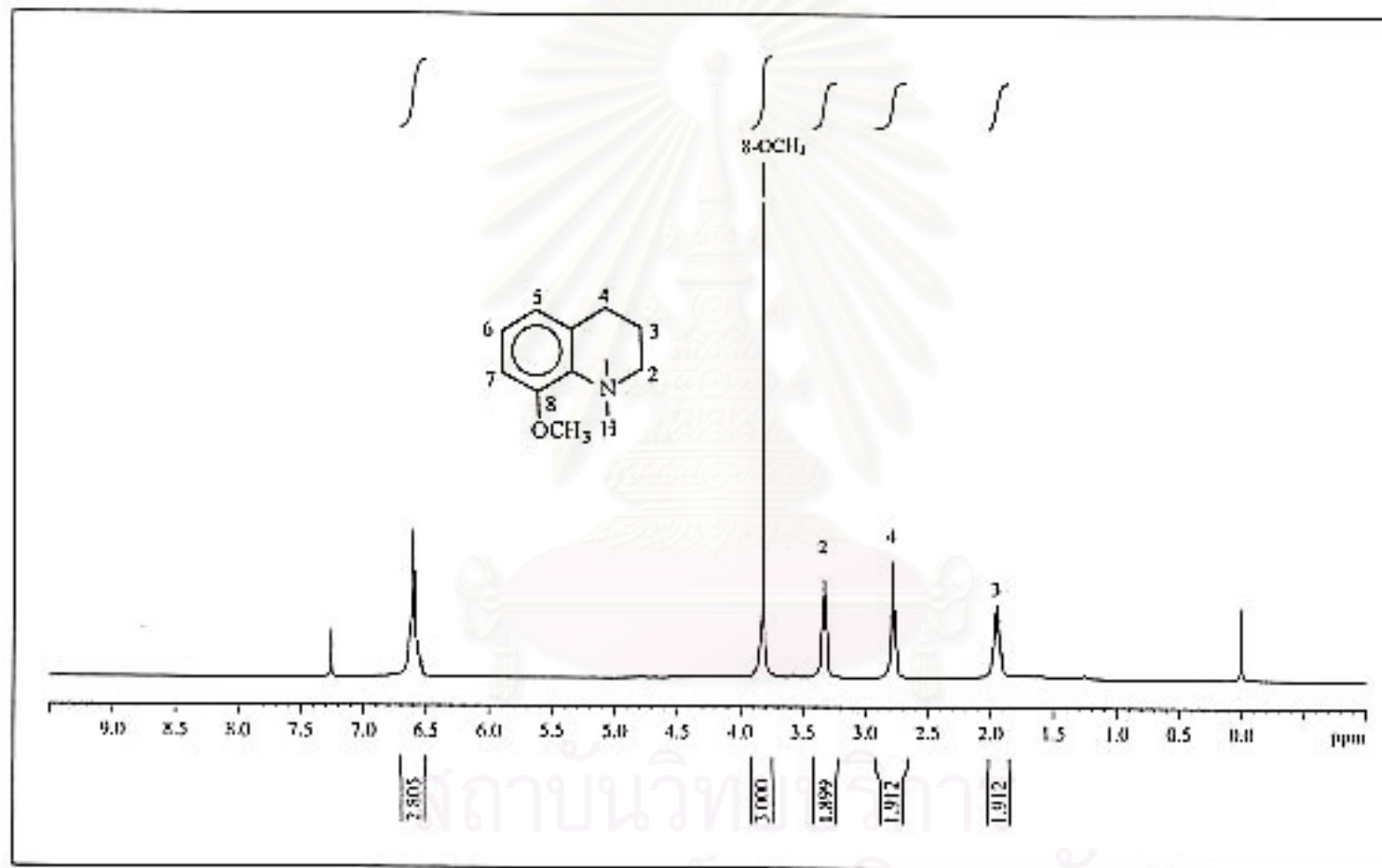
Figure 39. The 300 MHz 1H-NMR spectrum of 1,2,3,4-tetrahydro-8-methoxyquinoline (2h) in CDCl₃.
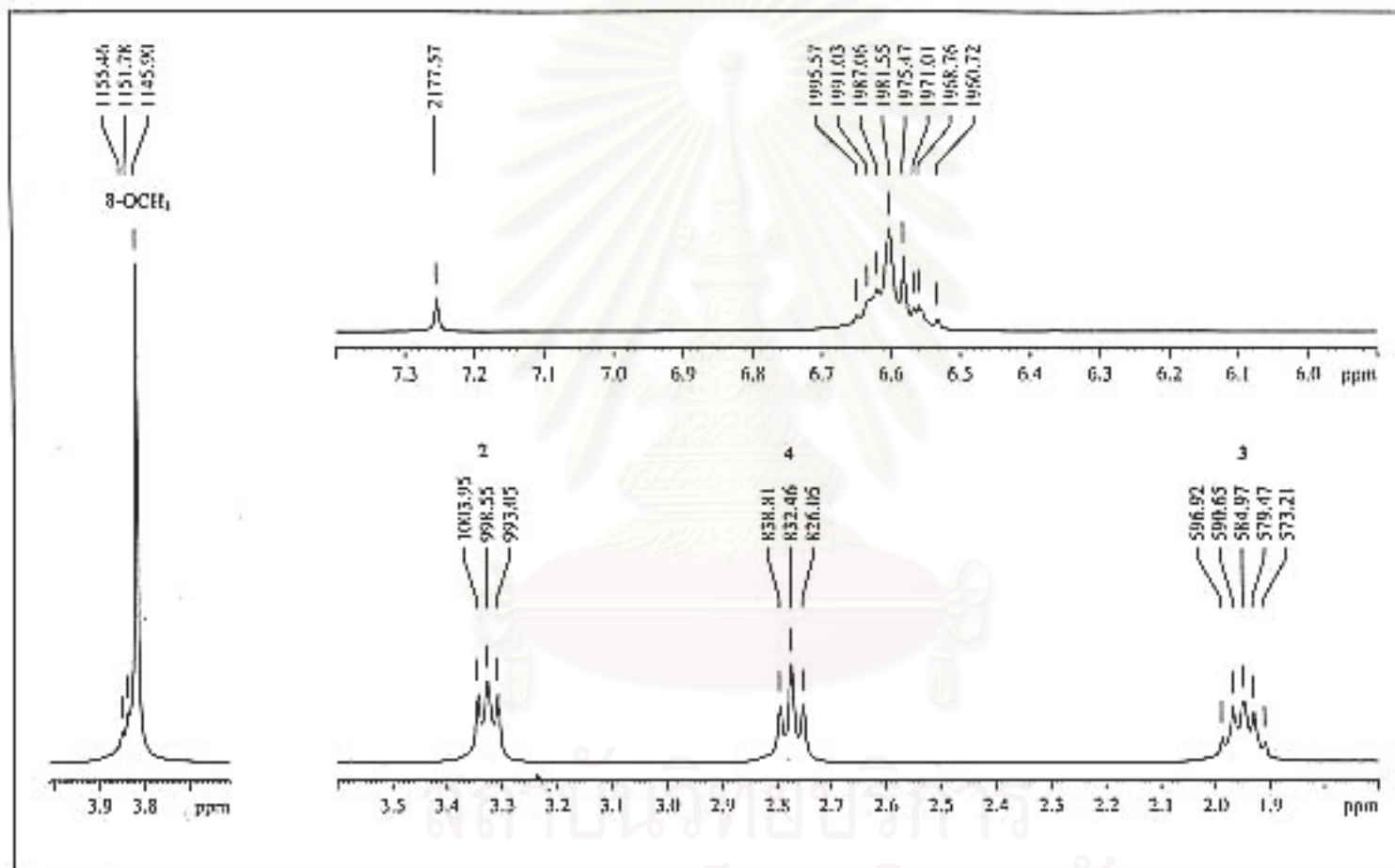
Figure 40. The 300 MHz 1H-NMR spectrum of 1,2,3,4-tetrahydro-8-methoxyquinoline (2h) in CDCl$_3$. (Enlarged scale)
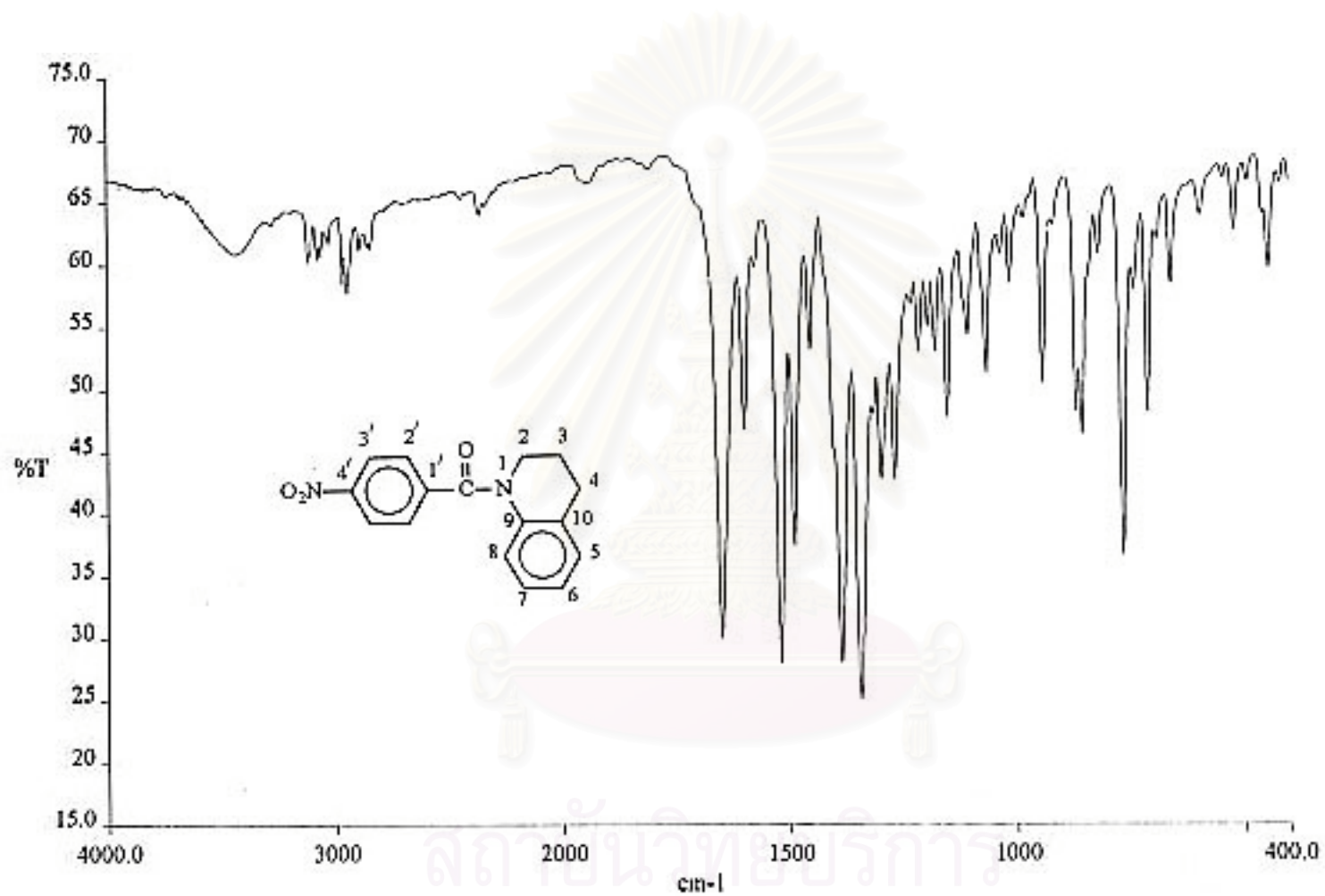
Figure 41. The IR spectrum (KBr) of N-(*p*-nitrobenzoyl)-1,2,3,4-tetrahydroquinoline (3a, CU-17-01).
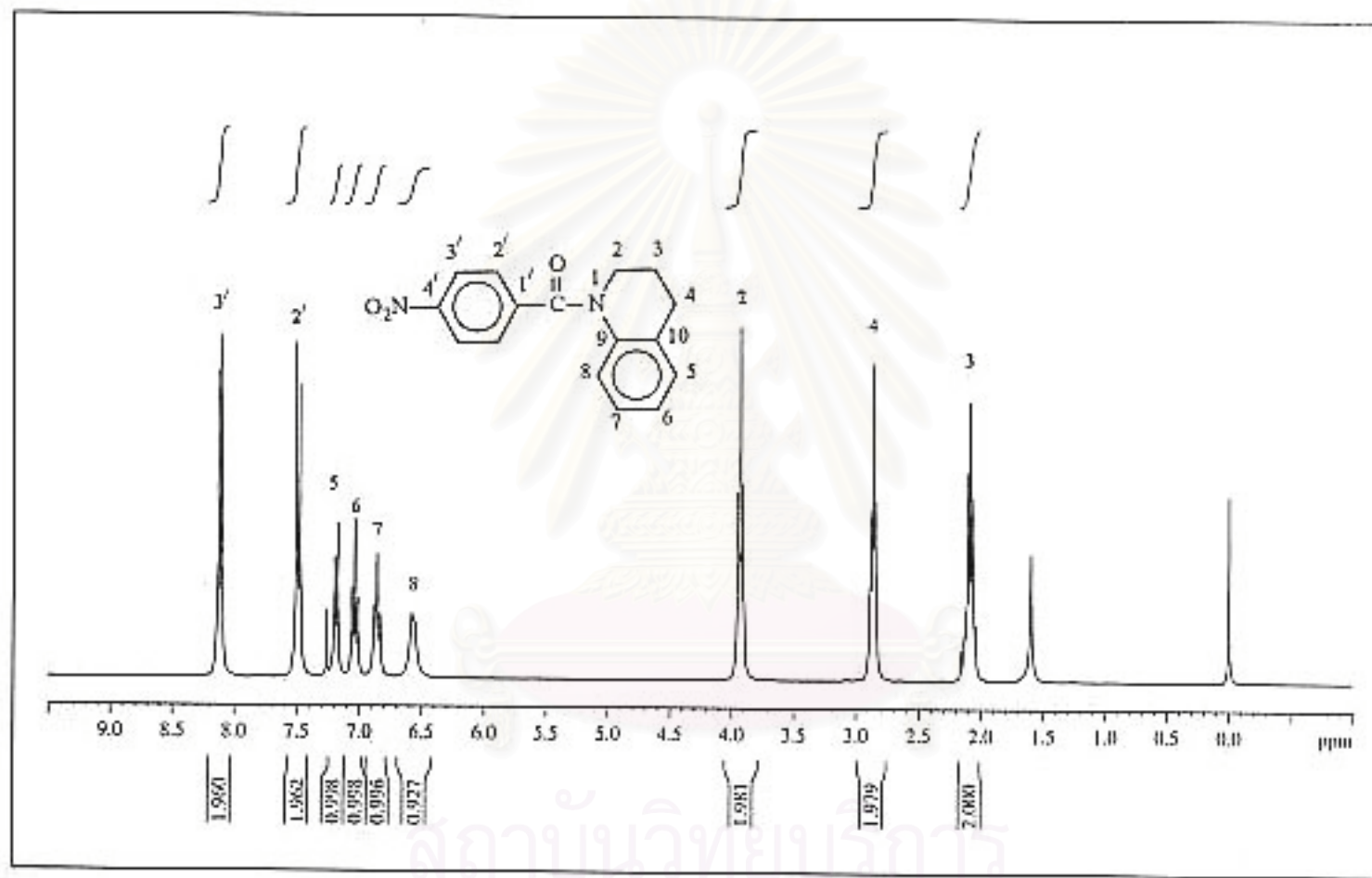
Figure 42. The 300 MHz 1H-NMR spectrum of N-(*p*-nitrobenzoyl)-1,2,3,4-tetrahydroquinoline (3a, CU-17-01) in CDCl₃.
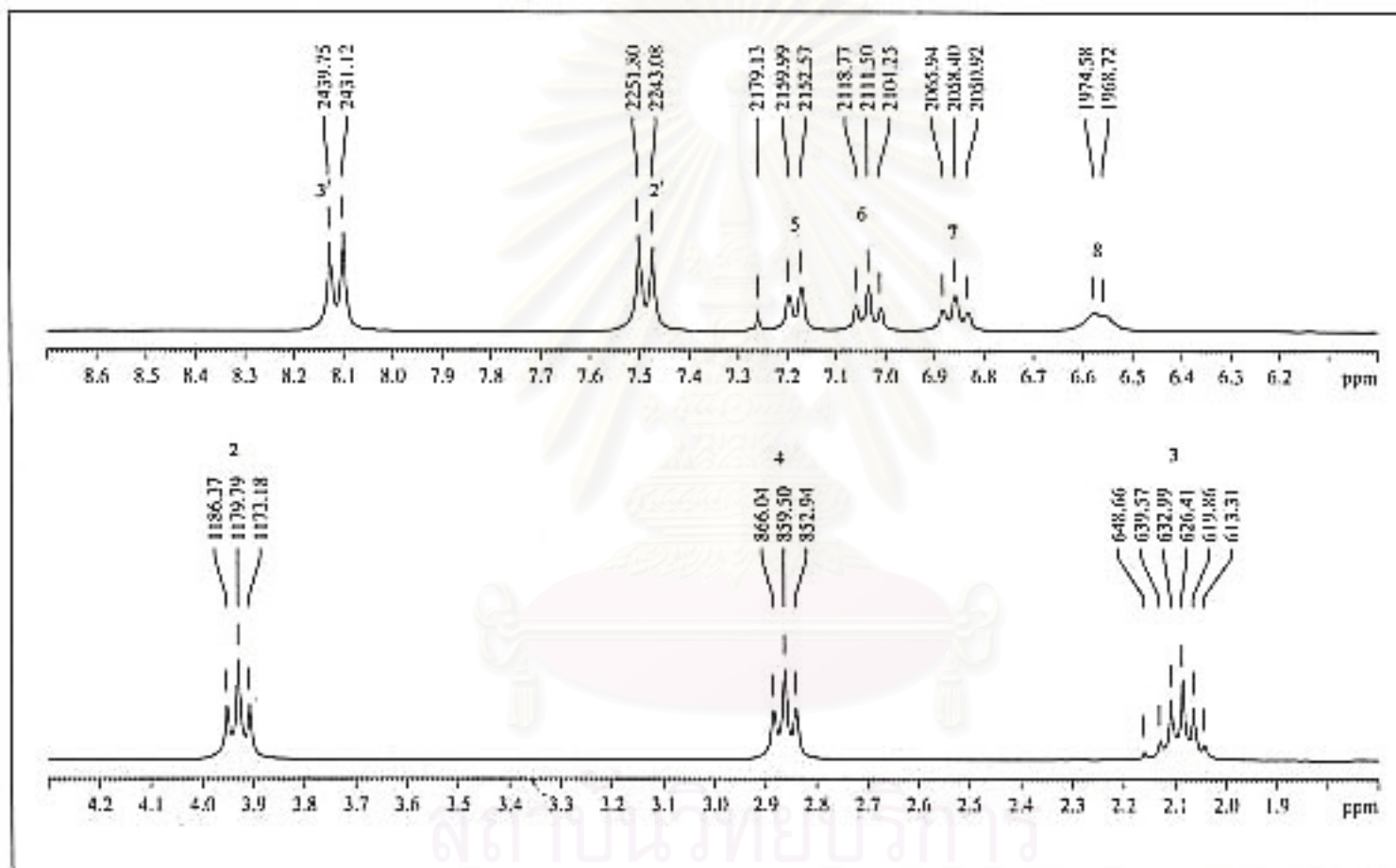
Figure 43. The 300 MHz 1H-NMR spectrum of N-(*p*-nitrobenzoyl)-1,2,3,4-tetrahydroquinoline (3a, CU-17-01) in CDCl₃. (Enlarged scale)
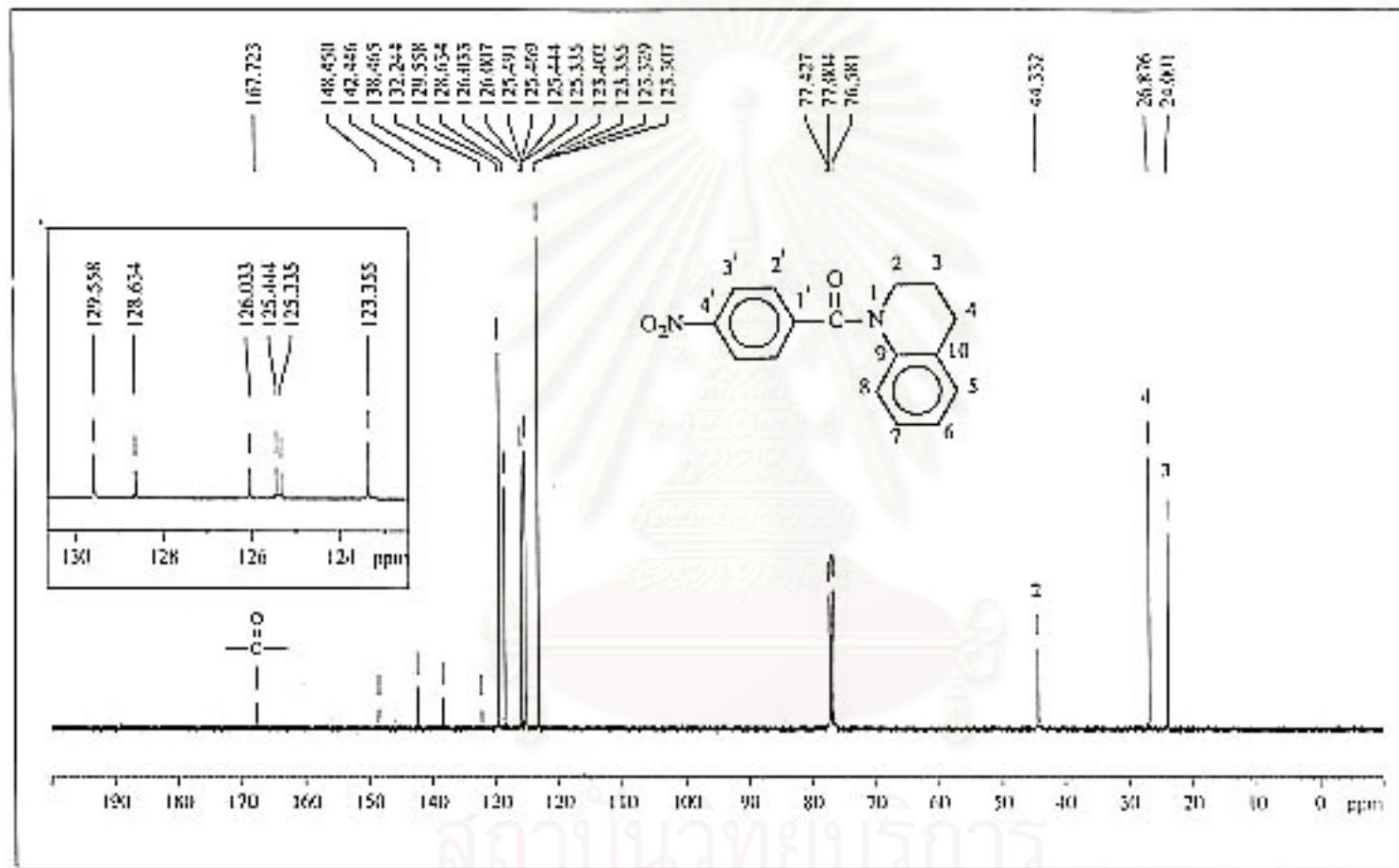
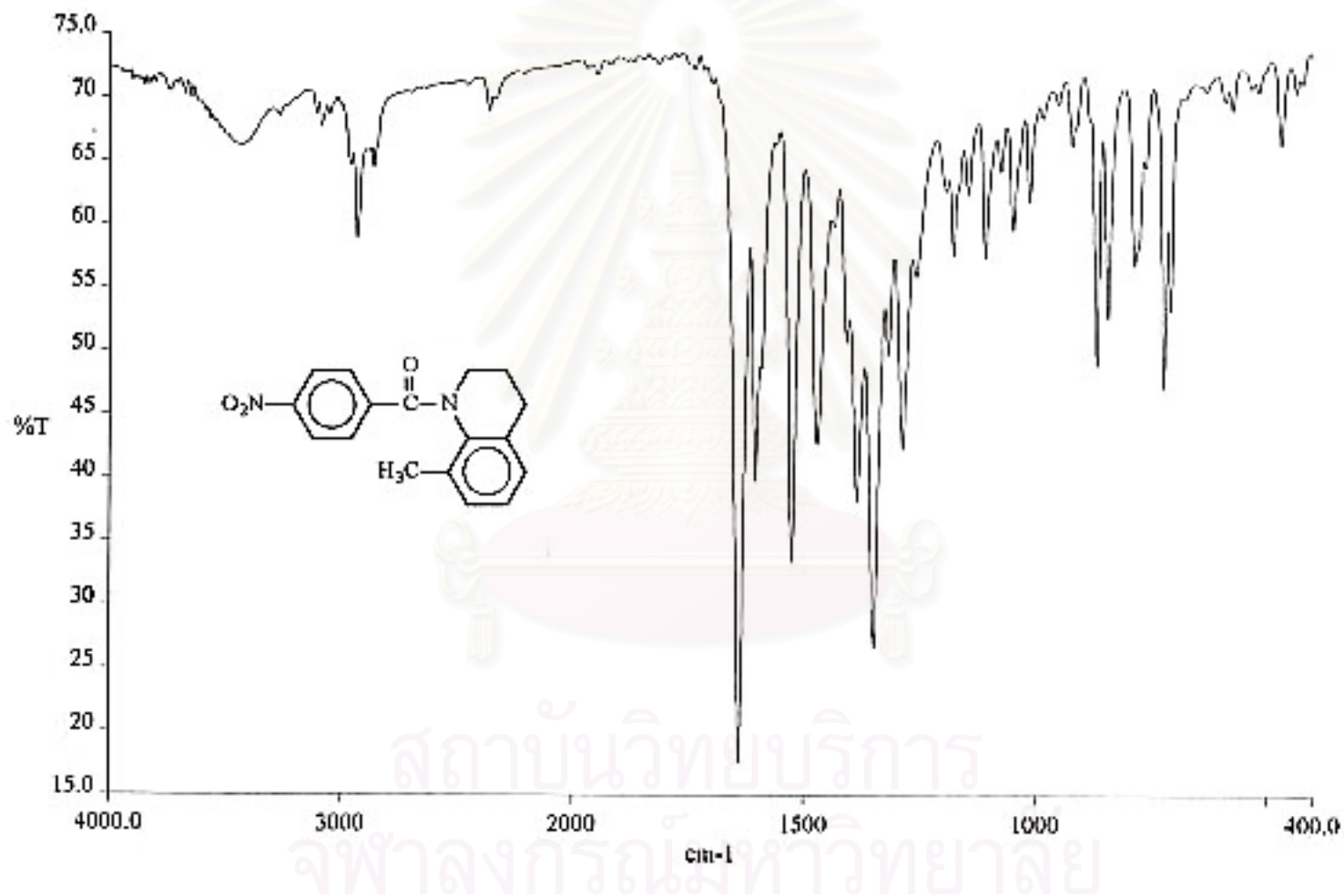Figure 44. The 75 MHz 13C-NMR decoupled spectrum of N-(*p*-nitrobenzoyl)-1,2,3,4-tetrahydroquinoline (3a, CU-17-01) in CDCl₃.
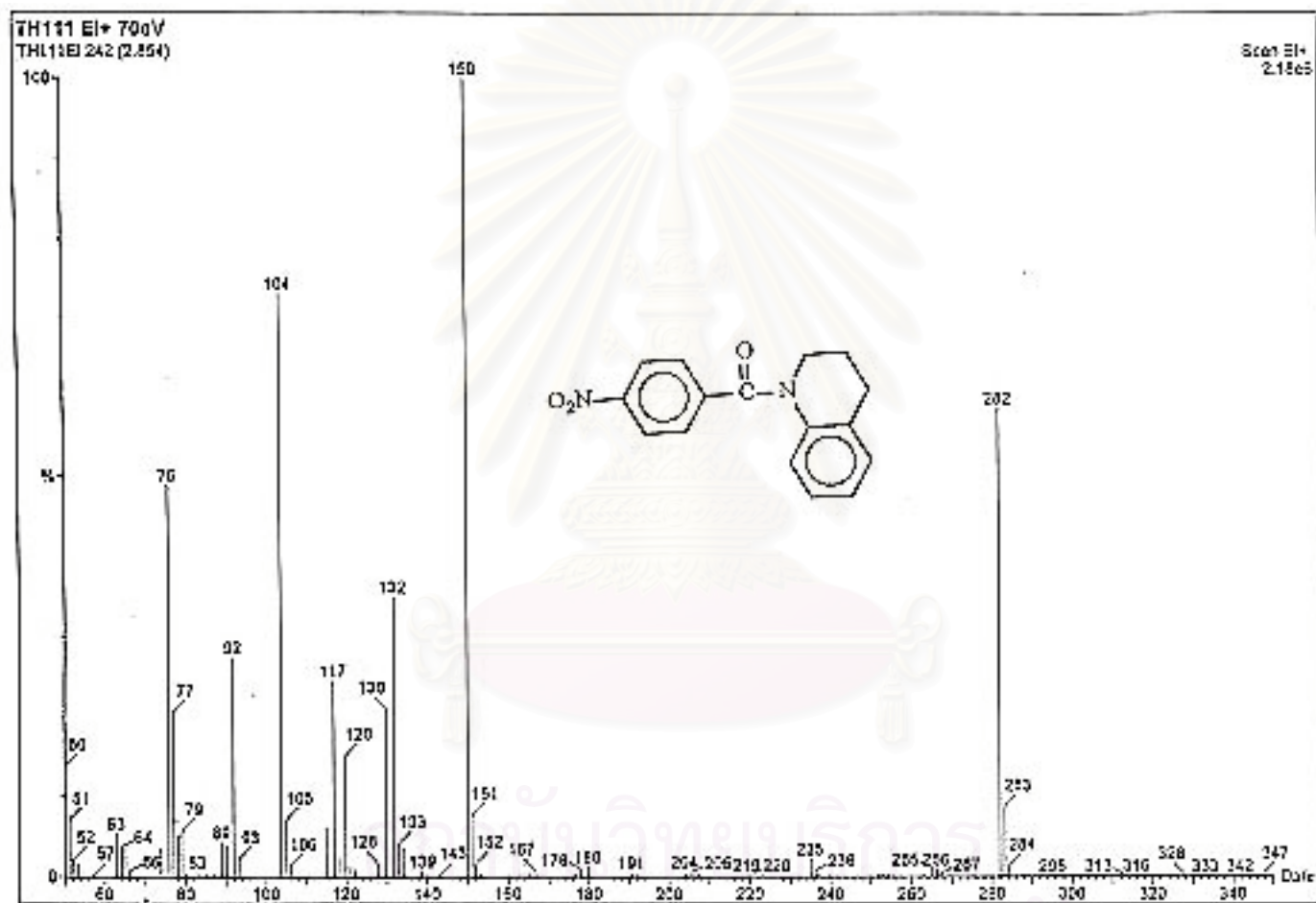
Figure 45. The electron impact mass spectrum of N-(*p*-nitrobenzoyl)-1,2,3,4-tetrahydroquinoline (3a, CU-17-01).
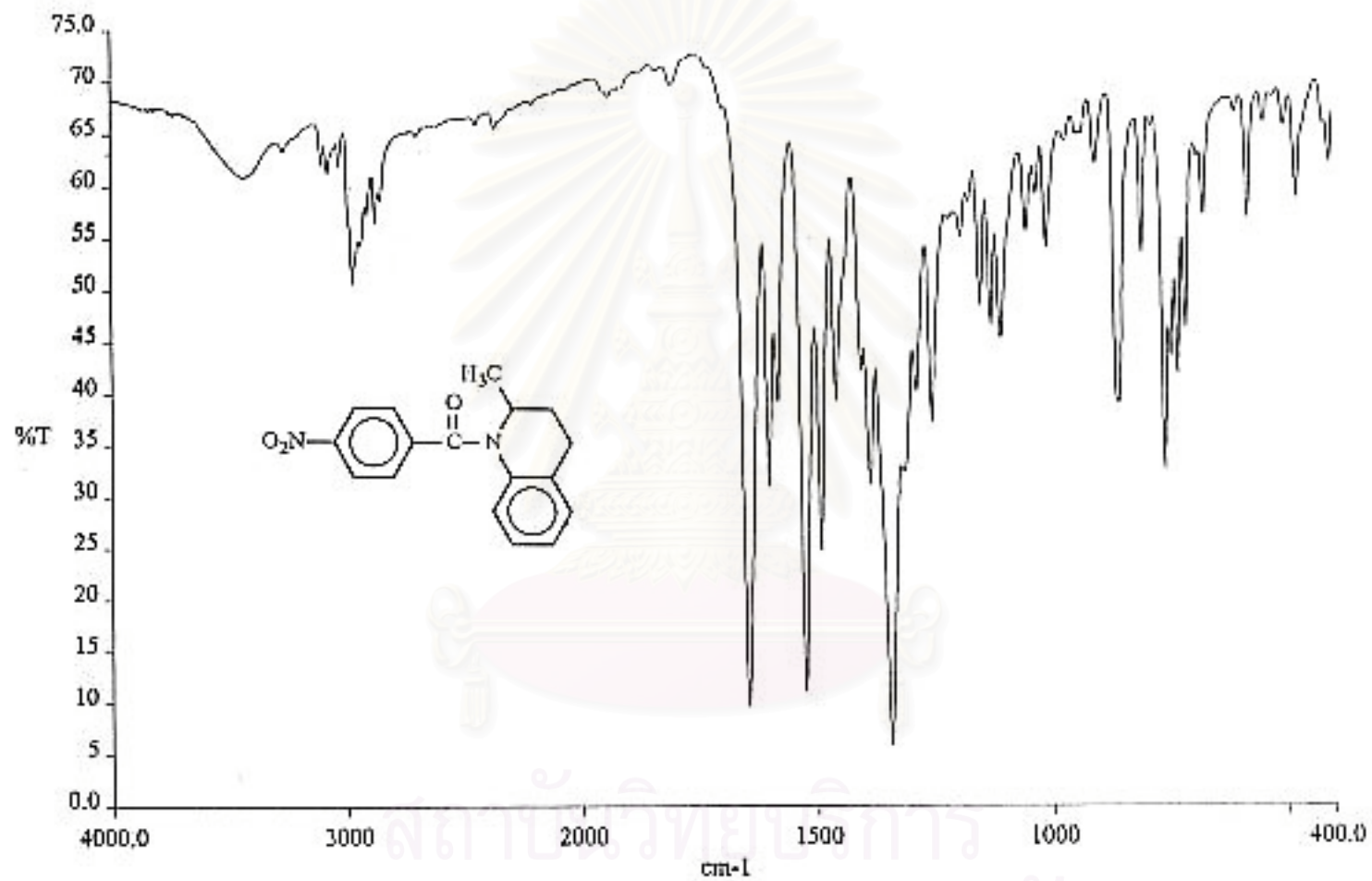
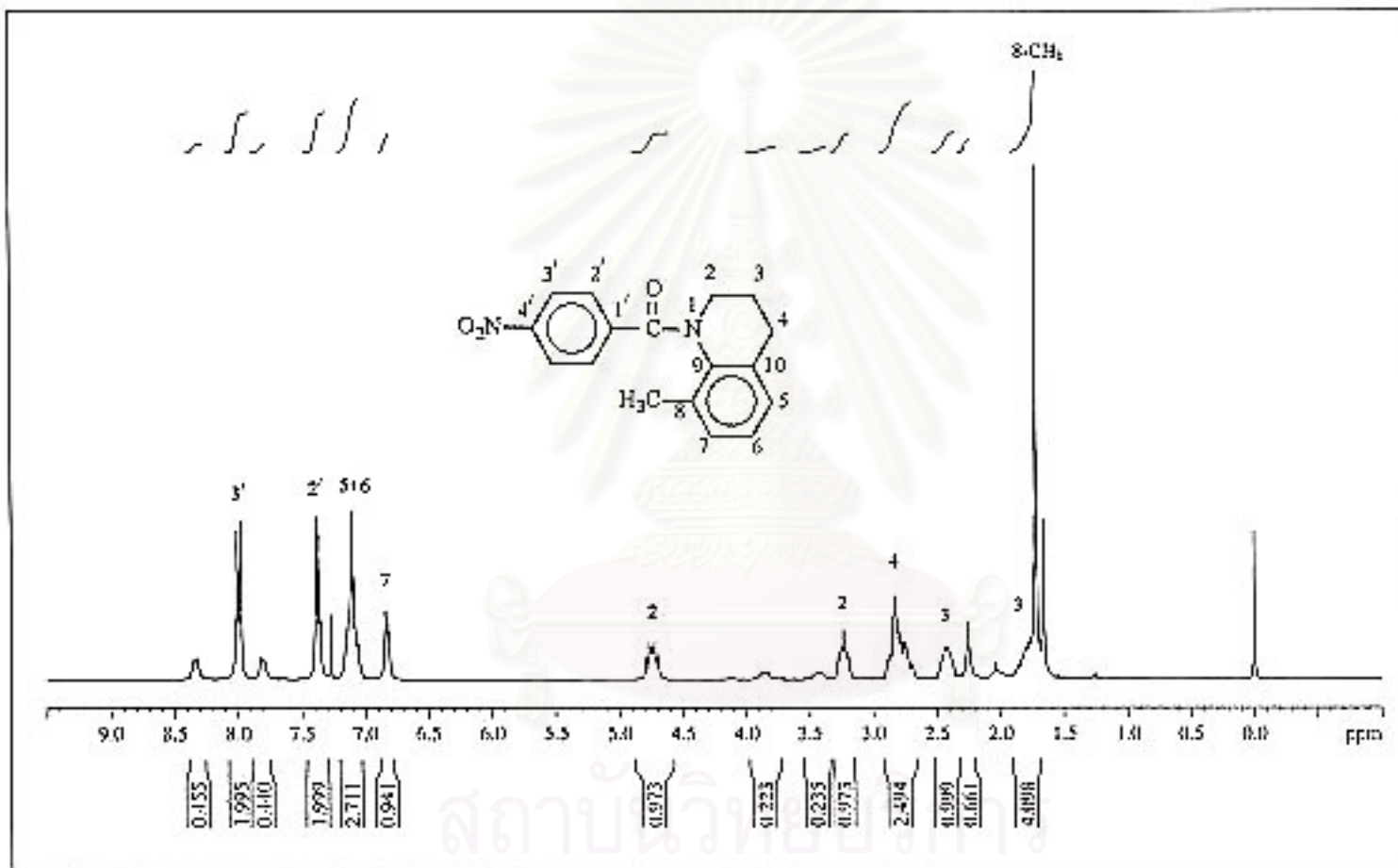Figure 46. The IR spectrum (KBr) of N-(*p*-nitrobenzoyl)-1,2,3,4-tetrahydro-2-methylquinoline (3b, CU-17-03).
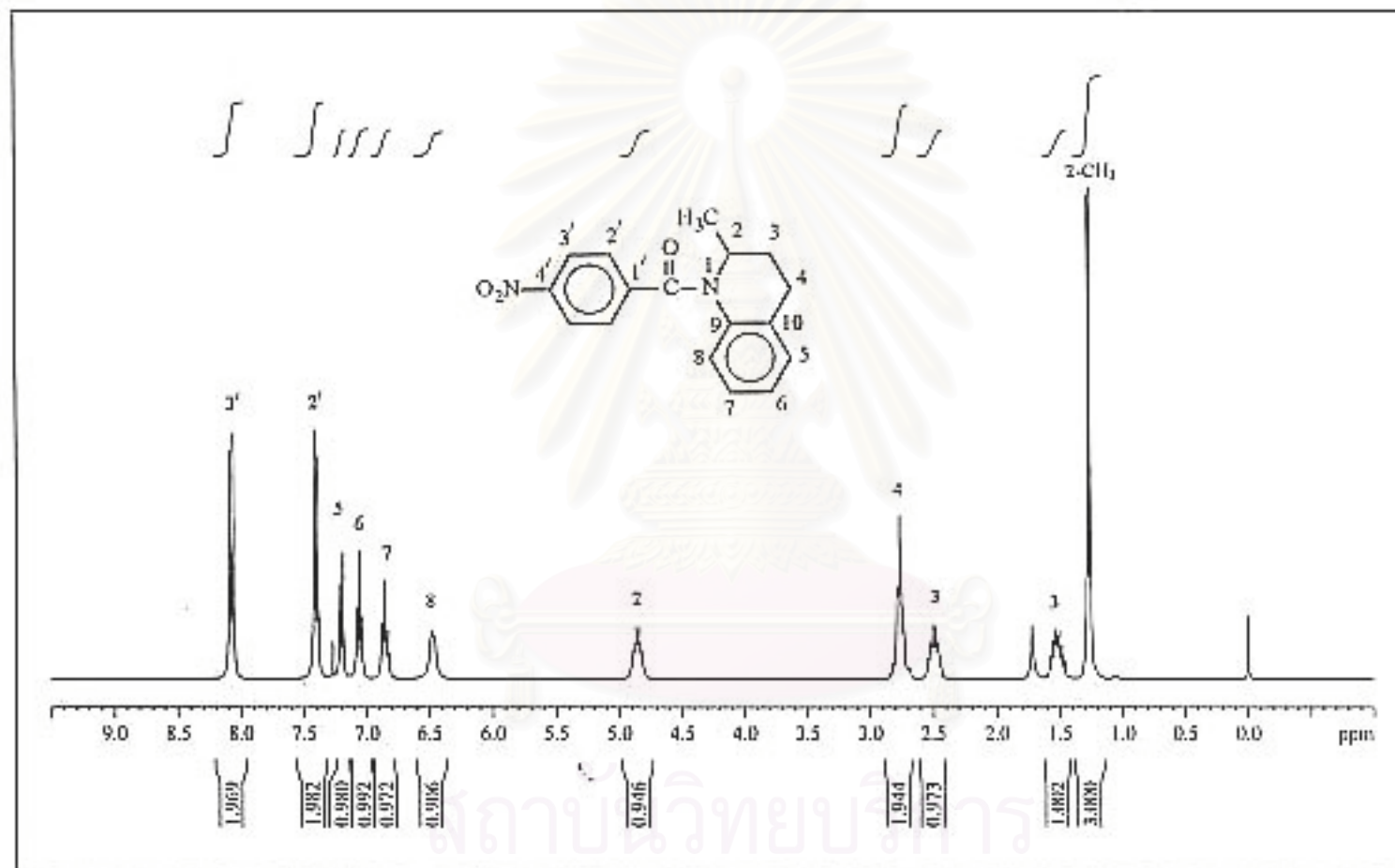
Figure 47. The 300 MHz 1H-NMR spectrum of N-(*p*-nitrobenzoyl)-1,2,3,4-tetrahydro-2-methylquinoline (3b, CU-17-03) in CDCl₃.
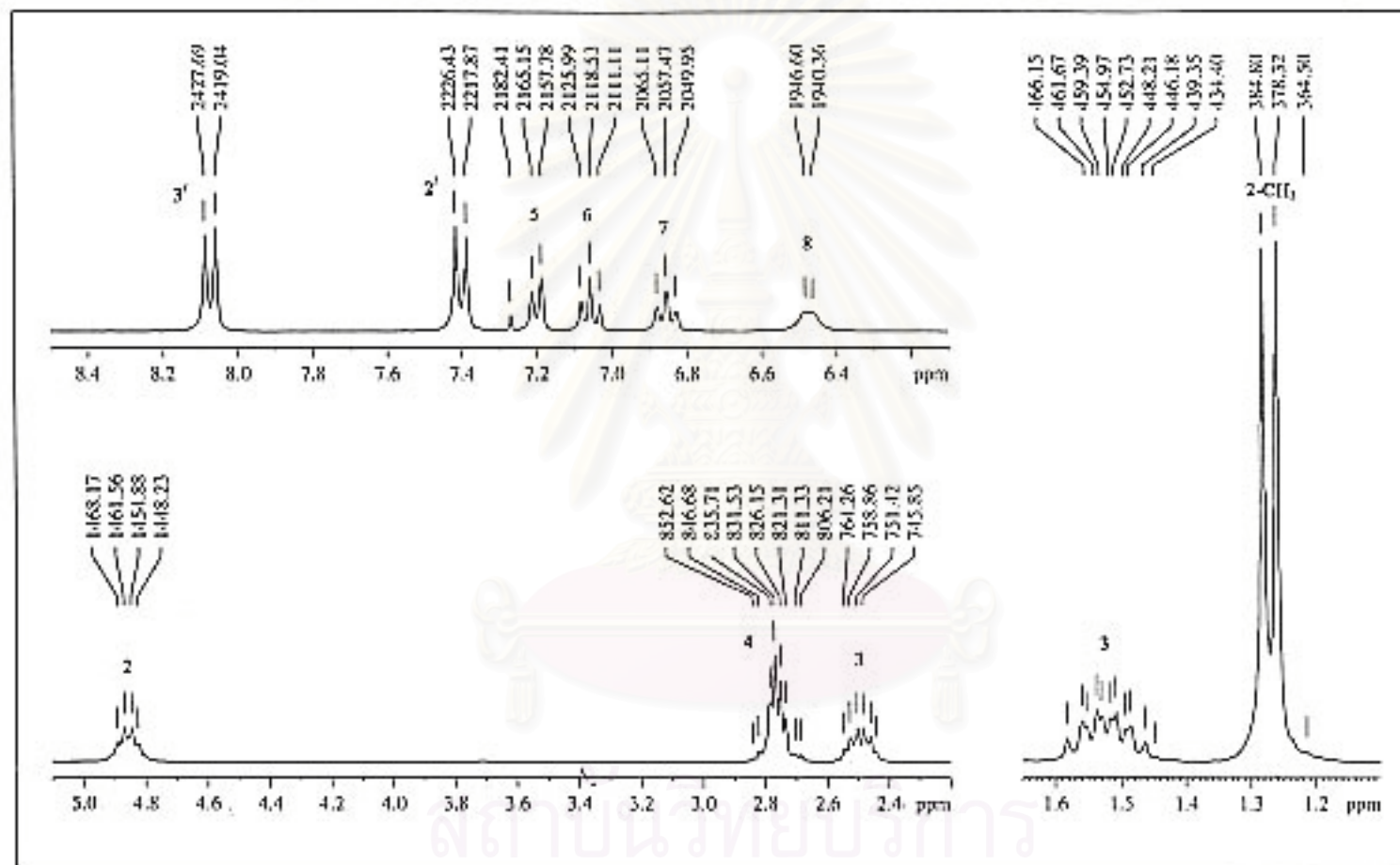
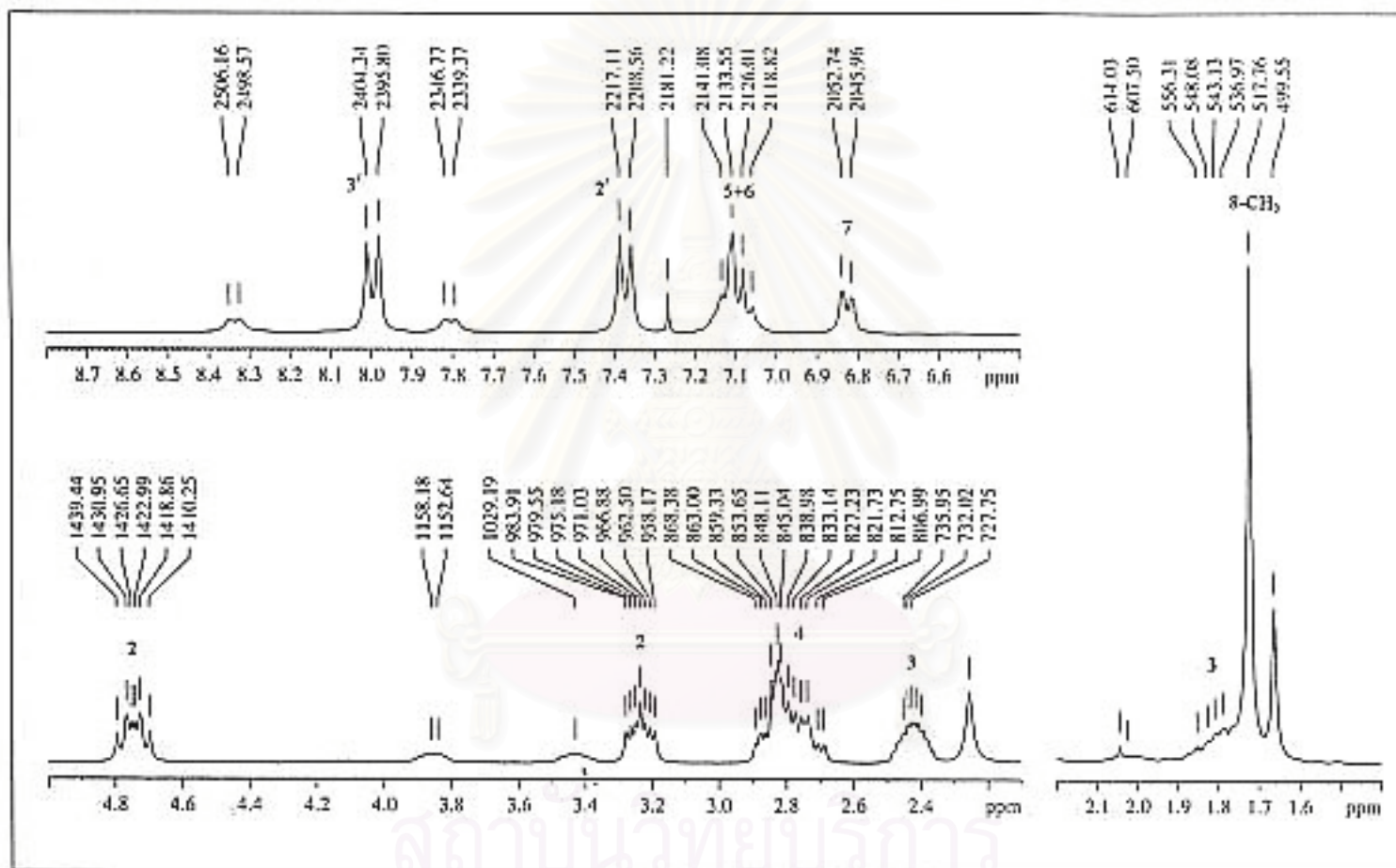Figure 48. The 300 MHz 1H-NMR spectrum of N-(*p*-nitrobenzoyl)-1,2,3,4-tetrahydro-2-methylquinoline (3b, CU-17-03) in CDCl₃. (Enlarged scale)
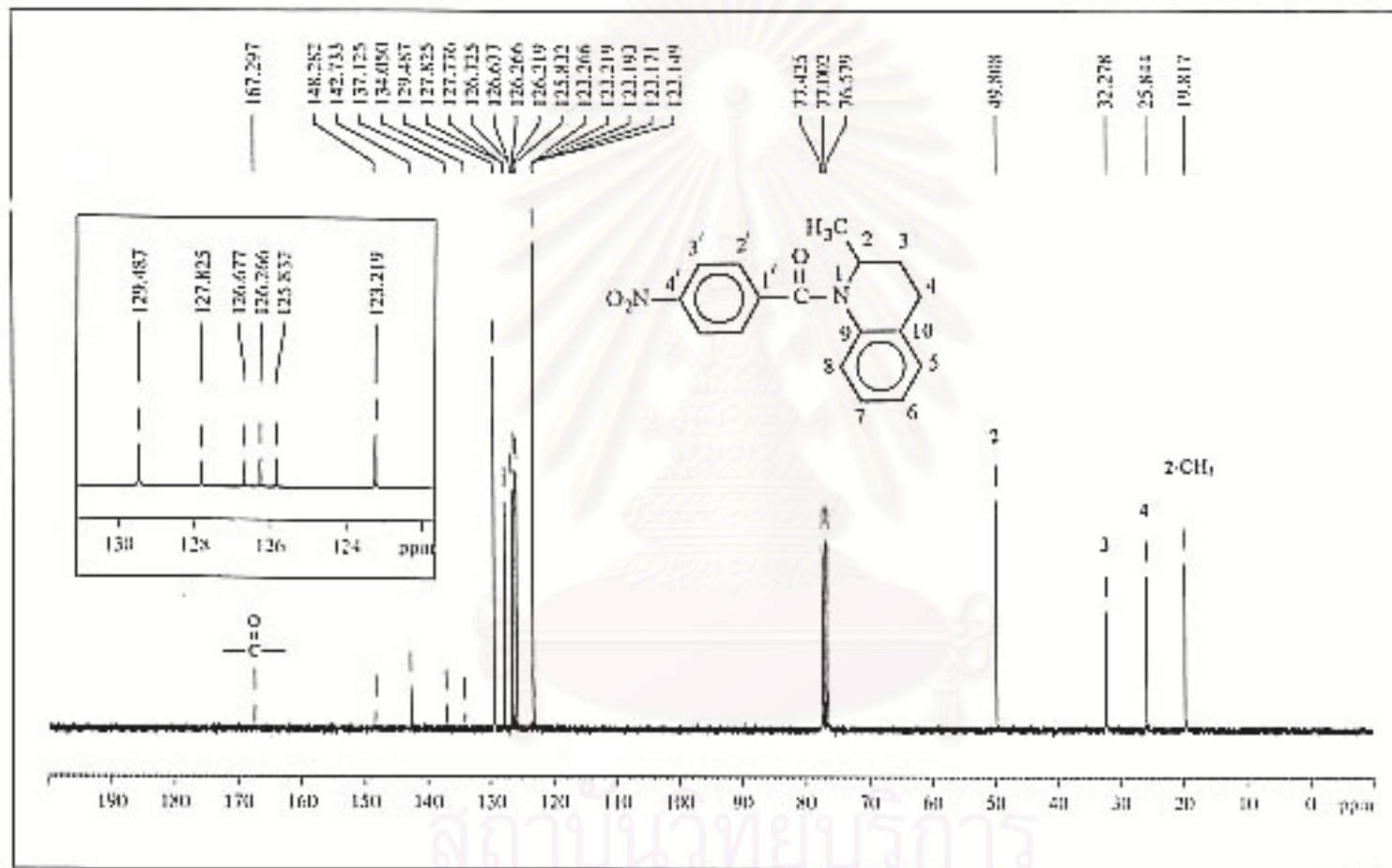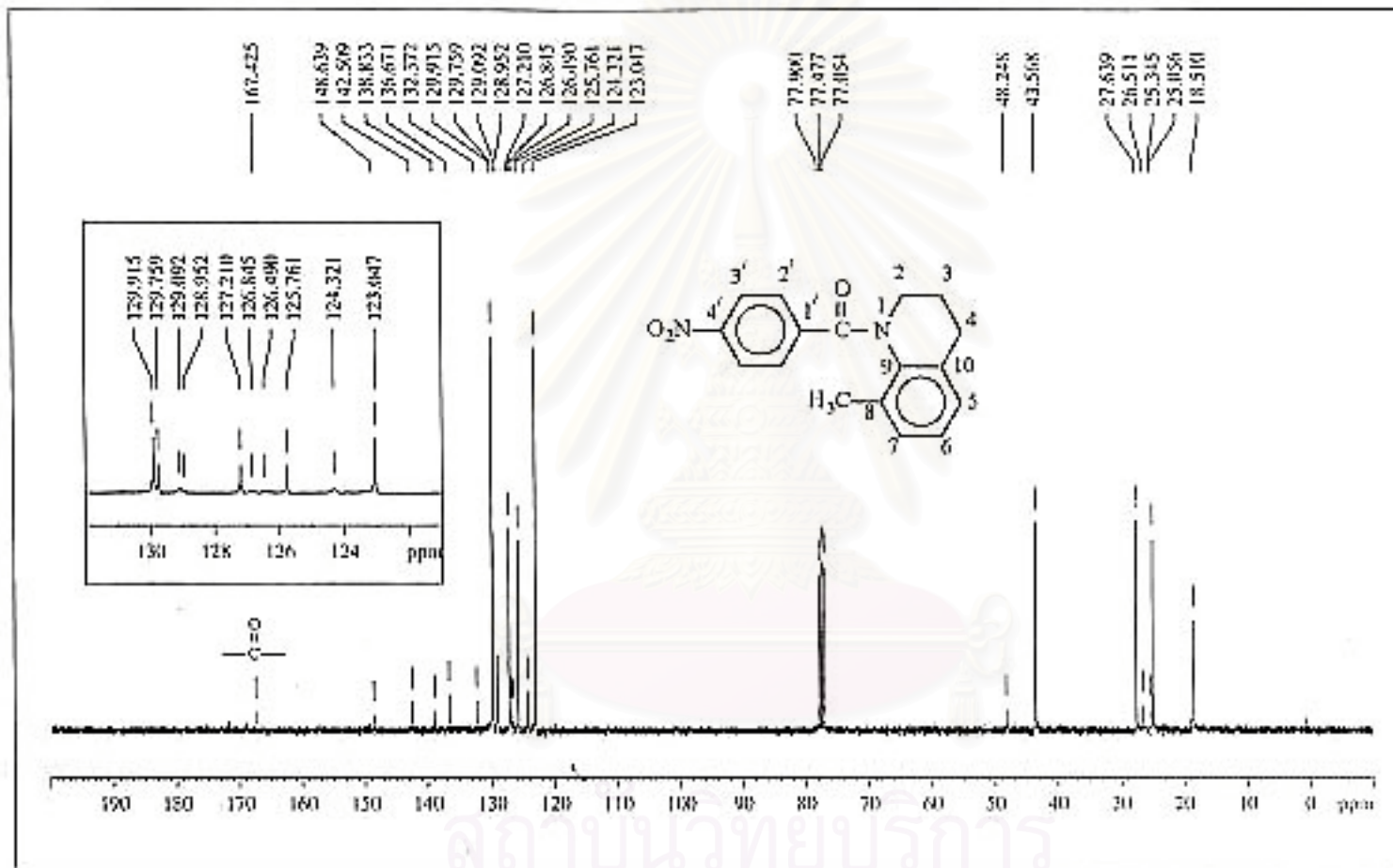
Figure 49. The 75 MHz 13C-NMR decoupled spectrum of N-(*p*-nitrobenzoyl)-1,2,3,4-tetrahydro-2-methylquinoline (3b, CU-17-03) in CDCl₃.
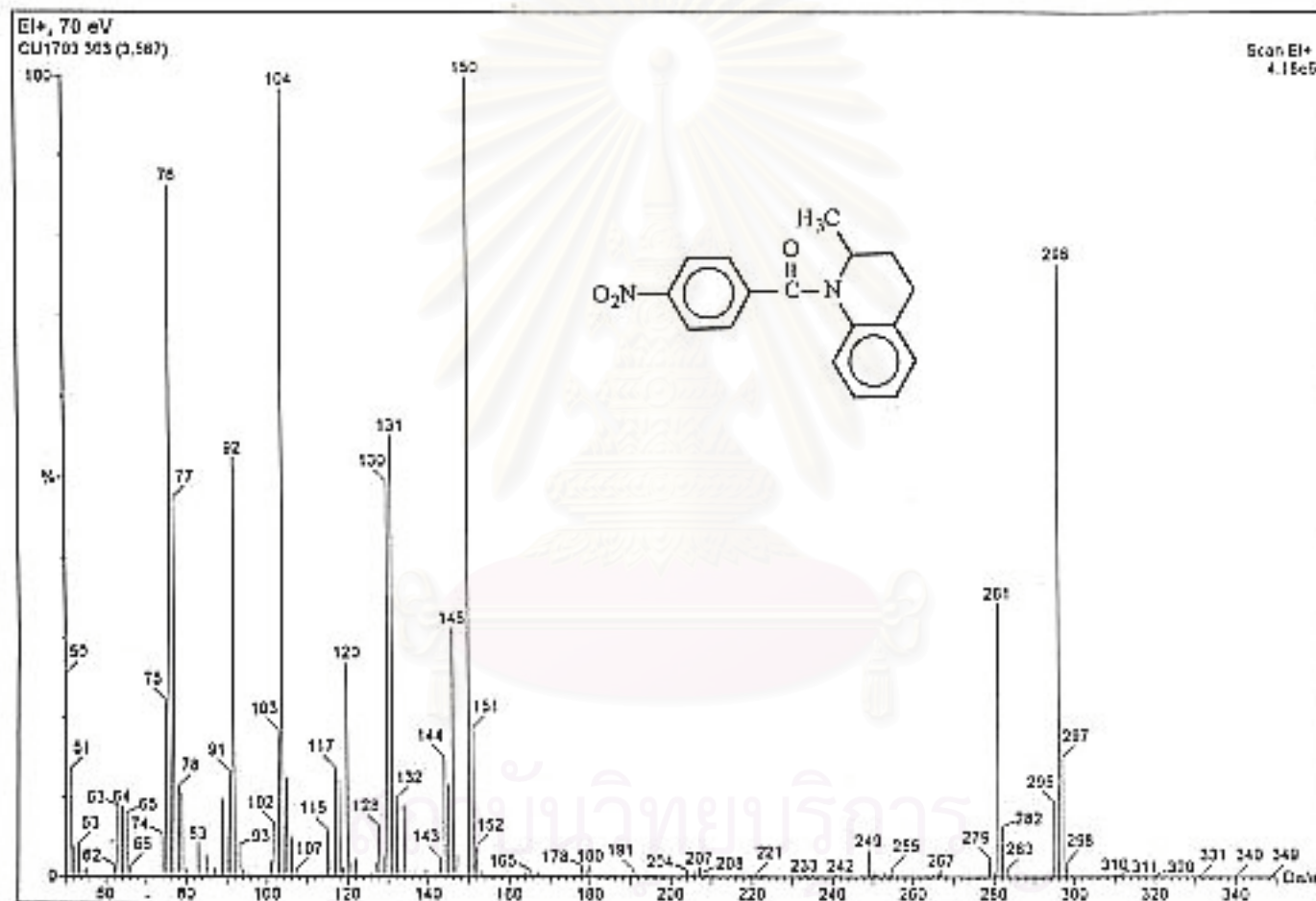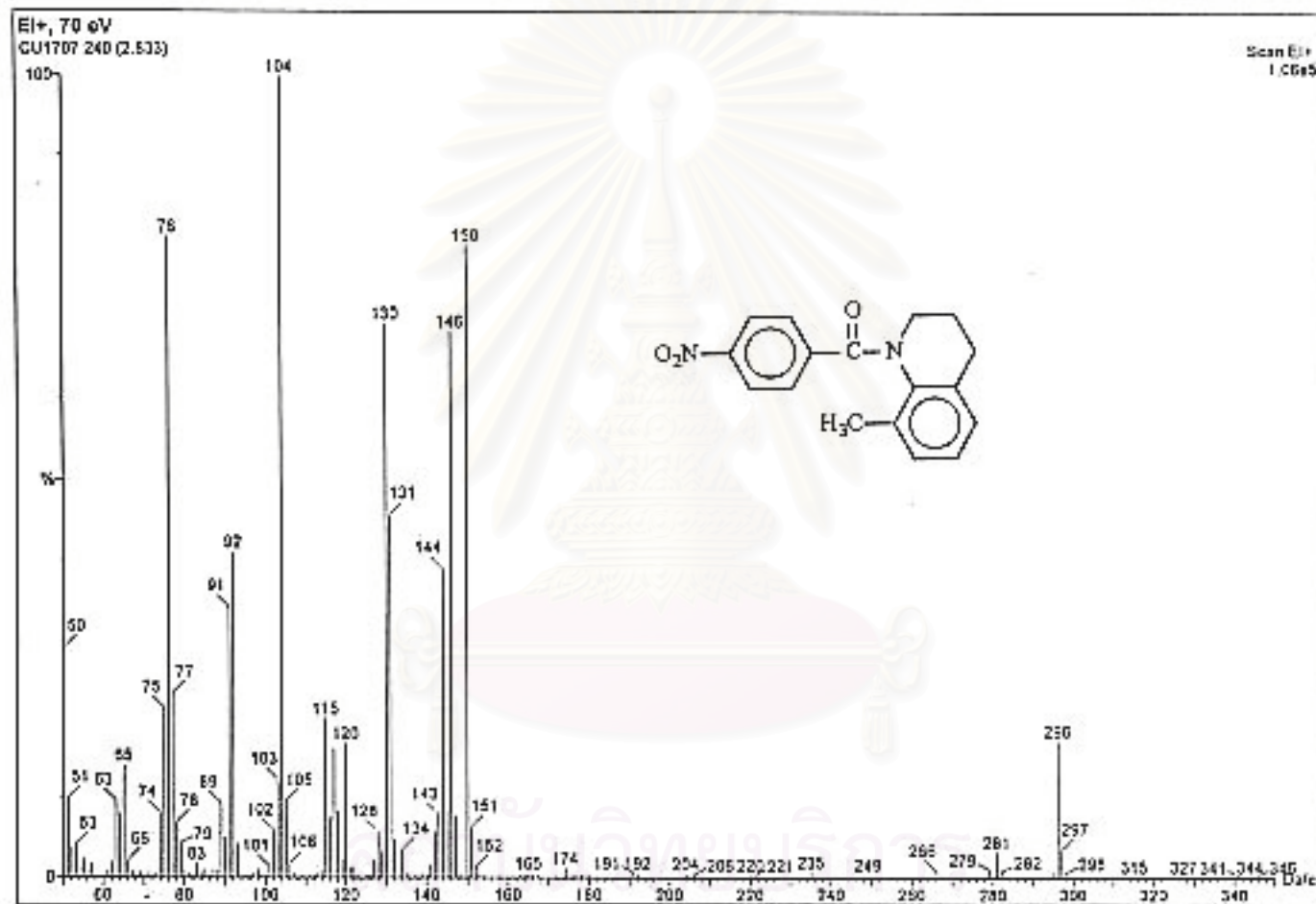
Figure 50. The electron impact mass spectrum of N-(*p*-nitrobenzoyl)-1,2,3,4-tetrahydro-2-methylquinoline (3b, CU-17-03).
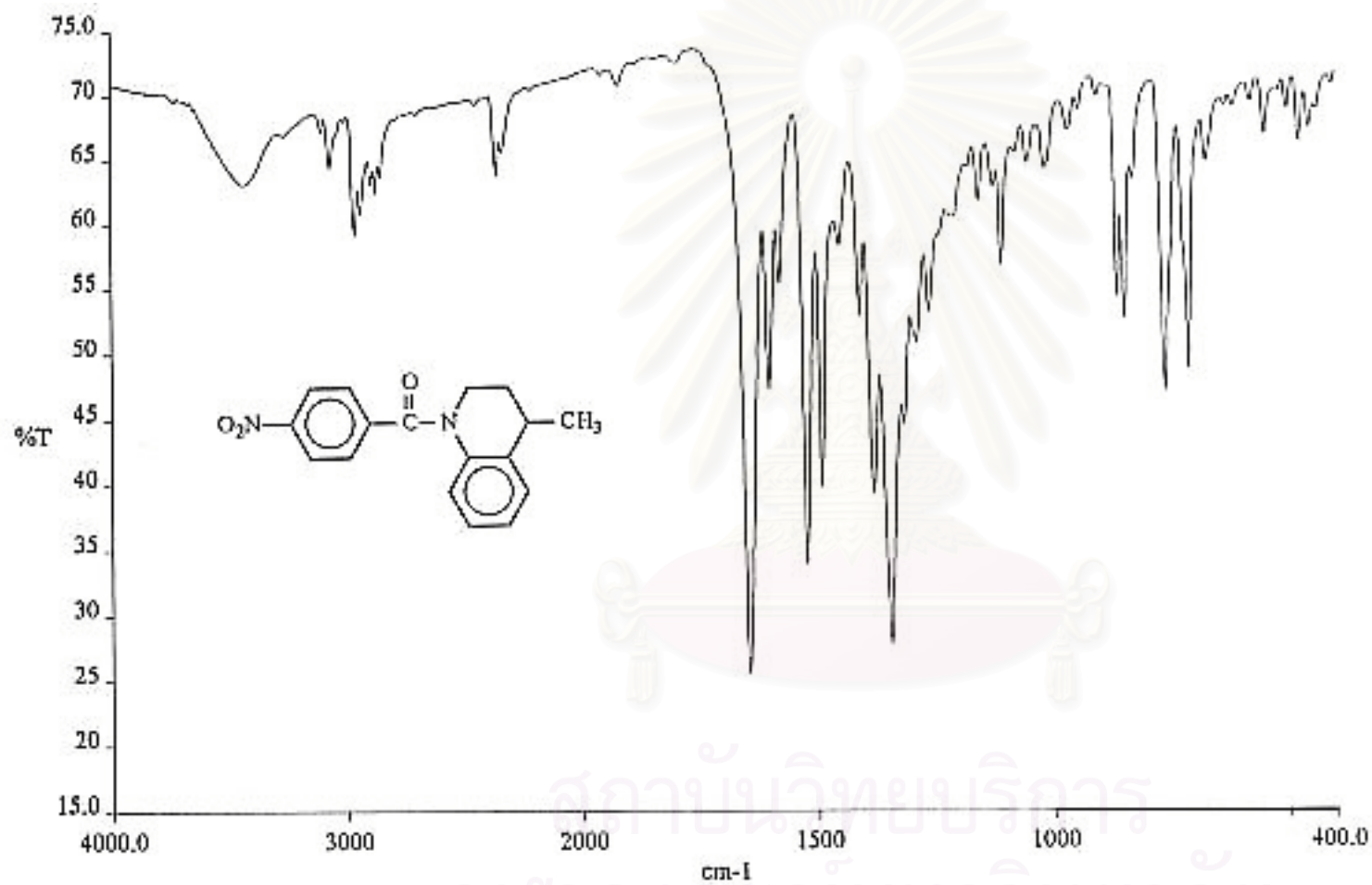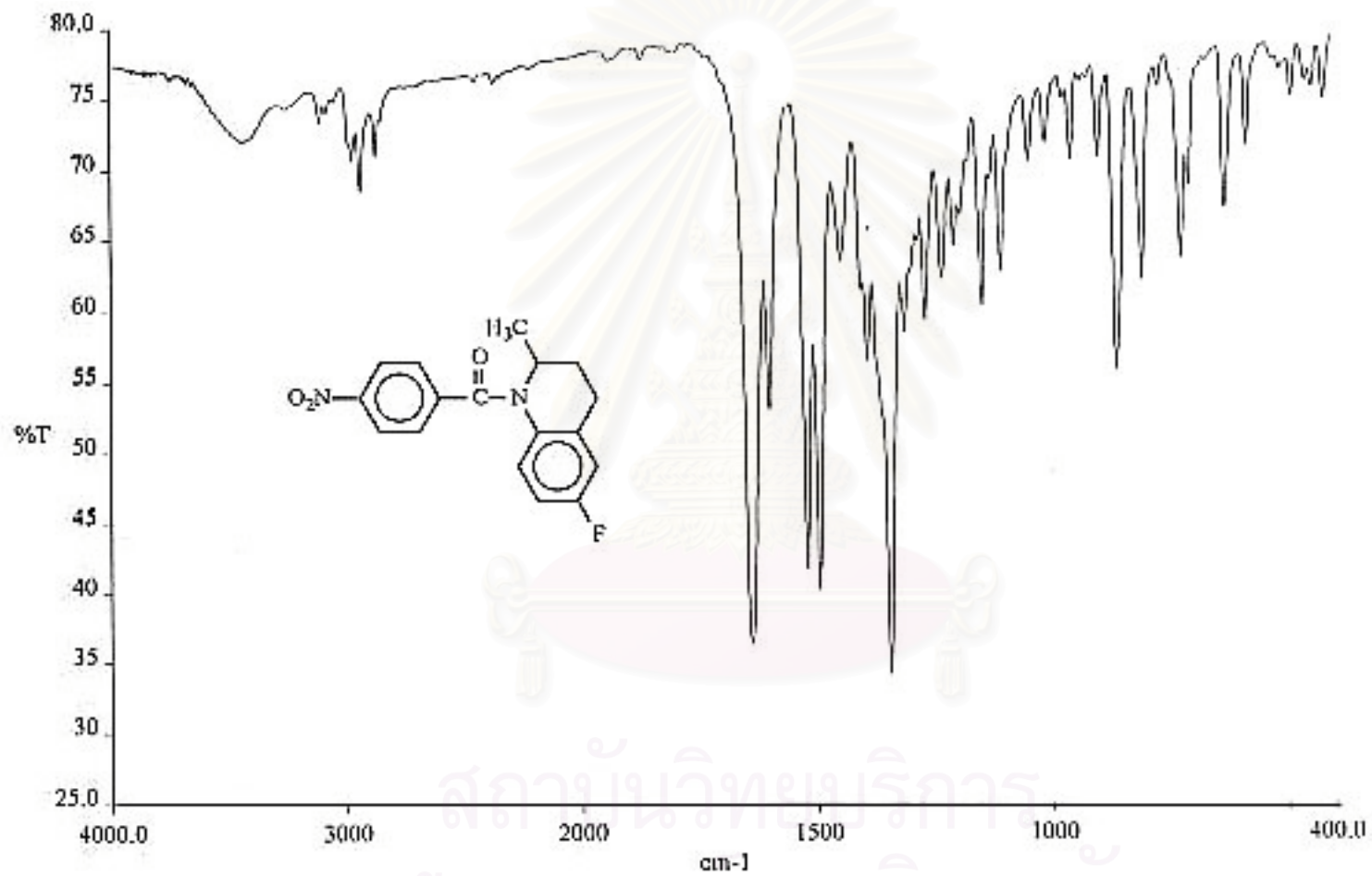
Figure 51. The IR spectrum (KBr) of N-(*p*-nitrobenzoyl)-1,2,3,4-tetrahydro-4-methylquinoline (3c, CU-17-05).
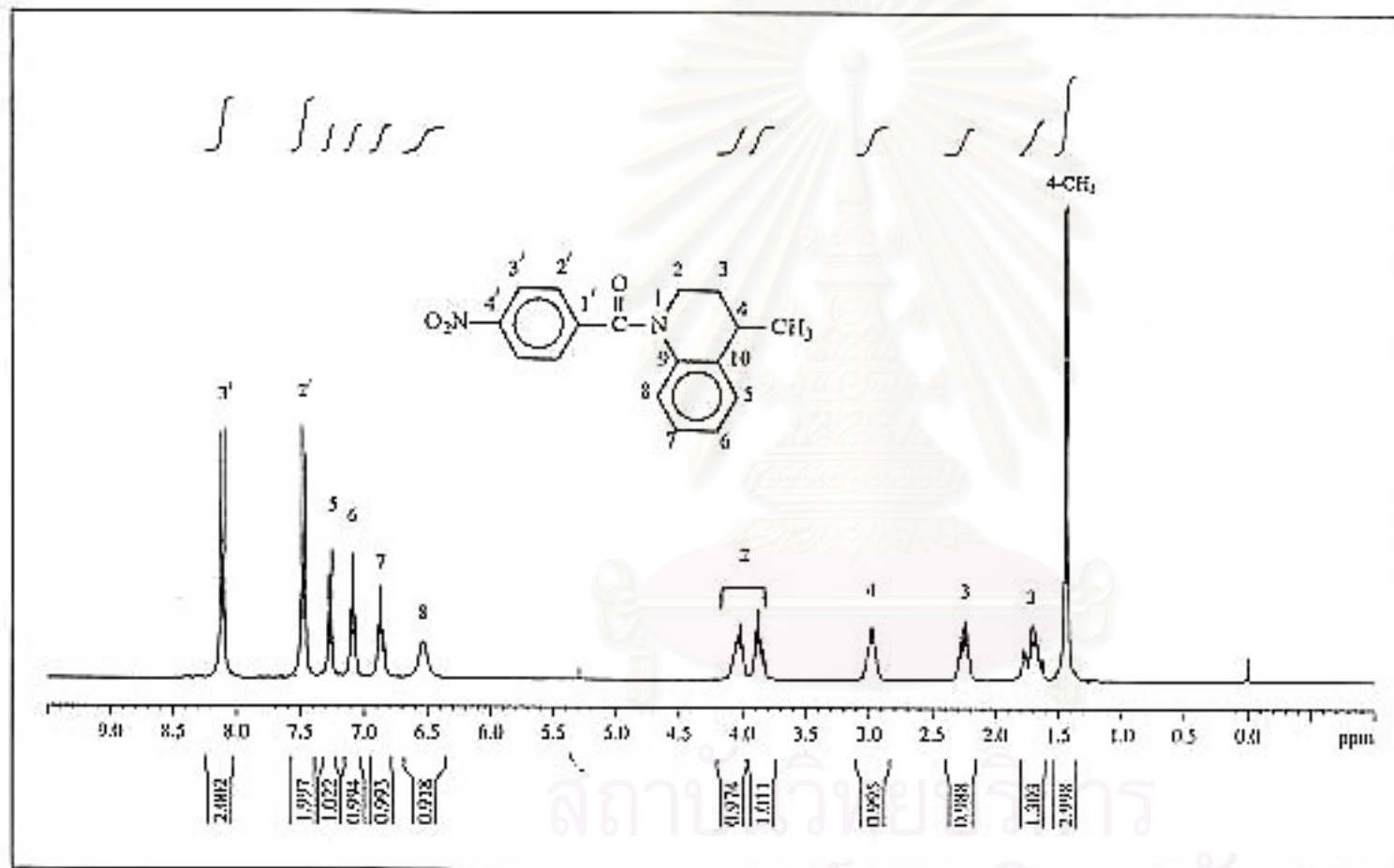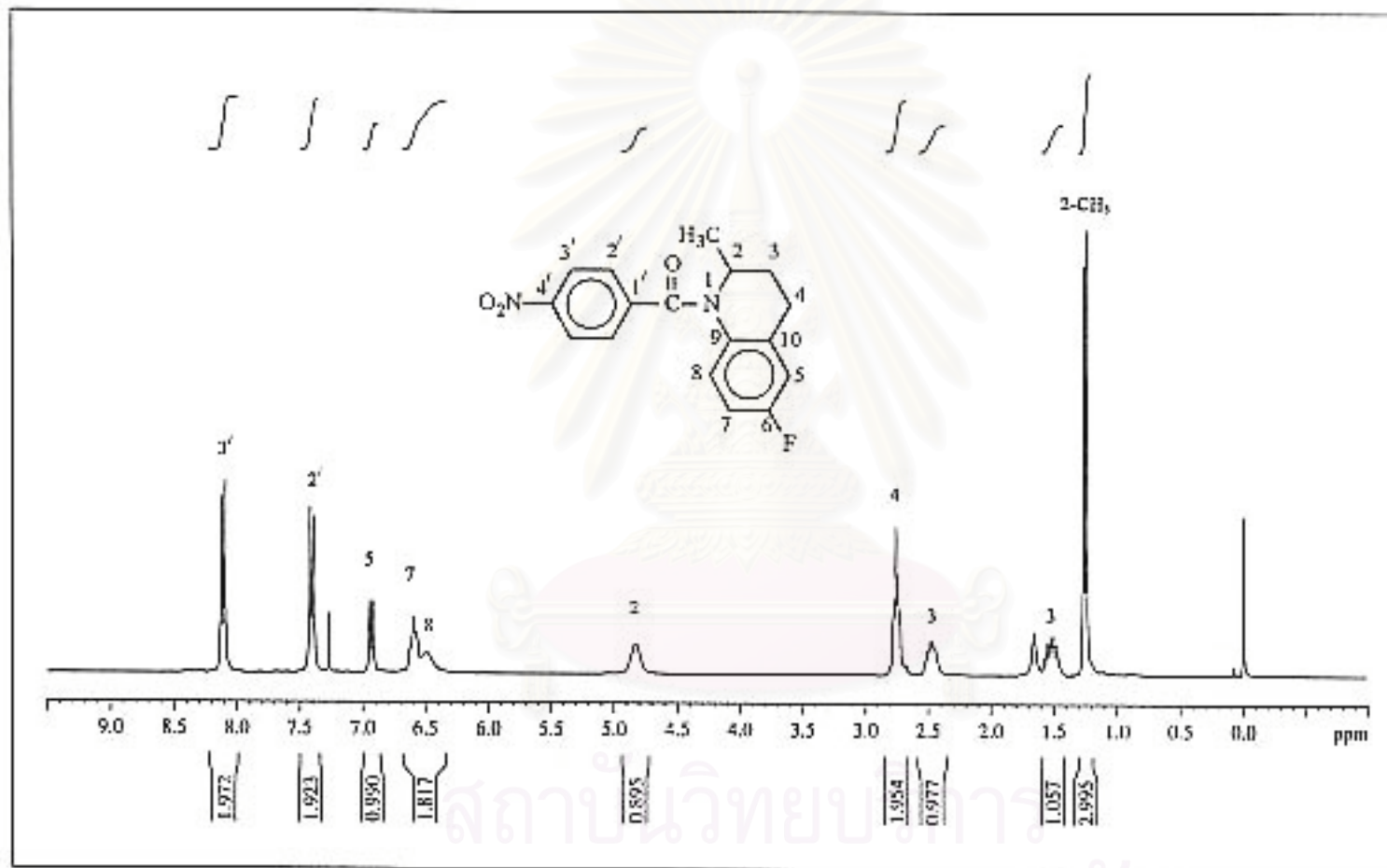
Figure 52. The 300 MHz 1H-NMR spectrum of N-(*p*-nitrobenzoyl)-1,2,3,4-tetrahydro-4-methylquinoline (3c, CU-17-05) in CDCl₃.
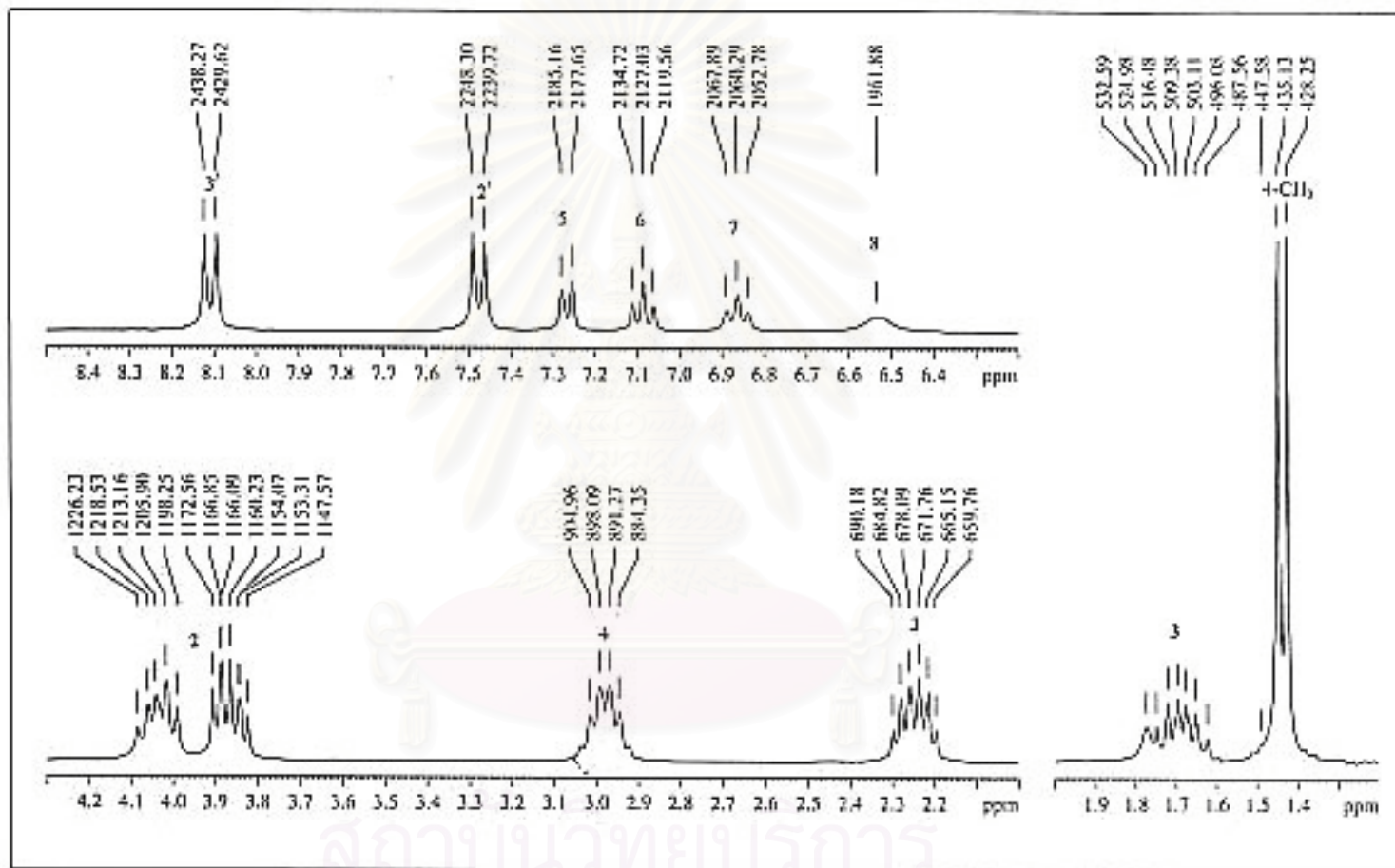
Figure 53. The 300 MHz 1H-NMR spectrum of N-(*p*-nitrobenzoyl)-1,2,3,4-tetrahydro-4-methylquinoline (3c, CU-17-05) in CDCl₃. (Enlarged scale)
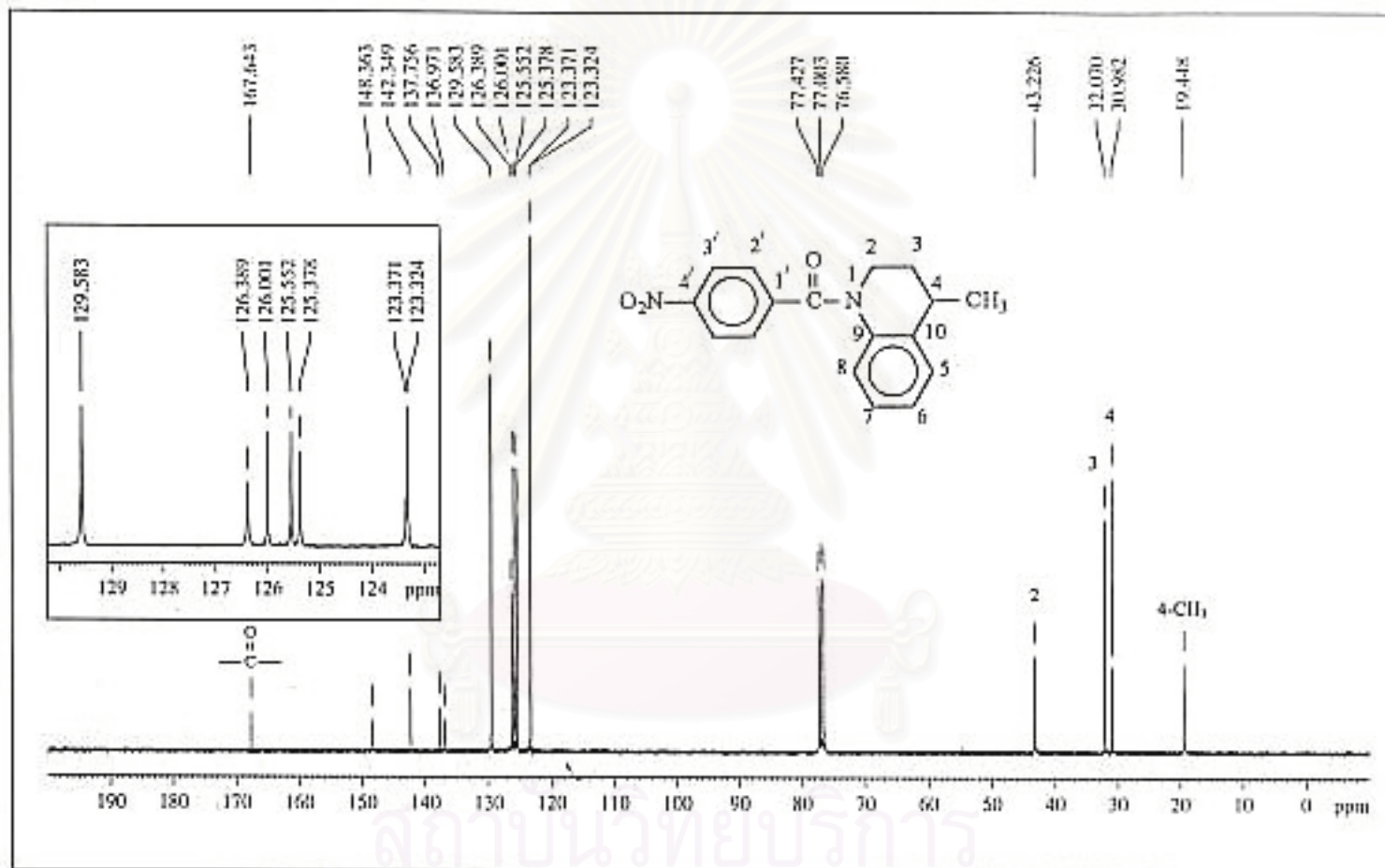
Figure 54. The 75 MHz 13C-NMR decoupled spectrum of N-(*p*-nitrobenzoyl)-1,2,3,4-tetrahydro-4-methylquinoline (3c, CU-17-05) in CDCl₃.
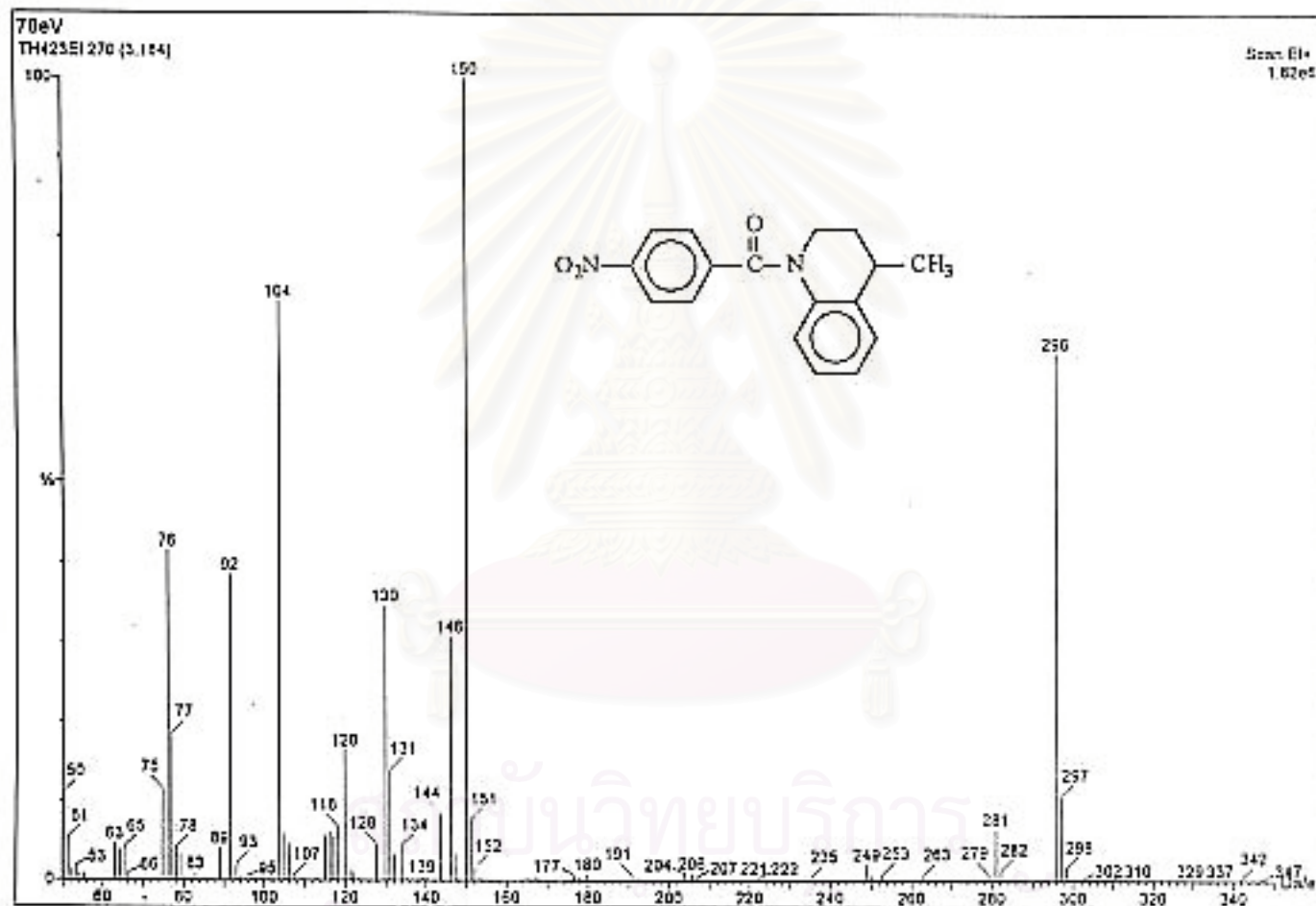
Figure 55. The electron impact mass spectrum of N-(*p*-nitrobenzoyl)-1,2,3,4-tetrahydro-4-methylquinoline (3c, CU-17-05).

Figure 56. The IR spectrum (KBr) of N-(*p*-nitrobenzoyl)-1,2,3,4-tetrahydro-8-methylquinoline (3d, CU-17-07).

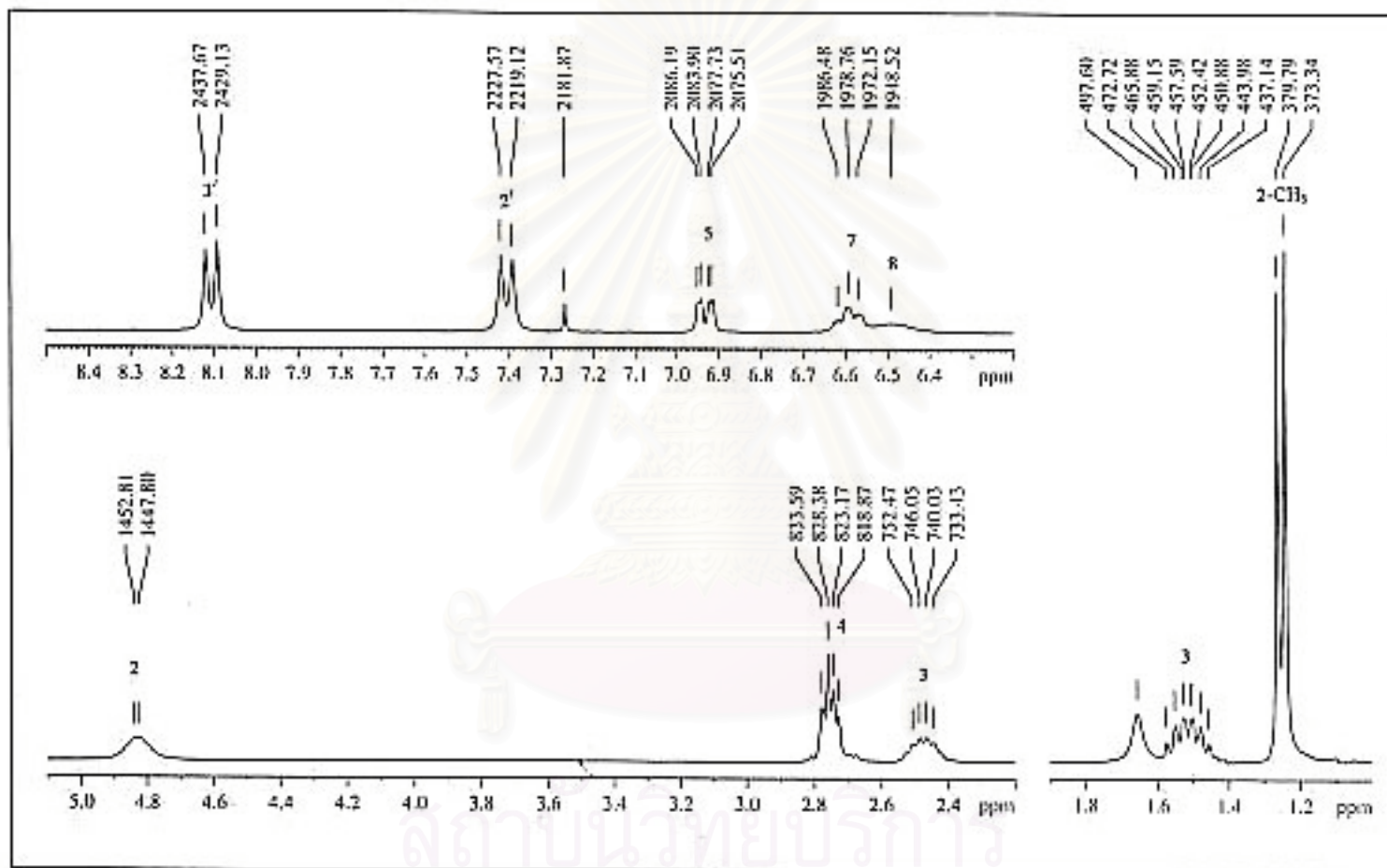Figure 57. The 300 MHz 1H-NMR spectrum of N-(*p*-nitrobenzoyl)-1,2,3,4-tetrahydro-8-methylquinoline (3d, CU-17-07) in CDCl₃.

Figure 58. The 300 MHz 1H-NMR spectrum of N-(*p*-nitrobenzoyl)-1,2,3,4-tetrahydro-8-methylquinoline (3d, CU-17-07) in CDCl₃. (Enlarged
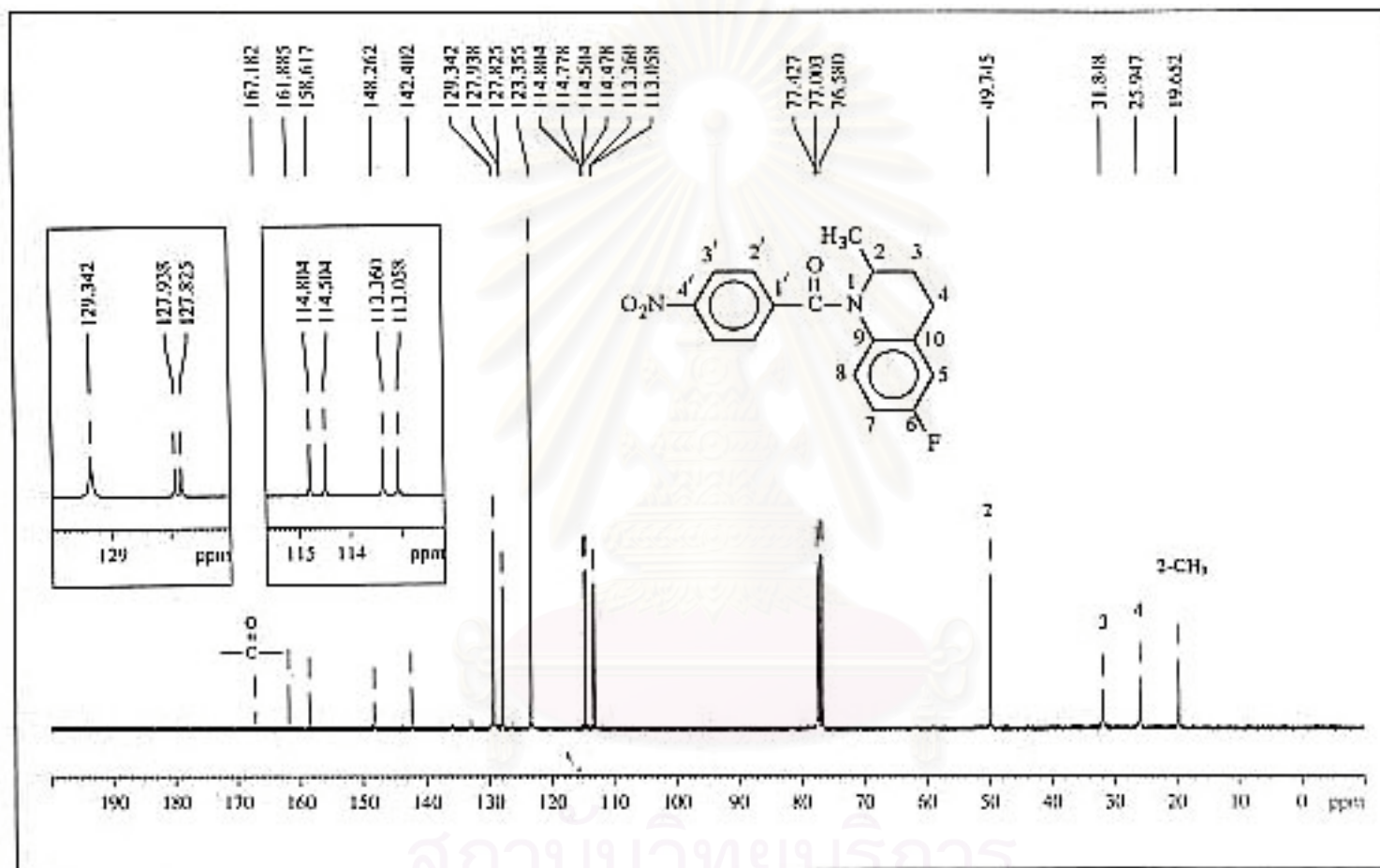
scale)

Figure 59. The 75 MHz 13C-NMR decoupled spectrum of N-(*p*-nitrobenzoyl)-1,2,3,4-tetrahydro-8-methylquinoline (3d, CU-17-07) in CDCl₃.
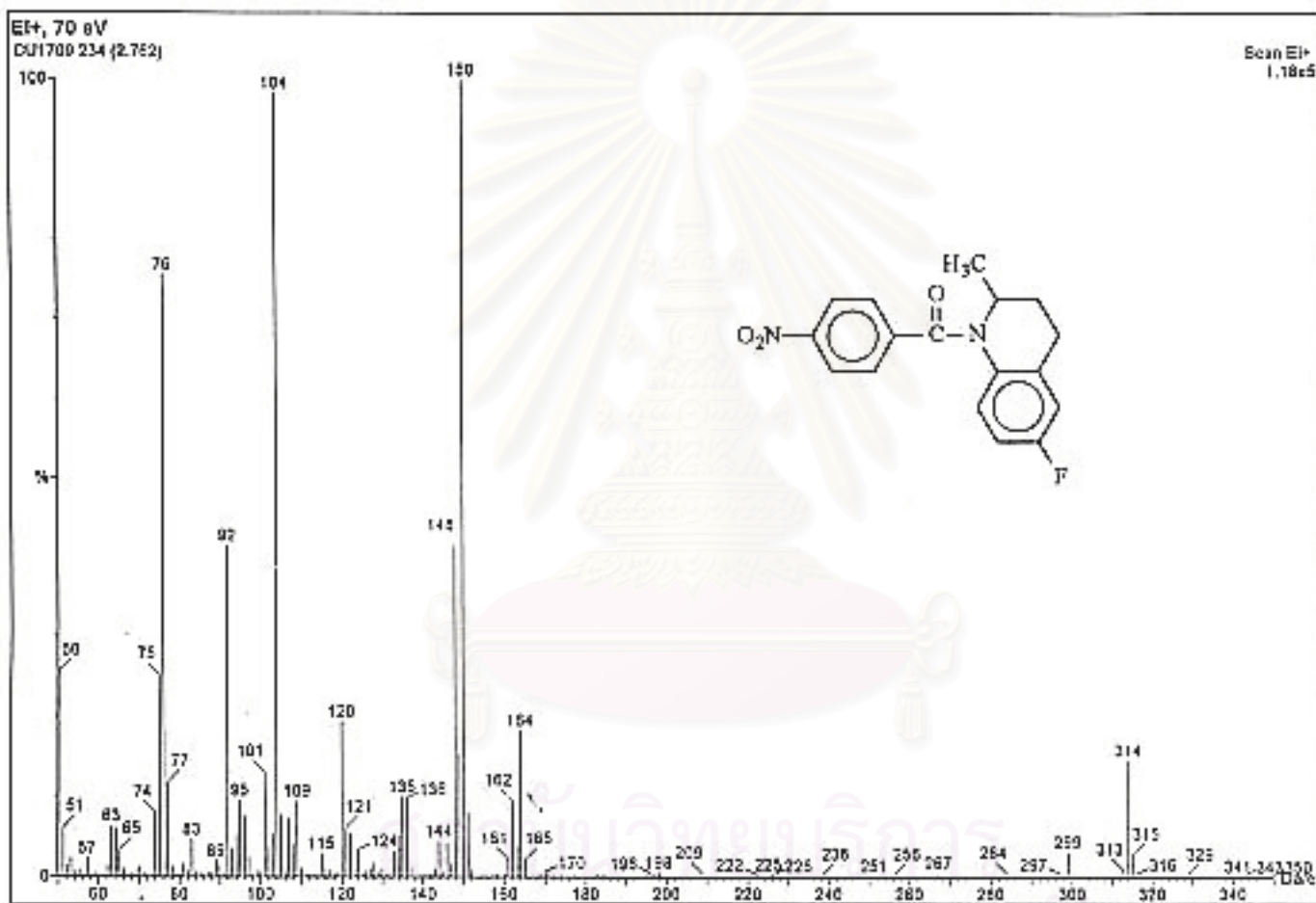
Figure 60. The electron impact mass spectrum of N-(*p*-nitrobenzoyl)-1,2,3,4-tetrahydro-8-methylquinoline (3d, CU-17-07).

Figure 61. The IR spectrum (KBr) of N-(*p*-nitrobenzoyl)-1,2,3,4-tetrahydro-6-fluoro-2-methylquinoline (3e, CU-17-09).

Figure 62. The 300 MHz 1H-NMR spectrum of N-(*p*-nitrobenzoyl)-1,2,3,4-tetrahydro-6-fluoro-2-methylquinoline (3e, CU-17-09) in CDCl₃.

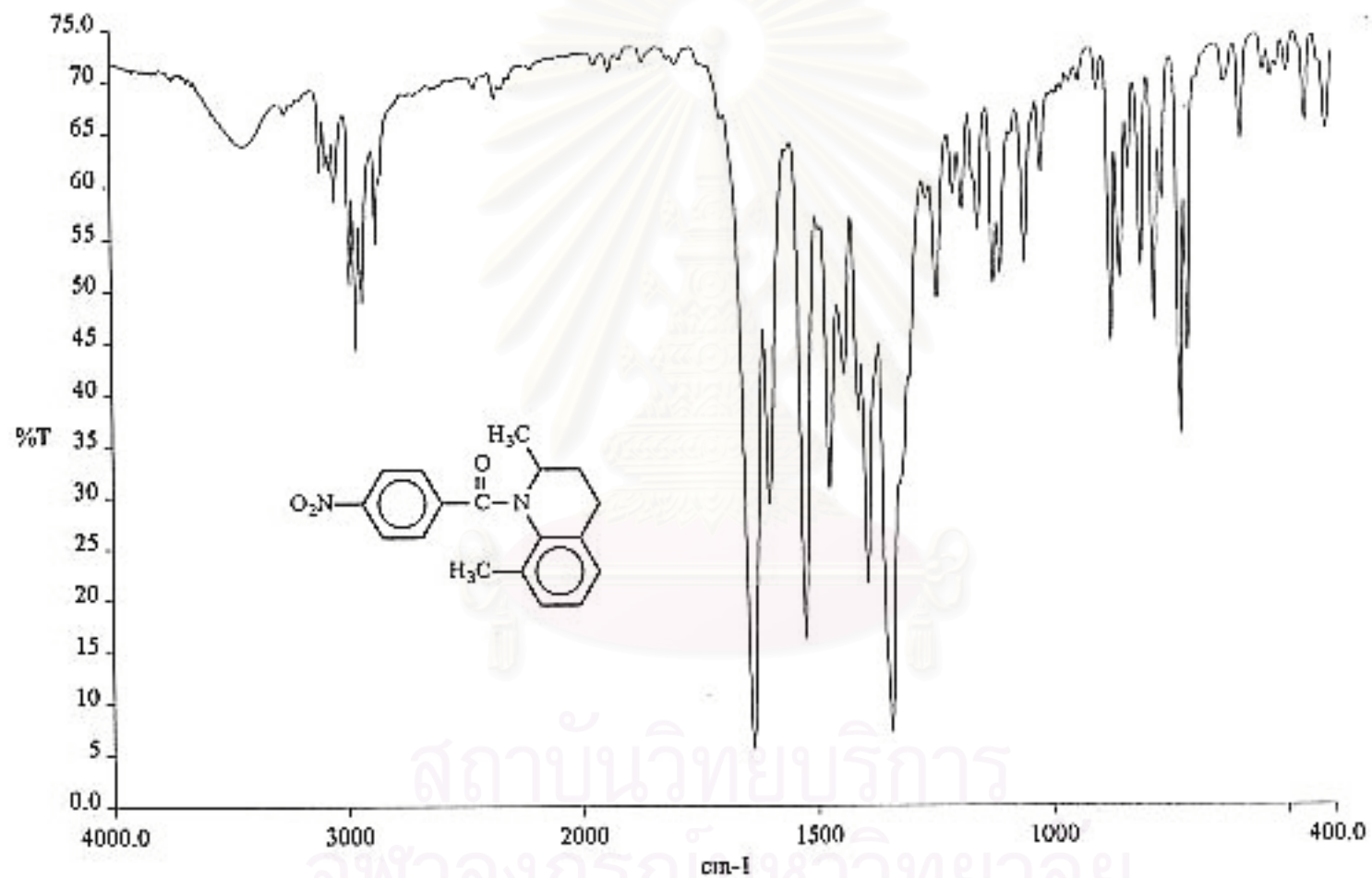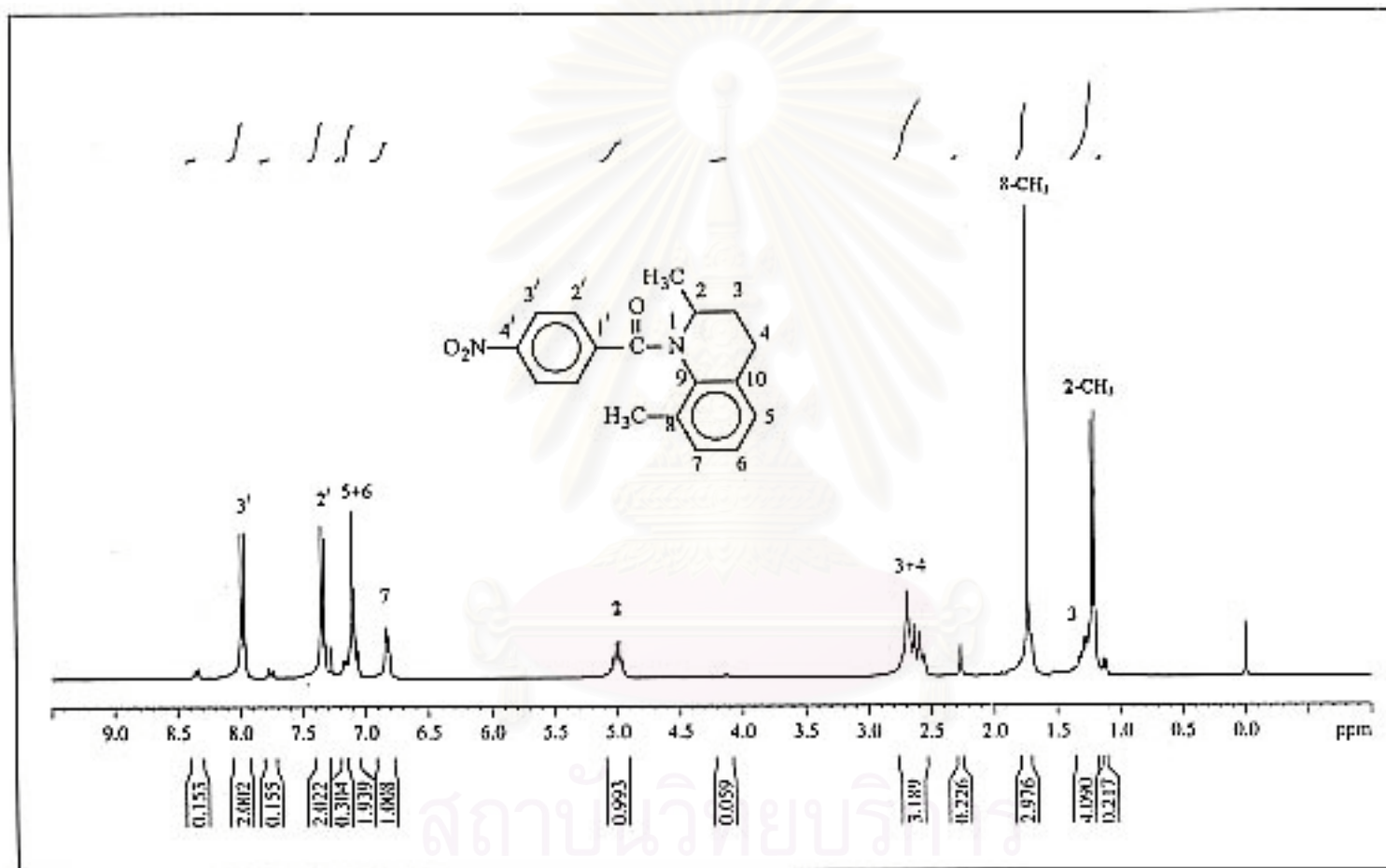Figure 63. The 300 MHz 1H-NMR spectrum of N-(*p*-nitrobenzoyl)-1,2,3,4-tetrahydro-6-fluoro-2-methylquinoline (3e, CU-17-09) in CDCl₃.

(Enlarged scale)

Figure 64. The 75 MHz 13C-NMR decoupled spectrum of N-(*p*-nitrobenzoyl)-1,2,3,4-tetrahydro-6-fluoro-2-methylquinoline (3e, CU-17-09) in CDCl₃.

Figure 65. The electron impact mass spectrum of N-(*p*-nitrobenzoyl)-1,2,3,4-tetrahydro-6-fluoro-2-methylquinoline (3e, CU-17-09).

Figure 66. The IR spectrum (KBr) of N-(*p*-nitrobenzoyl)-1,2,3,4-tetrahydro-2,8-dimethylquinoline (3f, CU-17-11).

Figure 67. The 300 MHz 1H-NMR spectrum of N-(*p*-nitrobenzoyl)-1,2,3,4-tetrahydro-2,8-dimethylquinoline (3f, CU-17-11) in CDCl₃.
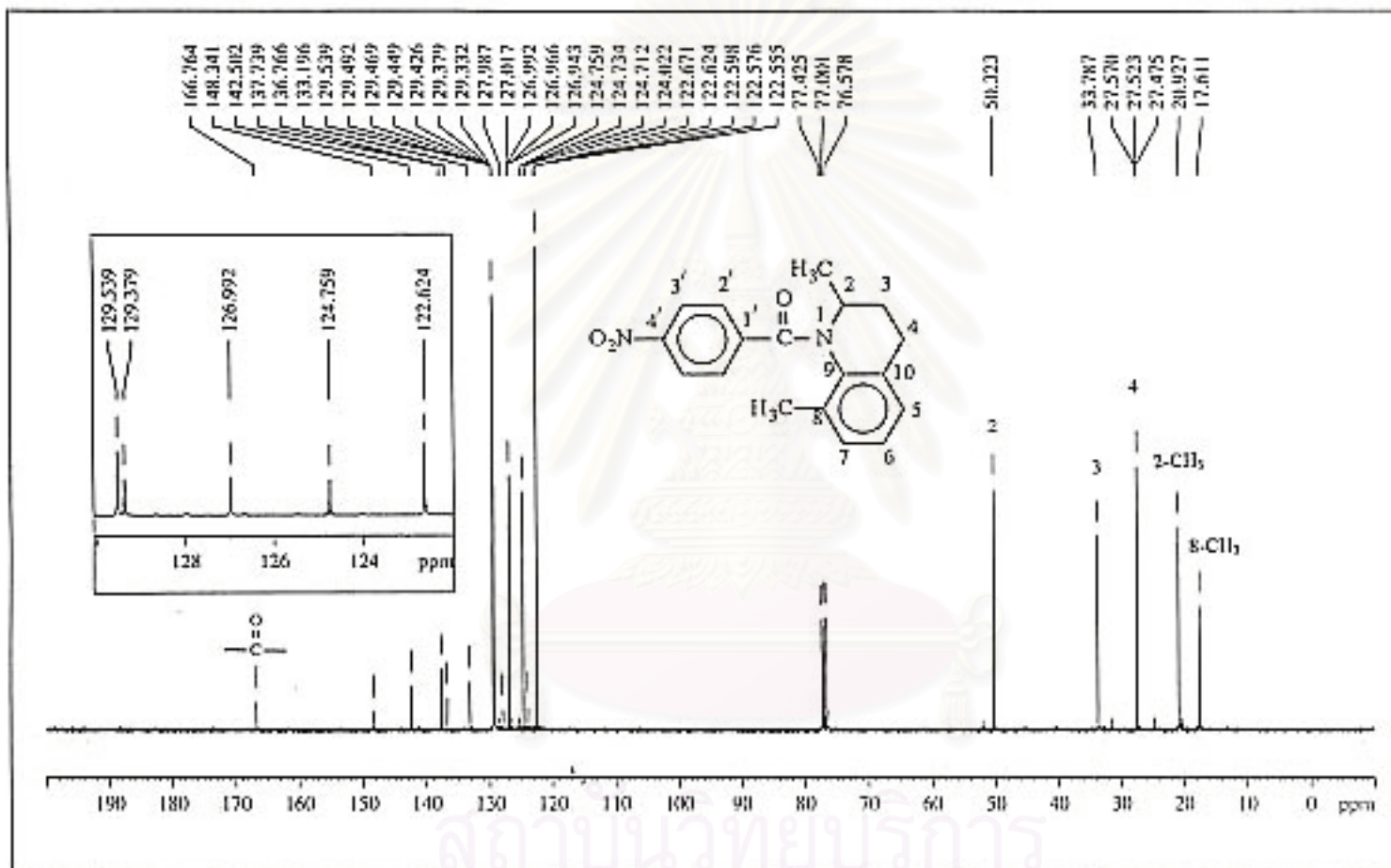
Figure 68. The 300 MHz 1H-NMR spectrum of N-(*p*-nitrobenzoyl)-1,2,3,4-tetrahydro-2,8-dimethylquinoline (3f, CU-17-11) in CDCl₃.

(Enlarged scale)

Figure 69. The 75 MHz 13C-NMR decoupled spectrum of N-(*p*-nitrobenzoyl)-1,2,3,4-tetrahydro-2,8-dimethylquinoline (3f, CU-17-11) in CDCl₃.
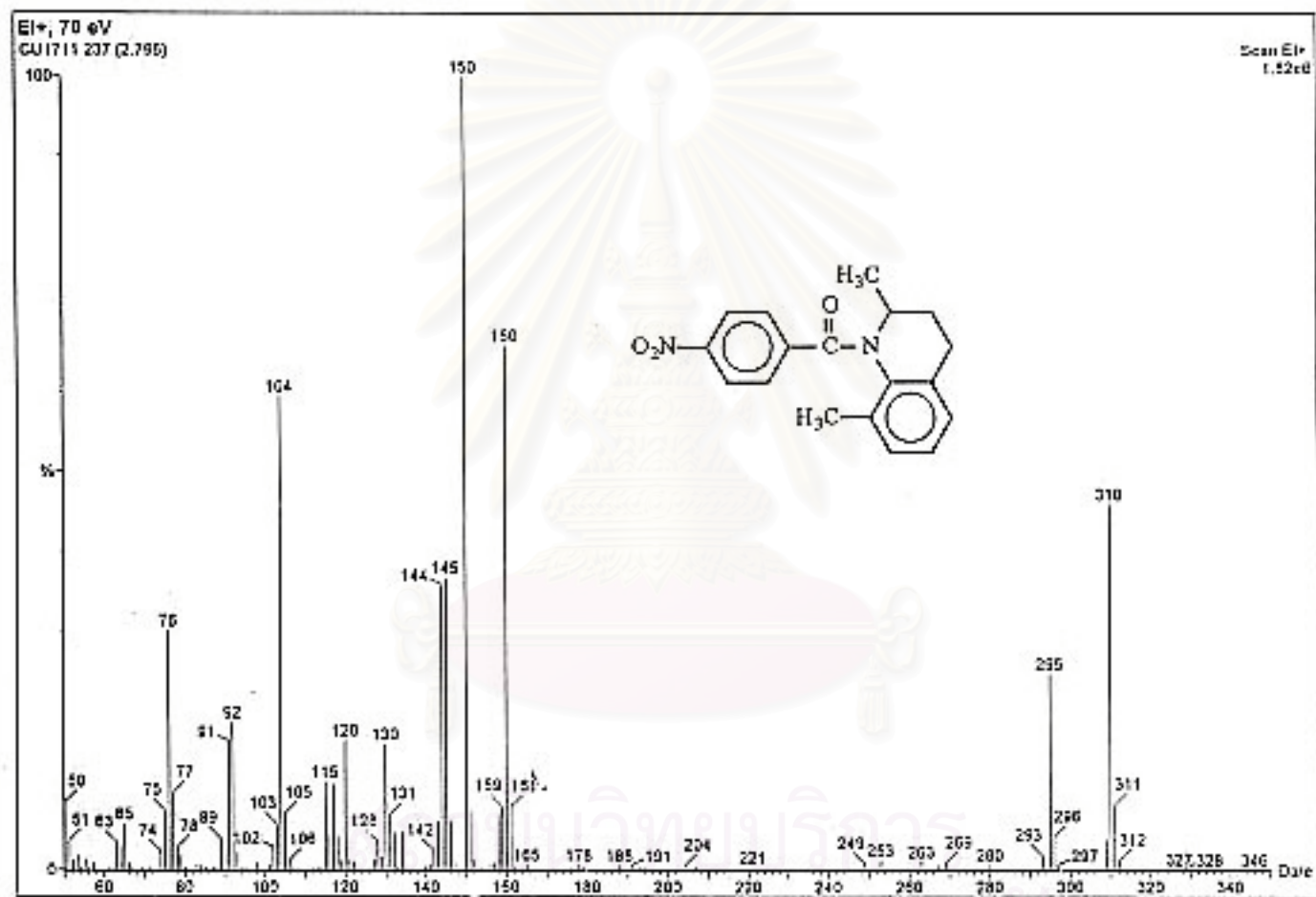
Figure 70. The electron impact mass spectrum of N-(*p*-nitrobenzoyl)-1,2,3,4-tetrahydro-2,8-dimethylquinoline (3f, CU-17-11).
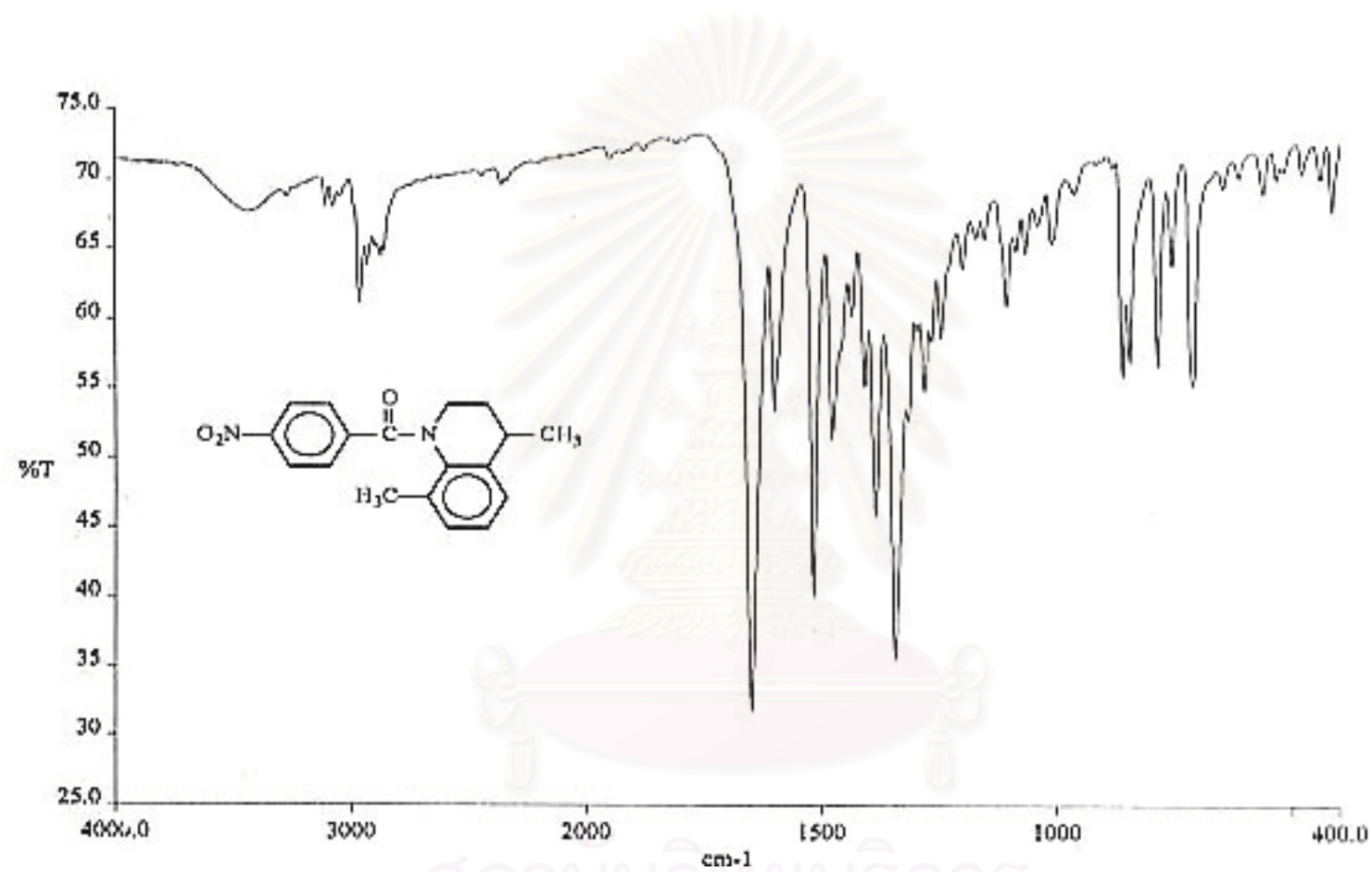
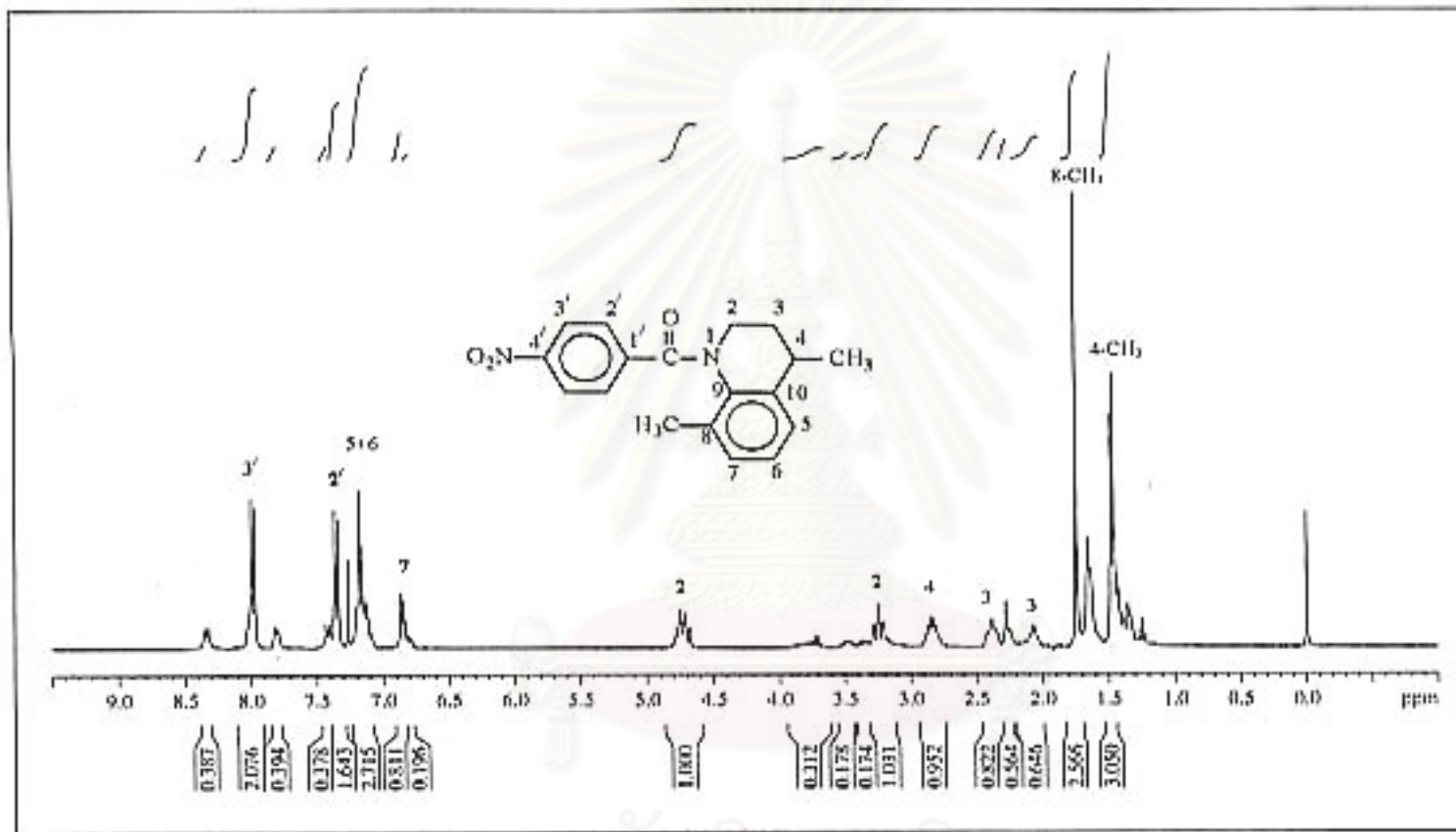Figure 71. The IR spectrum (KBr) of N-(*p*-nitrobenzoyl)-1,2,3,4-tetrahydro-4,8-dimethylquinoline (3g, CU-17-13).

Figure 72. The 300 MHz 1H-NMR spectrum of N-(*p*-nitrobenzoyl)-1,2,3,4-tetrahydro-4,8-dimethylquinoline (3g, CU-17-13) in CDCl₃.
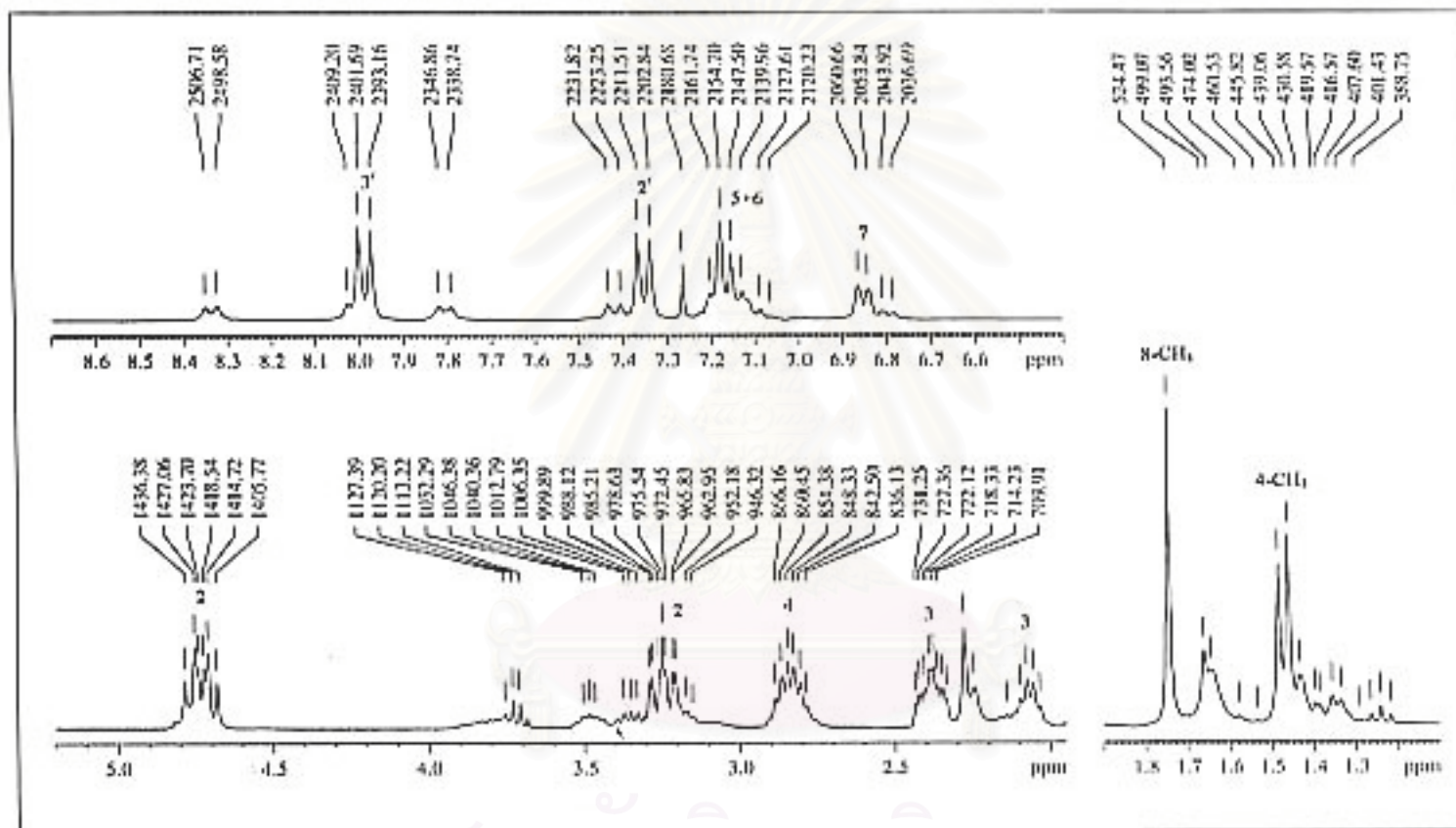
Figure 73. The 300 MHz 1H-NMR spectrum of N-(*p*-nitrobenzoyl)-1,2,3,4-tetrahydro-4,8-dimethylquinoline (3g, CU-17-13) in CDCl₃.
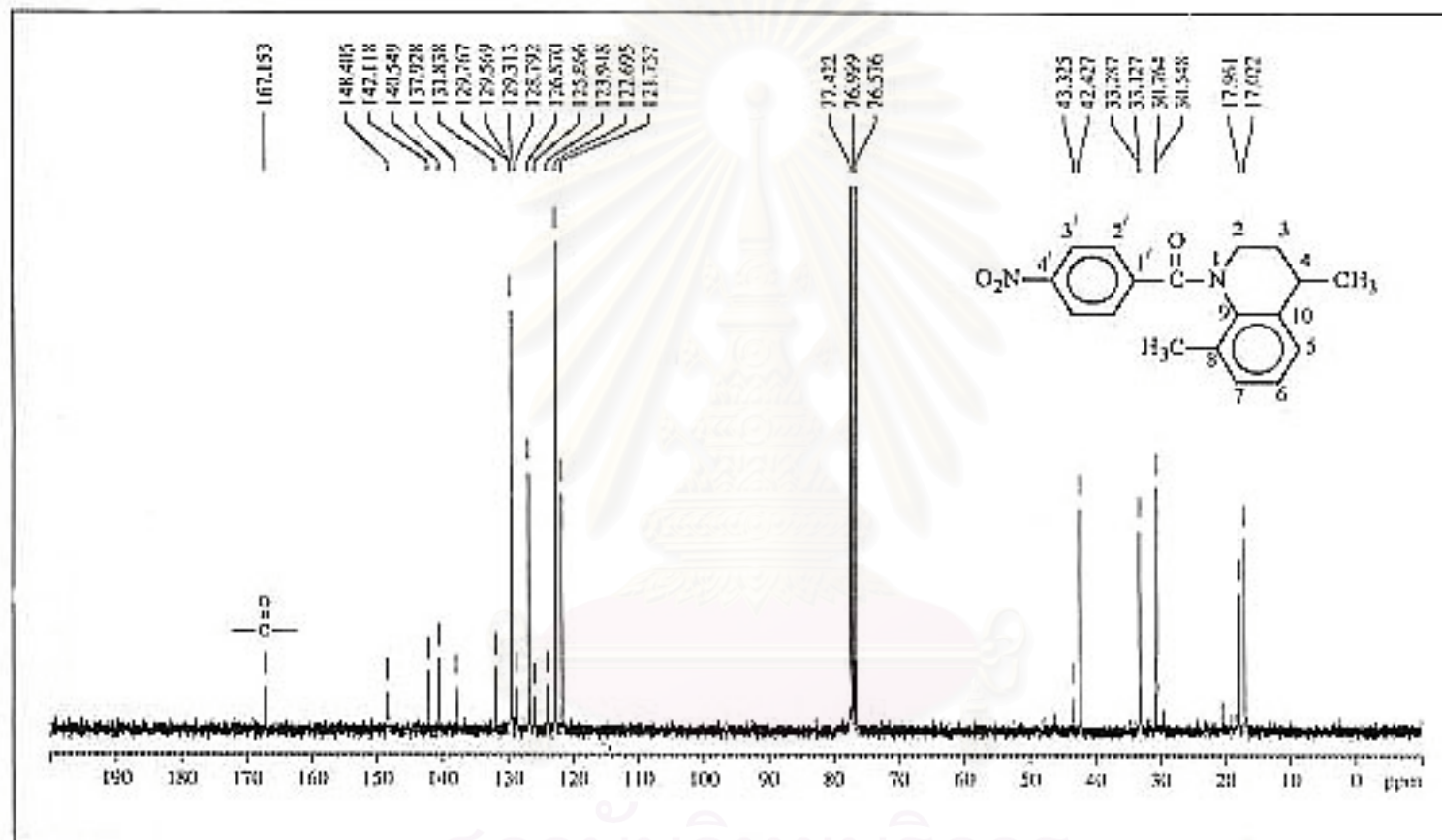
(Enlarged scale)

Figure 74. The 75 MHz 13C-NMR decoupled spectrum of N-(*p*-nitrobenzoyl)-1,2,3,4-tetrahydro-4,8-dimethylquinoline (3g, CU-17-13) in CDCl₃.
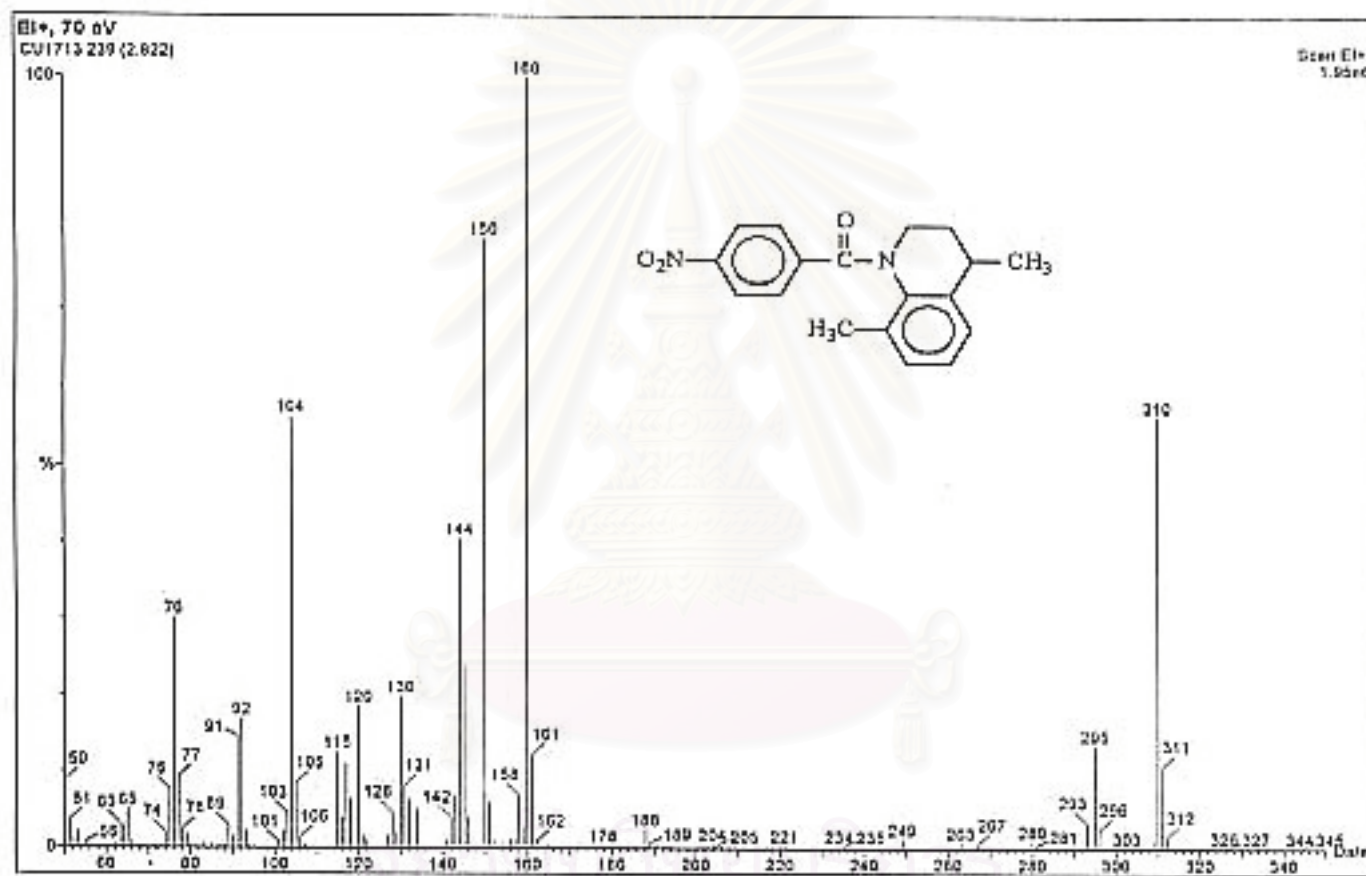
Figure 75. The electron impact mass spectrum of N-(*p*-nitrobenzoyl)-1,2,3,4-tetrahydro-4,8-dimethylquinoline (3g, CU-17-13).
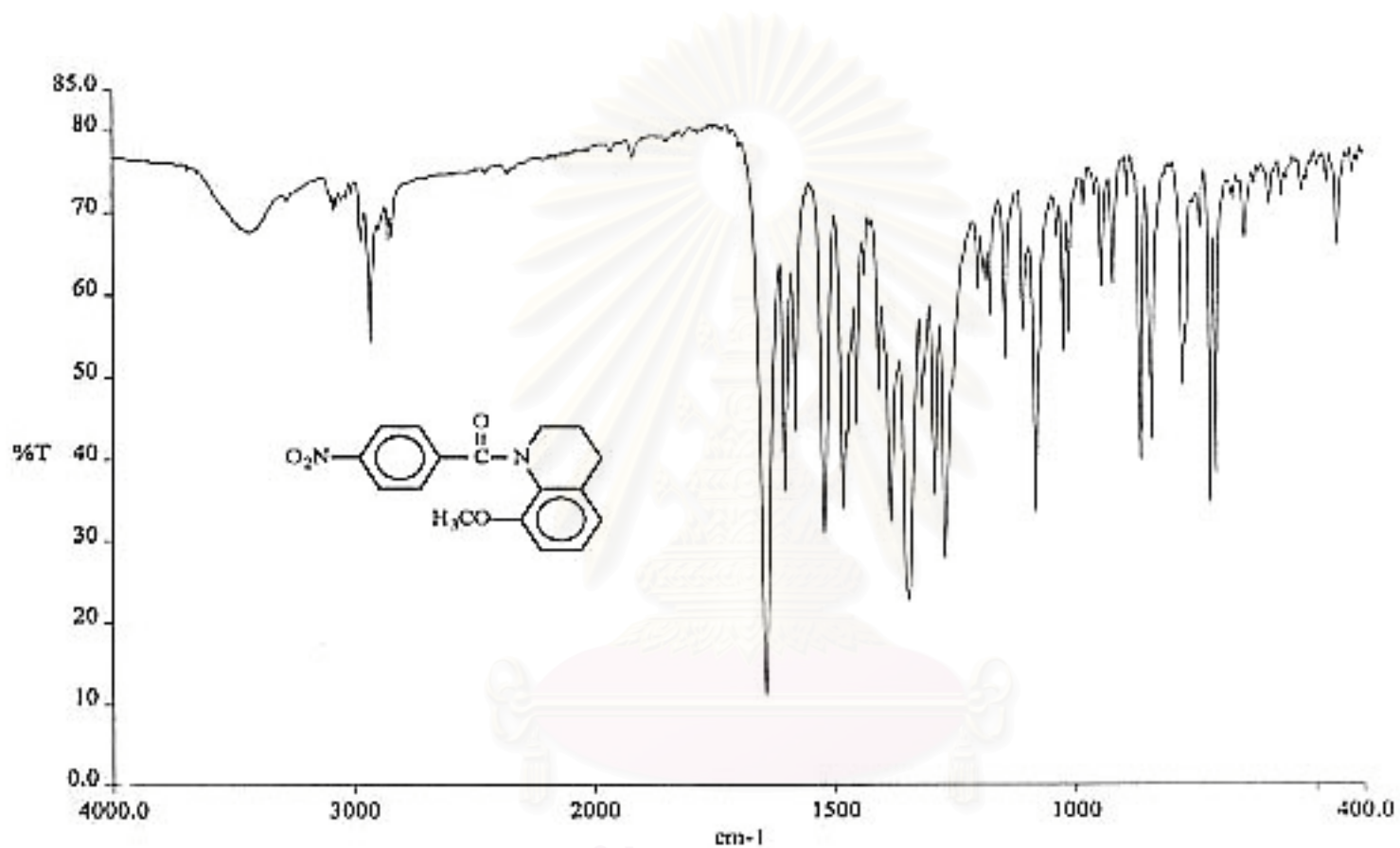
Figure 76. The IR spectrum (KBr) of N-(*p*-nitrobenzoyl)-1,2,3,4-tetrahydro-8-methoxyquinoline (3h, CU-17-15).
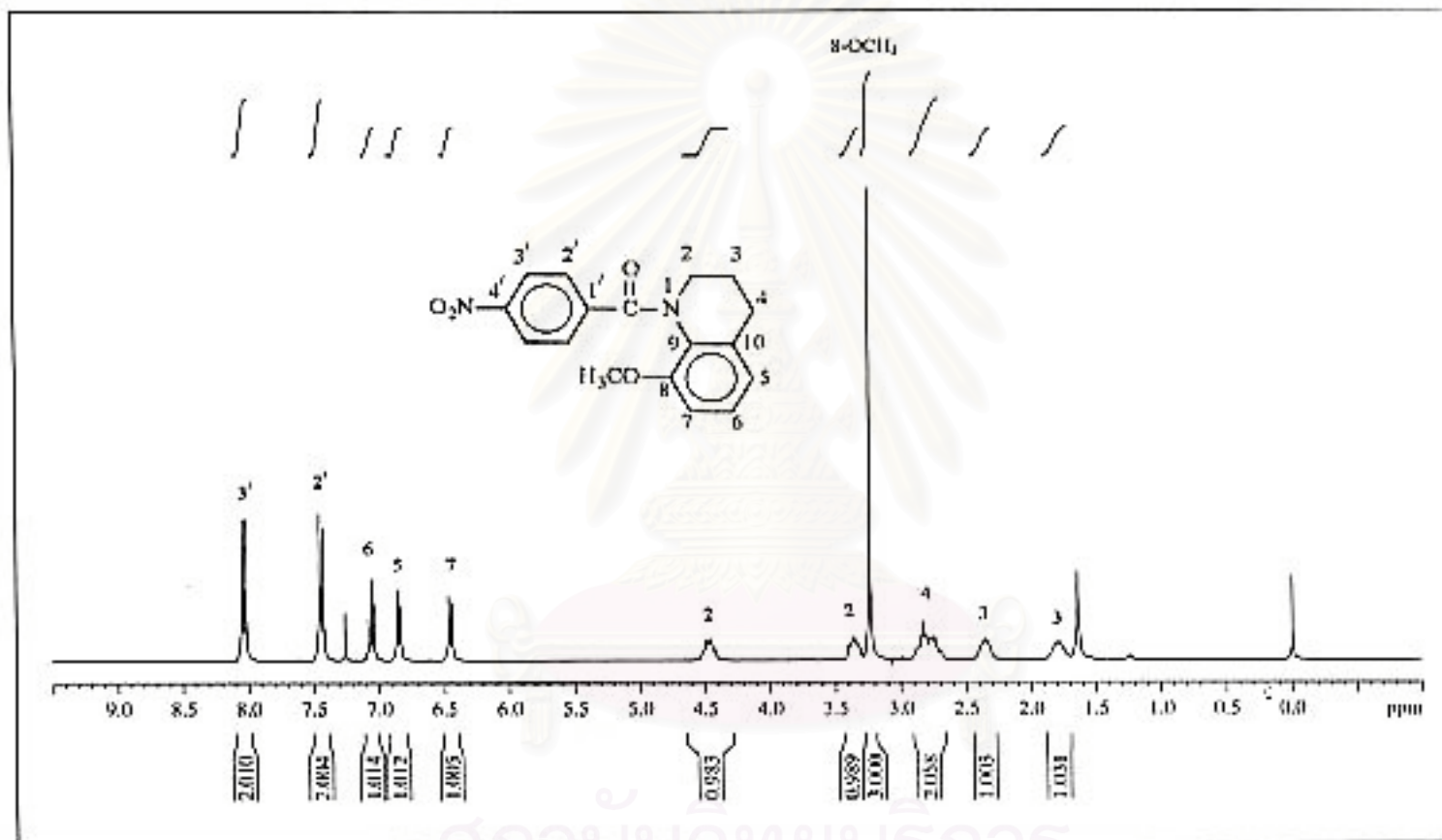
Figure 77. The 300 MHz 1H-NMR spectrum of N-(*p*-nitrobenzoyl)-1,2,3,4-tetrahydro-8-methoxyquinoline (3h, CU-17-15) in CDCl₃.
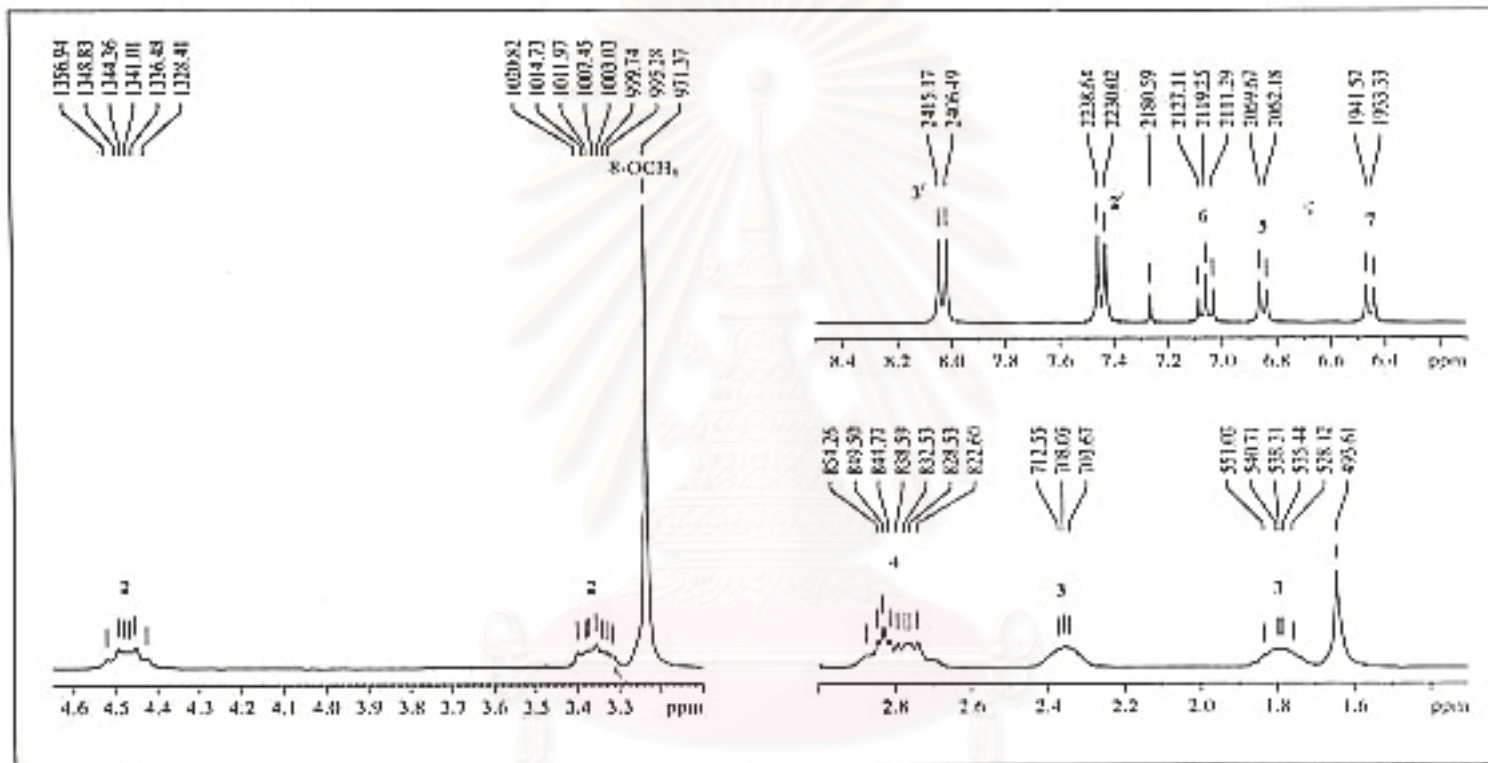
Figure 78. The 300 MHz 1H-NMR spectrum of N-(*p*-nitrobenzoyl)-1,2,3,4-tetrahydro-8-methoxyquinoline (3h, CU-17-15) in CDCl₃.

(Enlarged scale)

Figure 79. The 75 MHz 13C-NMR decoupled spectrum of N-(*p*-nitrobenzoyl)-1,2,3,4-tetrahydro-8-methoxyquinoline (3h, CU-17-15) in

CDCl₃.

Figure 80. The IR spectrum (KBr) of N-(*p*-aminobenzoyl)-1,2,3,4-tetrahydroquinoline (4a, CU-17-02).

Figure 81. The 300 MHz 1H-NMR spectrum of N-(*p*-aminobenzoyl)-1,2,3,4-tetrahydroquinoline (4a, CU-17-02) in CDCl₃.

Figure 82. The 300 MHz 1H-NMR spectrum of N-(*p*-aminobenzoyl)-1,2,3,4-tetrahydroquinoline (4a, CU-17-02) in CDCl₃. (Enlarged scale)
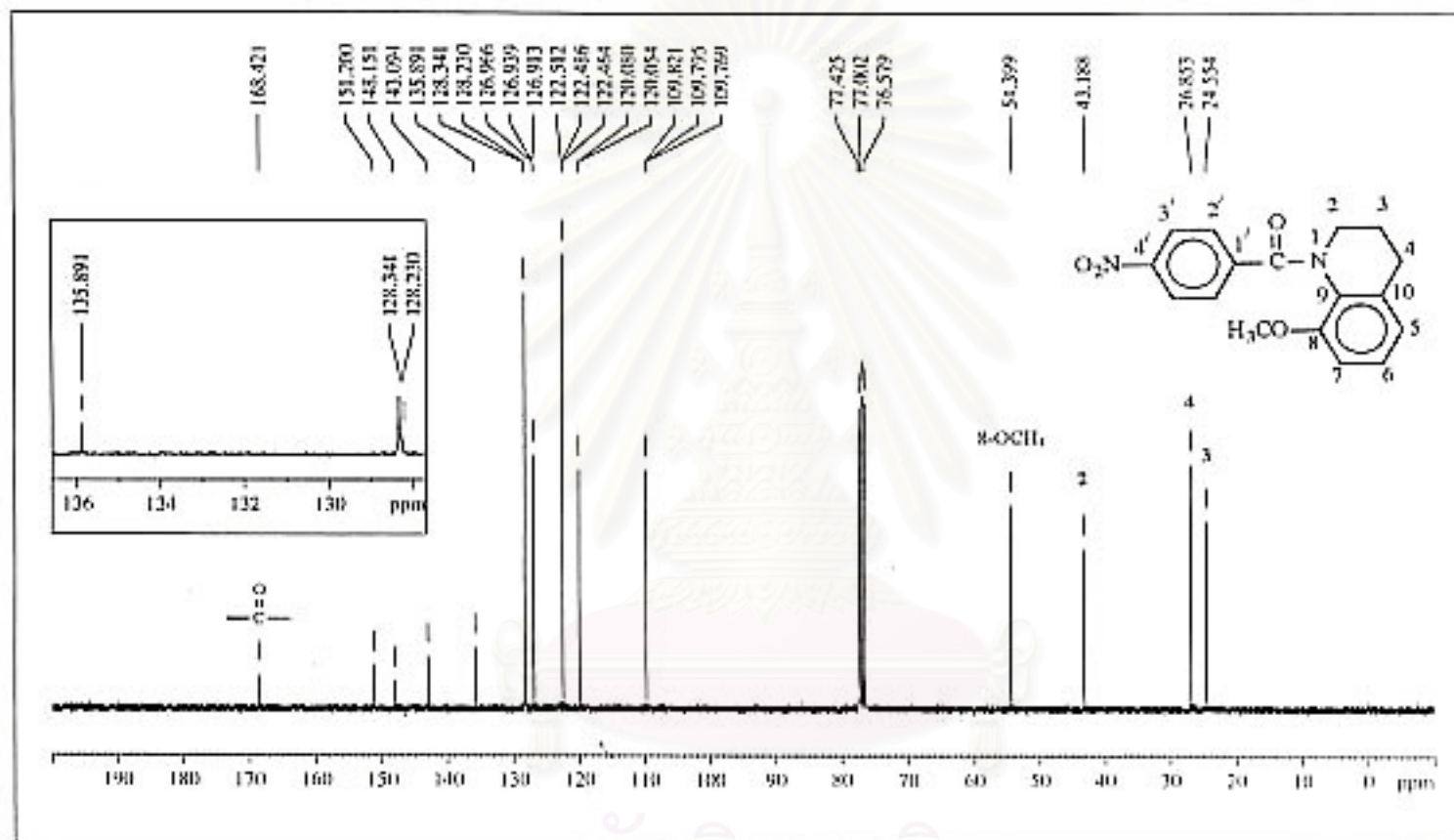
Figure 83. The 75 MHz 13C-NMR decoupled spectrum of N-(*p*-aminobenzoyl)-1,2,3,4-tetrahydroquinoline (4a, CU-17-02) in CDCl₃.
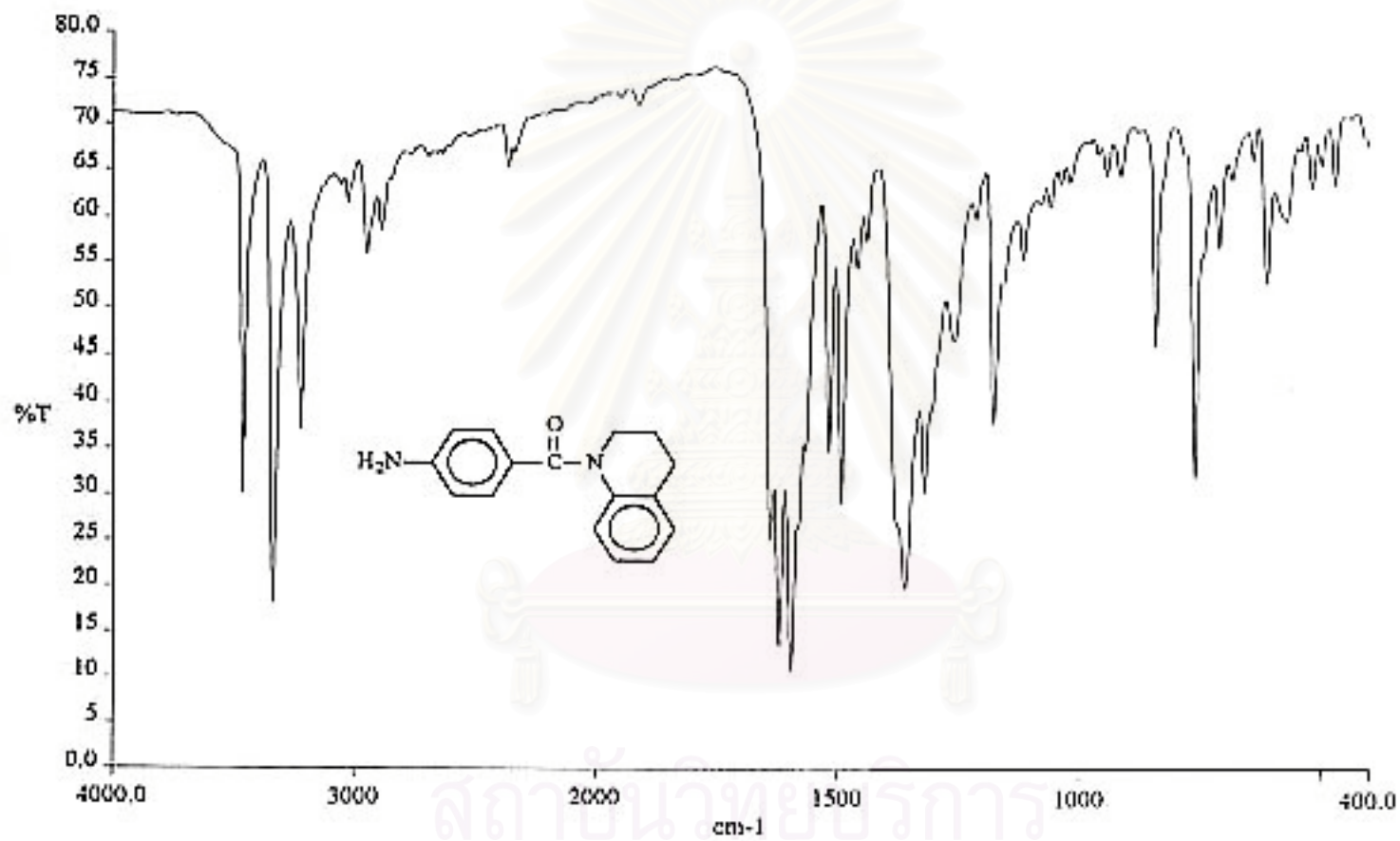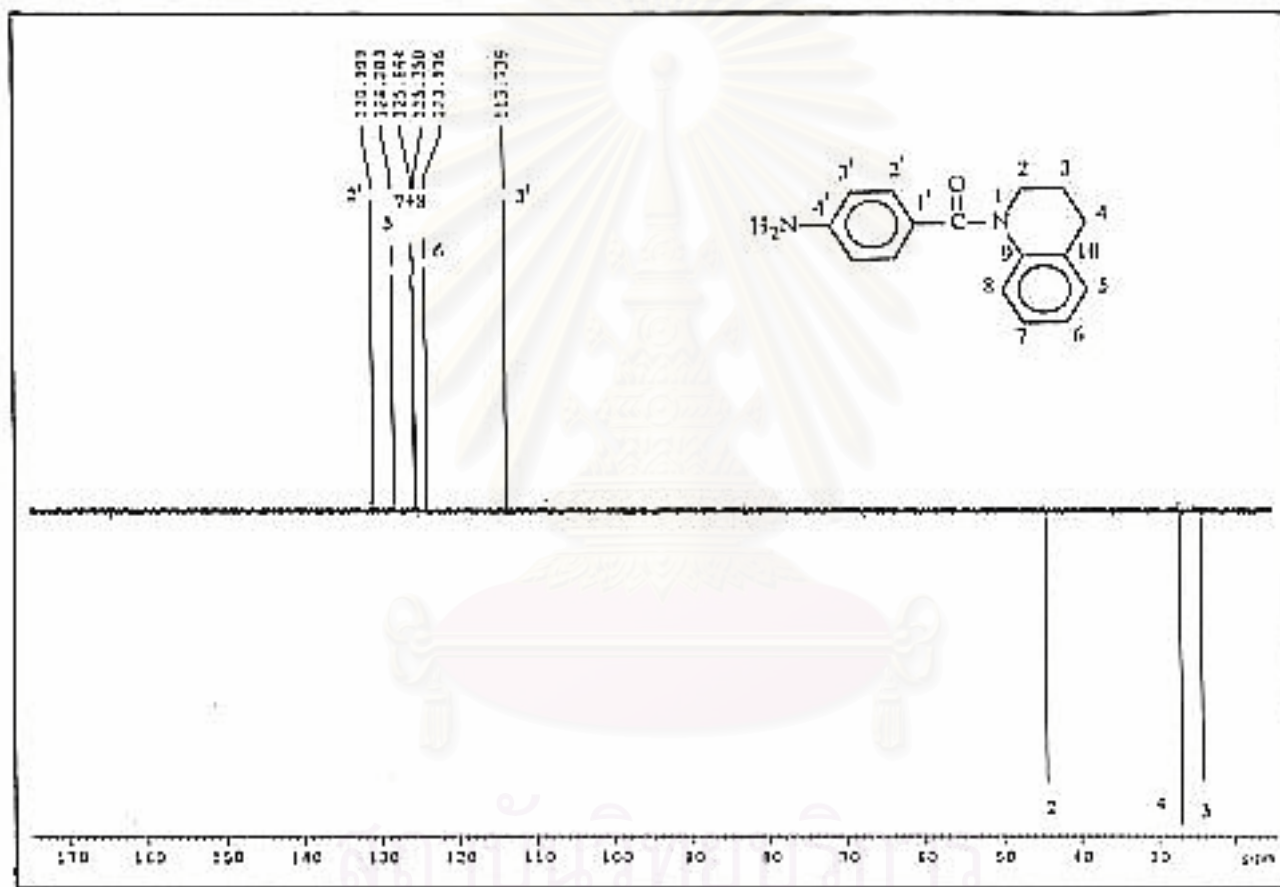
Figure 84. The 75 MHz DEPT-135 spectrum of N-(*p*-aminobenzoyl)-1,2,3,4-tetrahydroquinoline (4a, CU-17-02) in CDCl$_3$.
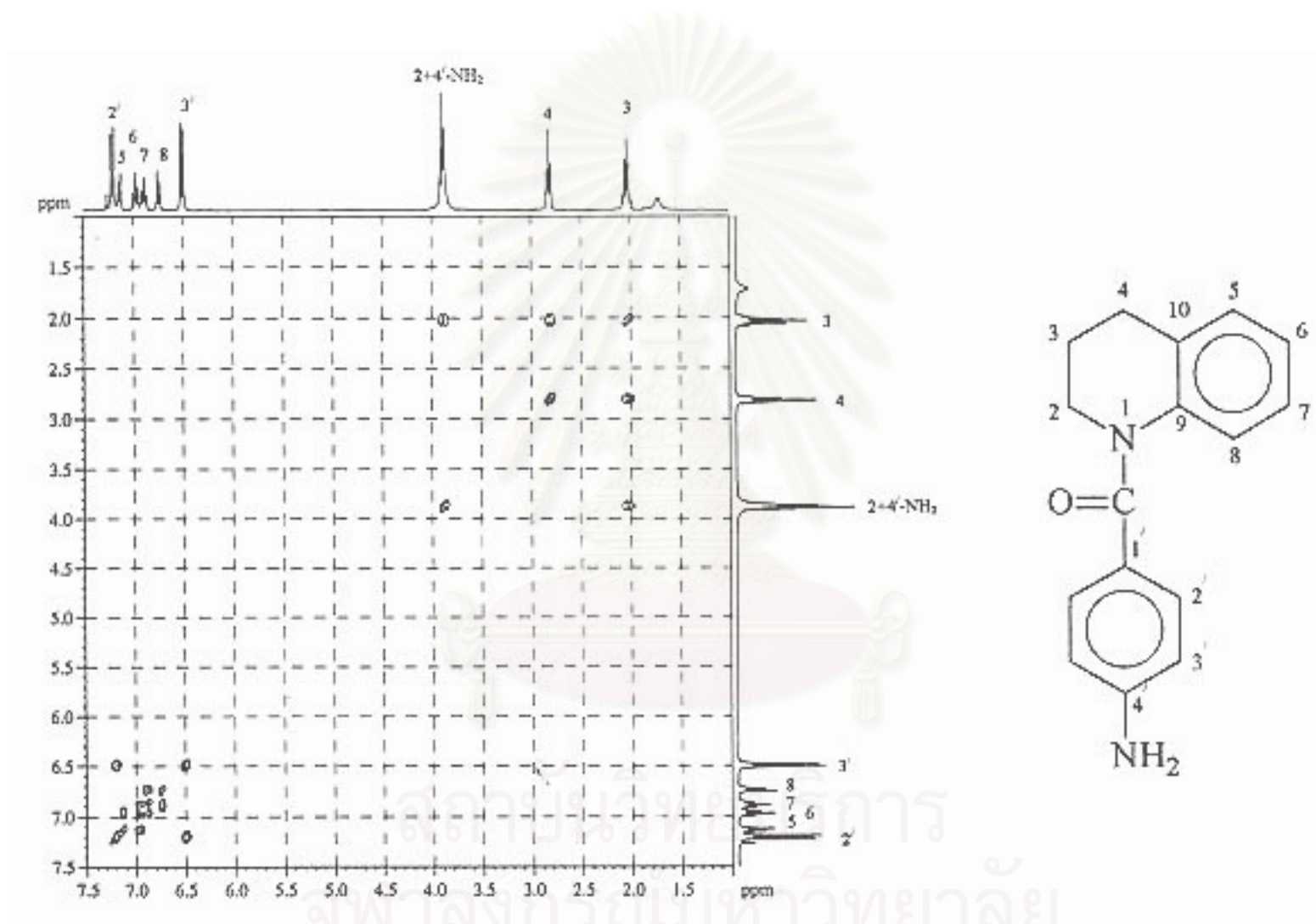
Figure 85. The 300 MHz HH COSY spectrum of N-(*p*-aminobenzoyl)-1,2,3,4-tetrahydroquinoline (4a, CU-17-02) in CDCl₃.

165

Figure 86. The 300 MHz HH COSY spectrum of N-(*p*-aminobenzoyl)-1,2,3,4-tetrahydroquinoline (4a, CU-17-02) in CDCl₃. (Enlarged scale)
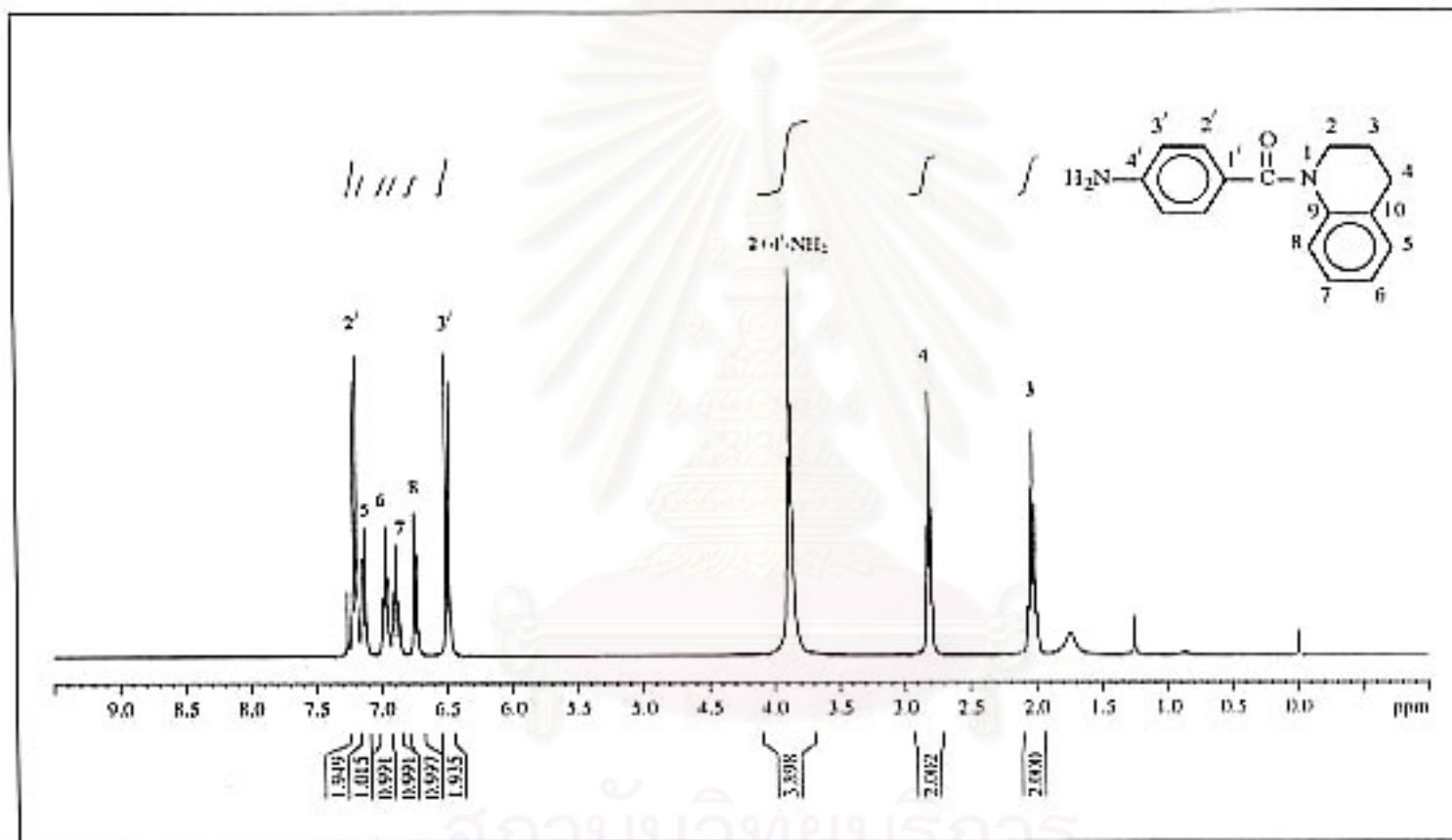
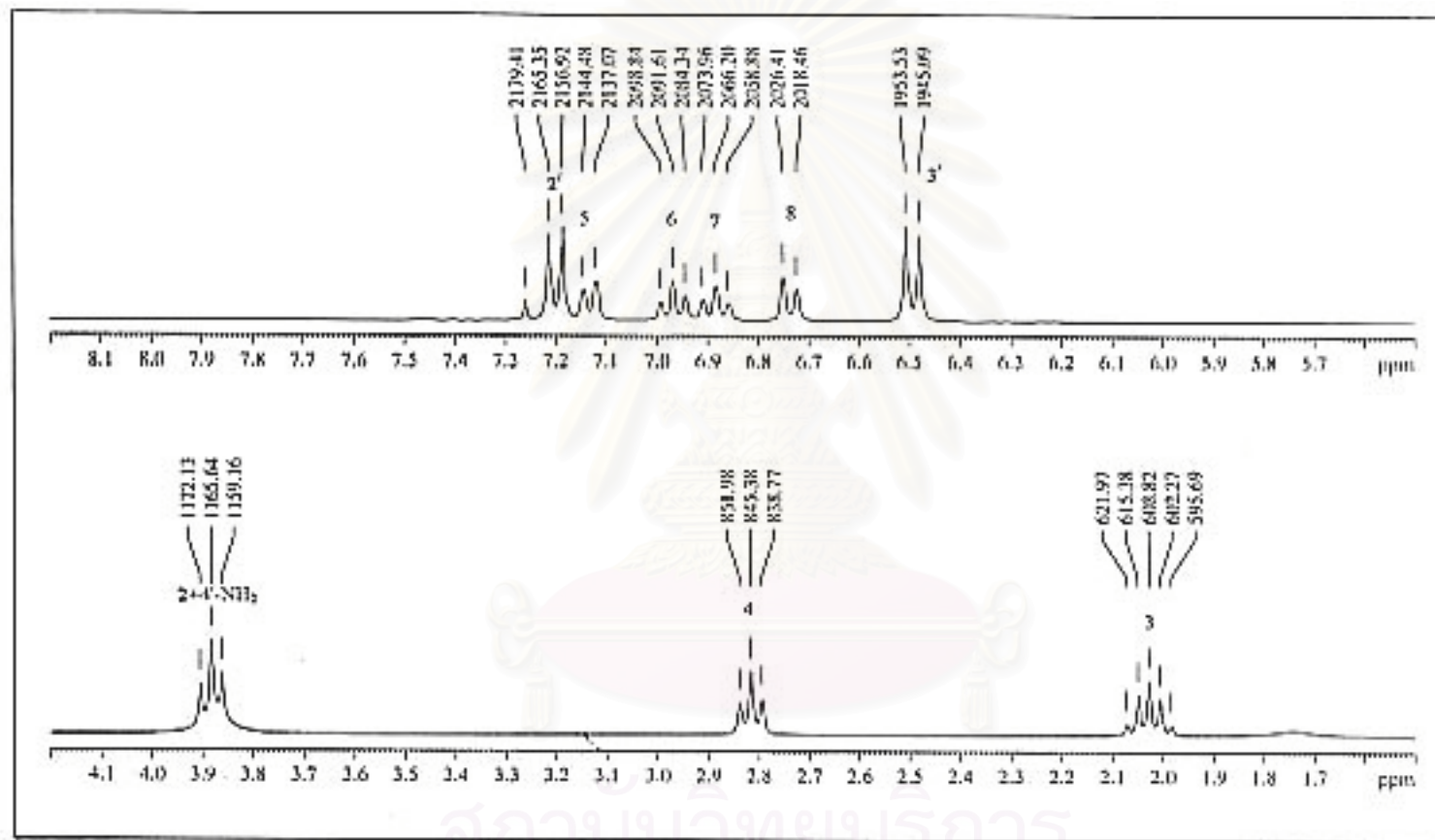Figure 87. The 300 MHz HMQC spectrum of N-(*p*-aminobenzoyl)-1,2,3,4-tetrahydroquinoline (4a, CU-17-02) in CDCl₃.

Figure 88. The 300 MHz HMQC spectrum of N-(*p*-aminobenzoyl)-1,2,3,4-tetrahydroquinoline (4a, CU-17-02) in CDCl₃. (Enlarged scale)
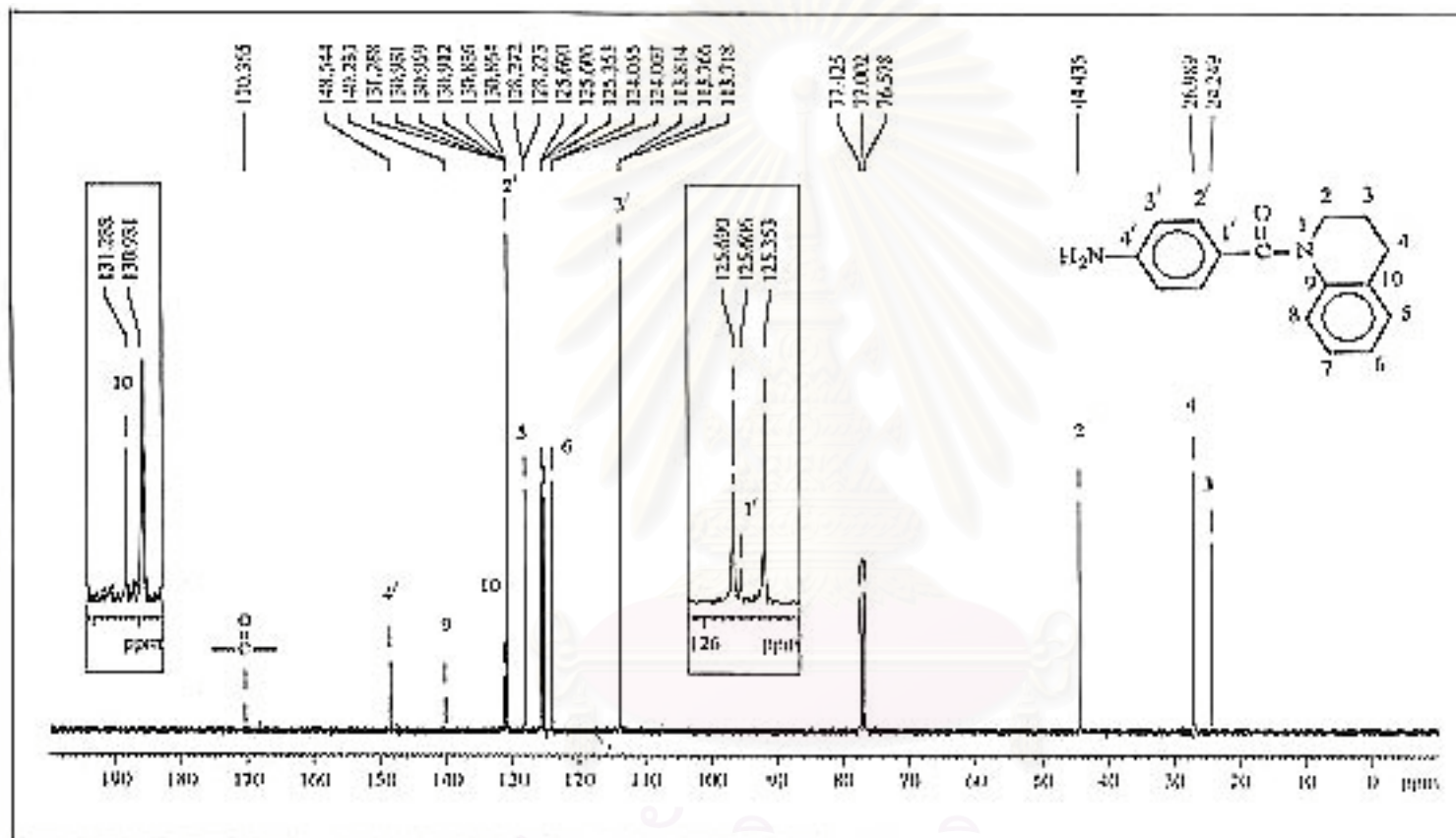
Figure 89. The 300 MHz HMBC spectrum (JHC = 8 Hz) of N-(*p*-aminobenzoyl)-1,2,3,4-tetrahydroquinoline (4a, CU-17-02) in CDCl₃.

Figure 90. The 300 MHz HMBC spectrum (JHC = 8 Hz) of N-(*p*-aminobenzoyl)-1,2,3,4-tetrahydroquinoline (4a, CU-17-02) in CDCl₃.

(Expanded: δH 1.9-4.0 ppm; δC 20-174 ppm)

Figure 91. The 300 MHz HMBC spectrum (JHC = 8 Hz) of N-(*p*-aminobenzoyl)-1,2,3,4-tetrahydroquinoline (4a, CU-17-02) in CDCl₃.

(Expanded: δH 6.3-7.4 ppm; δC 108-180 ppm)

Figure 92. The electron impact mass spectrum of N-(*p*-aminobenzoyl)-1,2,3,4-tetrahydroquinoline (4a, CU-17-02).

Figure 93. The IR spectrum (KBr) of N-(*p*-aminobenzoyl)-1,2,3,4-tetrahydro-2-methylquinoline (4b, CU-17-04).

Figure 94. The 300 MHz 1H-NMR spectrum of N-(*p*-aminobenzoyl)-1,2,3,4-tetrahydro-2-methylquinoline (4b, CU-17-04) in CDCl$_3$.

Figure 95. The 300 MHz 1H-NMR spectrum of N-(*p*-aminobenzoyl)-1,2,3,4-tetrahydro-2-methylquinoline (4b, CU-17-04) in CDCl₃. (Enlarged

scale)
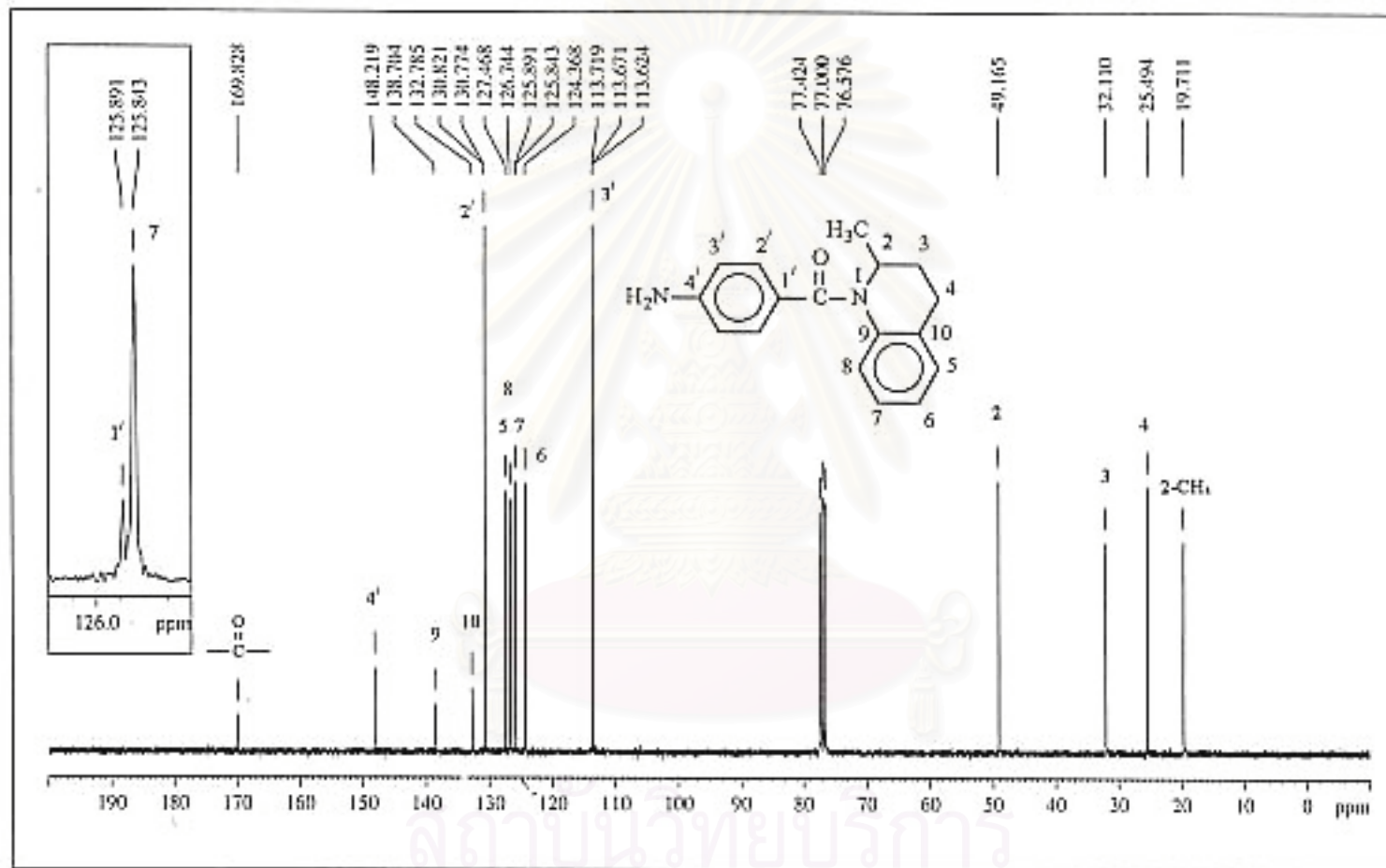
Figure 96. The 75 MHz 13C-NMR decoupled spectrum of N-(*p*-aminobenzoyl)-1,2,3,4-tetrahydro-2-methylquinoline (4b, CU-17-04) in CDCl₃.
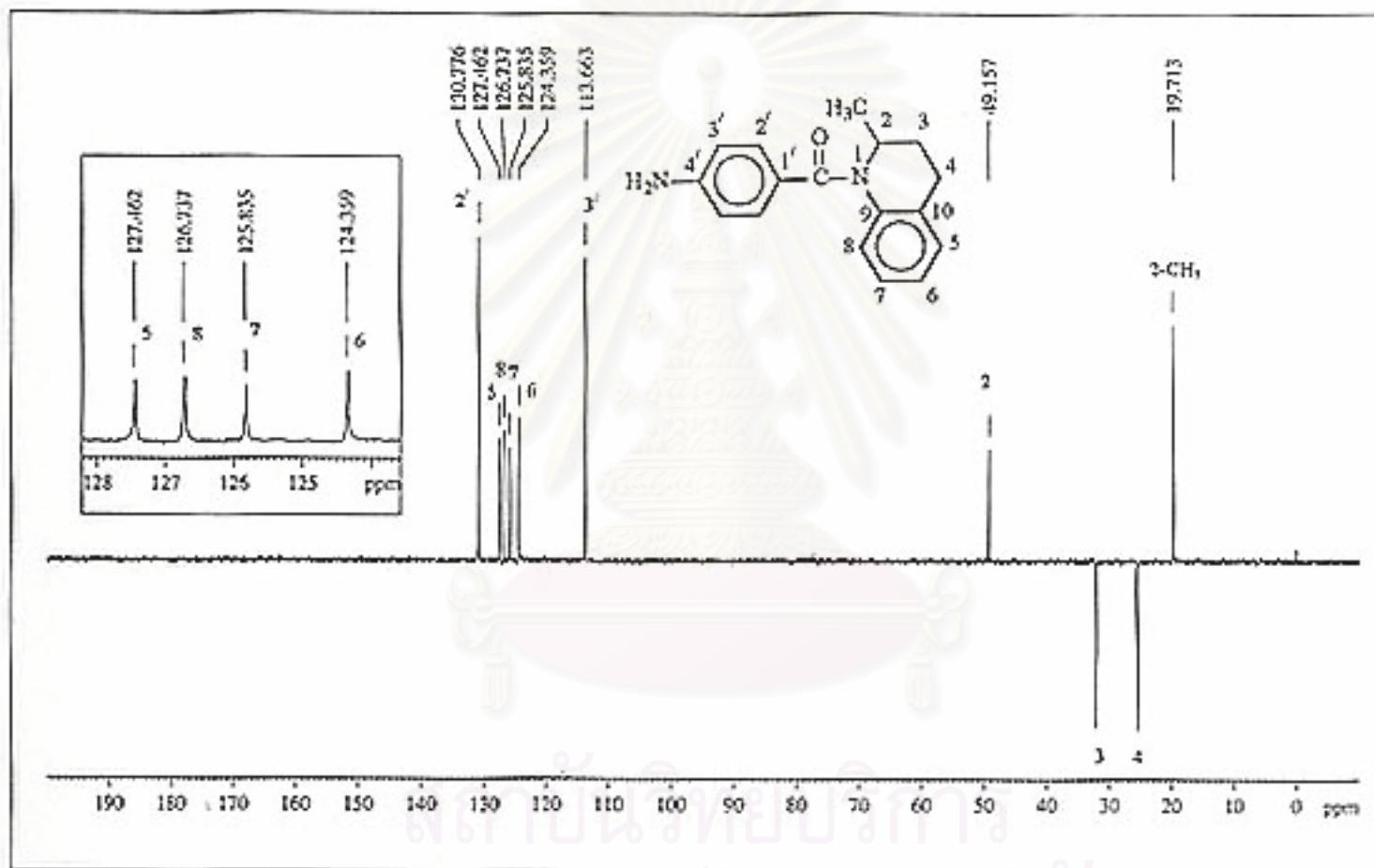
Figure 97. The 75 MHz DEPT-135 spectrum of N-(*p*-aminobenzoyl)-1,2,3,4-tetrahydro-2-methylquinoline (4b, CU-17-04) in CDCl₃.

Figure 98. The 300 MHz HH COSY spectrum of N-(*p*-aminobenzoyl)-1,2,3,4-tetrahydro-2-methylquinoline (4b, CU-17-04) in CDCl₃.
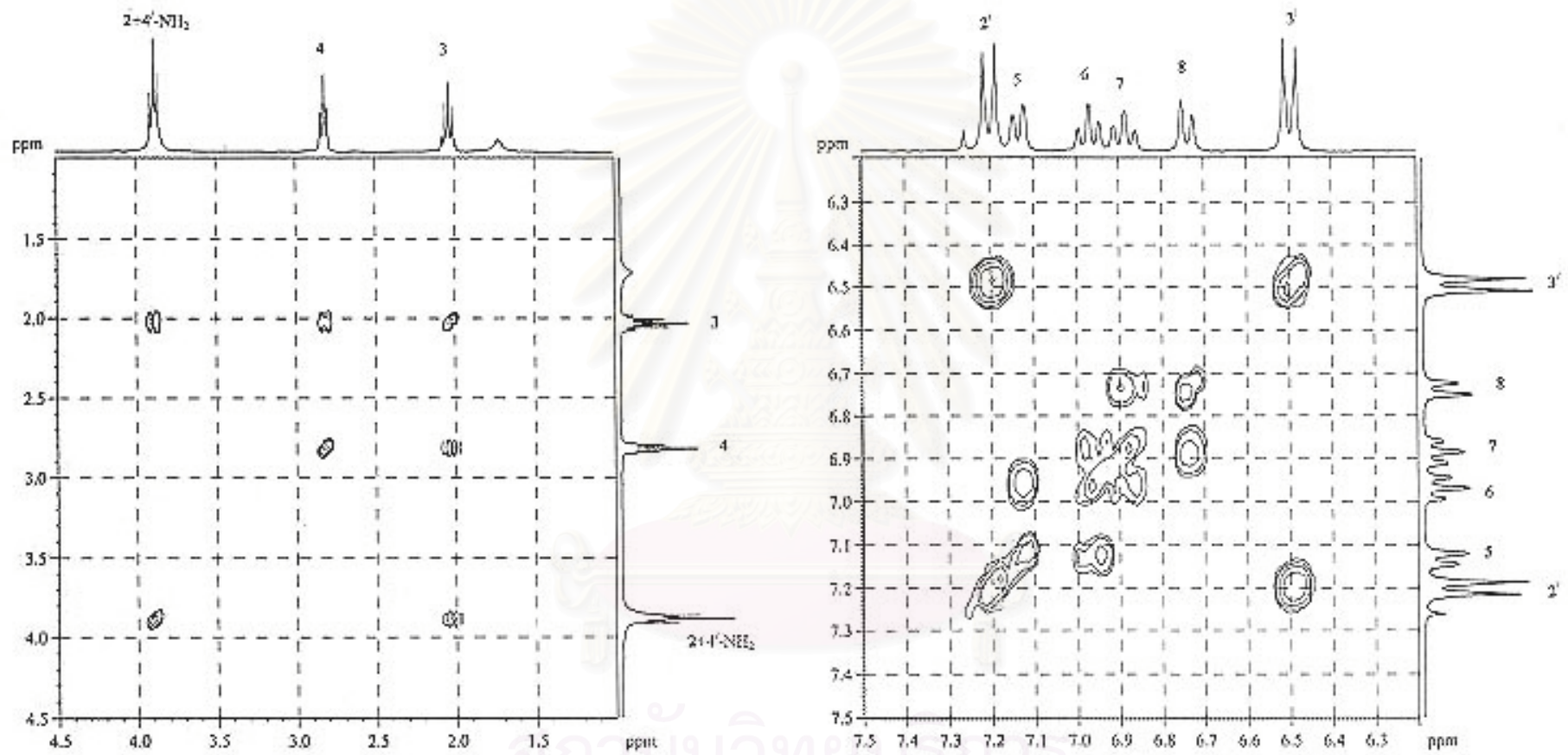
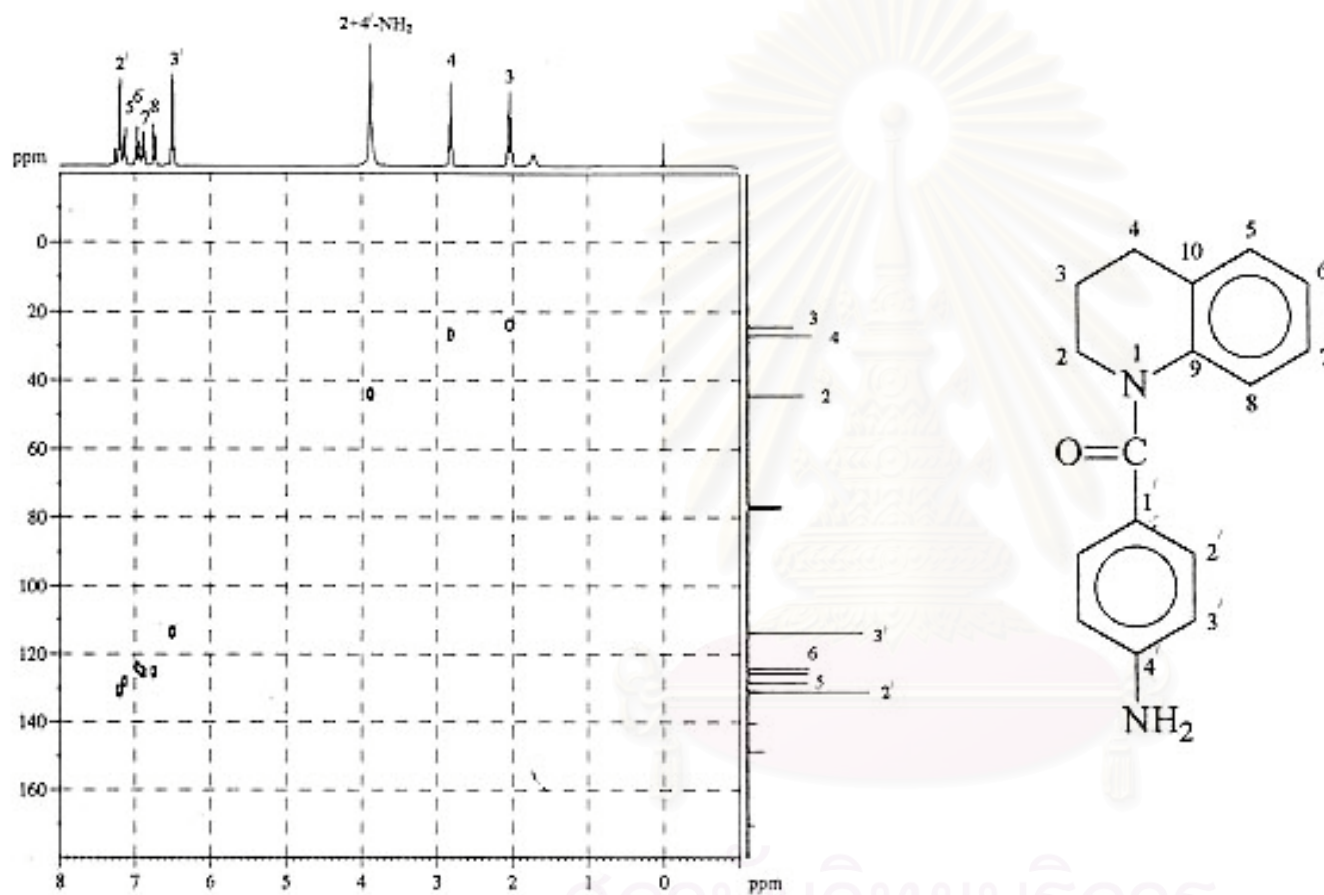Figure 99. The 300 MHz HH COSY spectrum of N-(*p*-aminobenzoyl)-1,2,3,4-tetrahydro-2-methylquinoline (4b, CU-17-04) in CDCl$_3$.

(Enlarged scale)

Figure 100. The 300 MHz HMQC spectrum of N-(*p*-aminobenzoyl)-1,2,3,4-tetrahydro-2-methylquinoline (4b, CU-17-04) in CDCl₃.
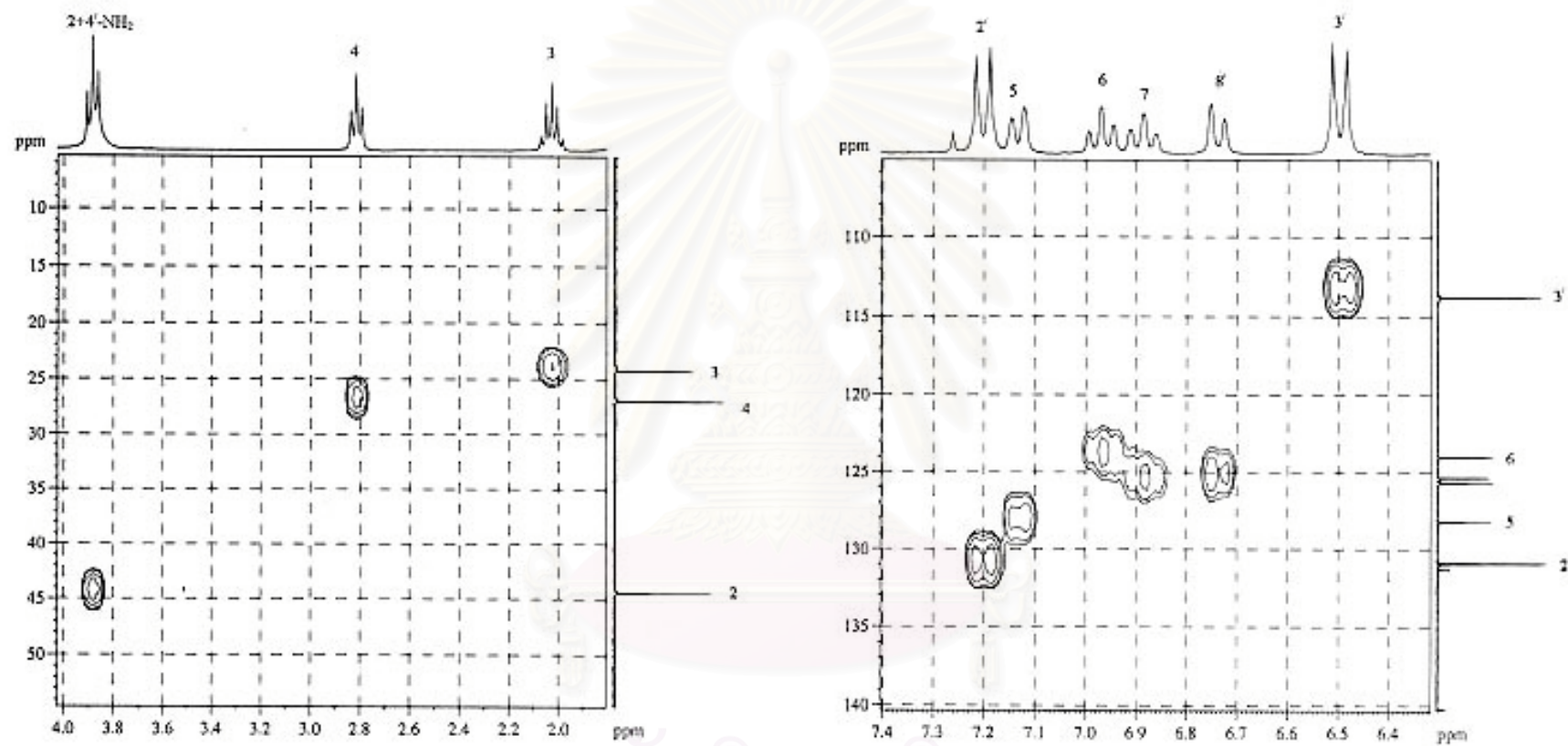
Figure 101. The 300 MHz HMQC spectrum of N-(*p*-aminobenzoyl)-1,2,3,4-tetrahydro-2-methylquinoline (4b, CU-17-04) in CDCl₃. (Enlarged scale)
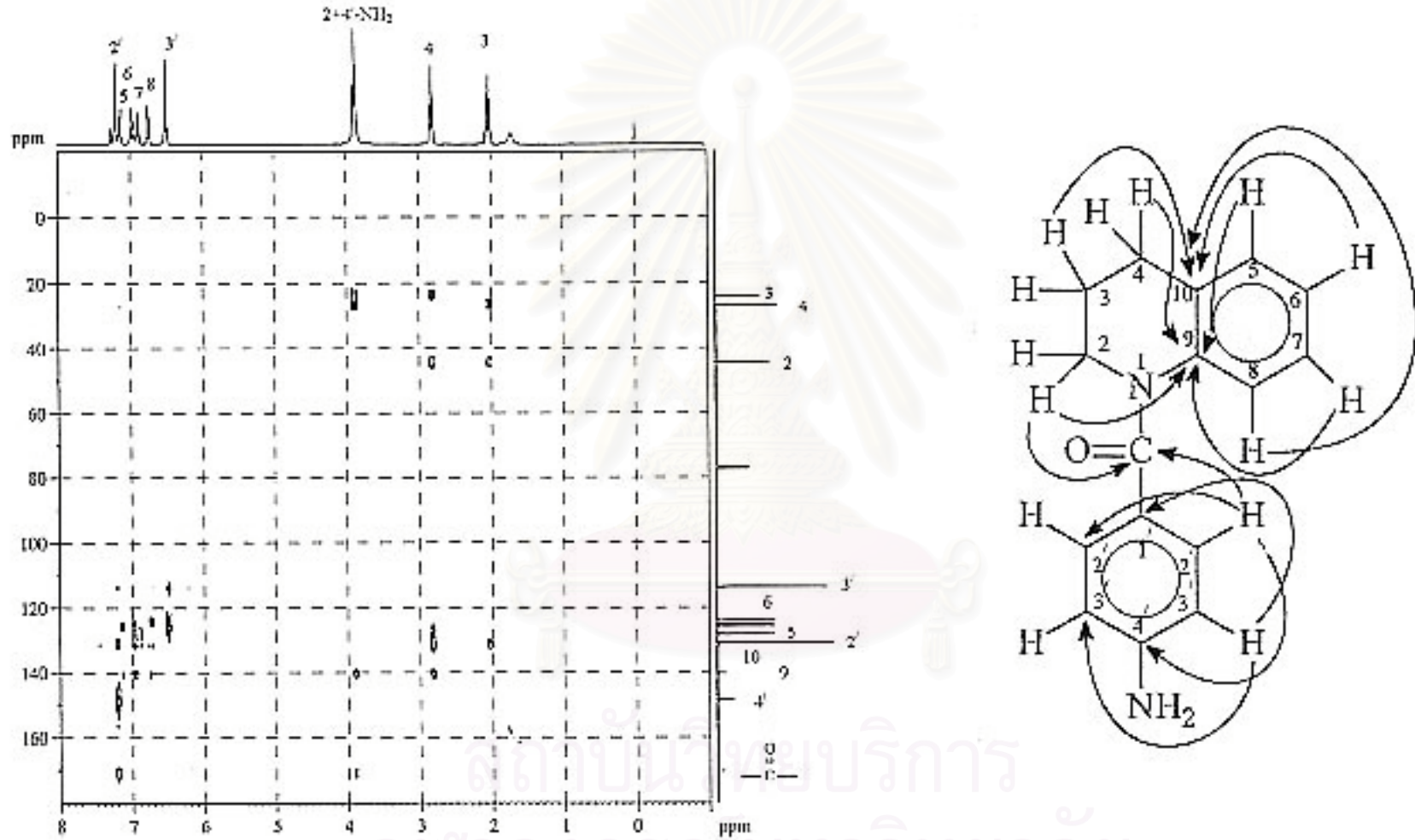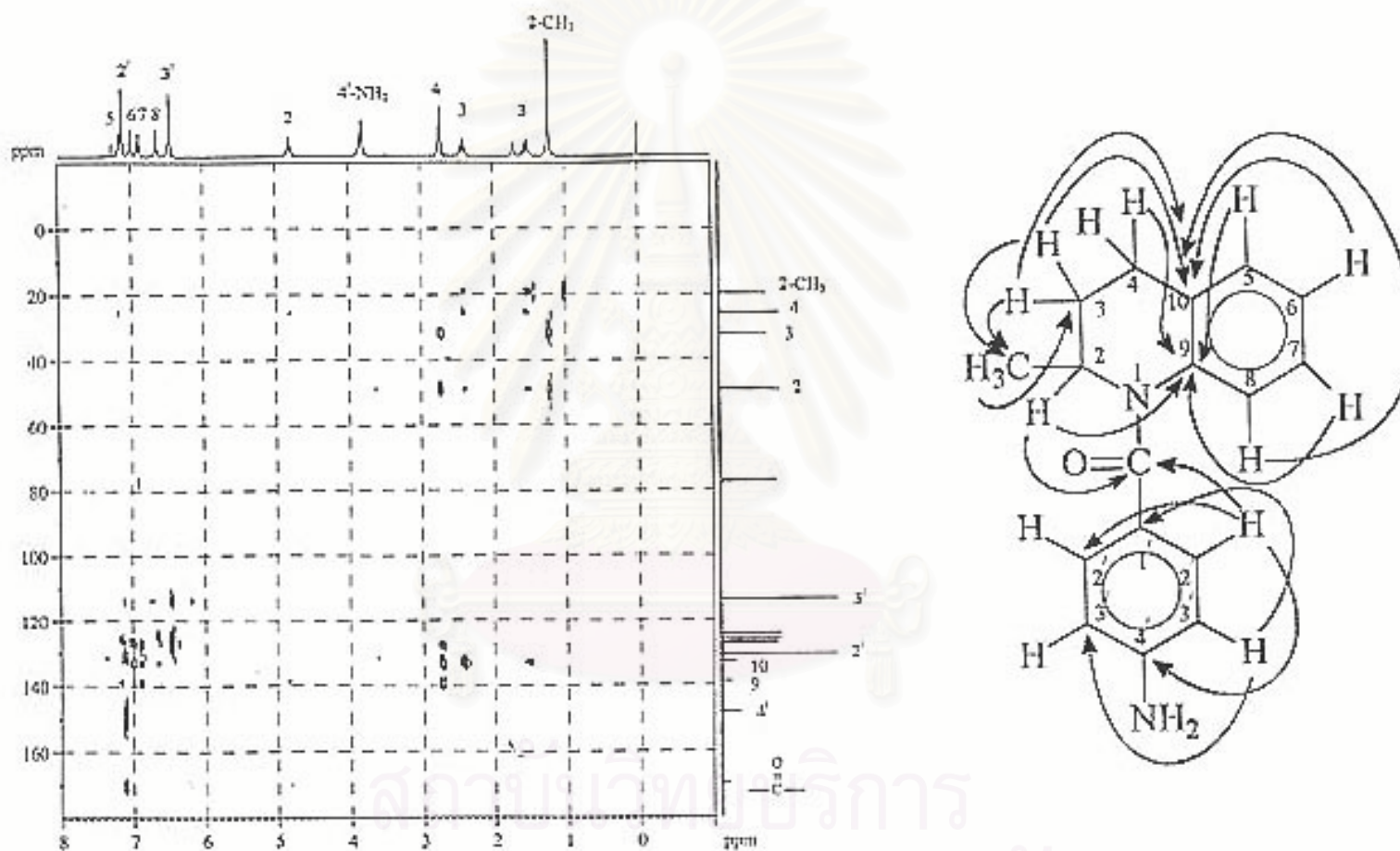
Figure 102. The 300 MHz HMBC spectrum (JHC = 8 Hz) of N-(*p*-aminobenzoyl)-1,2,3,4-tetrahydro-2-methylquinoline (4b, CU-17-04) in
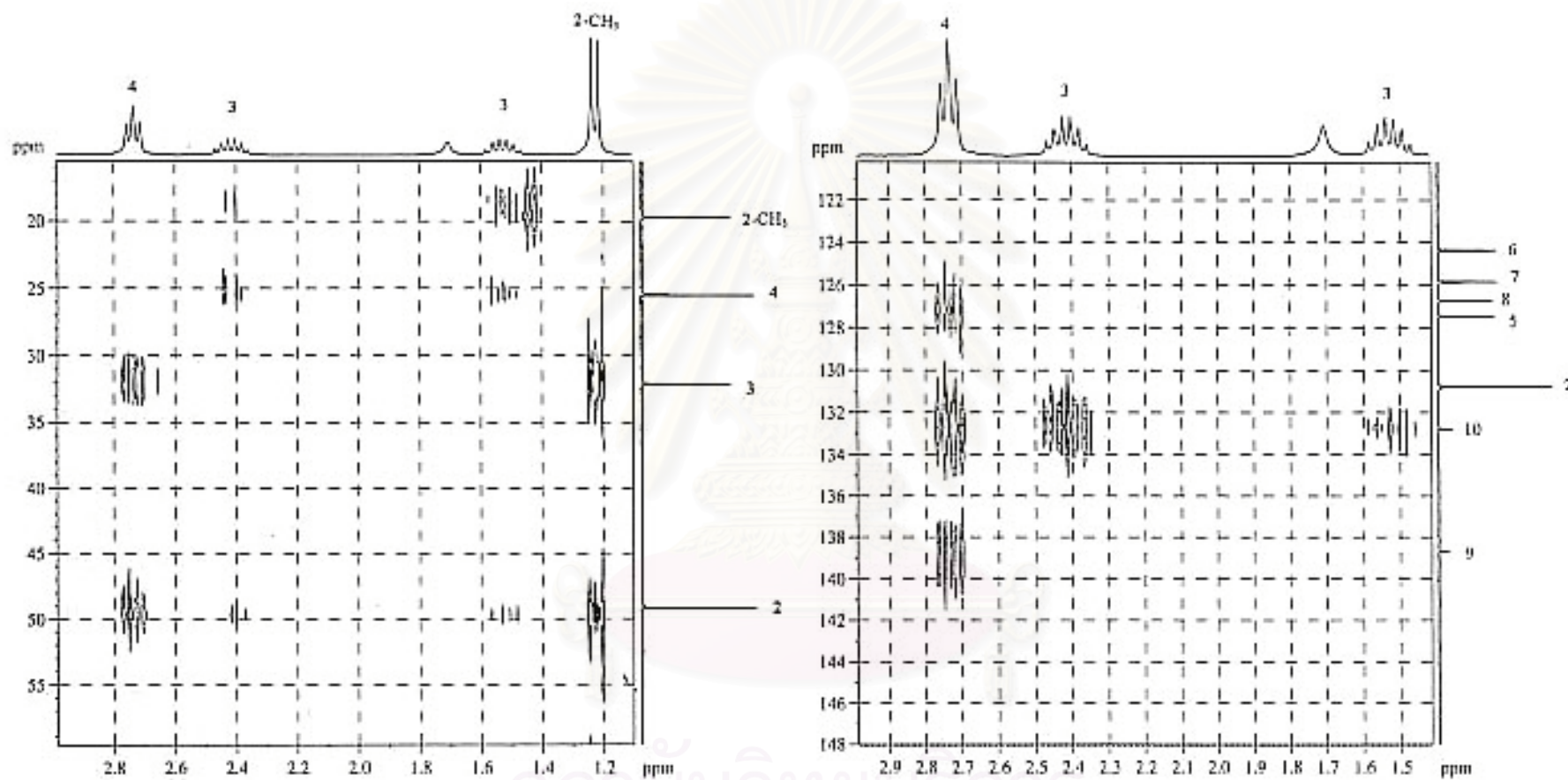
CDCl₃.

Figure 103. The 300 MHz HMBC spectrum (JHC = 8 Hz) of N-(*p*-aminobenzoyl)-1,2,3,4-tetrahydro-2-methylquinoline (4b, CU-17-04) in

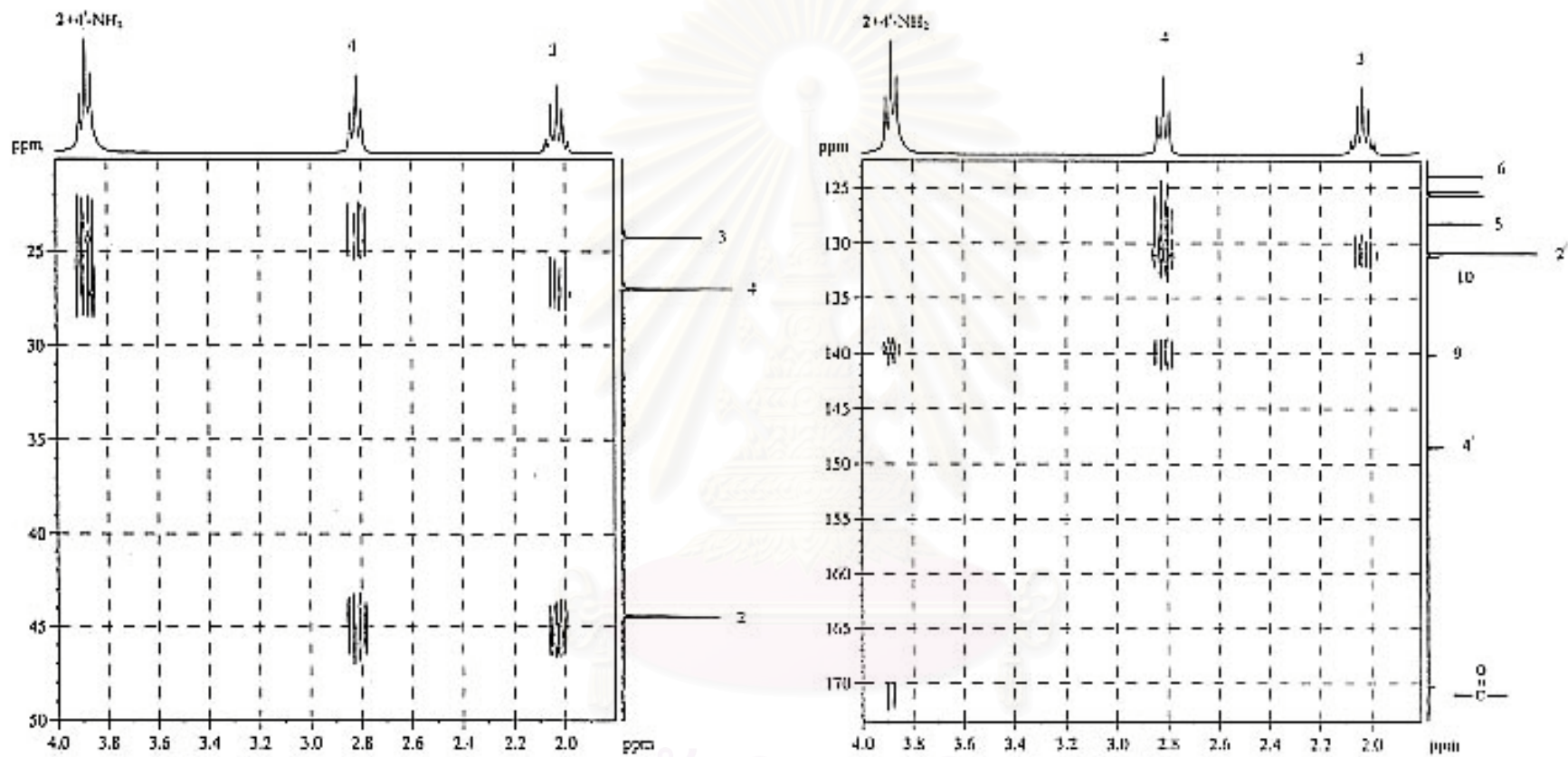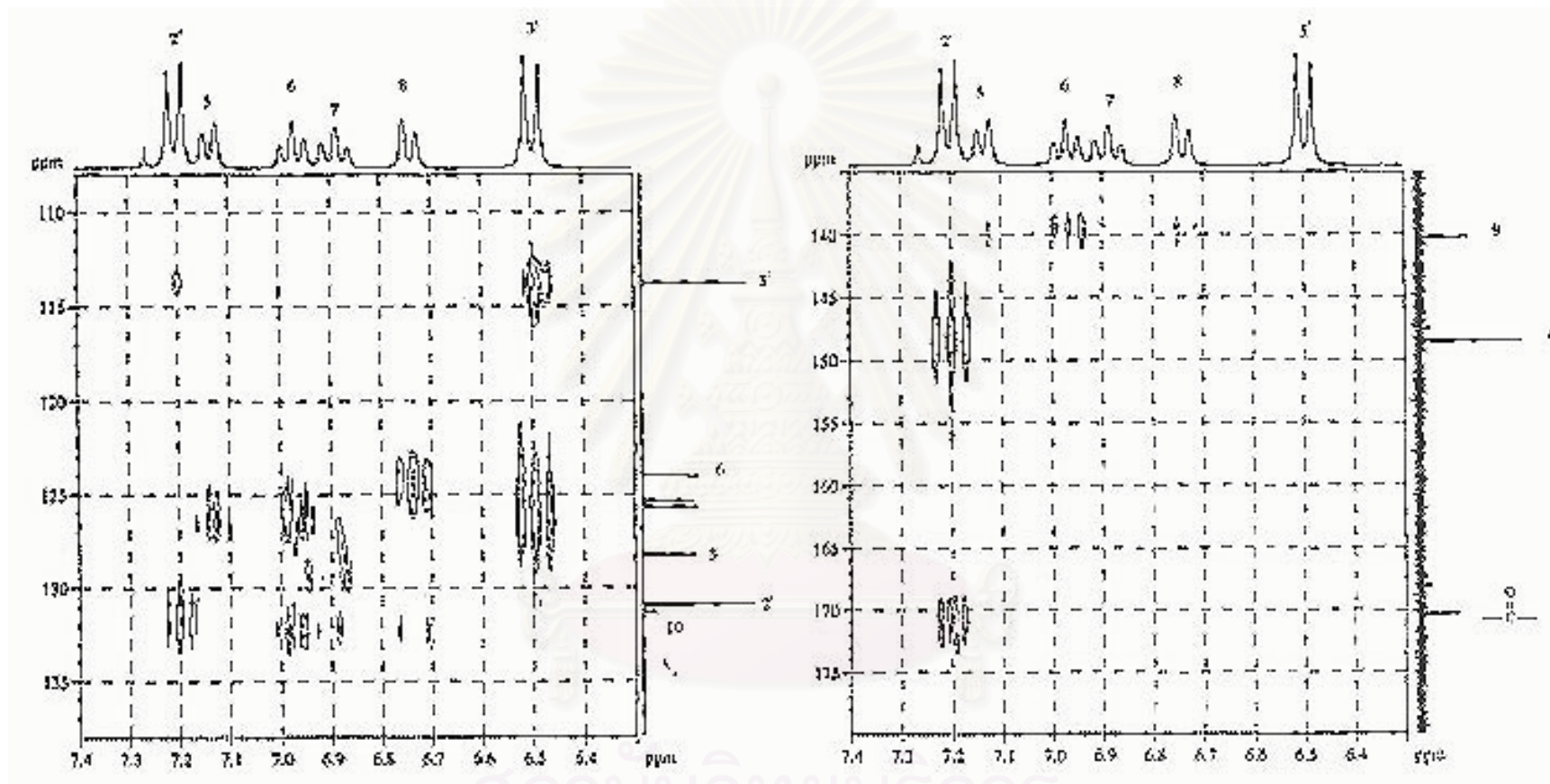CDCl₃. (Expanded: Left; δH 1.1-3.0 ppm; δC 15-60 ppm: Right; δH 1.4-3.0 ppm; δC 120-148 ppm)
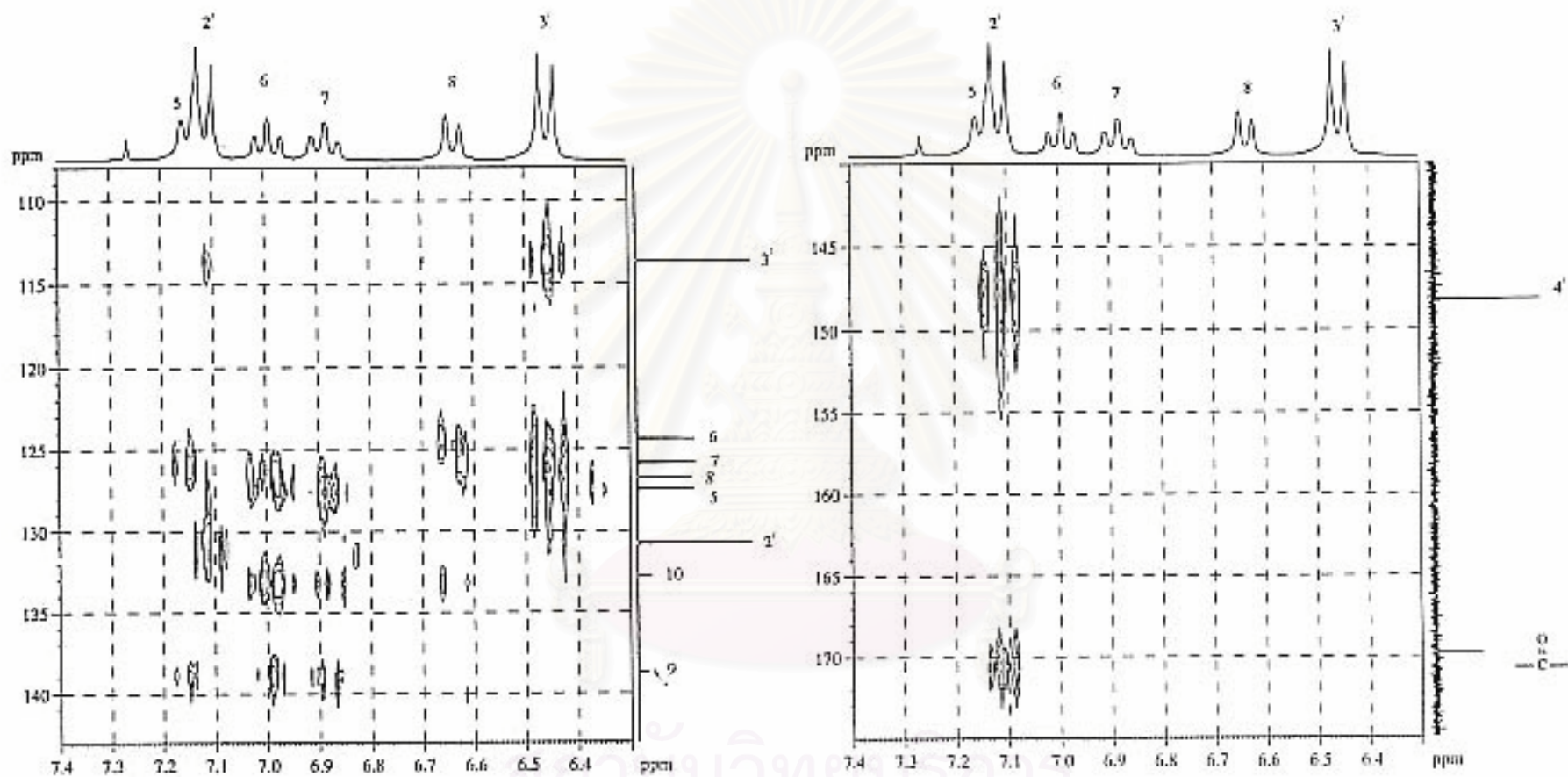
Figure 104. The 300 MHz HMBC spectrum (JHC = 8 Hz) of N-(*p*-aminobenzoyl)-1,2,3,4-tetrahydro-2-methylquinoline (4b, CU-17-04) in
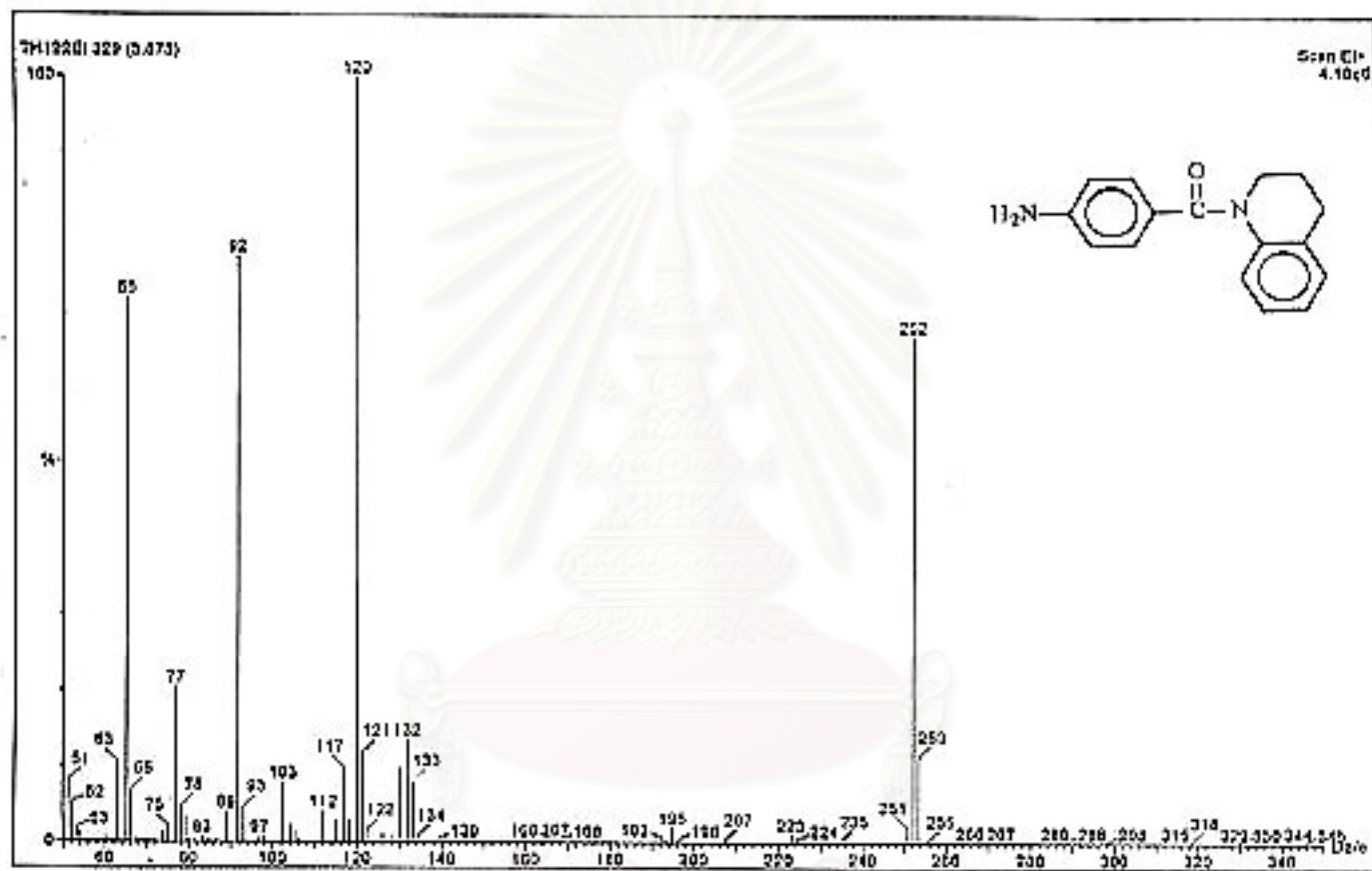
CDCl₃. (Expanded: δH 6.3-7.4 ppm; δC 108-175 ppm)

Figure 105. The electron impact mass spectrum of N-(*p*-aminobenzoyl)-1,2,3,4-tetrahydro-2-methylquinoline (4b, CU-17-04).
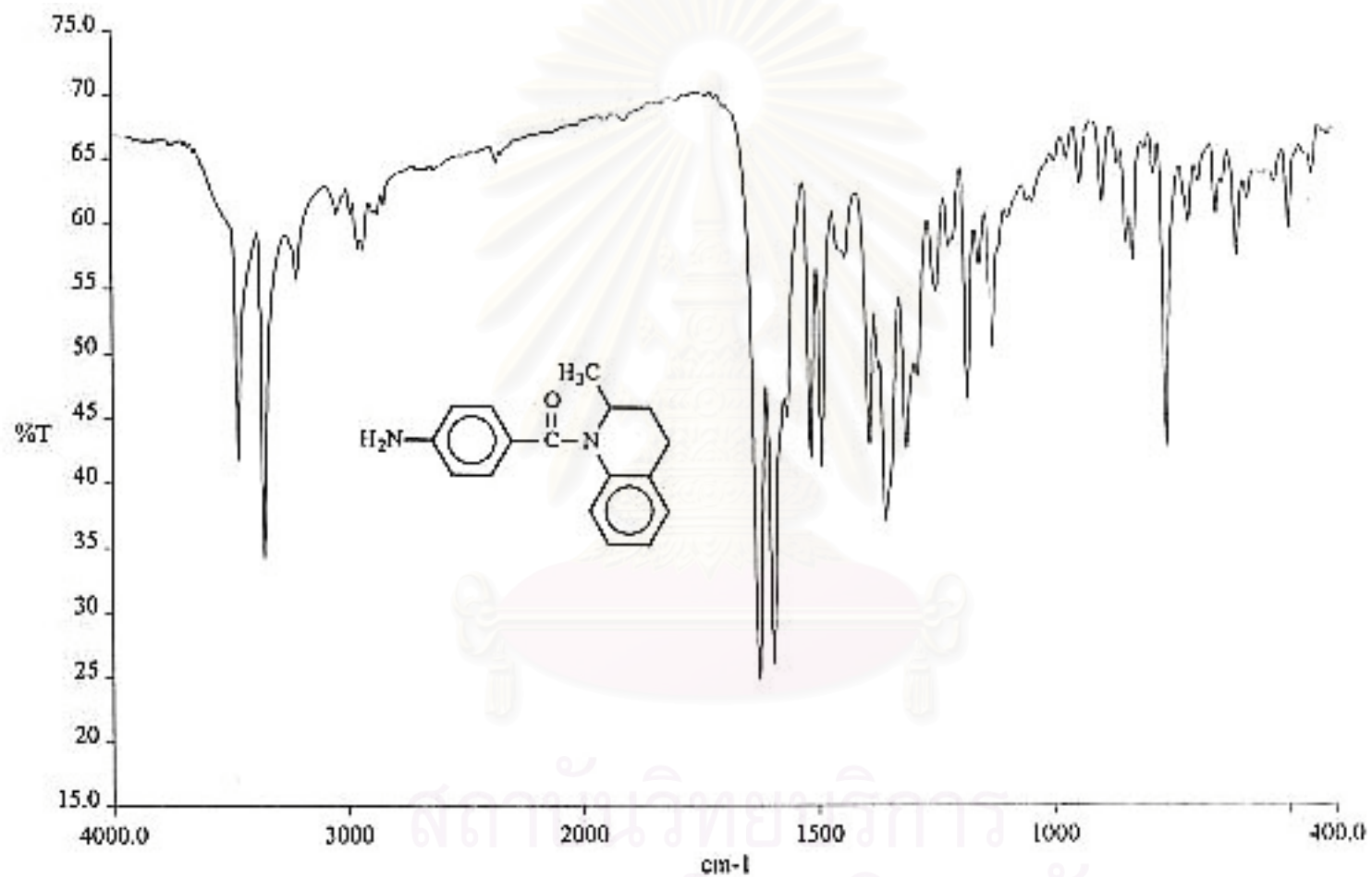
Figure 106. The IR spectrum (KBr) of N-(*p*-aminobenzoyl)-1,2,3,4-tetrahydro-4-methylquinoline (4c, CU-17-06).
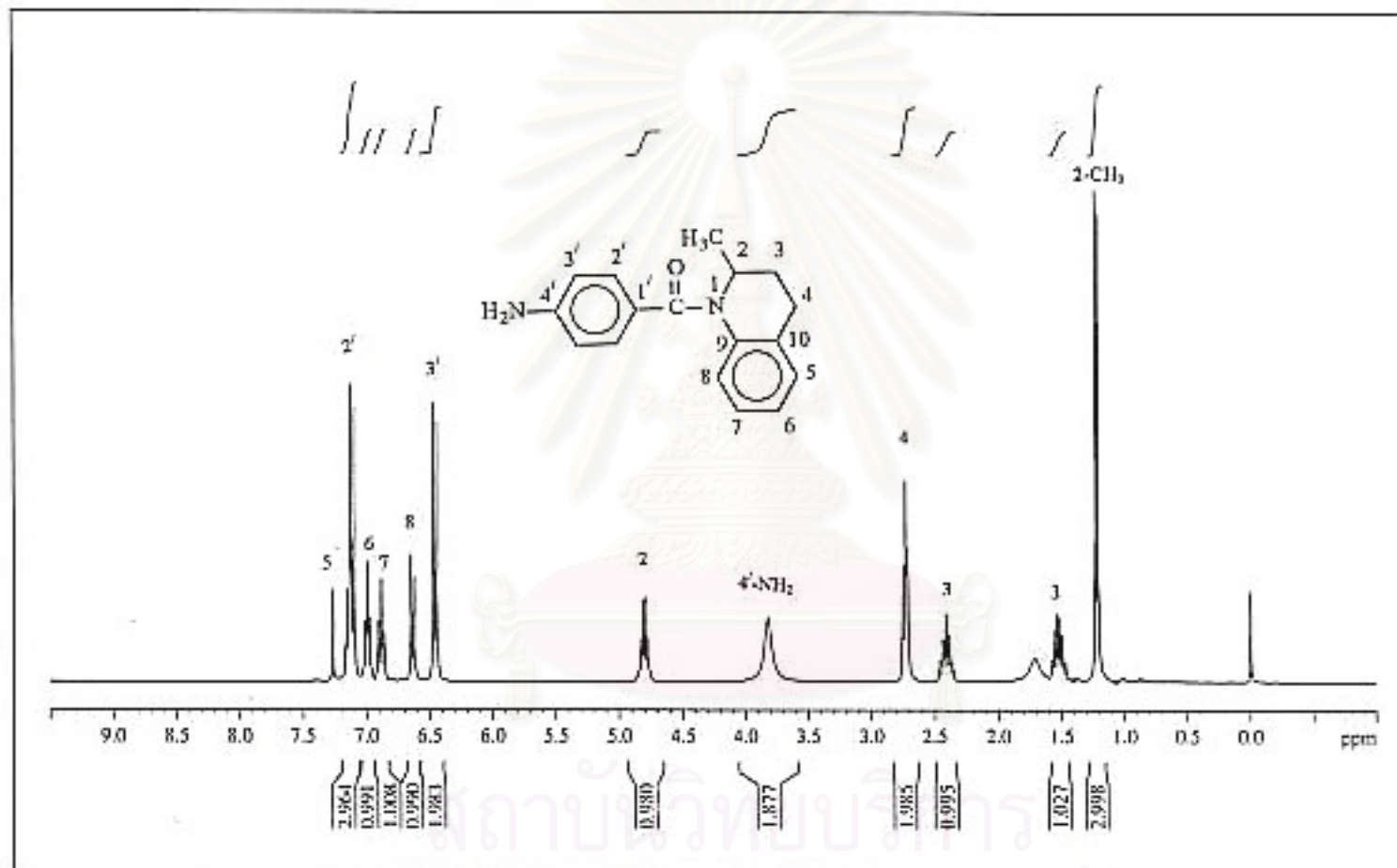
Figure 107. The 300 MHz 1H-NMR spectrum of N-(*p*-aminobenzoyl)-1,2,3,4-tetrahydro-4-methylquinoline (4c, CU-17-06) in CDCl₃.

Figure 108. The 300 MHz 1H-NMR spectrum of N-(*p*-aminobenzoyl)-1,2,3,4-tetrahydro-4-methylquinoline (4c, CU-17-06) in CDCl₃.

(Enlarged scale)
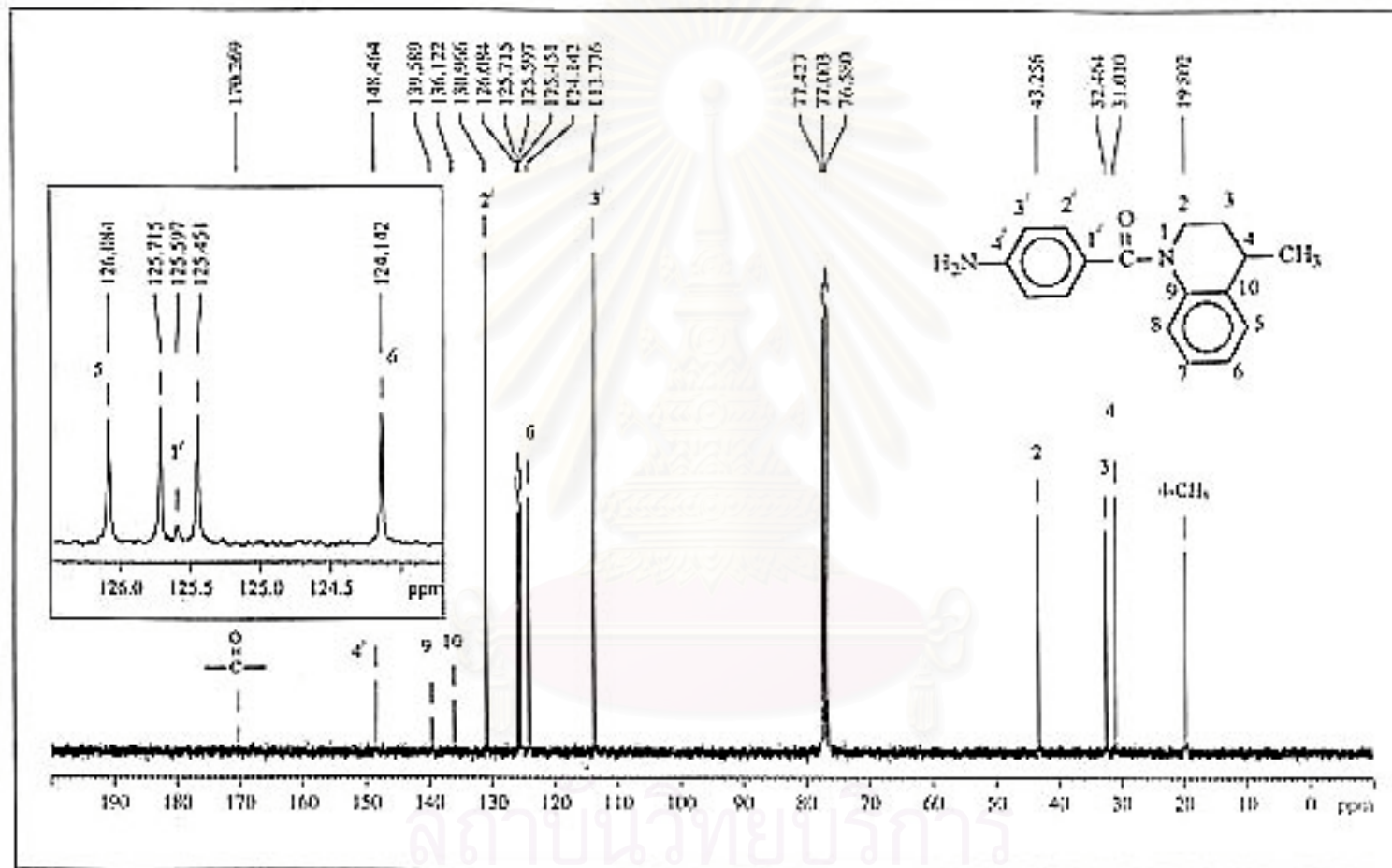
Figure 109. The 75 MHz 13C-NMR decoupled spectrum of N-(*p*-aminobenzoyl)-1,2,3,4-tetrahydro-4-methylquinoline (4c, CU-17-06) in
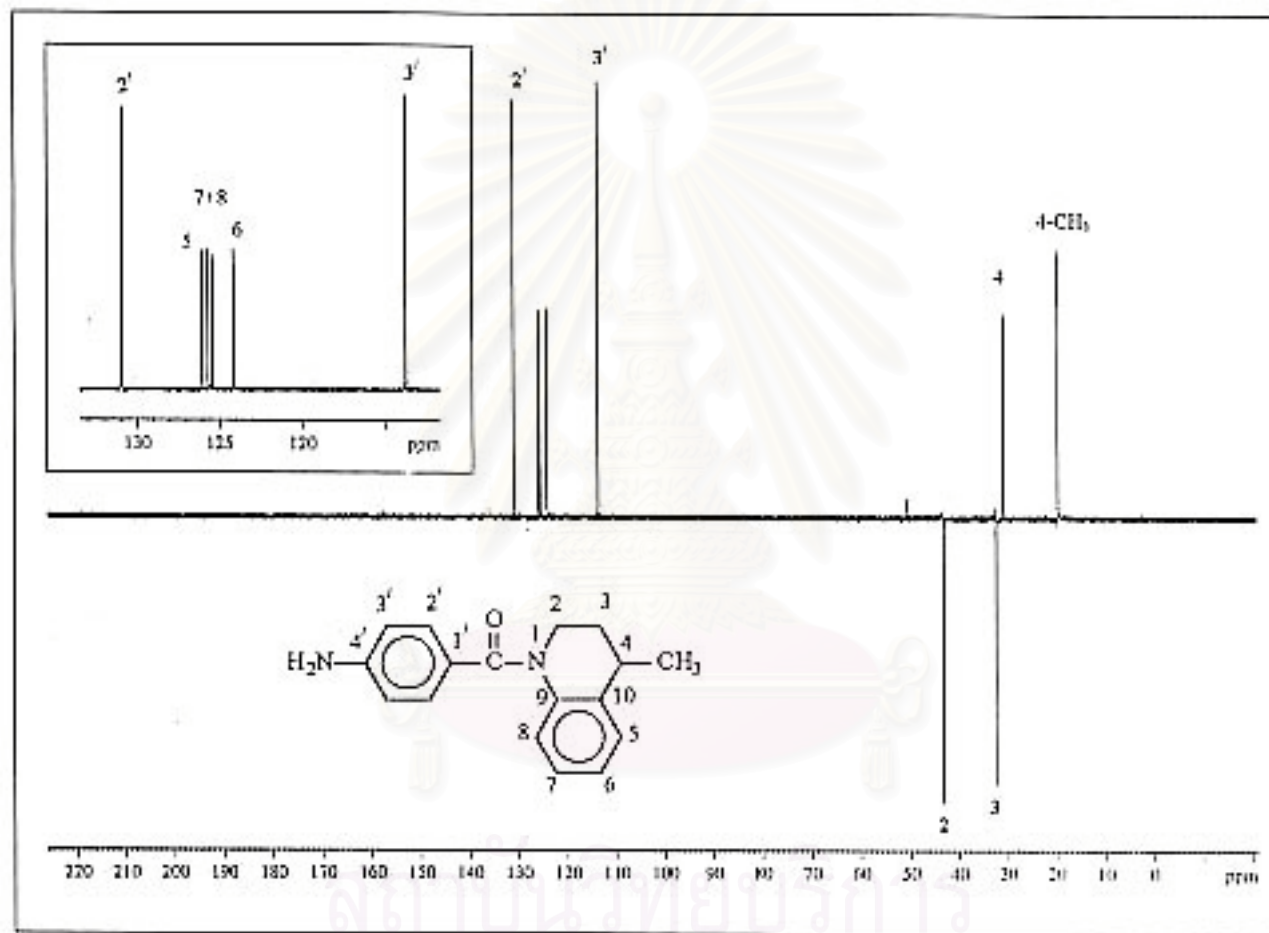
CDCl₃.

Figure 110. The 75 MHz DEPT-135 spectrum of N-(*p*-aminobenzoyl)-1,2,3,4-tetrahydro-4-methylquinoline (4c, CU-17-06) in CDCl₃.
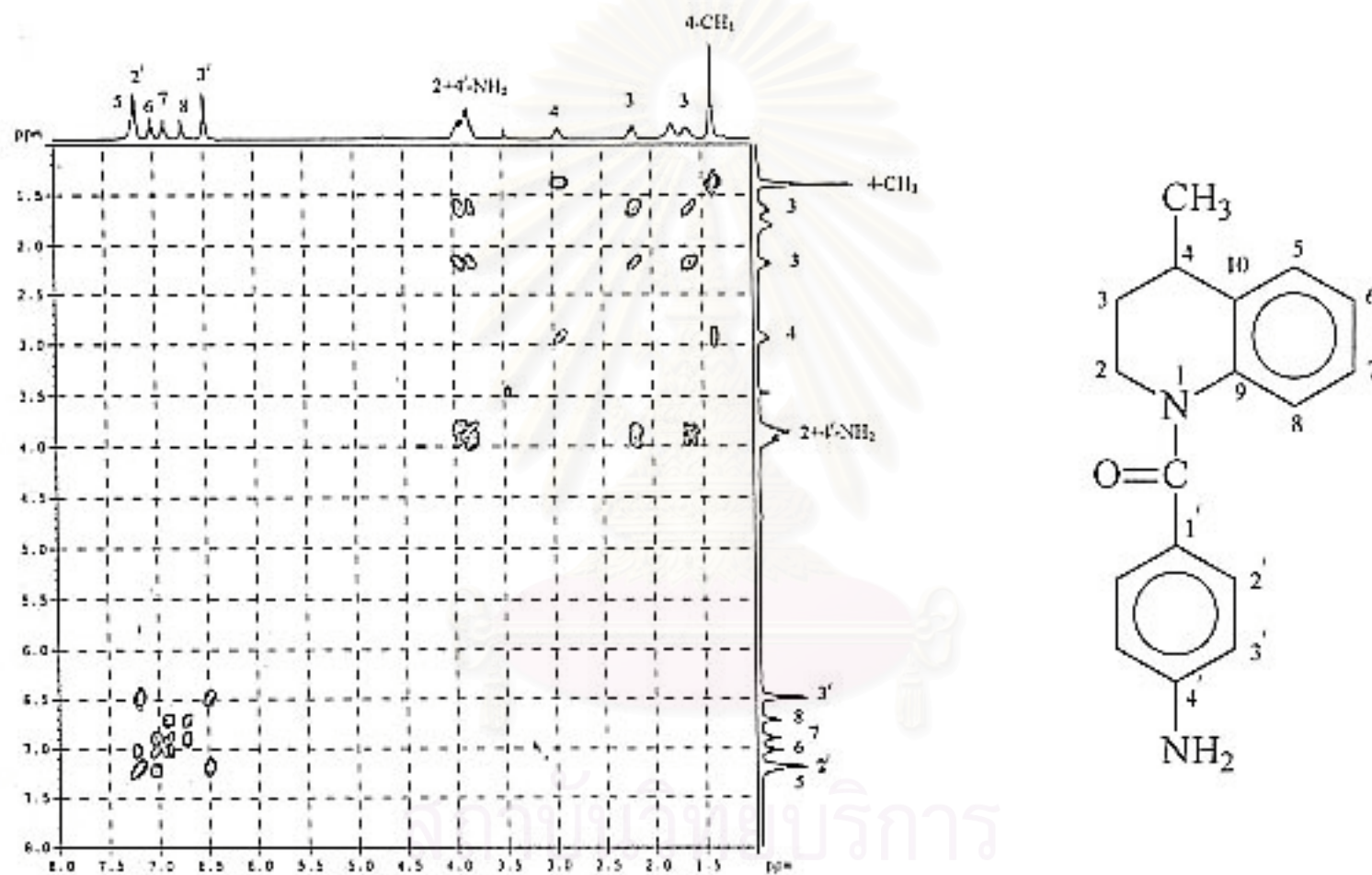
Figure 111. The 300 MHz HH COSY spectrum of N-(*p*-aminobenzoyl)-1,2,3,4-tetrahydro-4-methylquinoline (4c, CU-17-06) in CDCl$_3$.
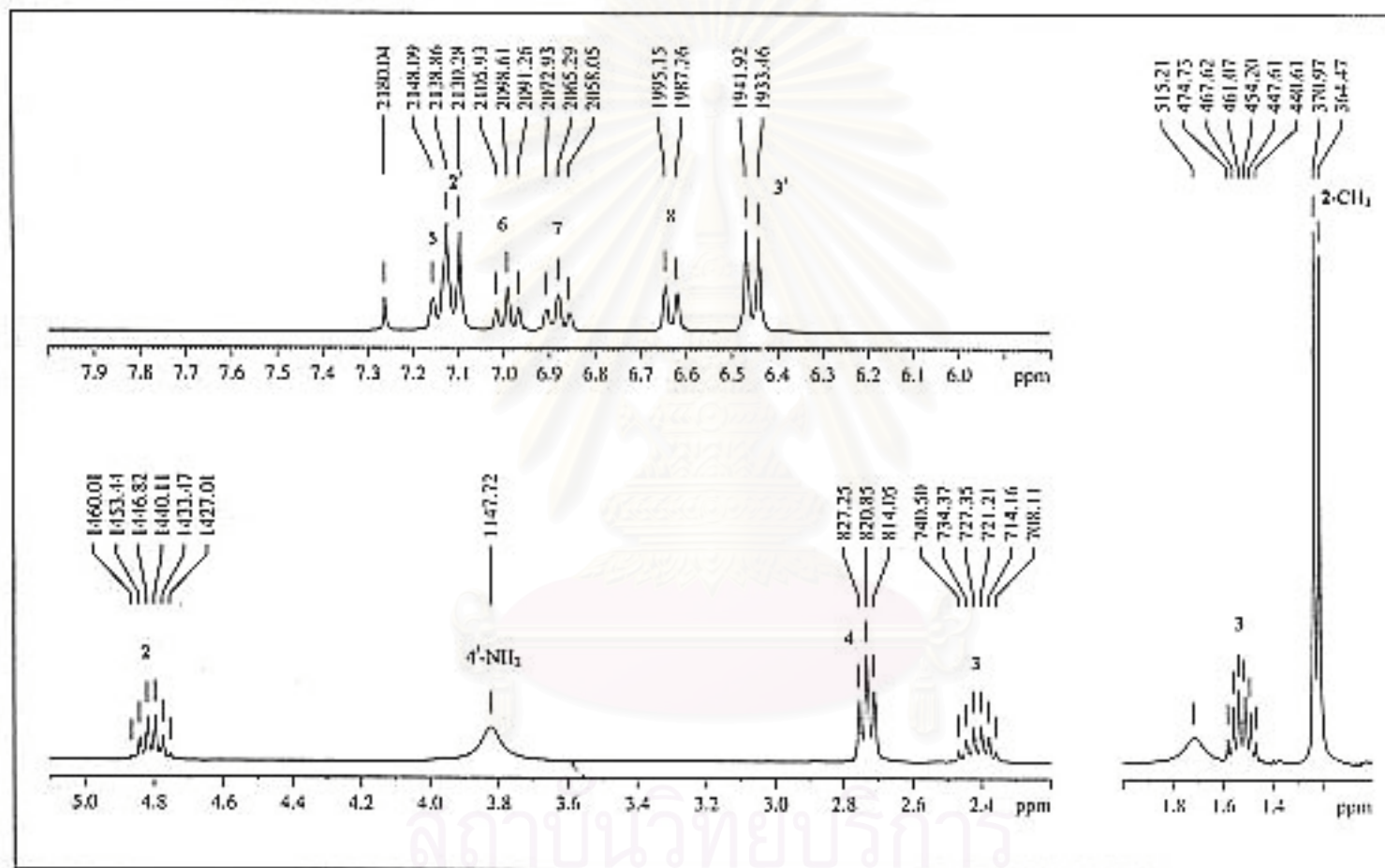
Figure 112. The 300 MHz HH COSY spectrum of N-(*p*-aminobenzoyl)-1,2,3,4-tetrahydro-4-methylquinoline (4c, CU-17-06) in CDCl₃.

(Enlarged scale)

Figure 113. The 300 MHz HMQC spectrum of N-(*p*-aminobenzoyl)-1,2,3,4-tetrahydro-4-methylquinoline (4c, CU-17-06) in CDCl₃.

Figure 114. The 300 MHz HMQC spectrum of N-(*p*-aminobenzoyl)-1,2,3,4-tetrahydro-4-methylquinoline (4c, CU-17-06) in CDCl₃. (Enlarged scale)
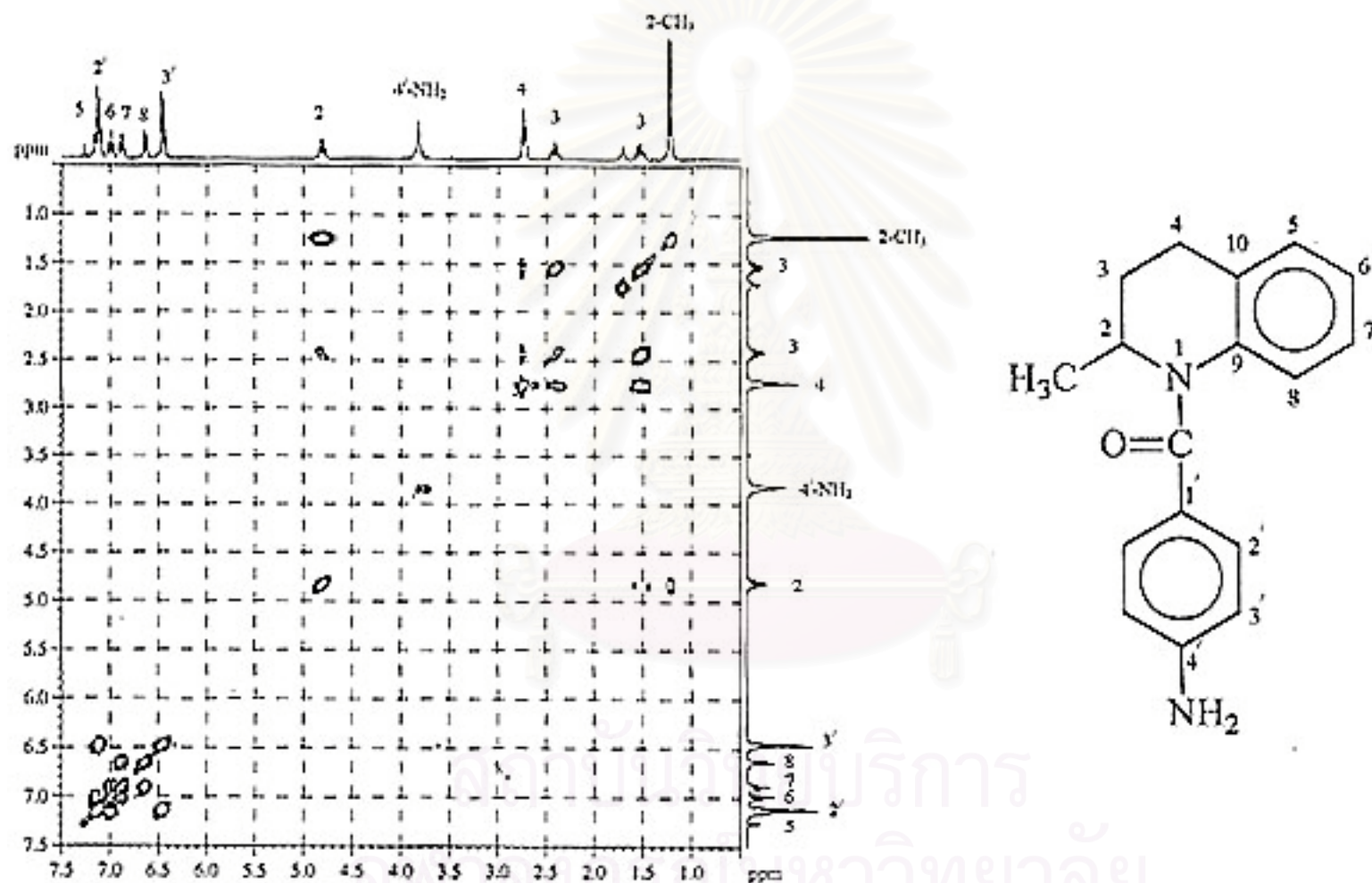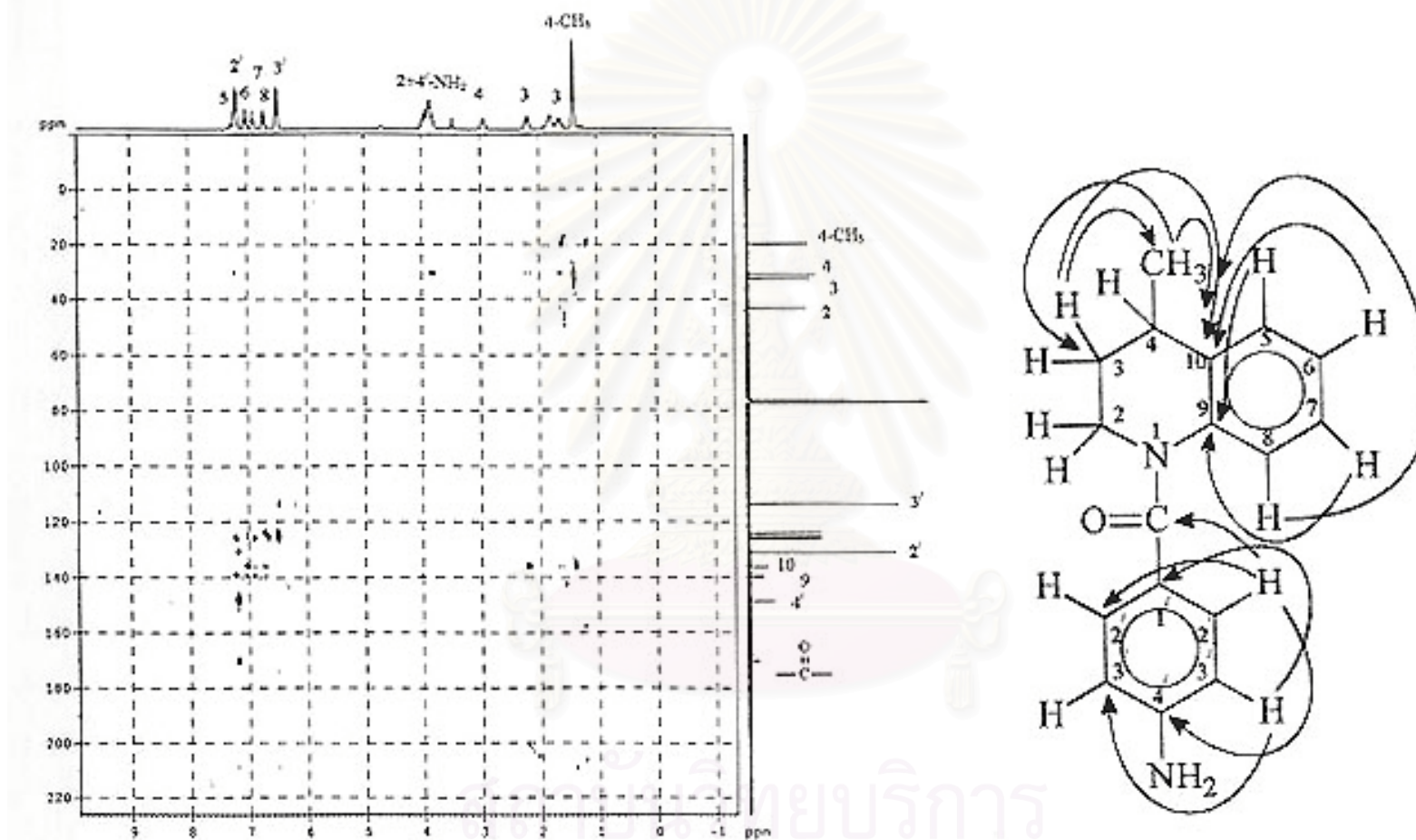
Figure 115. The 300 MHz HMBC spectrum (JHC = 8 Hz) of N-(*p*-aminobenzoyl)-1,2,3,4-tetrahydro-4-methylquinoline (4c, CU-17-06) in

CDCl₃.

Figure 116. The 300 MHz HMBC spectrum (JHC = 8 Hz) of N-(*p*-aminobenzoyl)-1,2,3,4-tetrahydro-4-methylquinoline (4c, CU-17-06) in

CDCl₃. (Expanded: Left; δH 1.0-4.5 ppm; δC (-1)-55 ppm: Right; δH 1.1-2.4 ppm; δC 105-175 ppm)

Figure 117. The 300 MHz HMBC spectrum (JHC = 8 Hz) of N-(*p*-aminobenzoyl)-1,2,3,4-tetrahydro-4-methylquinoline (4c, CU-17-06) in

CDCl₃. (Expanded: Left; δH 6.3-7.5 ppm; δc 105-175 ppm: Right; δH 6.4-7.4 ppm; δC 120-146 ppm)
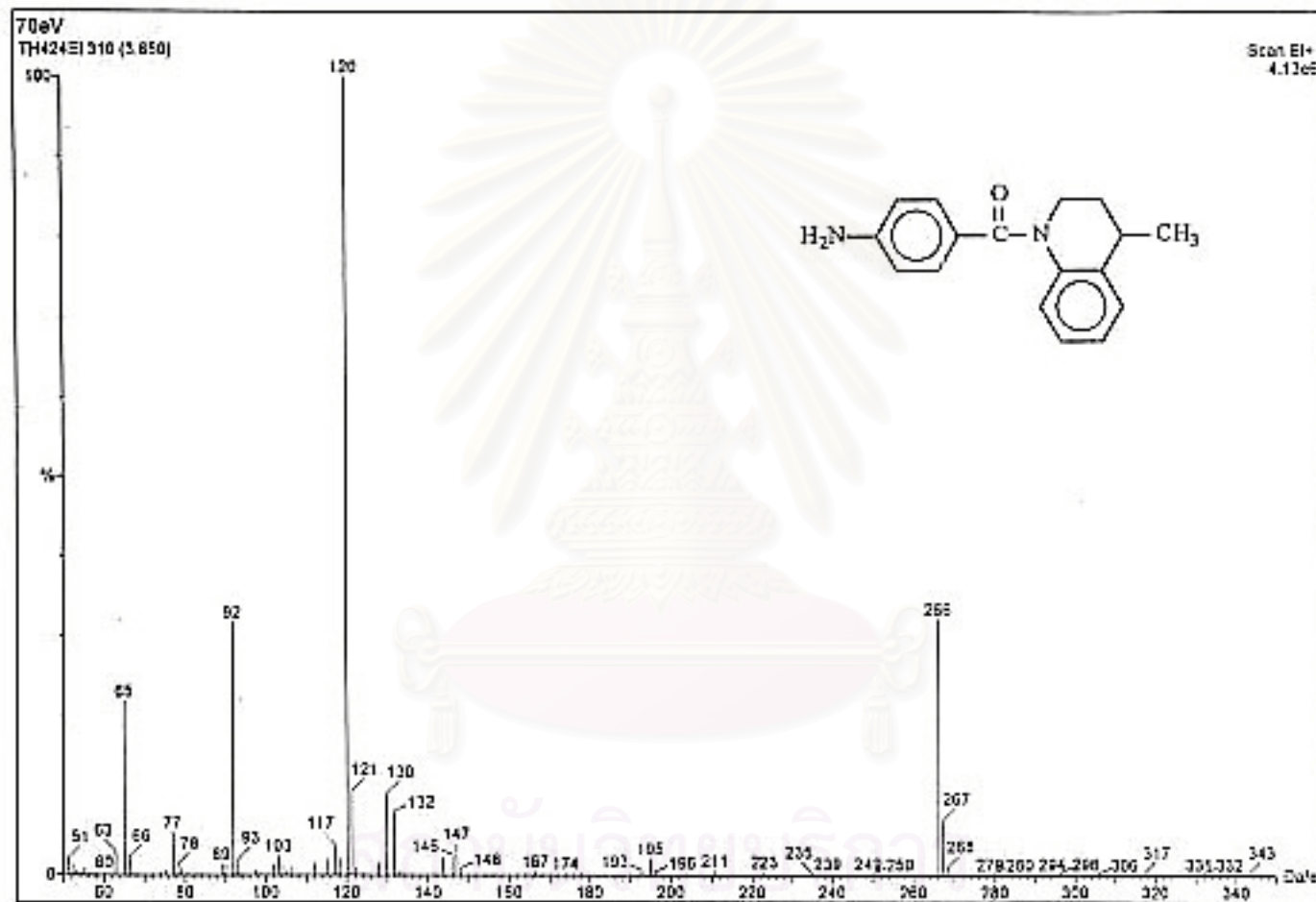
Figure 118. The electron impact mass spectrum of N-(*p*-aminobenzoyl)-1,2,3,4-tetrahydro-4-methylquinoline (4c, CU-17-06).

Figure 119. The IR spectrum (KBr) of N-(*p*-aminobenzoyl)-1,2,3,4-tetrahydro-8-methylquinoline (4d, CU-17-08).

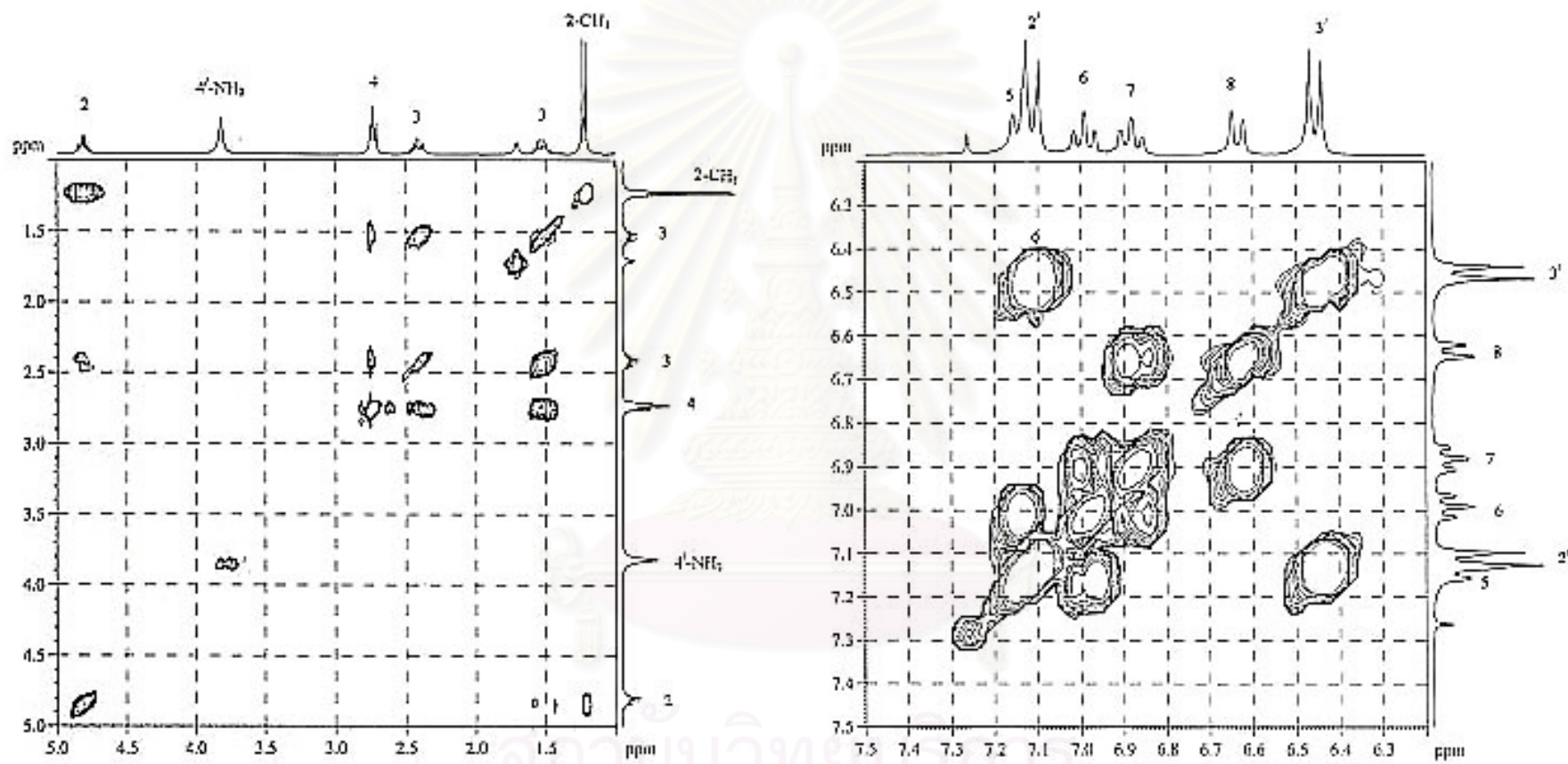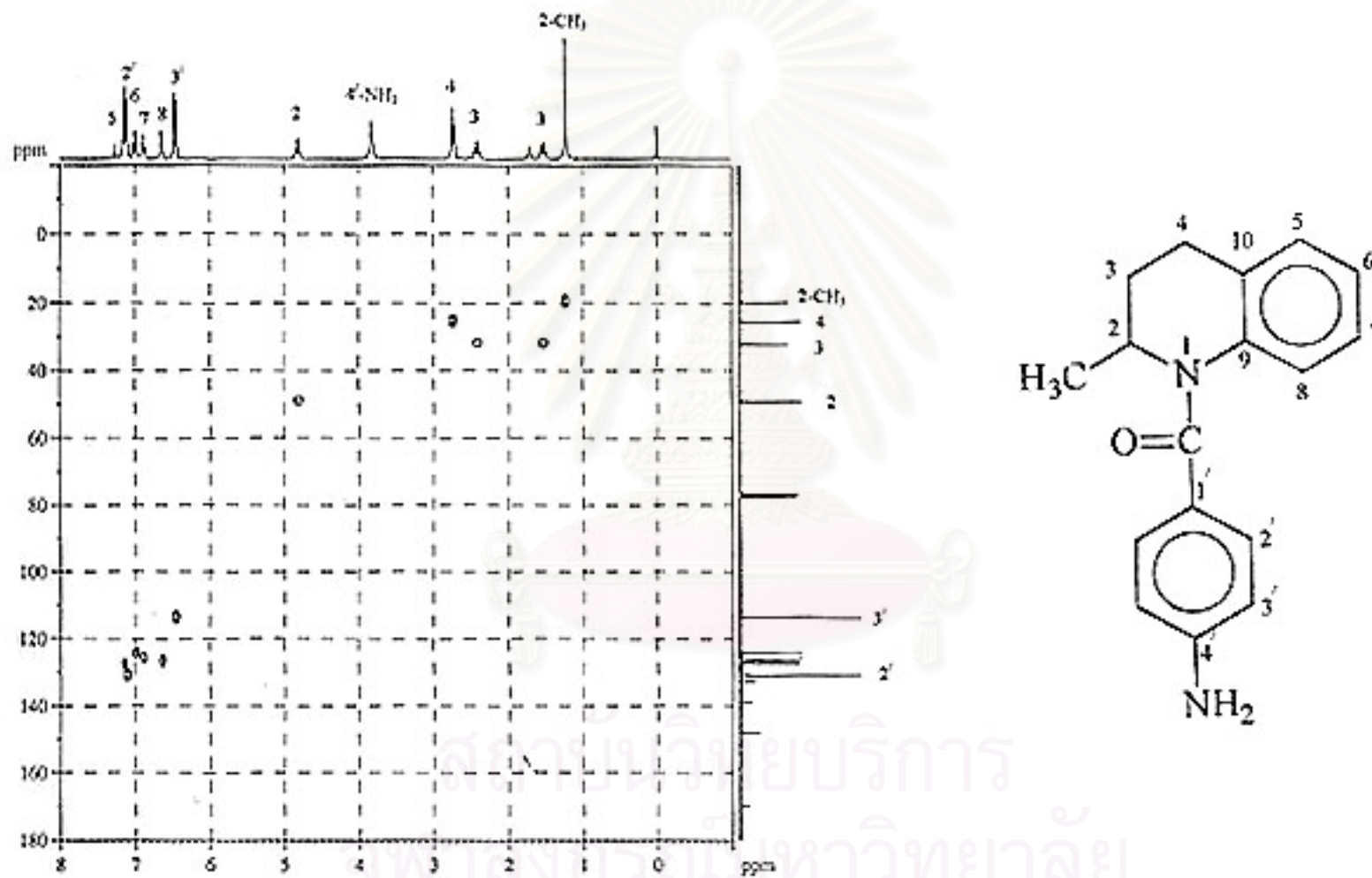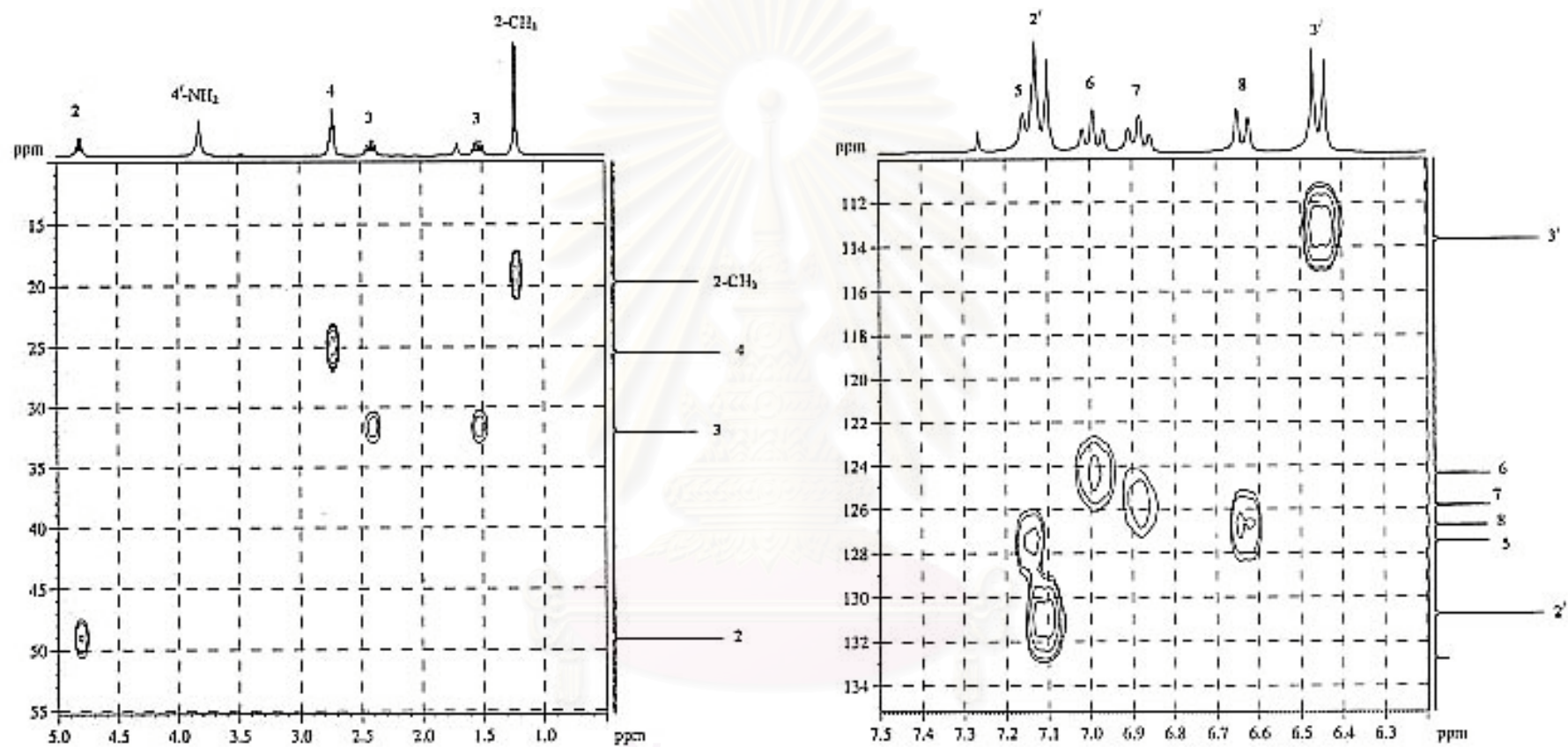Figure 120. The 300 MHz 1H-NMR spectrum of N-(*p*-aminobenzoyl)-1,2,3,4-tetrahydro-8-methylquinoline (4d, CU-17-08) in CDCl$_3$.

Figure 121. The 500 MHz 1H-NMR spectra of N-(*p*-aminobenzoyl)-1,2,3,4-tetrahydro-8-methylquinoline (4d, CU-17-08) in CDCl$_3$ at room temperature (RT), 15 °C, 0 °C, -15 °C and -30 °C.

Figure 122. The 500 MHz 1H-NMR spectra of N-(*p*-aminobenzoyl)-1,2,3,4-tetrahydro-8-methylquinoline (4d, CU-17-08) in CDCl₃ at room

temperature (RT), 15 °C, 0 °C, -15 °C and -30 °C. (Enlarged scale)

Figure 123. The 500 MHz 1H-NMR spectrum of N-(*p*-aminobenzoyl)-1,2,3,4-tetrahydro-8-methylquinoline (4d, CU-17-08) in CDCl$_3$ at

-30 °C.

Figure 124. The 500 MHz 1H-NMR spectrum of N-(*p*-aminobenzoyl)-1,2,3,4-tetrahydro-8-methylquinoline (4d, CU-17-08) in CDCl₃ at
-30 °C. (Enlarged scale)

Figure 125. The electron impact mass spectrum of N-(*p*-aminobenzoyl)-1,2,3,4-tetrahydro-8-methylquinoline (4d, CU-17-08).
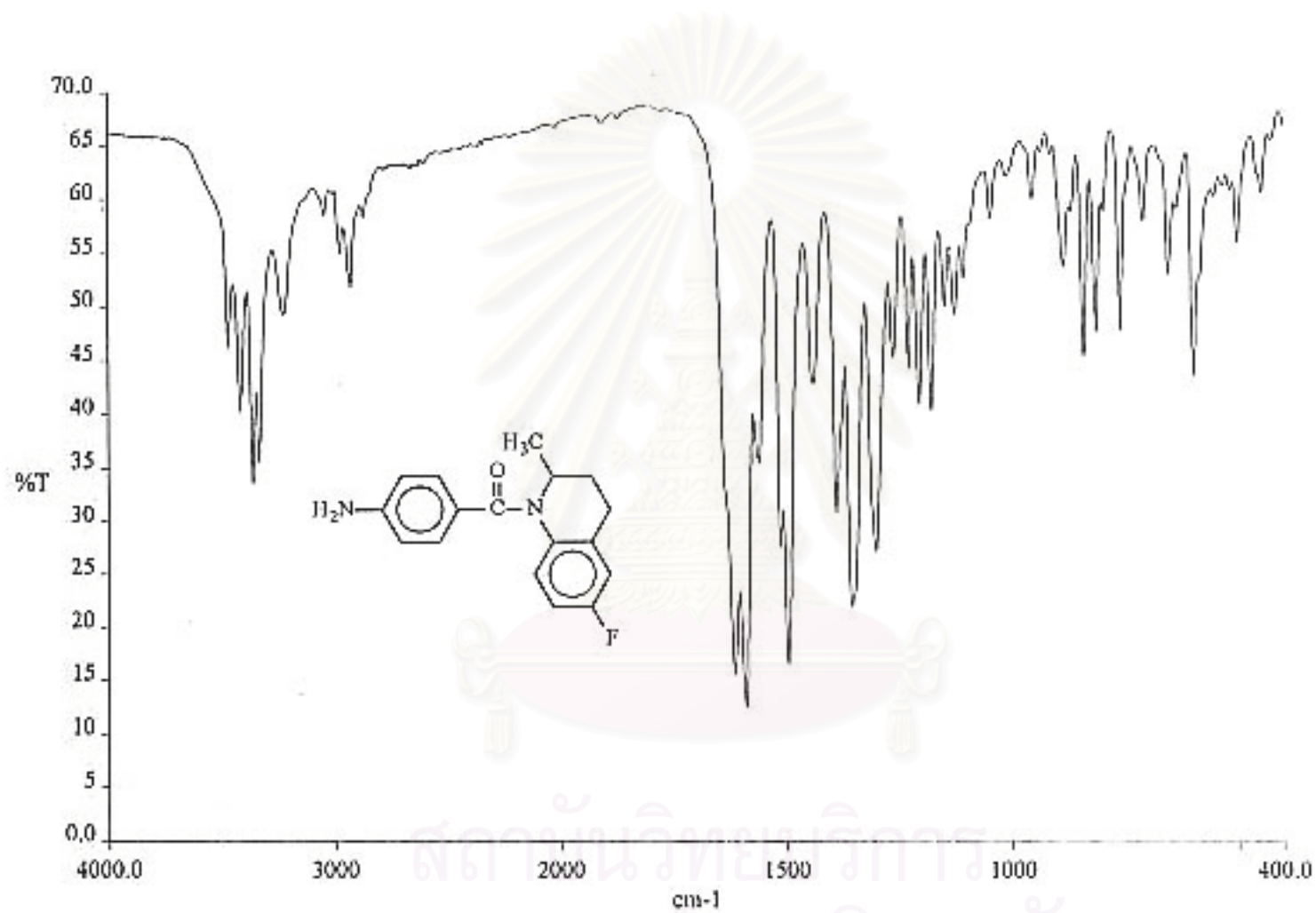
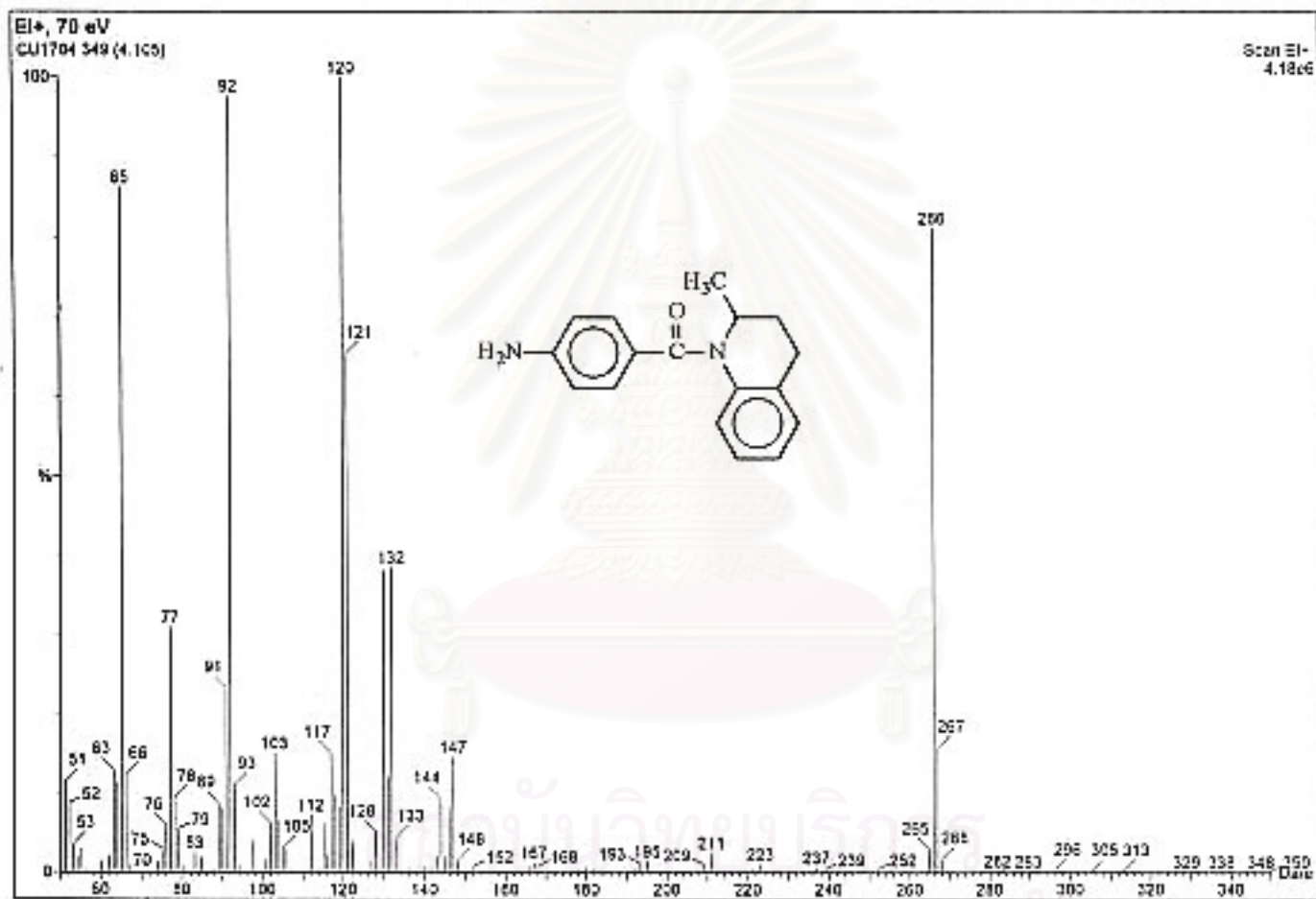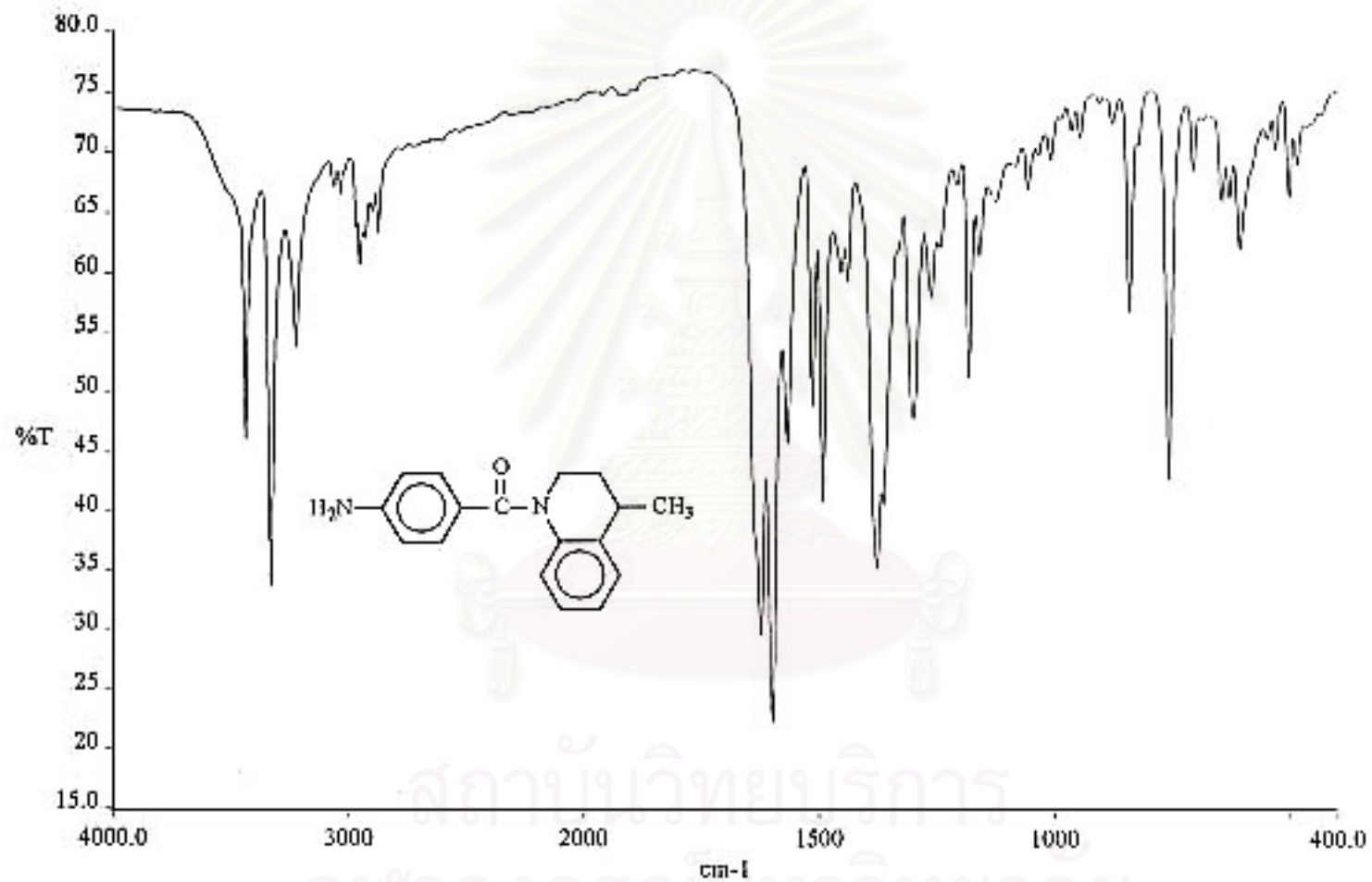Figure 126. The IR spectrum (KBr) of N-(*p*-aminobenzoyl)-1,2,3,4-tetrahydro-6-fluoro-2-methylquinoline (4e, CU-17-10).

Figure 127. The 300 MHz 1H-NMR spectrum of N-(*p*-aminobenzoyl)-1,2,3,4-tetrahydro-6-fluoro-2-methylquinoline (4e, CU-17-10) in CDCl₃.

Figure 128. The 300 MHz 1H-NMR spectrum of N-(*p*-aminobenzoyl)-1,2,3,4-tetrahydro-6-fluoro-2-methylquinoline (4e, CU-17-10) in CDCl₃.

(Enlarged scale)
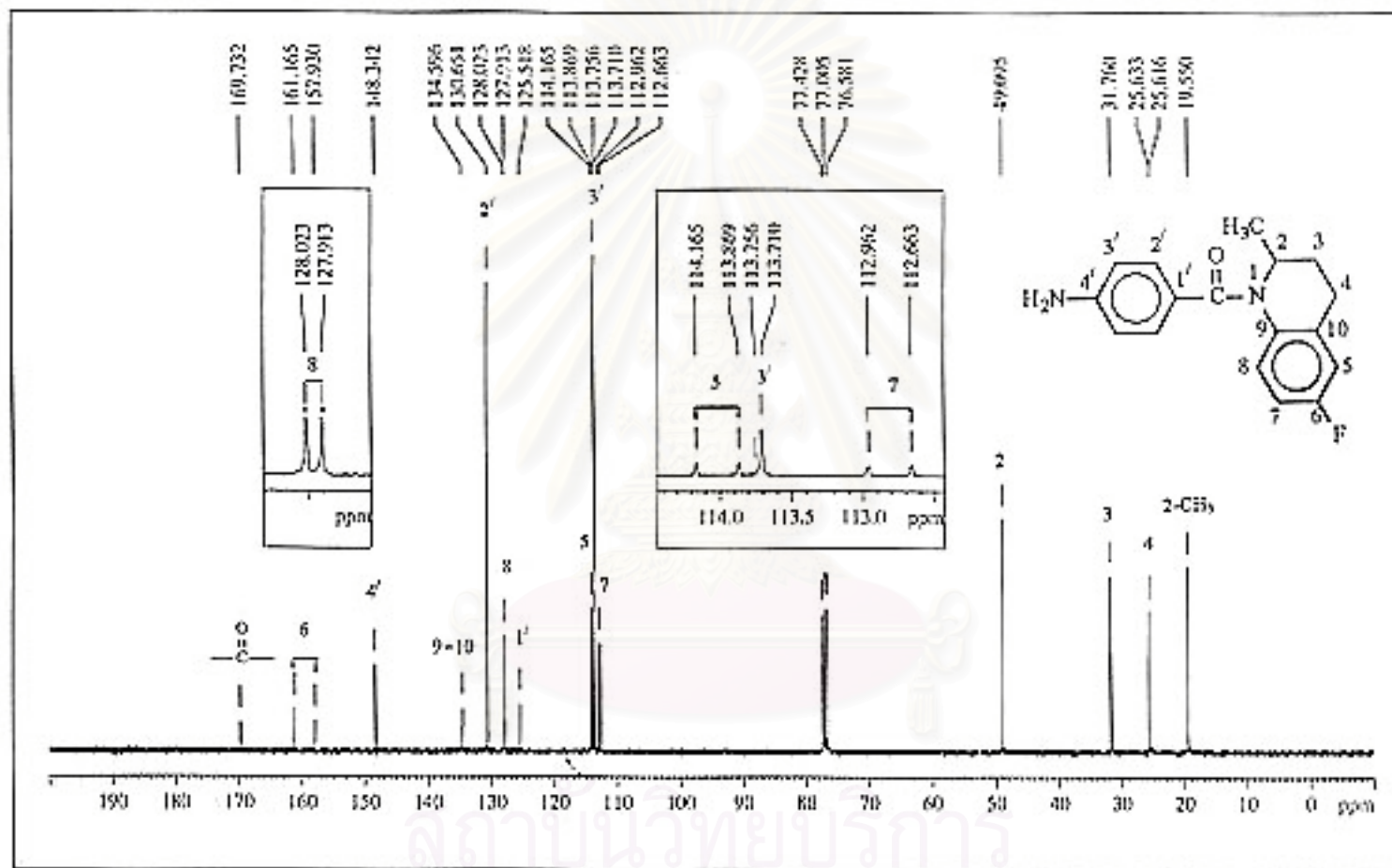
Figure 129. The 75 MHz 13C-NMR decoupled spectrum of N-(*p*-aminobenzoyl)-1,2,3,4-tetrahydro-6-fluoro-2-methylquinoline (4e, CU-17-10) in CDCl₃.
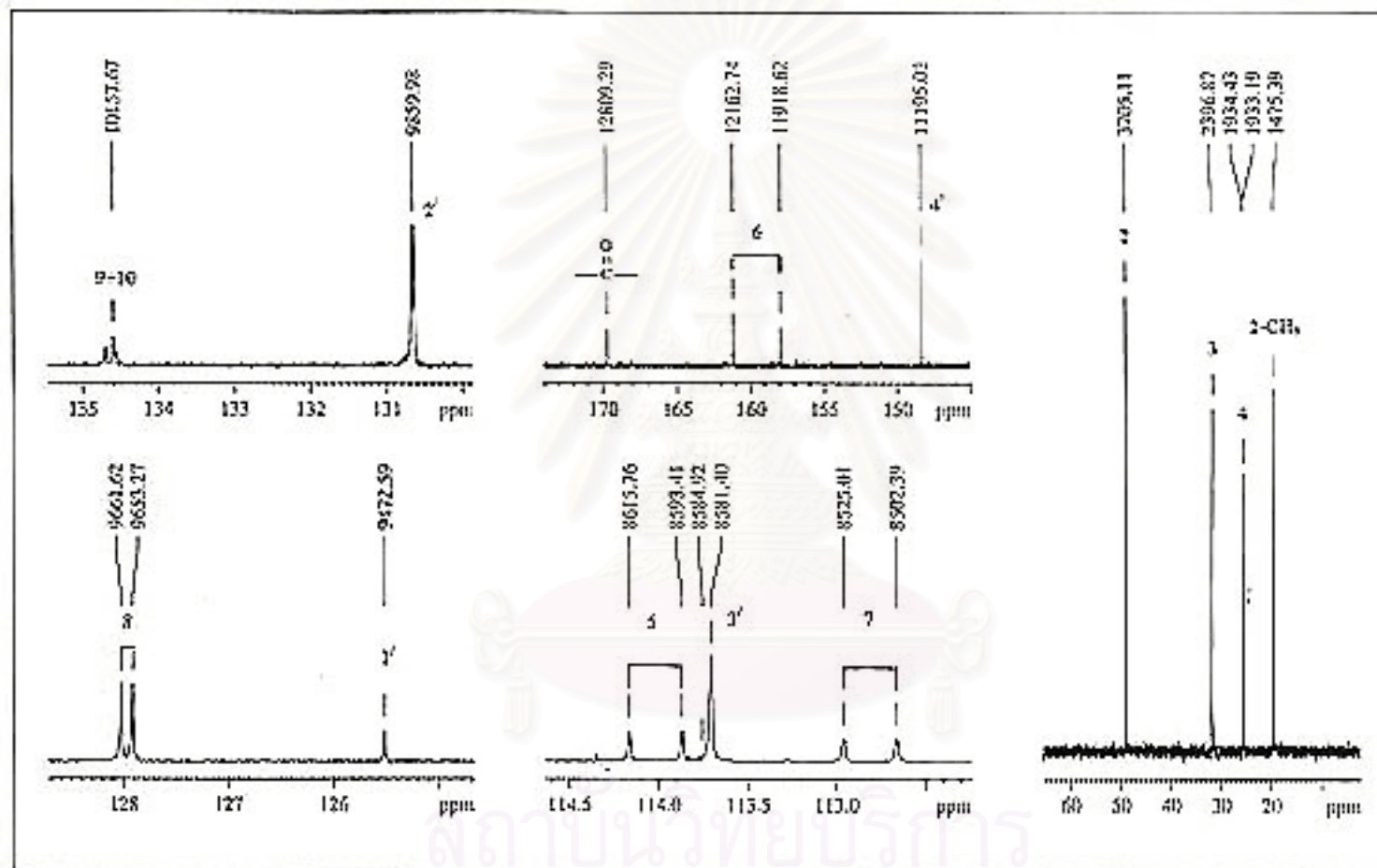
Figure 130. The 75 MHz 13C-NMR decoupled spectrum of N-(*p*-aminobenzoyl)-1,2,3,4-tetrahydro-6-fluoro-2-methylquinoline (4e, CU-17-10) in CDCl₃. (Enlarged scale)
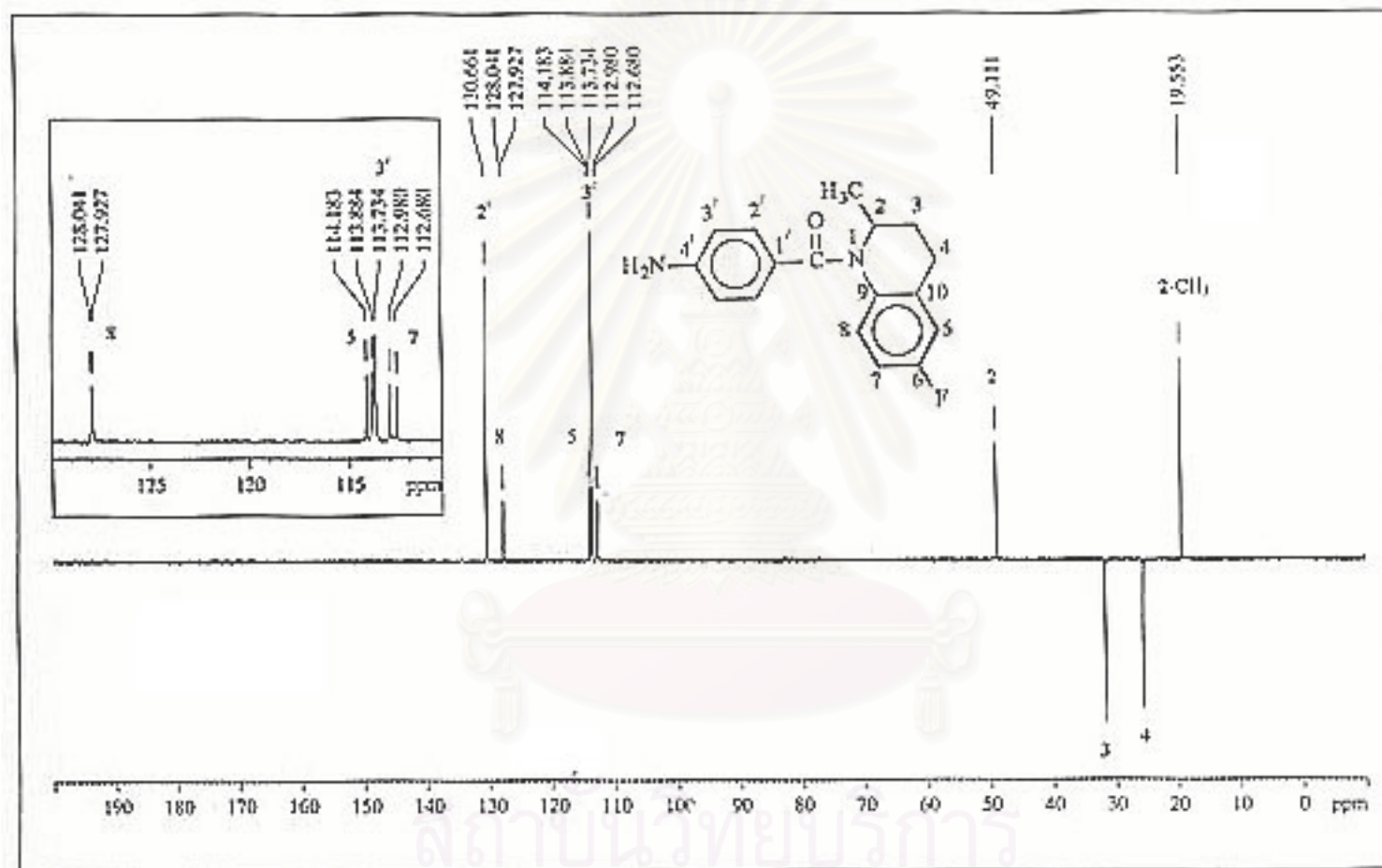
Figure 131. The 75 MHz DEPT-135 spectrum of N-(*p*-aminobenzoyl)-1,2,3,4-tetrahydro-6-fluoro-2-methylquinoline (4e, CU-17-10) in CDCl₃.
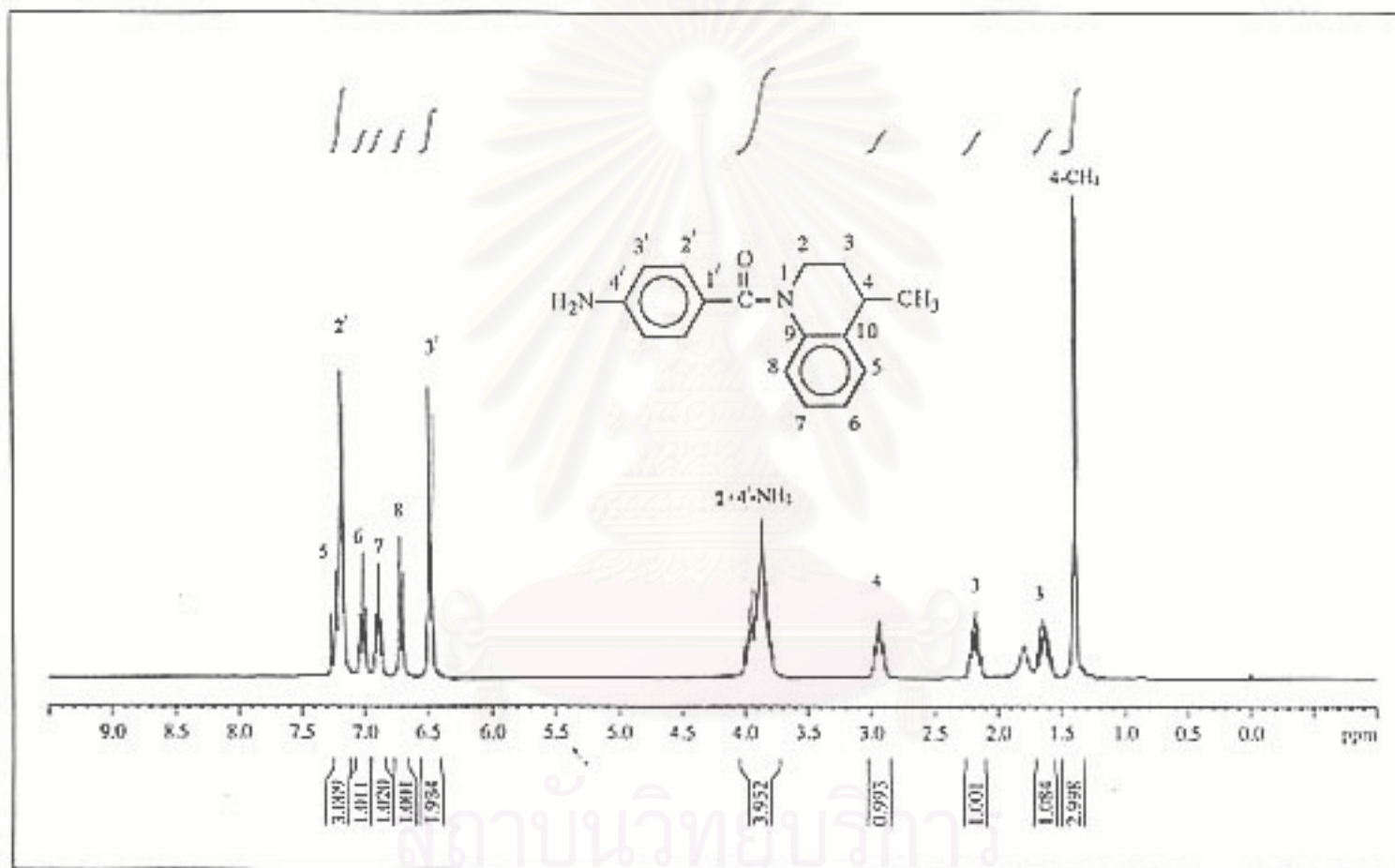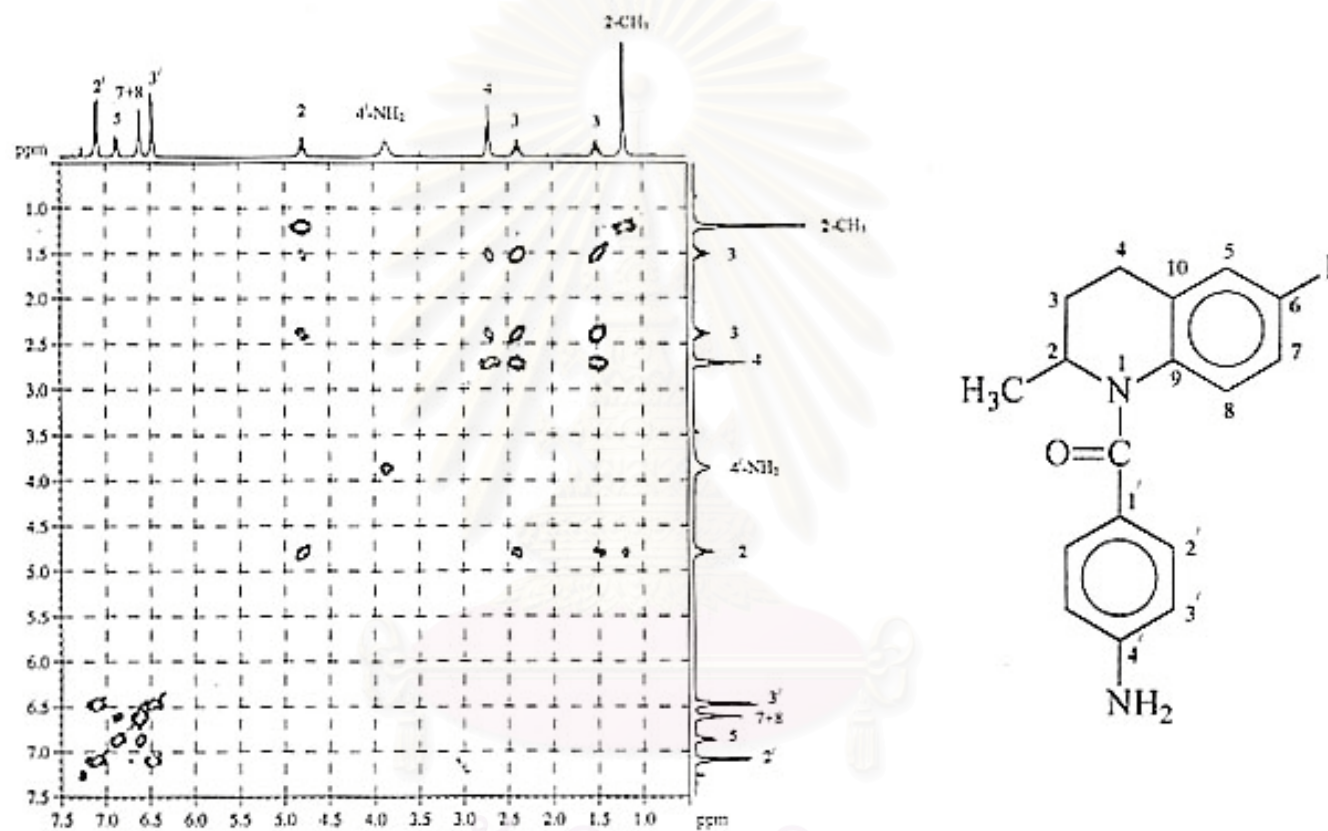
Figure 132. The 300 MHz HH COSY spectrum of N-(*p*-aminobenzoyl)-1,2,3,4-tetrahydro-6-fluoro-2-methylquinoline (4e, CU-17-10) in CDCl₃.
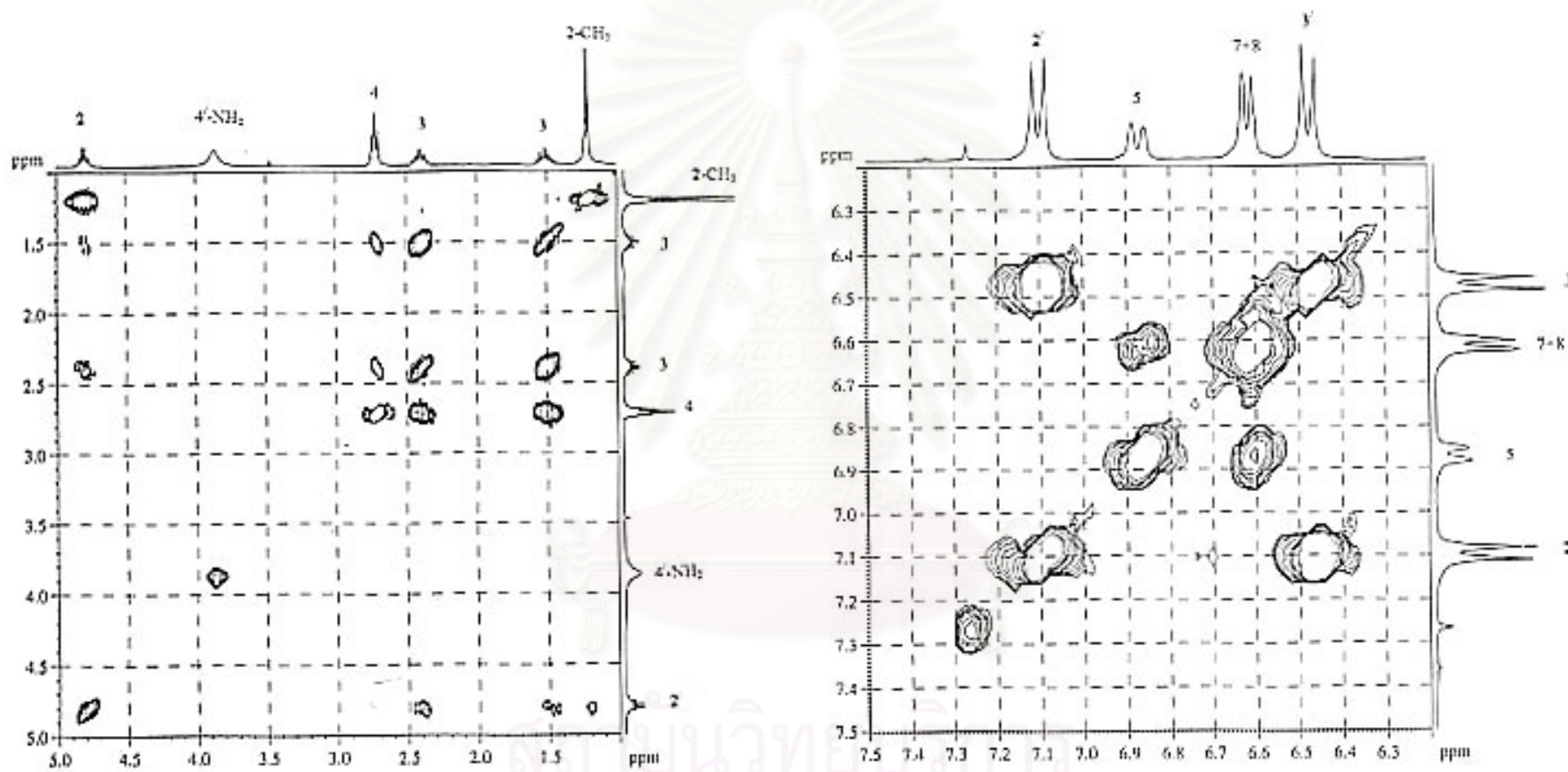
Figure 133. The 300 MHz HH COSY spectrum of N-(*p*-aminobenzoyl)-1,2,3,4-tetrahydro-6-fluoro-2-methylquinoline (4e, CU-17-10) in

CDCl$_3$. (Enlarged scale)
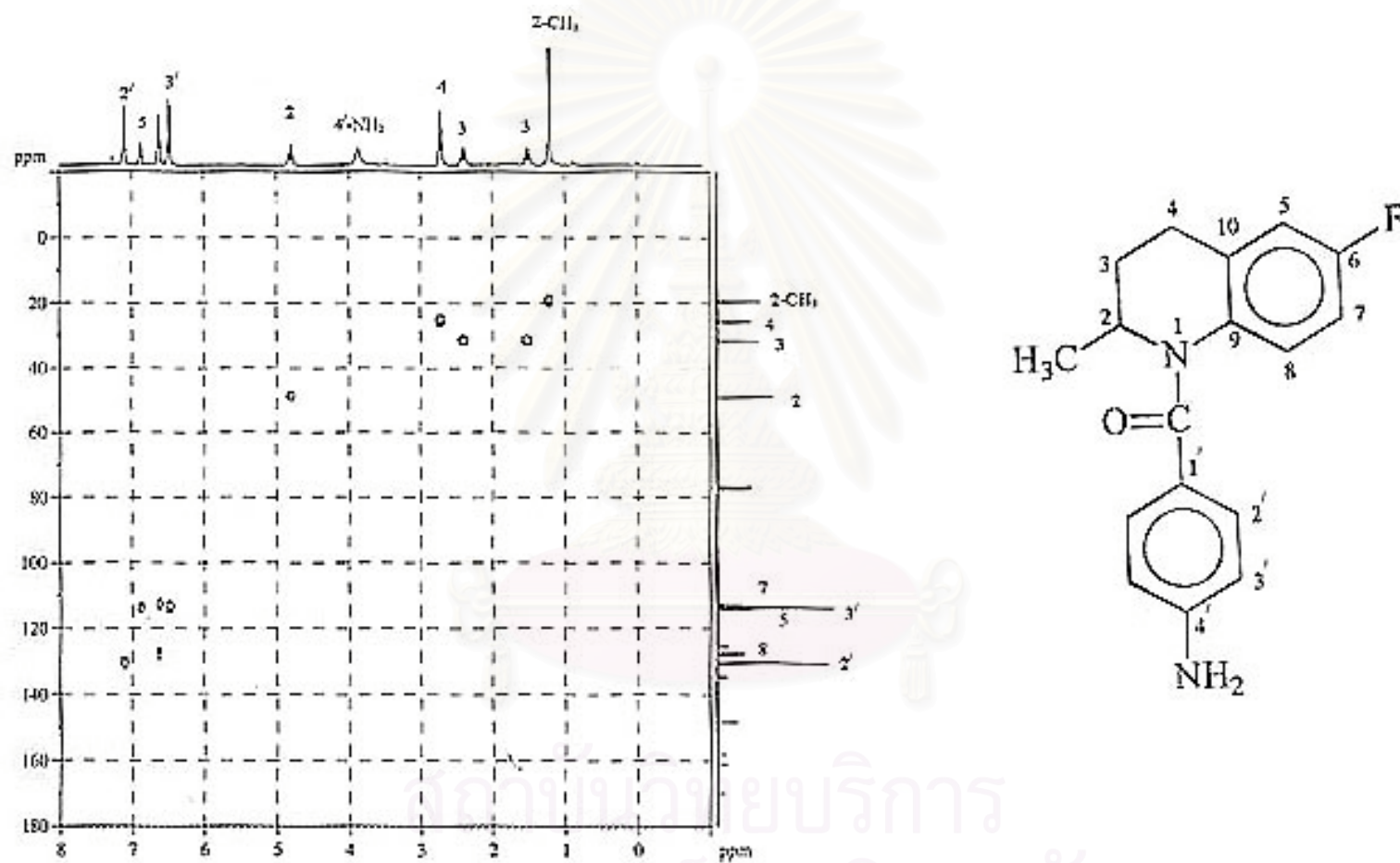
Figure 134. The 300 MHz HMQC spectrum of N-(*p*-aminobenzoyl)-1,2,3,4-tetrahydro-6-fluoro-2-methylquinoline (4e, CU-17-10) in CDCl₃.
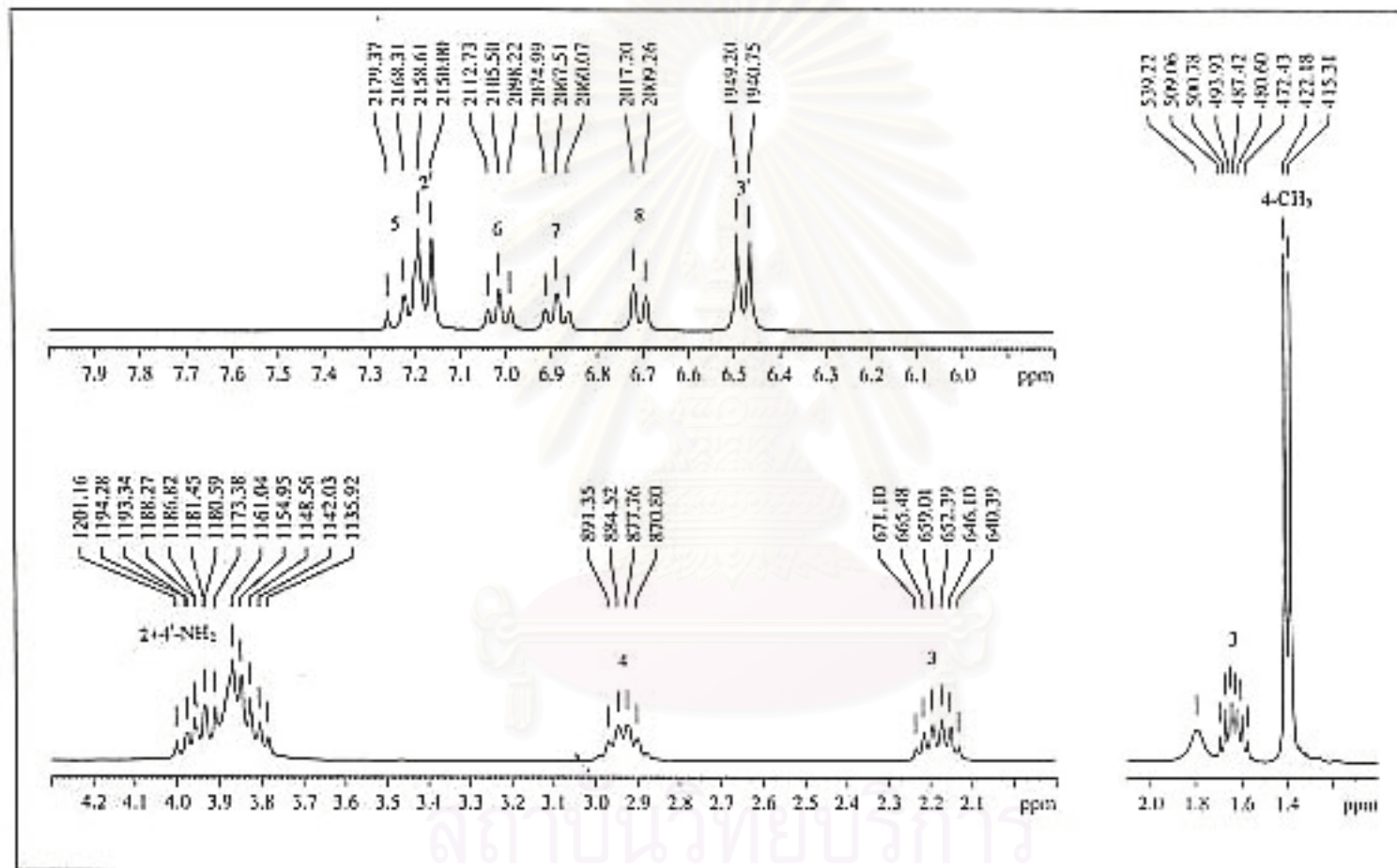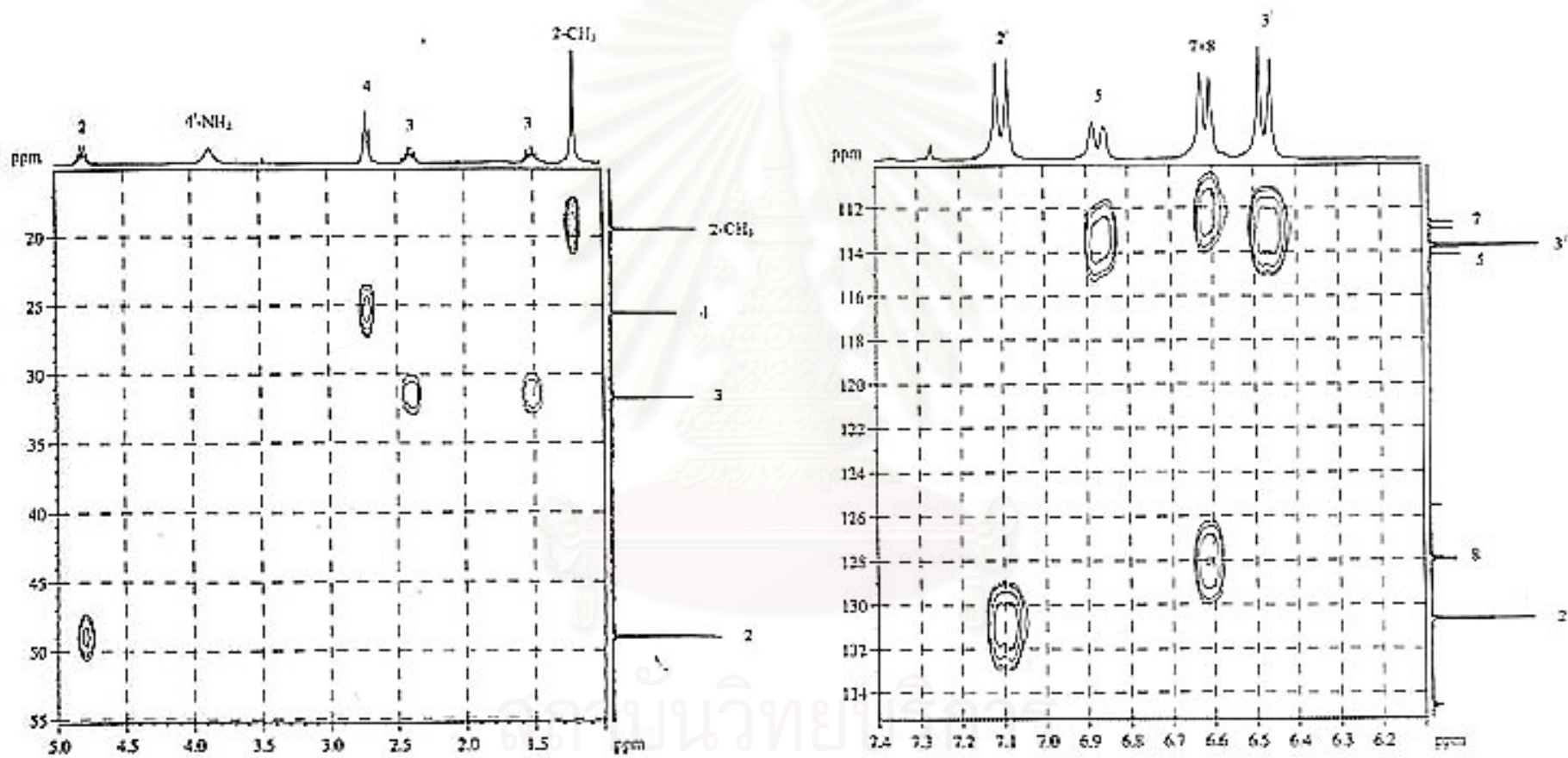
Figure 135. The 300 MHz HMQC spectrum of N-(*p*-aminobenzoyl)-1,2,3,4-tetrahydro-6-fluoro-2-methylquinoline (4e, CU-17-10) in CDCl₃.

(Enlarged scale)
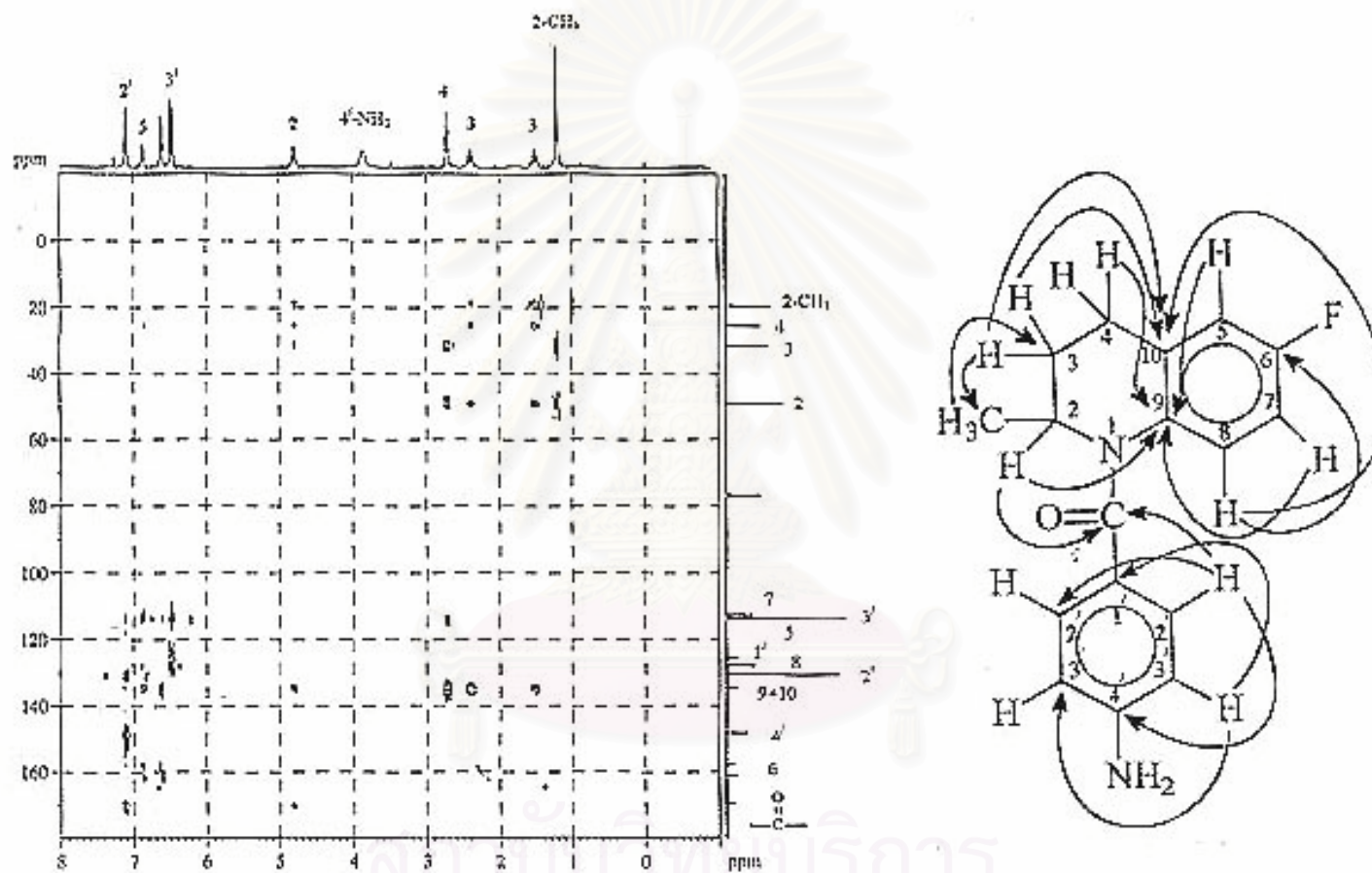
Figure 136. The 300 MHz HMBC spectrum (JHC = 8 Hz) of N-(*p*-aminobenzoyl)-1,2,3,4-tetrahydro-6-fluoro-2-methylquinoline (4e, CU-17-10) in CDCl₃.
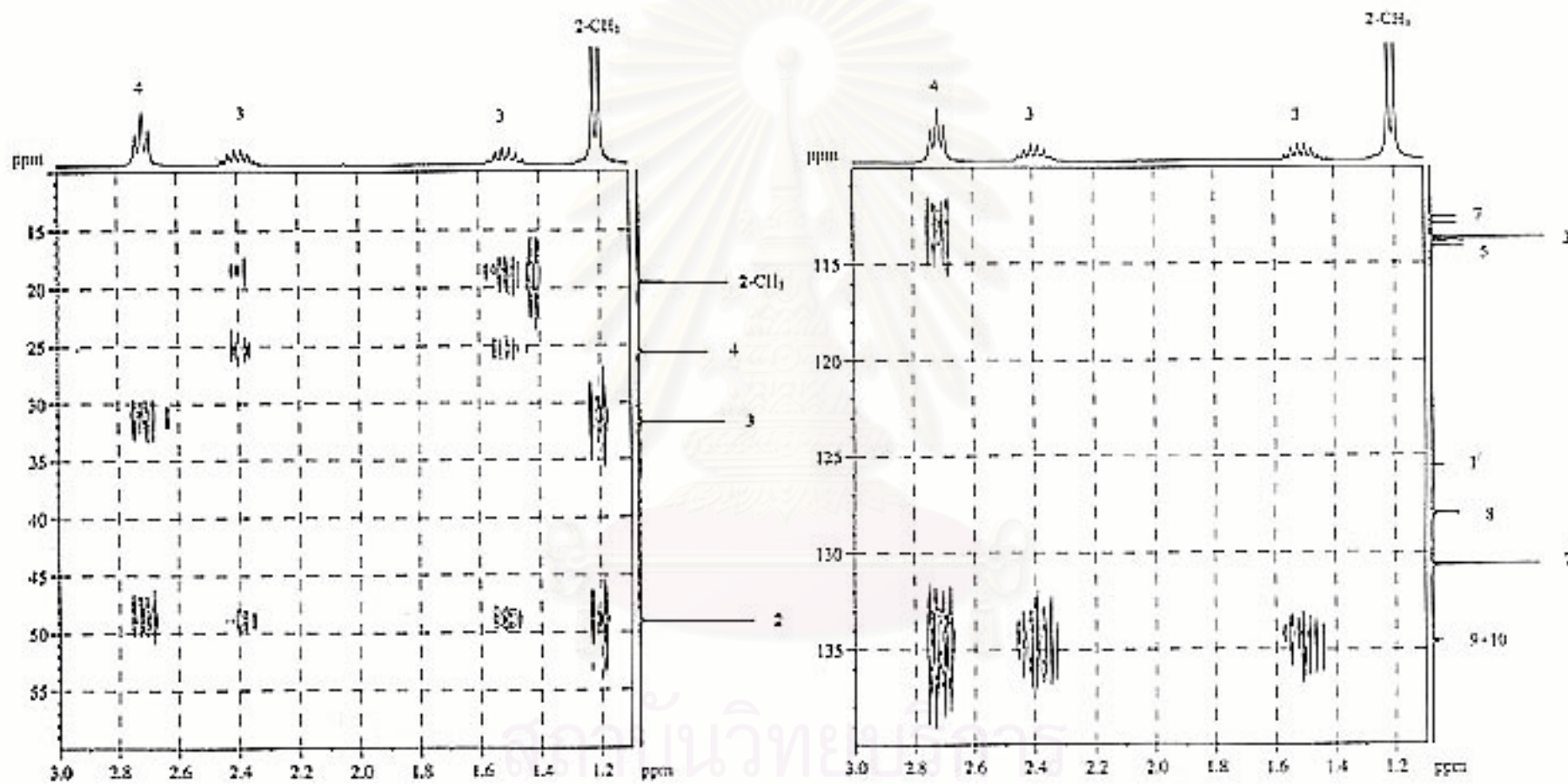
Figure 137. The 300 MHz HMBC spectrum (JHC = 8 Hz) of N-(*p*-aminobenzoyl)-1,2,3,4-tetrahydro-6-fluoro-2-methylquinoline

(4e, CU-17-10) in CDCl₃. (Expanded: δH 1.1-3.0 ppm; δC 10-140 ppm)
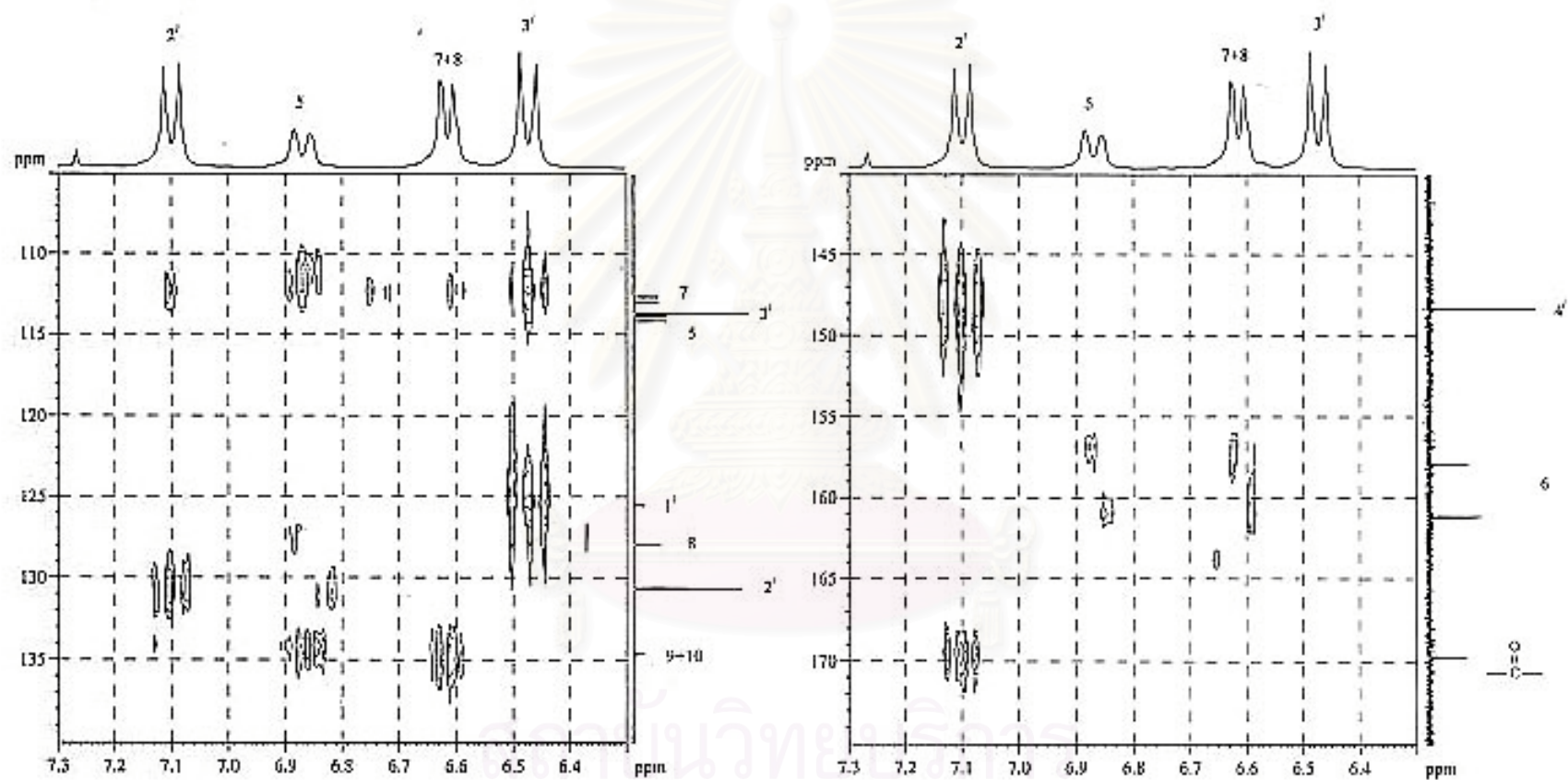
Figure 138. The 300 MHz HMBC spectrum (JHC = 8 Hz) of N-(*p*-aminobenzoyl)-1,2,3,4-tetrahydro-6-fluoro-2-methylquinoline (4e, CU-17-10)

in CDCl$_3$. (Expanded: δH 6.3-7.3 ppm; δC 105-175 ppm)
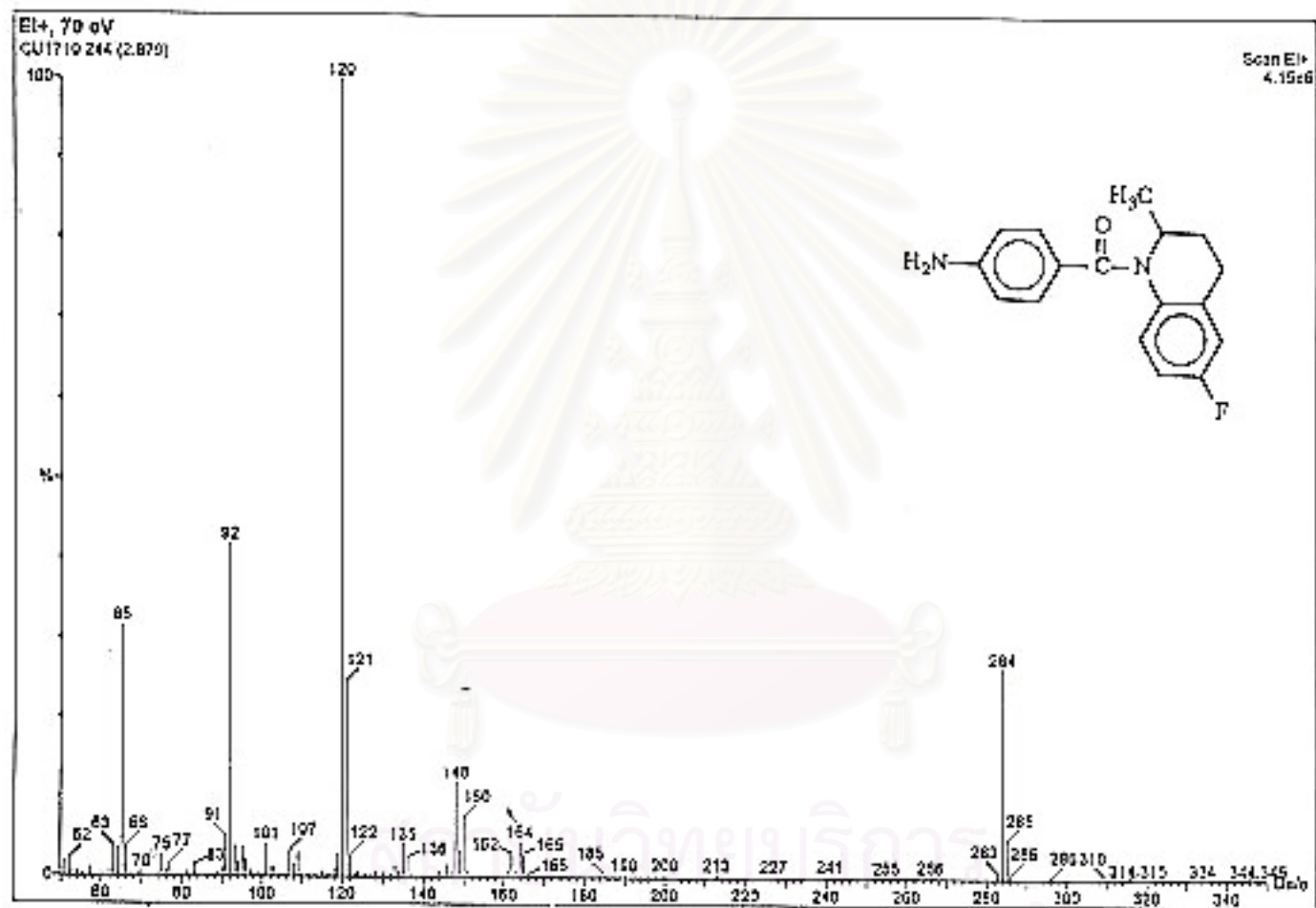
Figure 139. The electron impact mass spectrum of N-(*p*-aminobenzoyl)-1,2,3,4-tetrahydro-6-fluoro-2-methylquinoline (4e, CU-17-10).
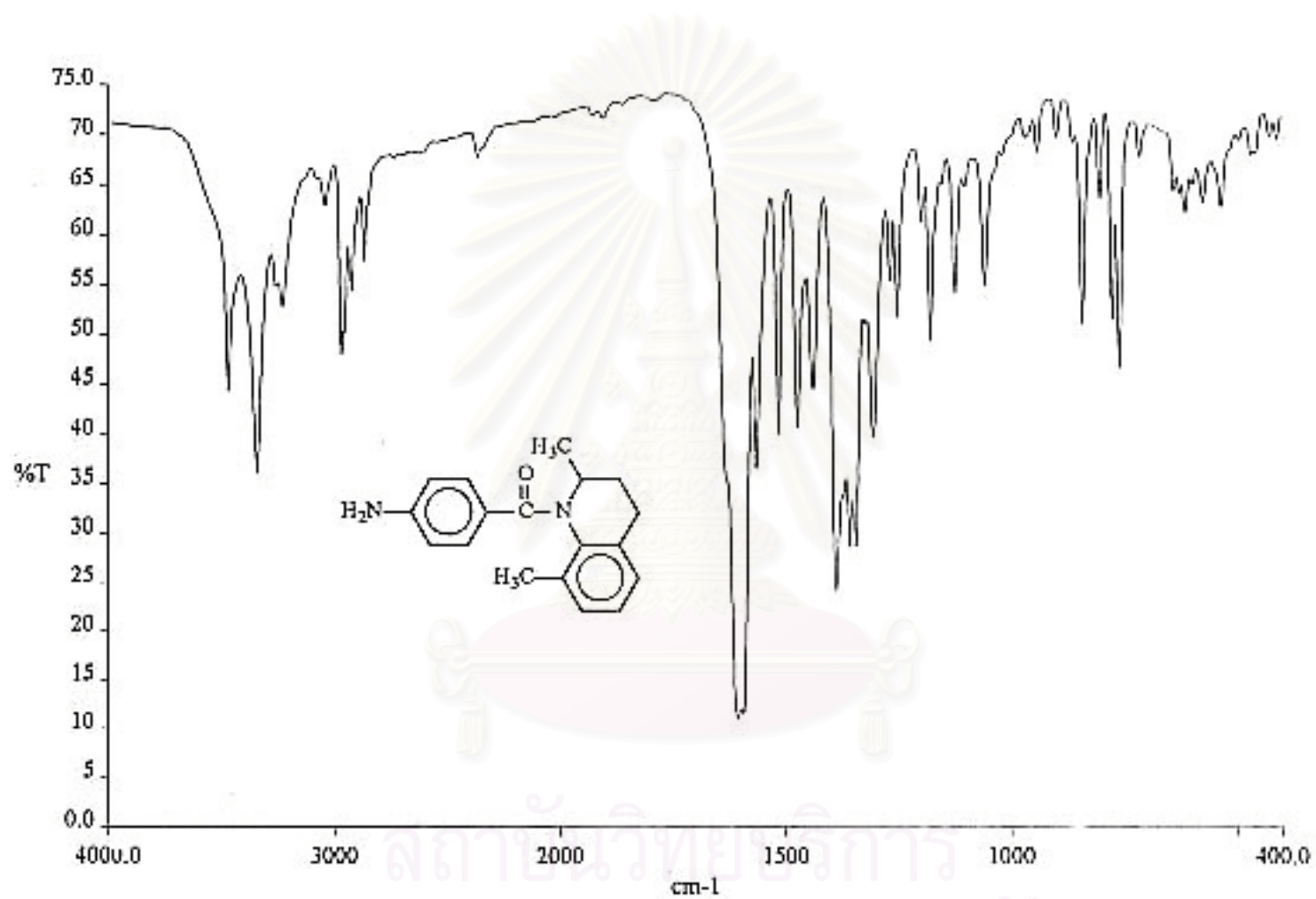
Figure 140. The IR spectrum (KBr) of N-(*p*-aminobenzoyl)-1,2,3,4-tetrahydro-2,8-dimethylquinoline (4f, CU-17-12).
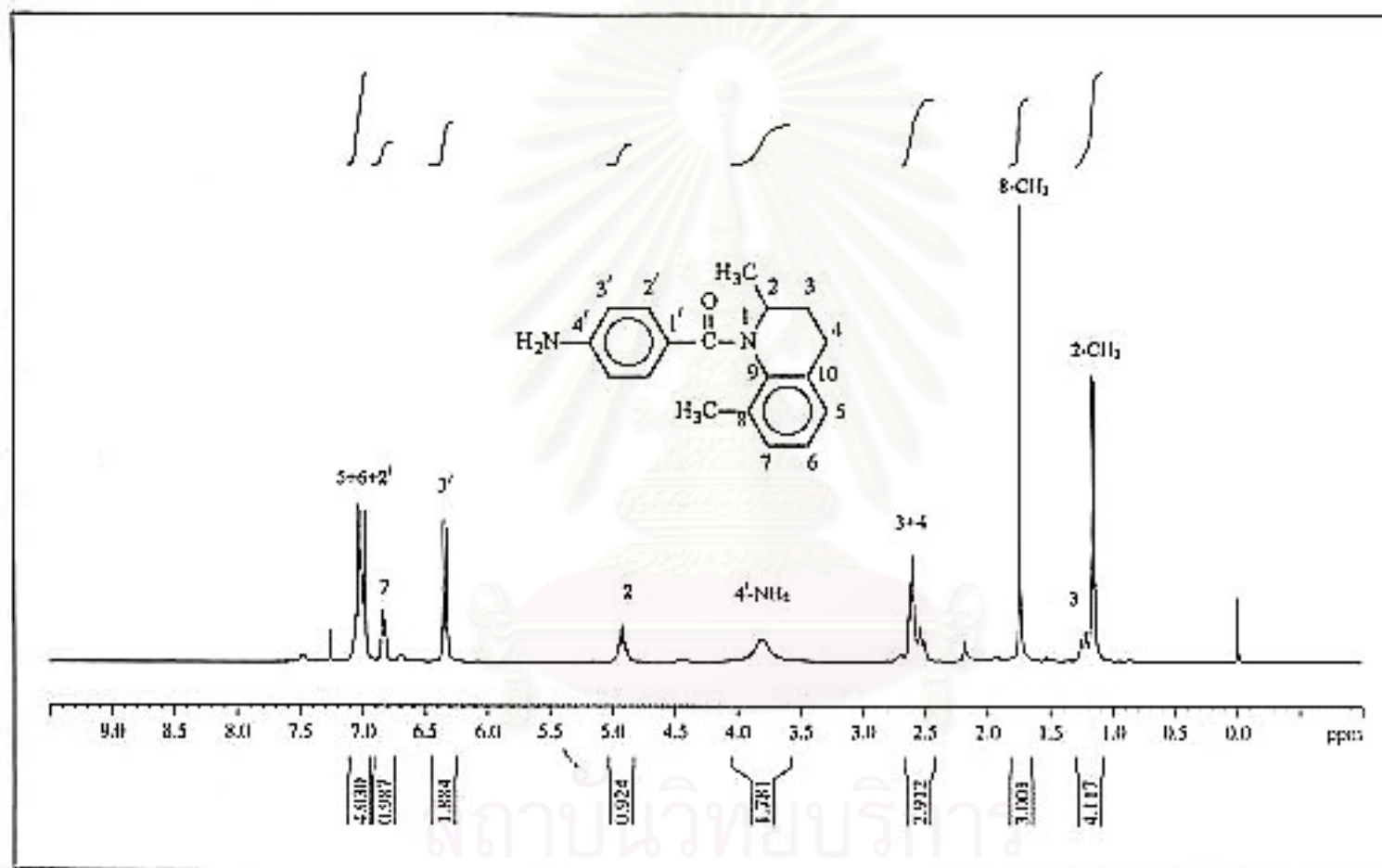
Figure 141. The 300 MHz 1H-NMR spectrum of N-(*p*-aminobenzoyl)-1,2,3,4-tetrahydro-2,8-dimethylquinoline (4f, CU-17-12) in CDCl₃.
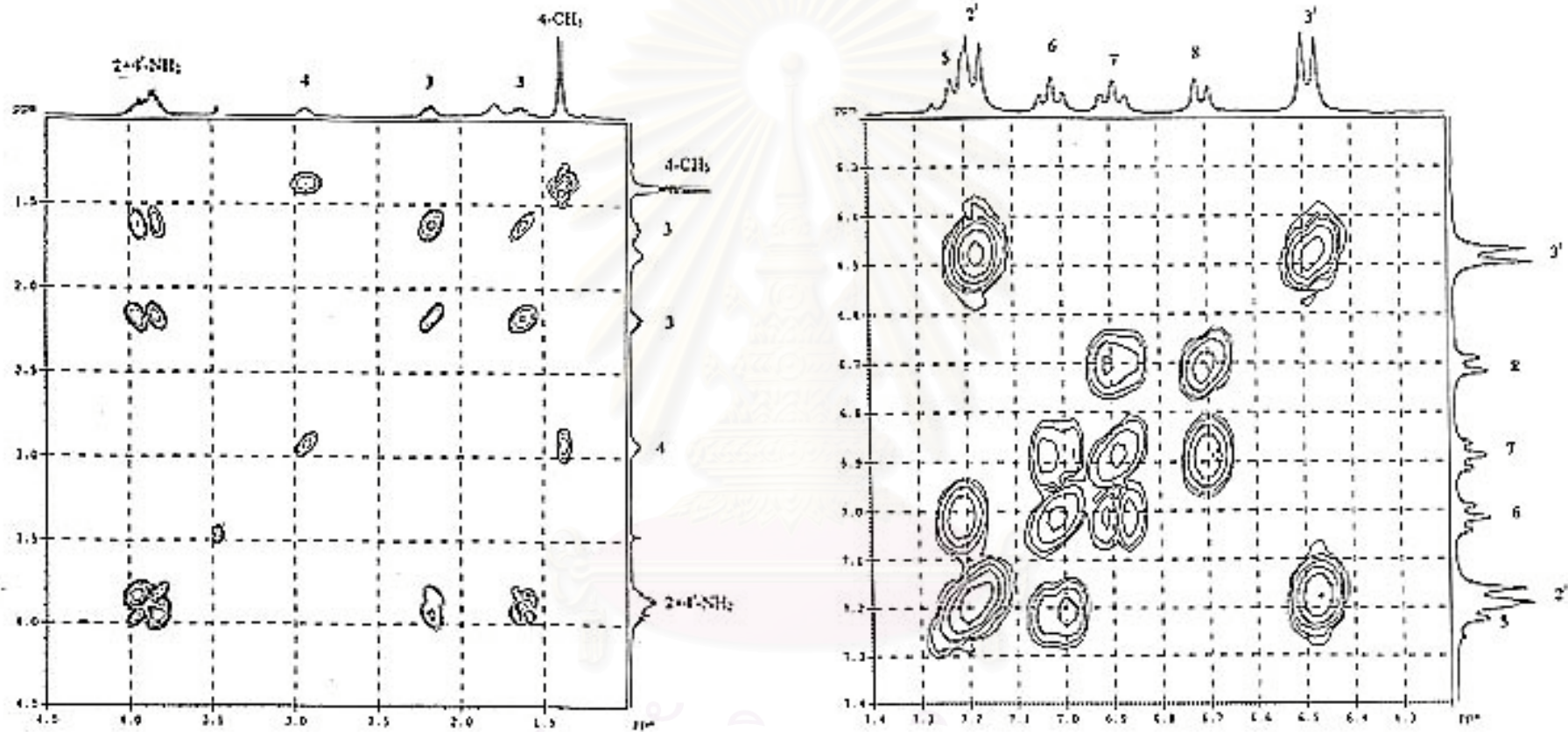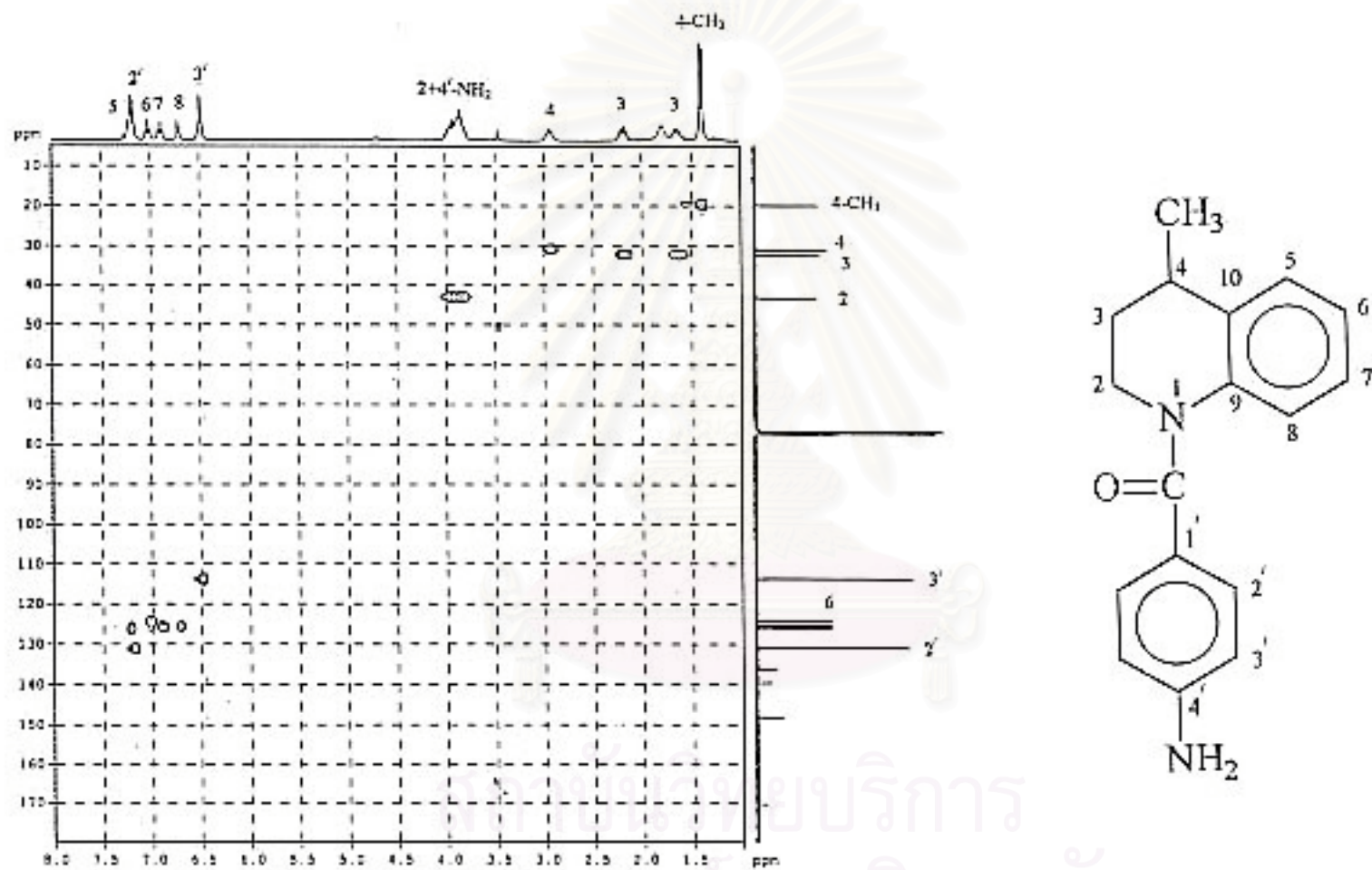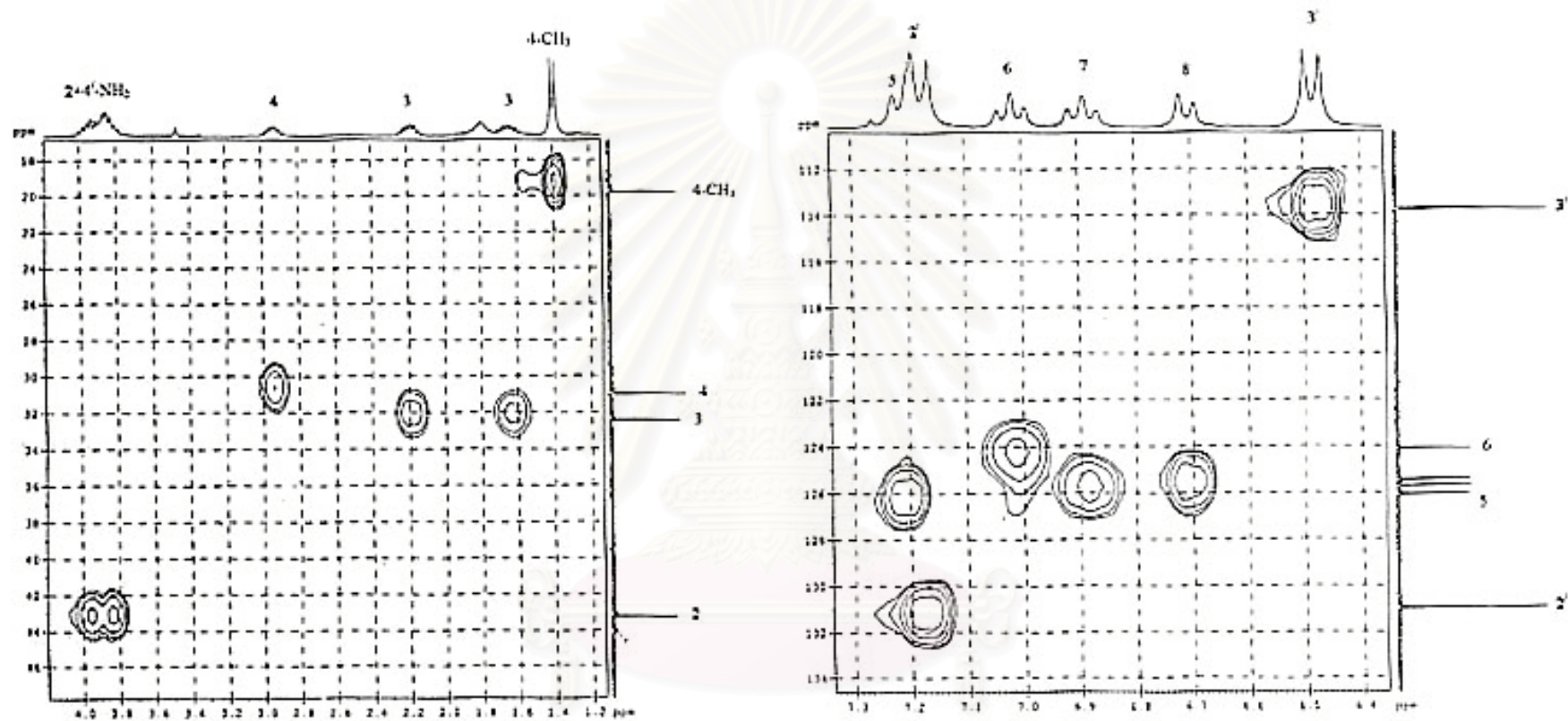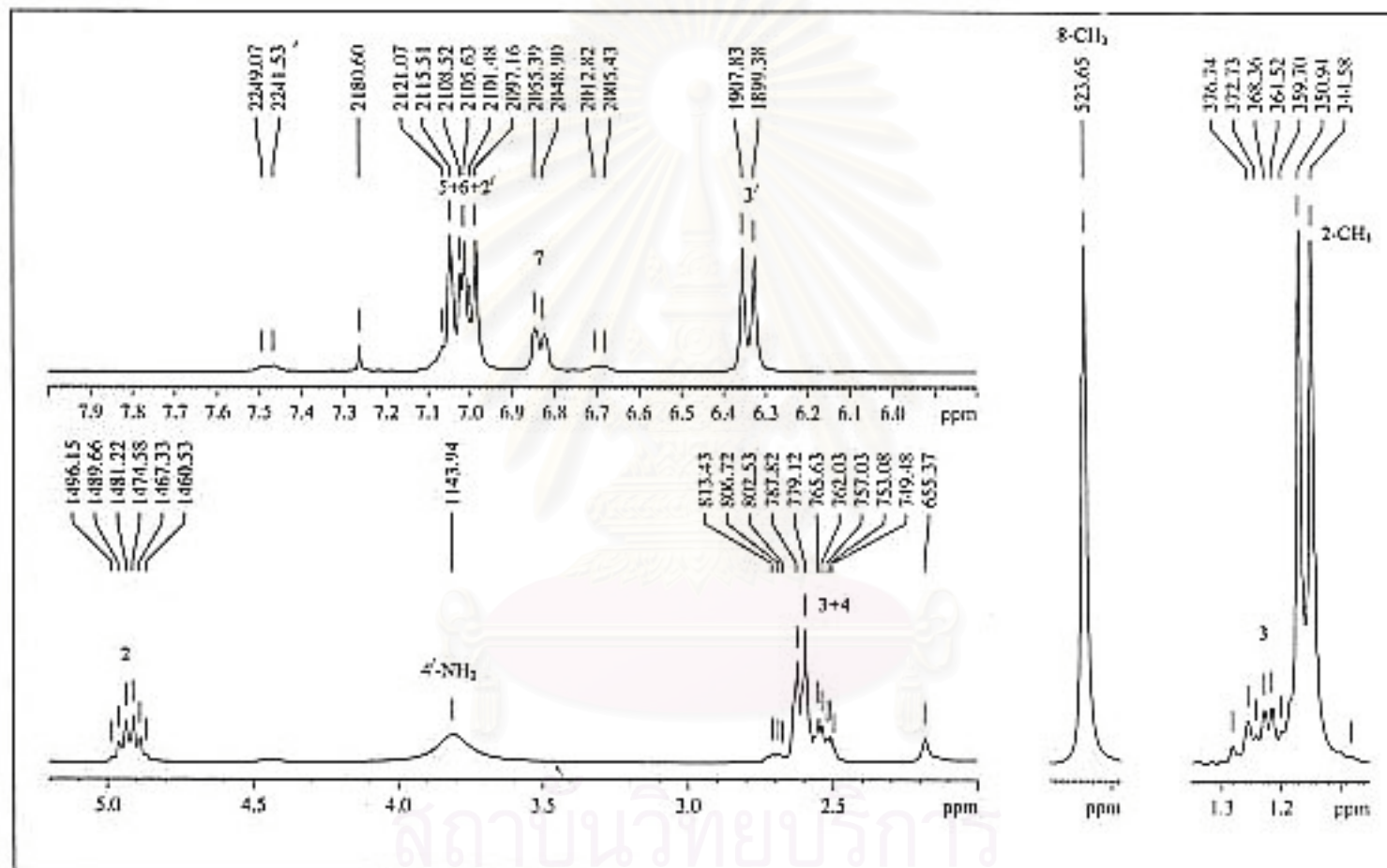
Figure 142. The 300 MHz 1H-NMR spectrum of N-(*p*-aminobenzoyl)-1,2,3,4-tetrahydro-2,8-dimethylquinoline (4f, CU-17-12) in CDCl₃.

(Enlarged scale)
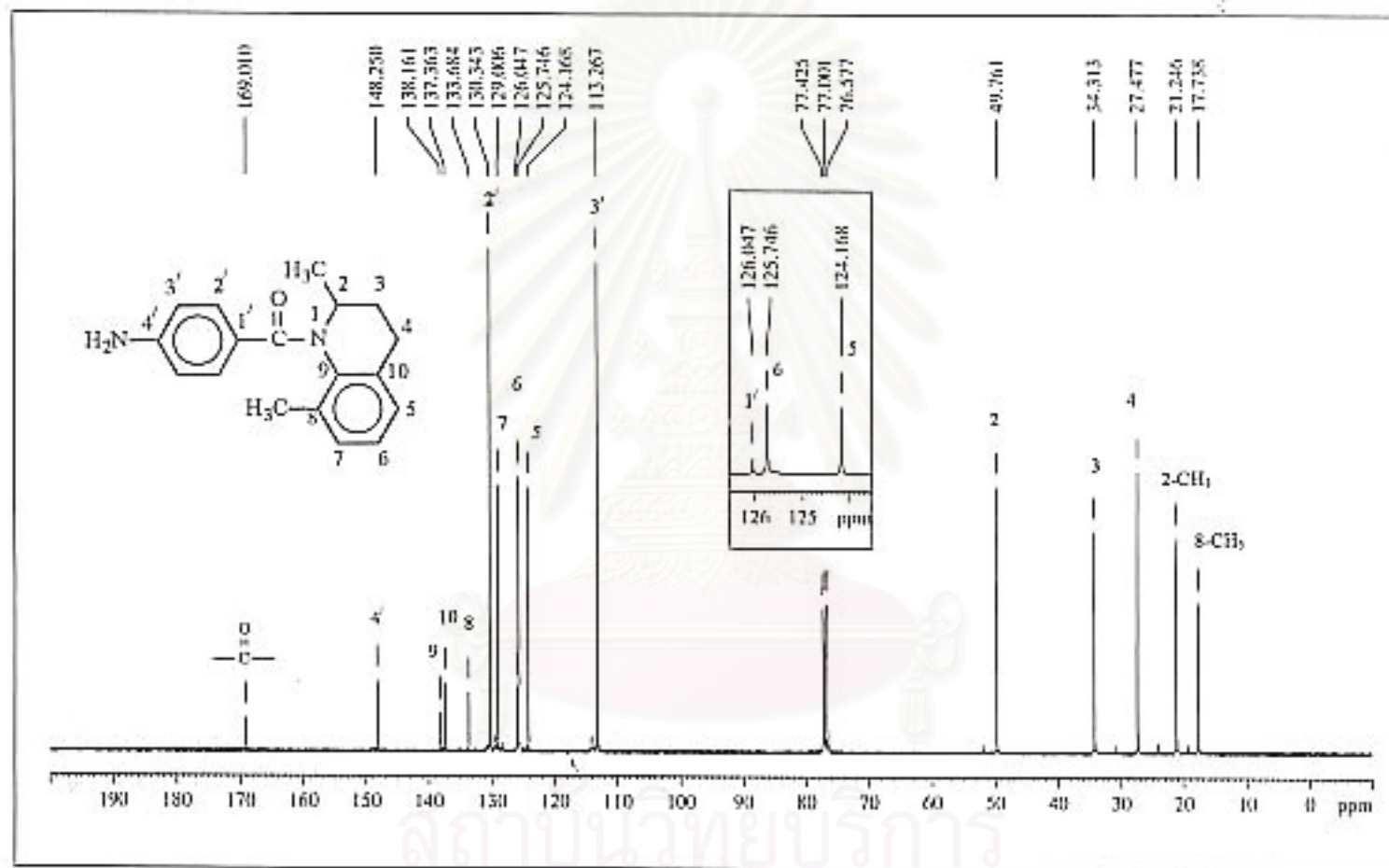
Figure 143. The 75 MHz 13C-NMR decoupled spectrum of N-(*p*-aminobenzoyl)-1,2,3,4-tetrahydro-2,8-dimethylquinoline (4f, CU-17-12) in
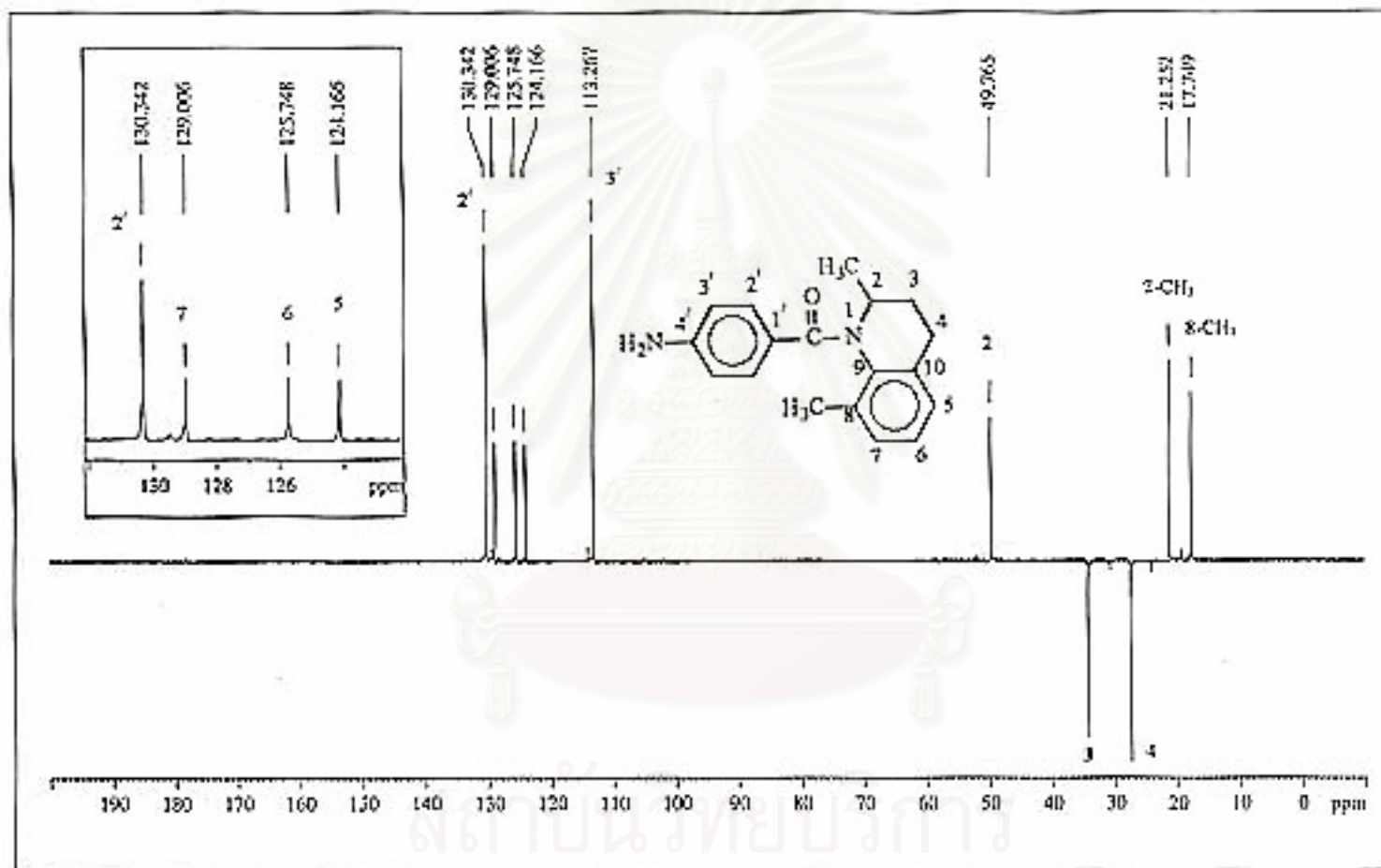
CDCl$_3$.

Figure 144. The 75 MHz DEPT-135 spectrum of N-(*p*-aminobenzoyl)-1,2,3,4-tetrahydro-2,8-dimethylquinoline (4f, CU-17-12) in CDCl₃.
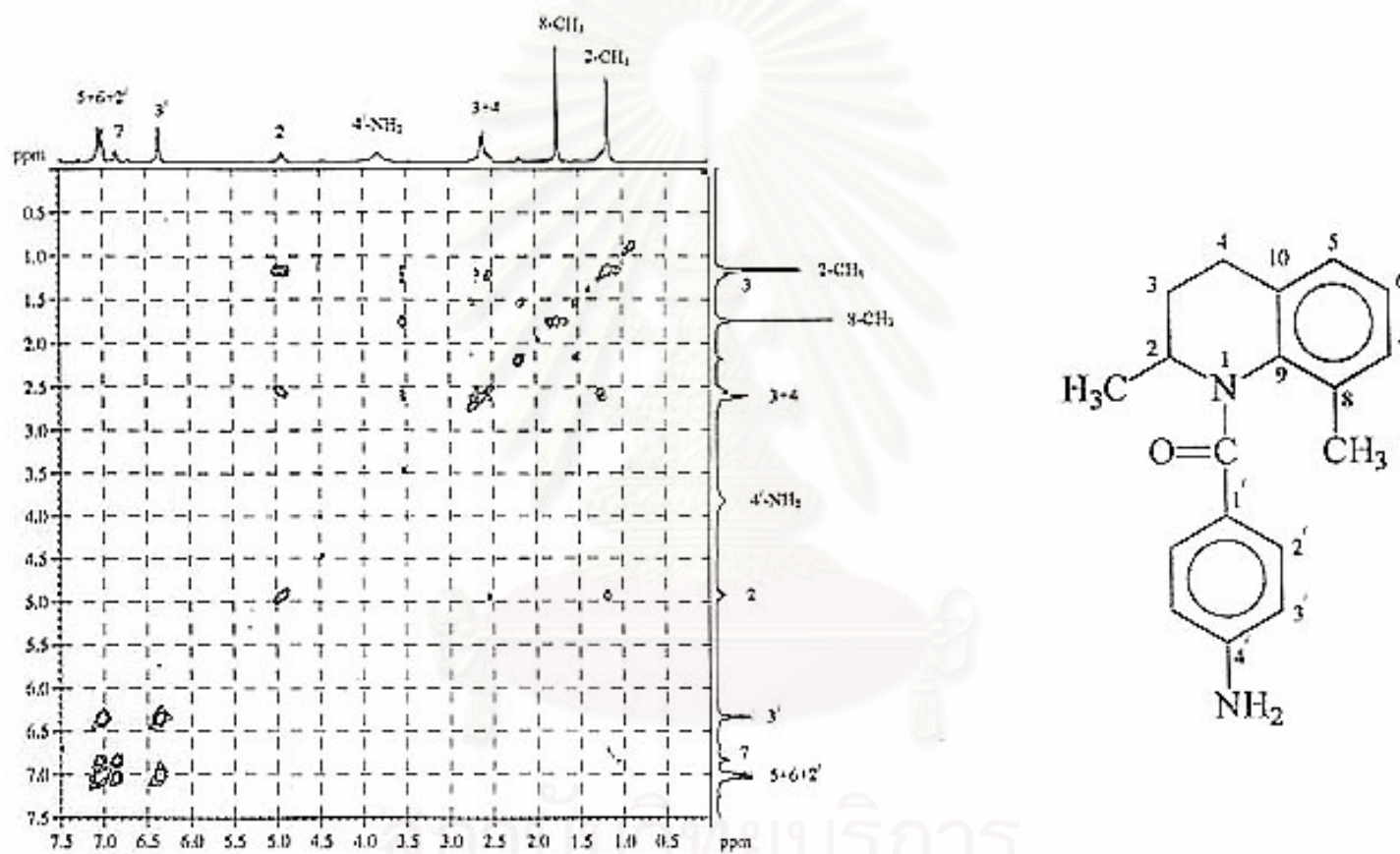
Figure 145. The 300 MHz HH COSY spectrum of N-(*p*-aminobenzoyl)-1,2,3,4-tetrahydro-2,8-dimethylquinoline (4f, CU-17-12) in CDCl$_3$.
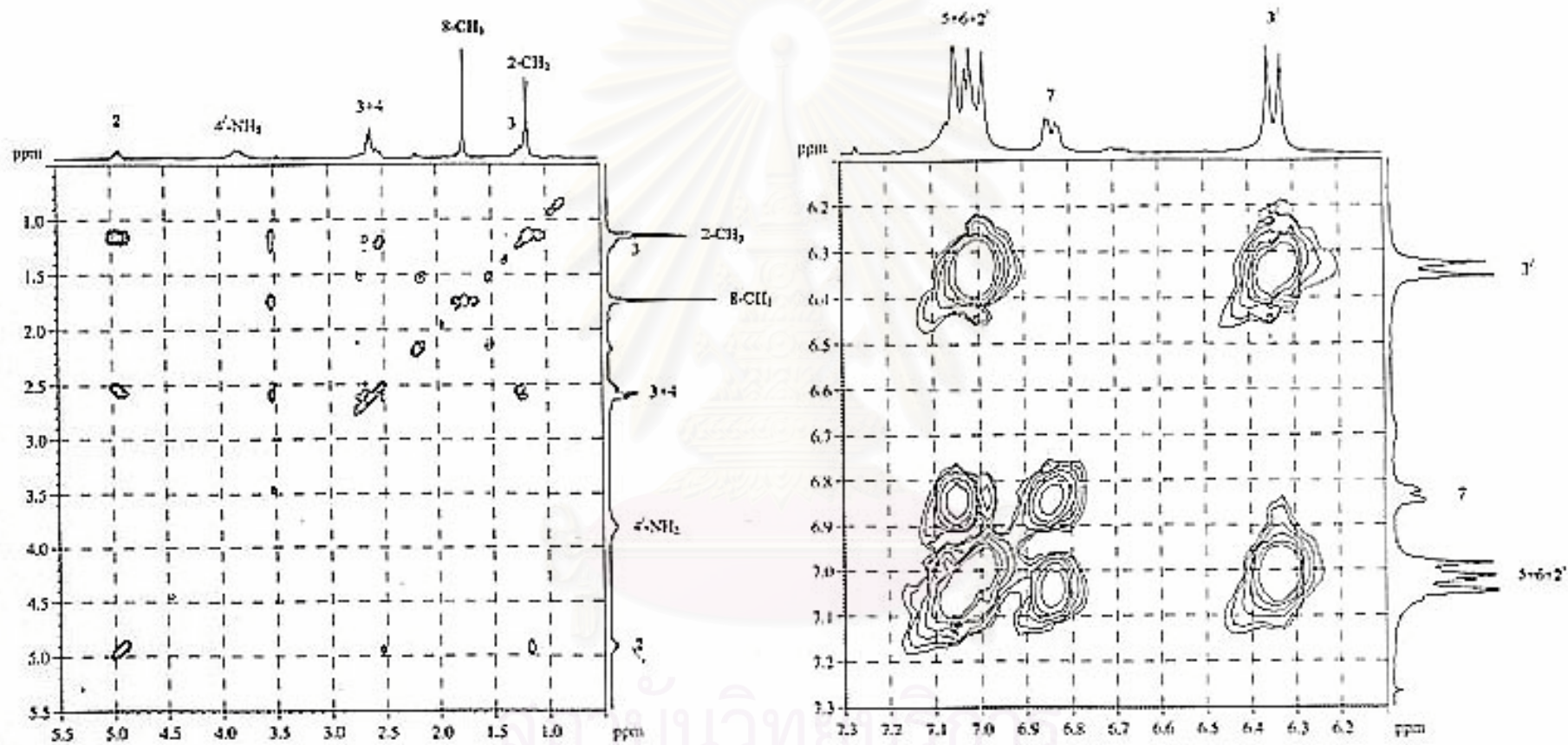
Figure 146. The 300 MHz HH COSY spectrum of N-(*p*-aminobenzoyl)-1,2,3,4-tetrahydro-2,8-dimethylquinoline (4f, CU-17-12) in CDCl₃.
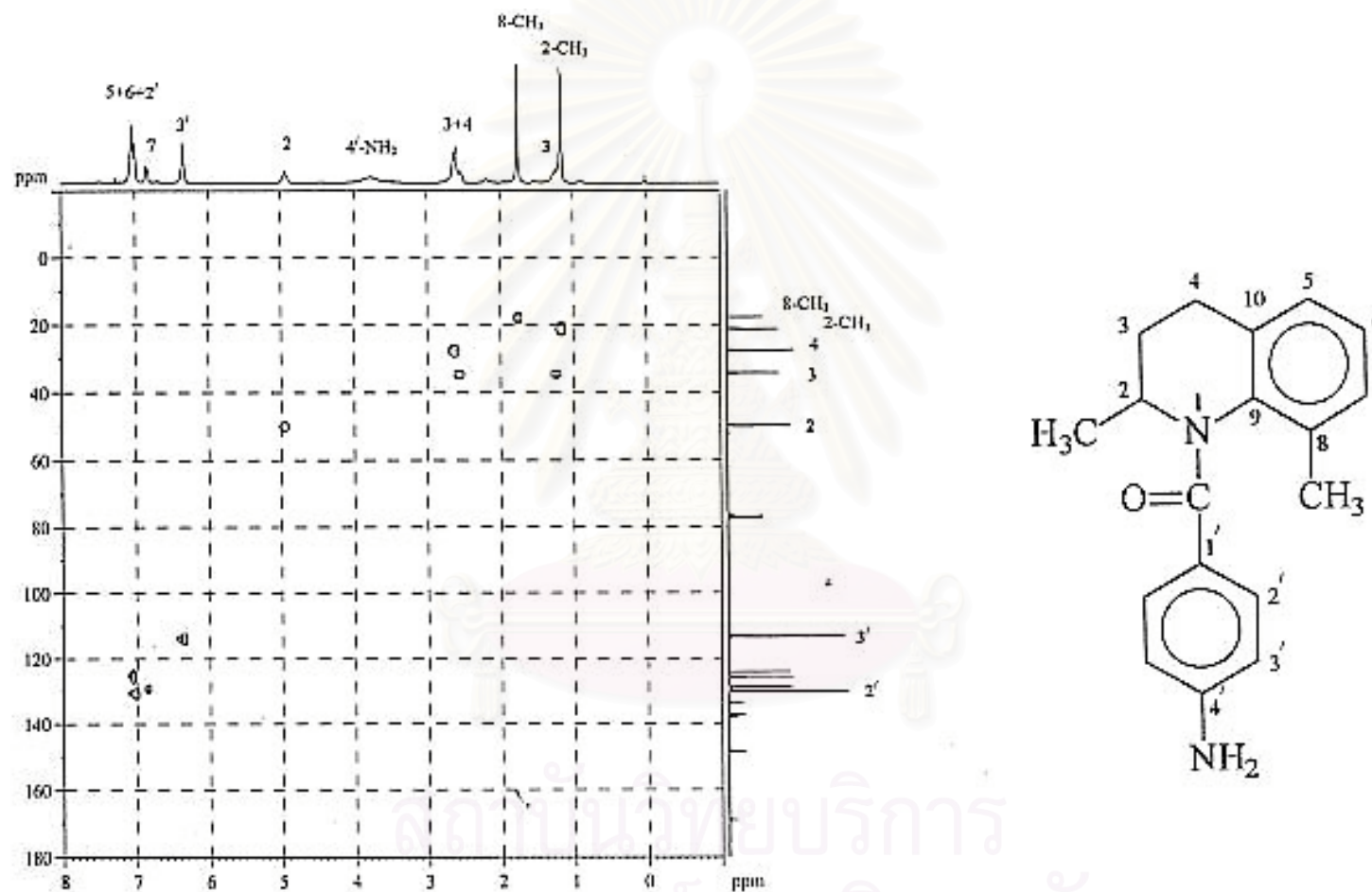
(Enlarged scale)

Figure 147. The 300 MHz HMQC spectrum of N-(*p*-aminobenzoyl)-1,2,3,4-tetrahydro-2,8-dimethylquinoline (4f, CU-17-12) in CDCl$_3$.
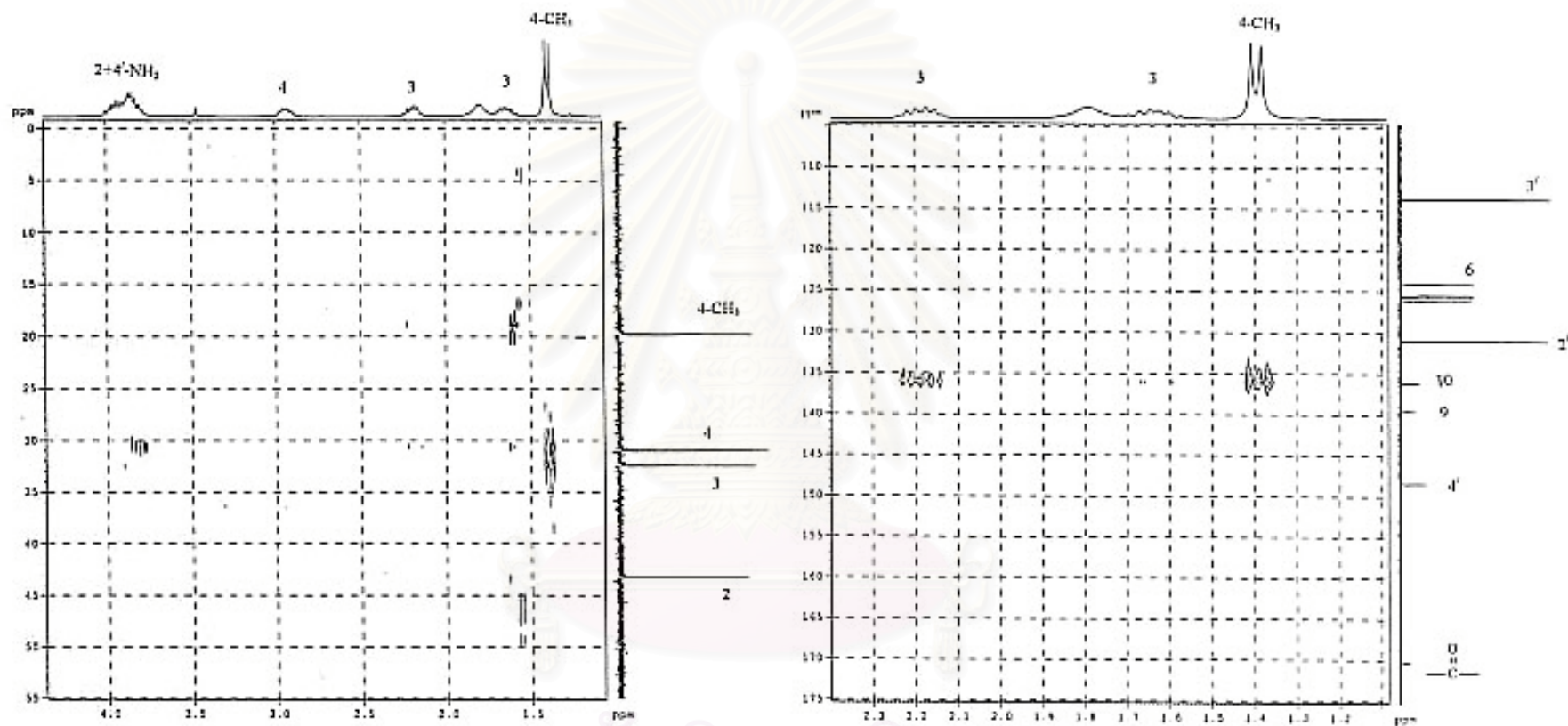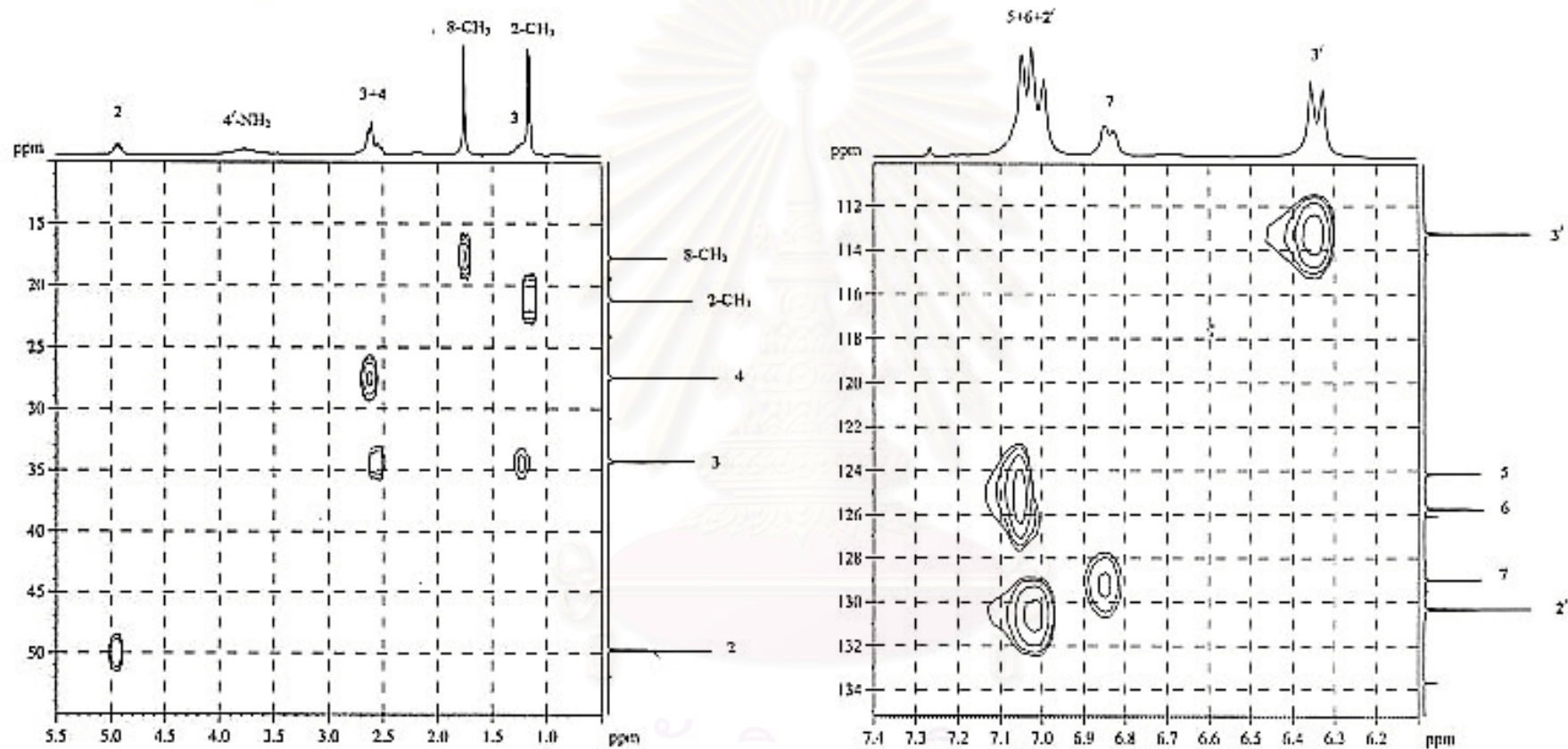
Figure 148. The 300 MHz HMQC spectrum of N-(*p*-aminobenzoyl)-1,2,3,4-tetrahydro-2,8-dimethylquinoline (4f, CU-17-12) in CDCl₃.

(Enlarged scale)
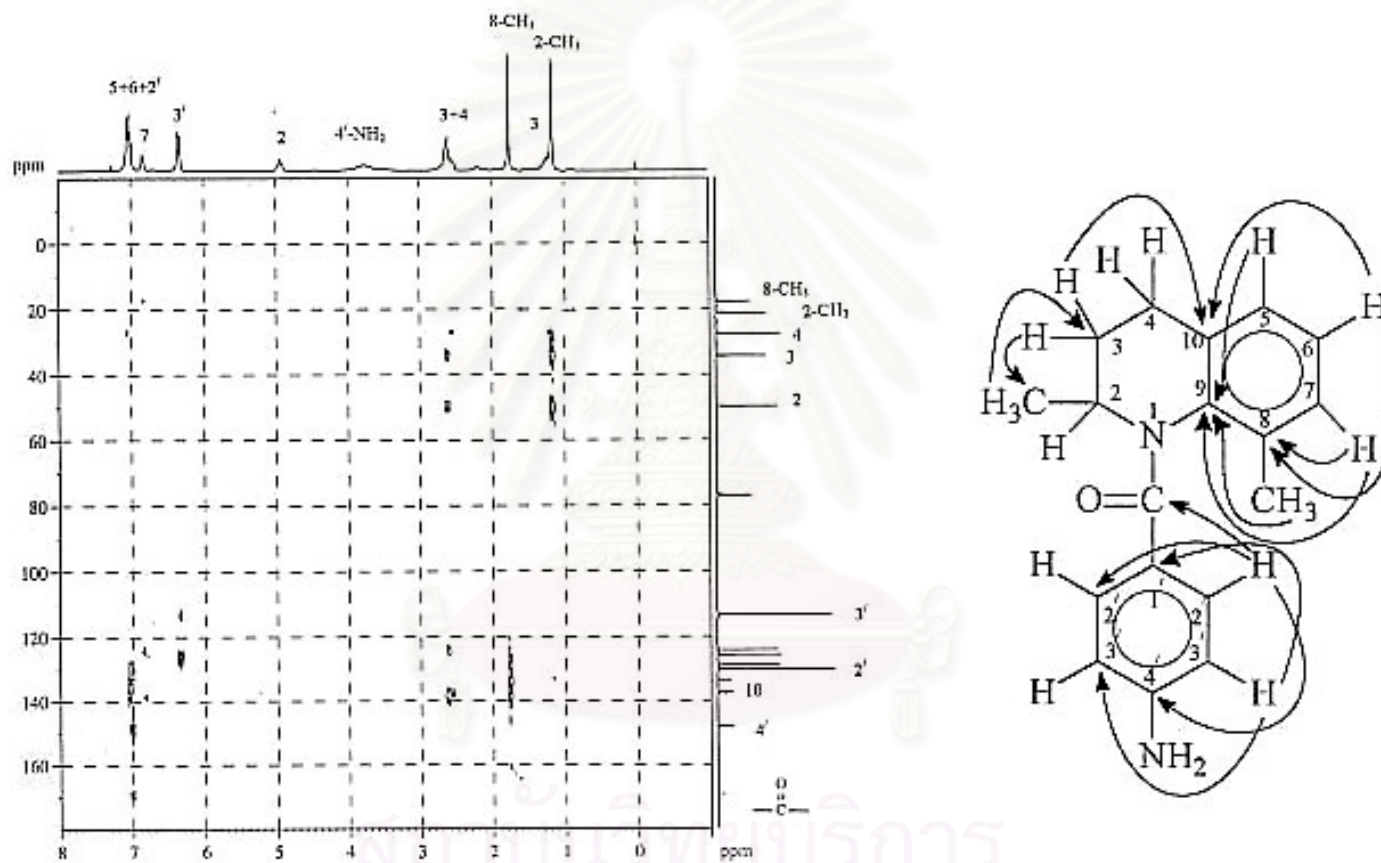
Figure 149. The 300 MHz HMBC spectrum (JHC = 8 Hz) of N-(*p*-aminobenzoyl)-1,2,3,4-tetrahydro-2,8-dimethylquinoline (4f, CU-17-12) in
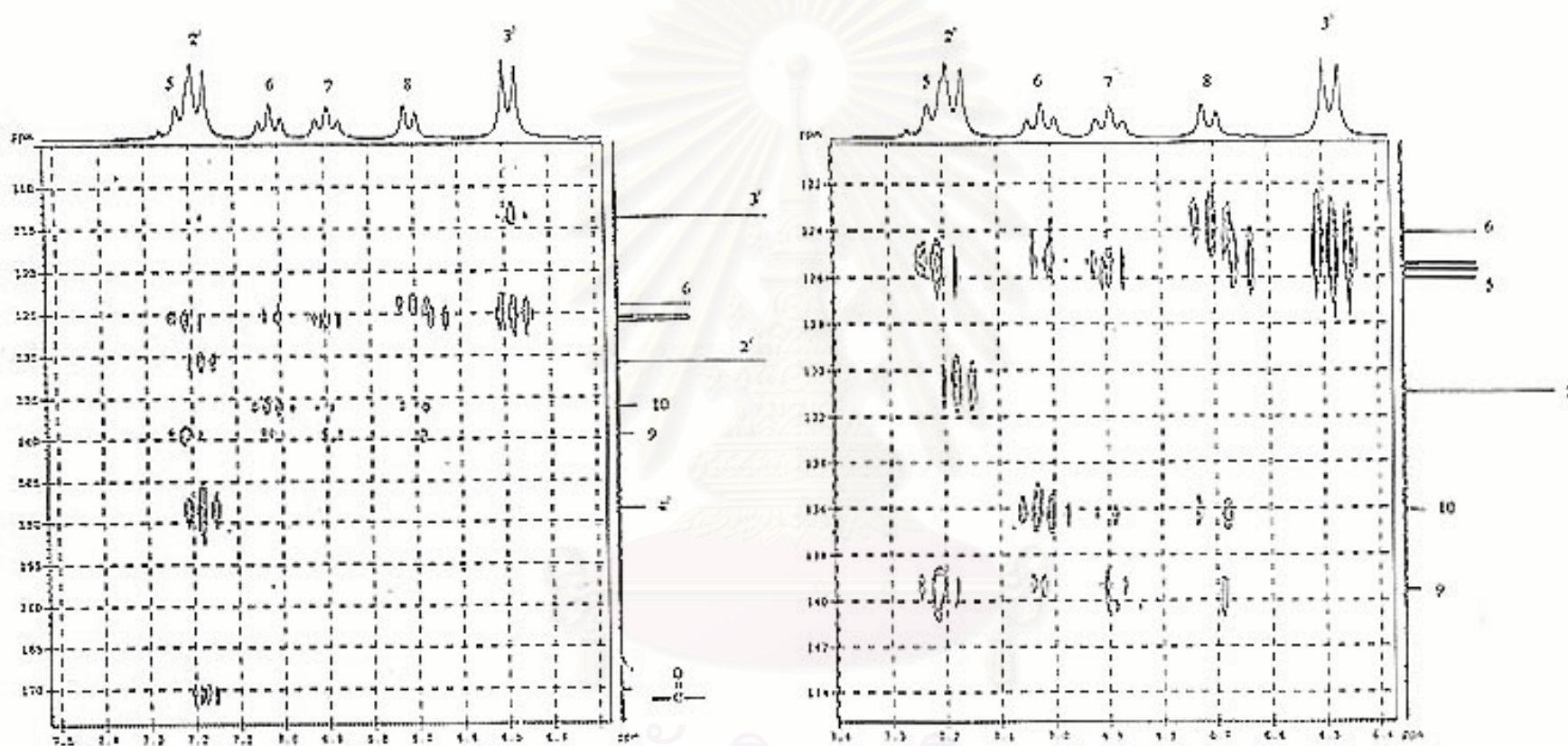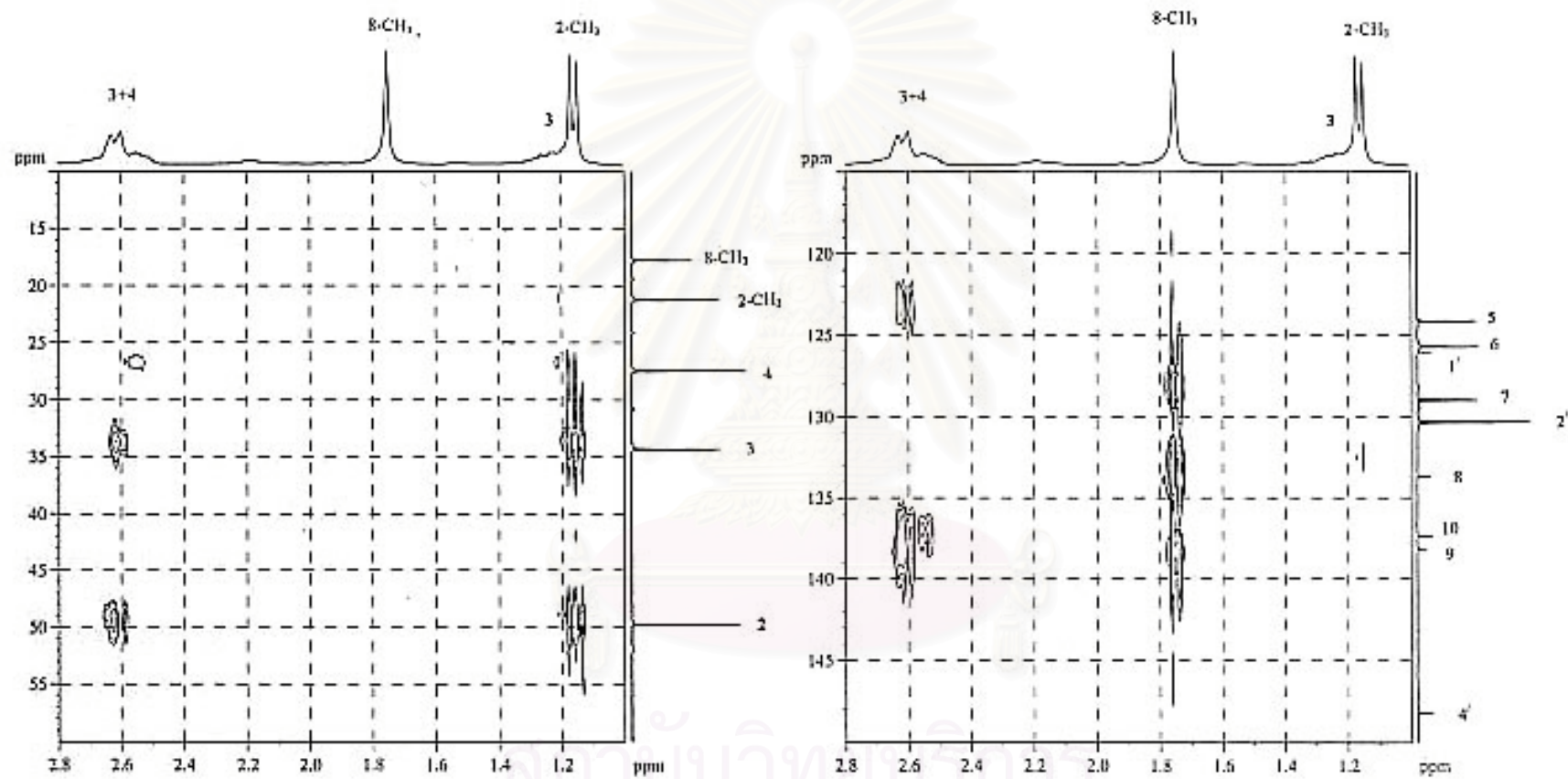
CDCl₃.

Figure 150. The 300 MHz HMBC spectrum (JHC = 8 Hz) of N-(*p*-aminobenzoyl)-1,2,3,4-tetrahydro-2,8-dimethylquinoline (4f, CU-17-12) in

CDCl₃. (Expanded: δH 1.0-2.8 ppm; δC 10-150 ppm)
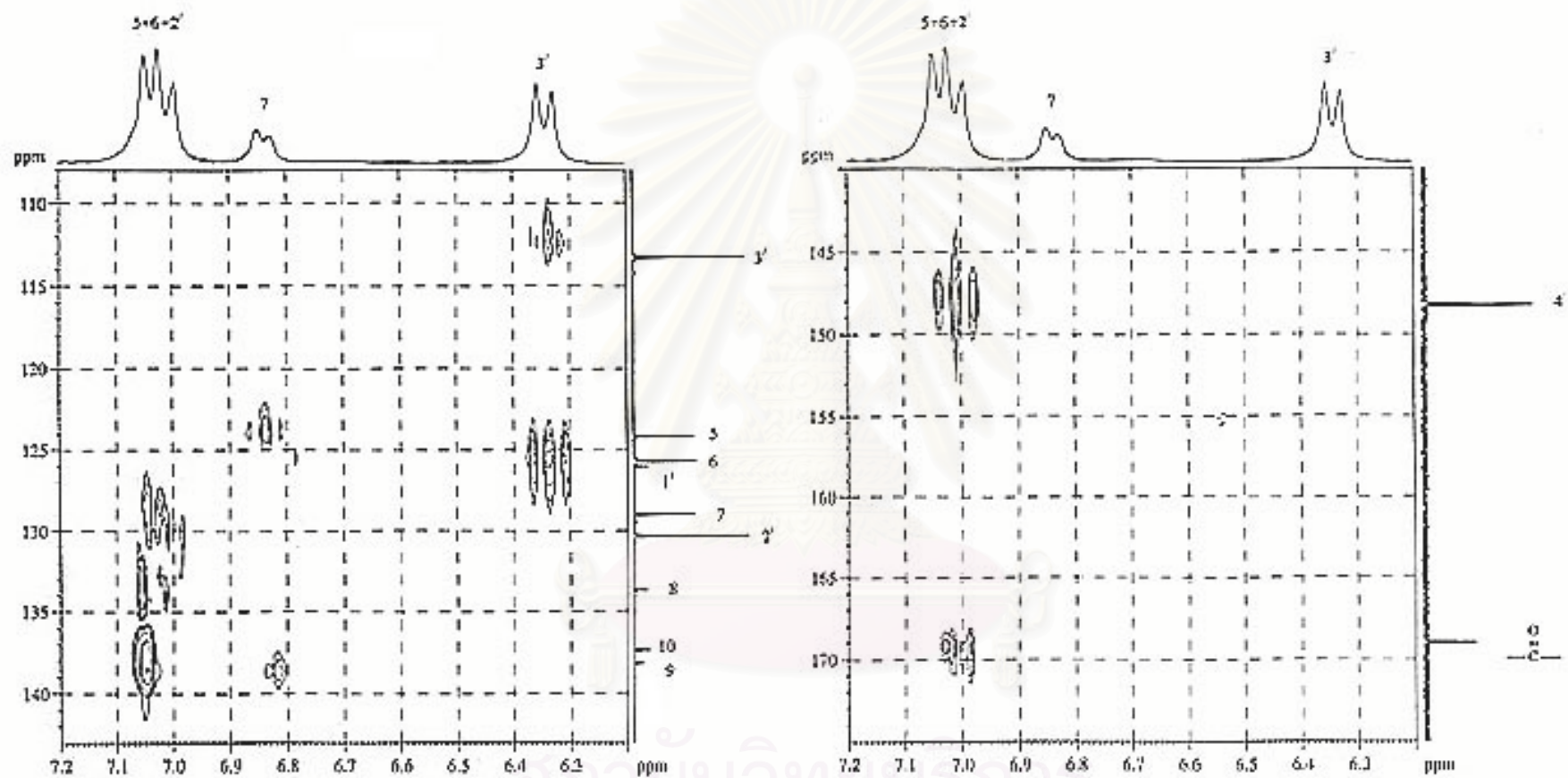
Figure 151. The 300 MHz HMBC spectrum (JHC = 8 Hz) of N-(*p*-aminobenzoyl)-1,2,3,4-tetrahydro-2,8-dimethylquinoline (4f, CU-17-12) in

CDCl₃. (Expanded: δH 6.2-7.2 ppm; δC 108-175 ppm)
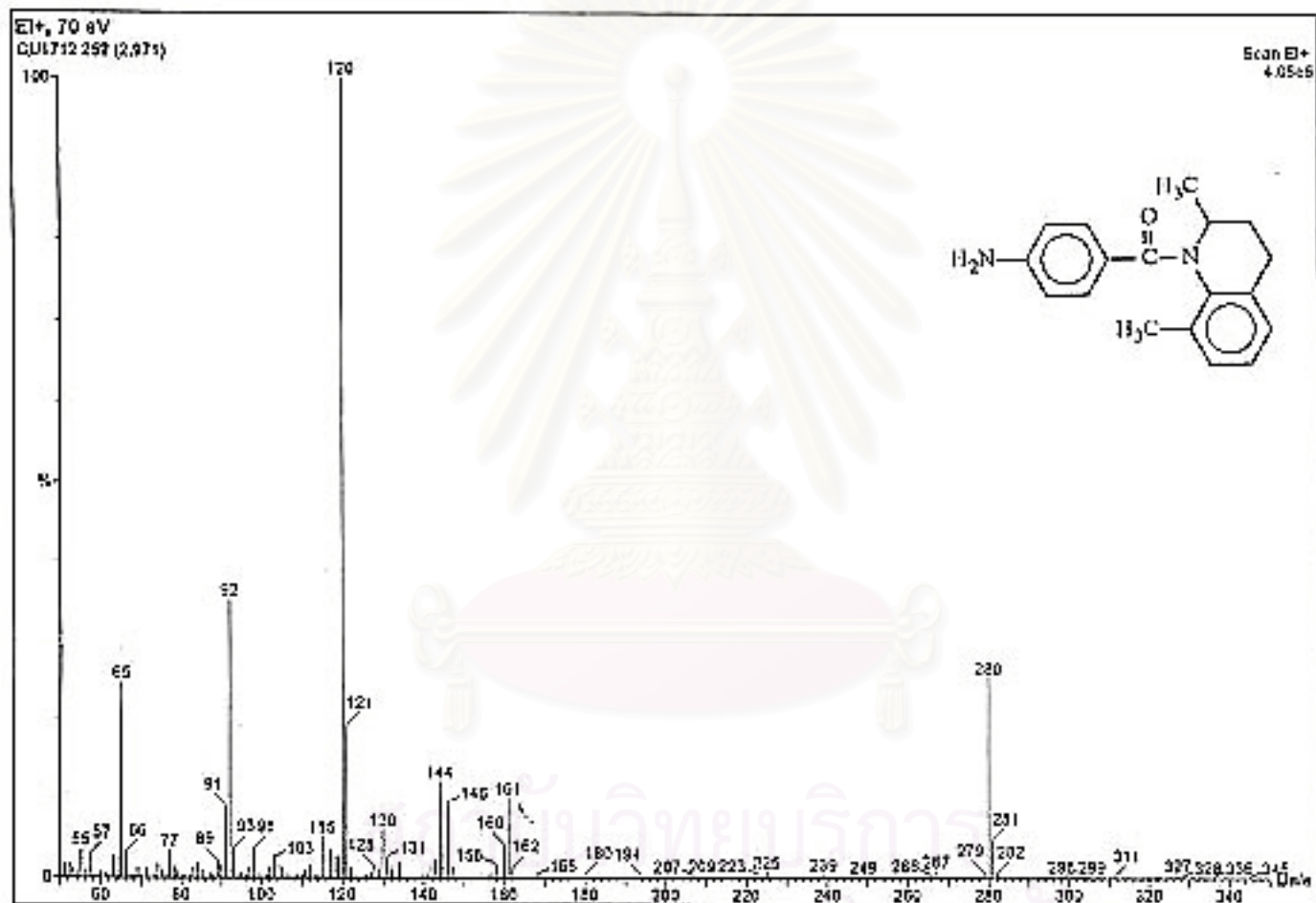
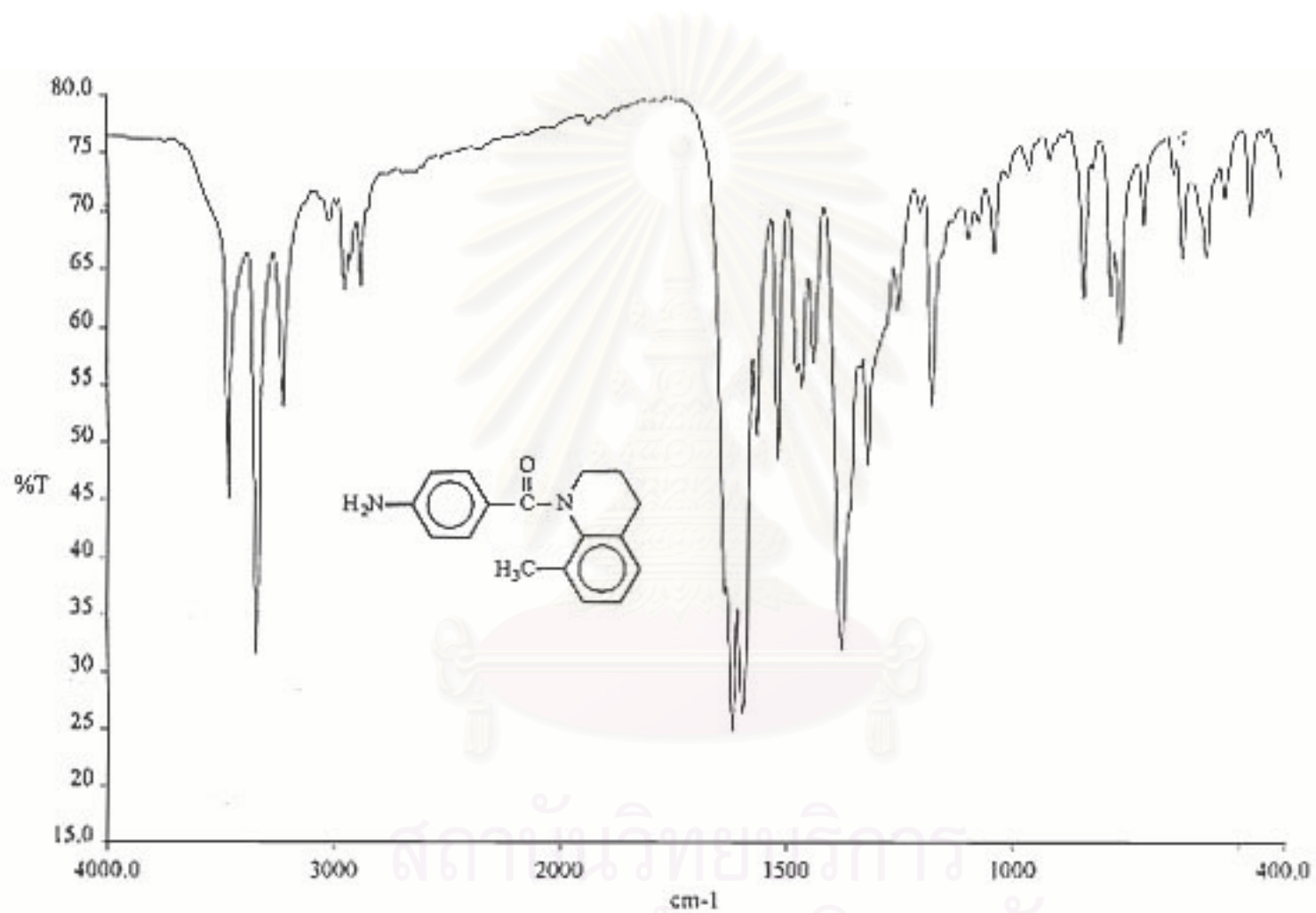Figure 152. The electron impact mass spectrum of N-(*p*-aminobenzoyl)-1,2,3,4-tetrahydro-2,8-dimethylquinoline (4f, CU-17-12).
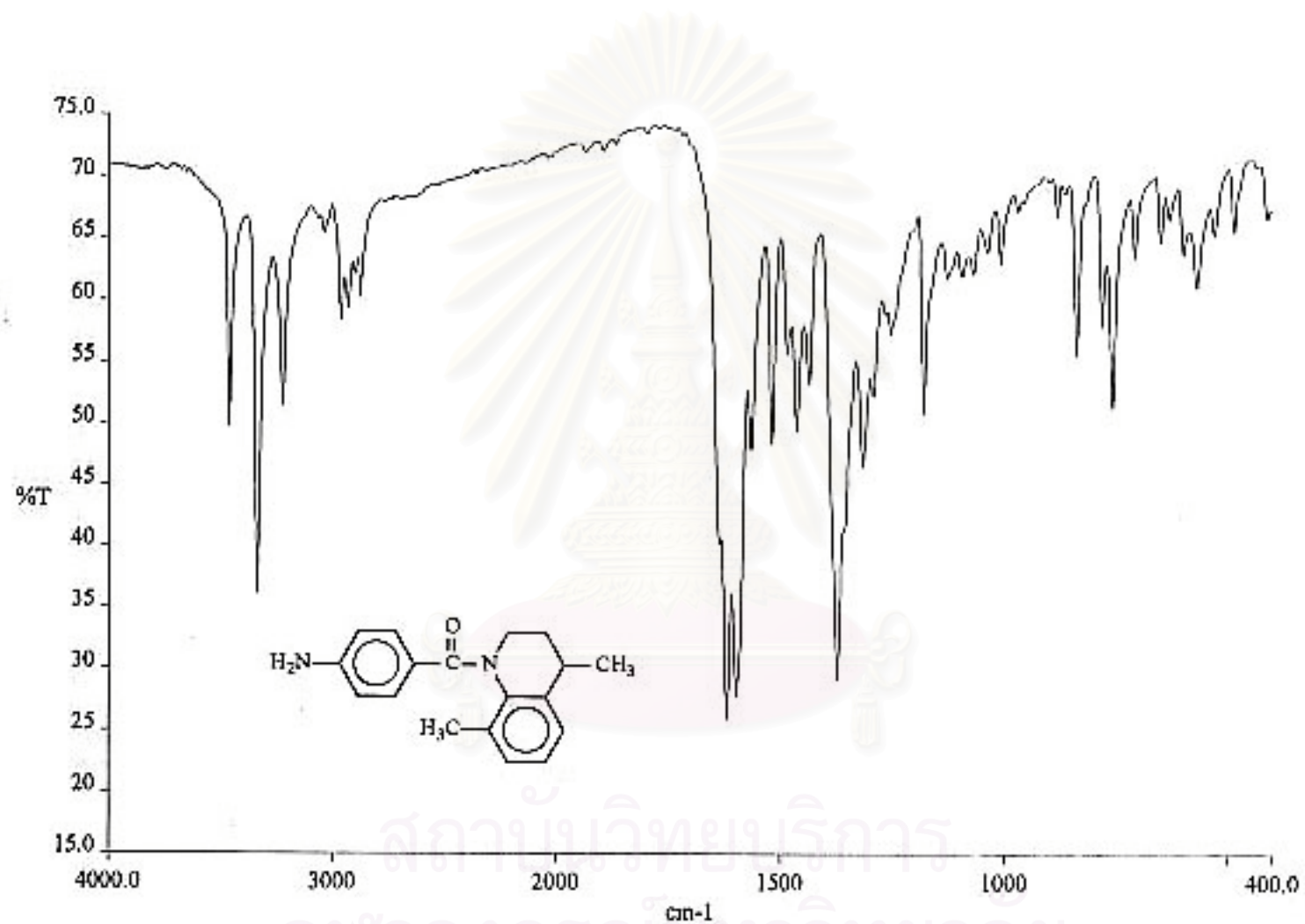
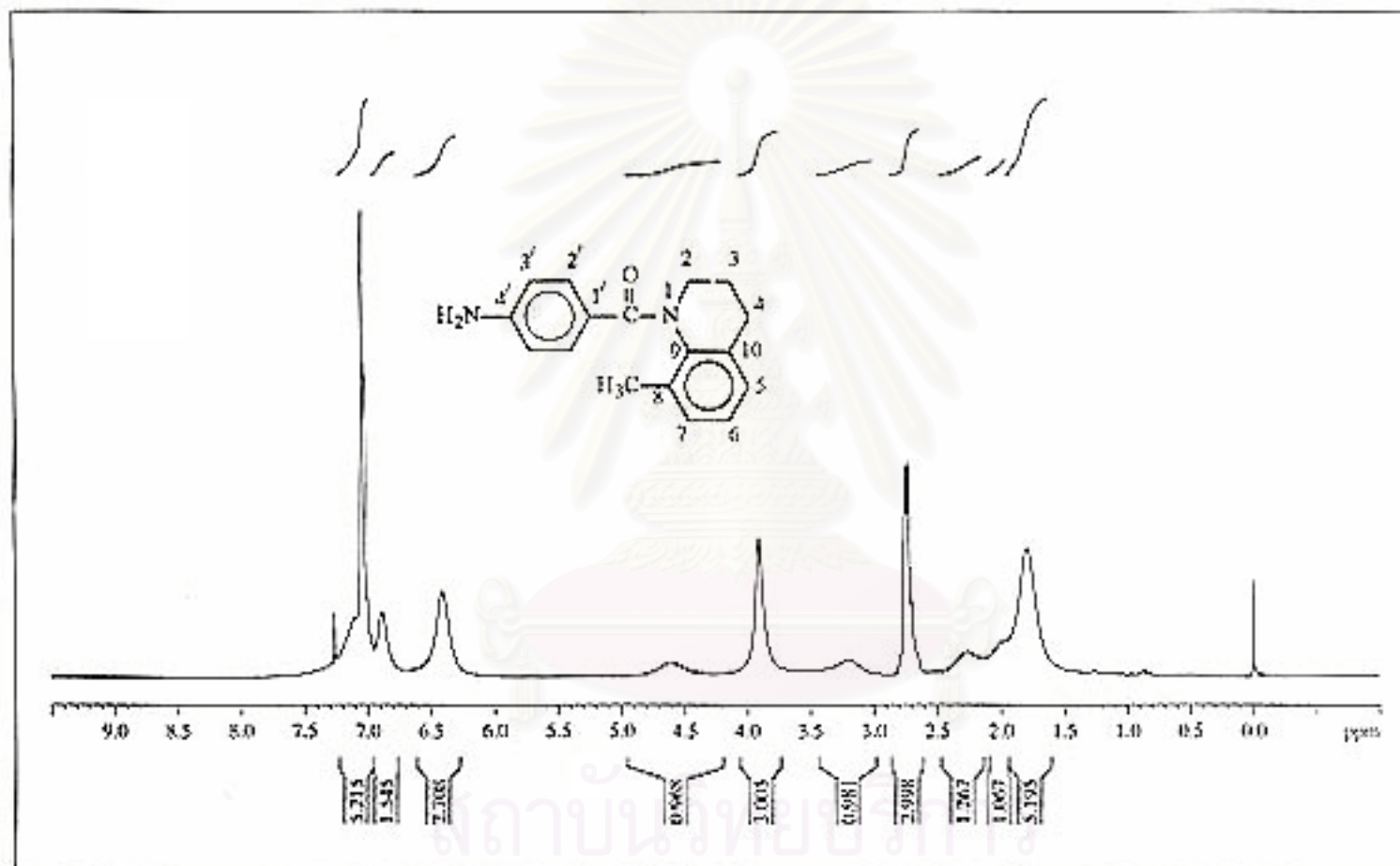Figure 153. The IR spectrum (KBr) of N-(*p*-aminobenzoyl)-1,2,3,4-tetrahydro-4,8-dimethylquinoline (4g, CU-17-14).
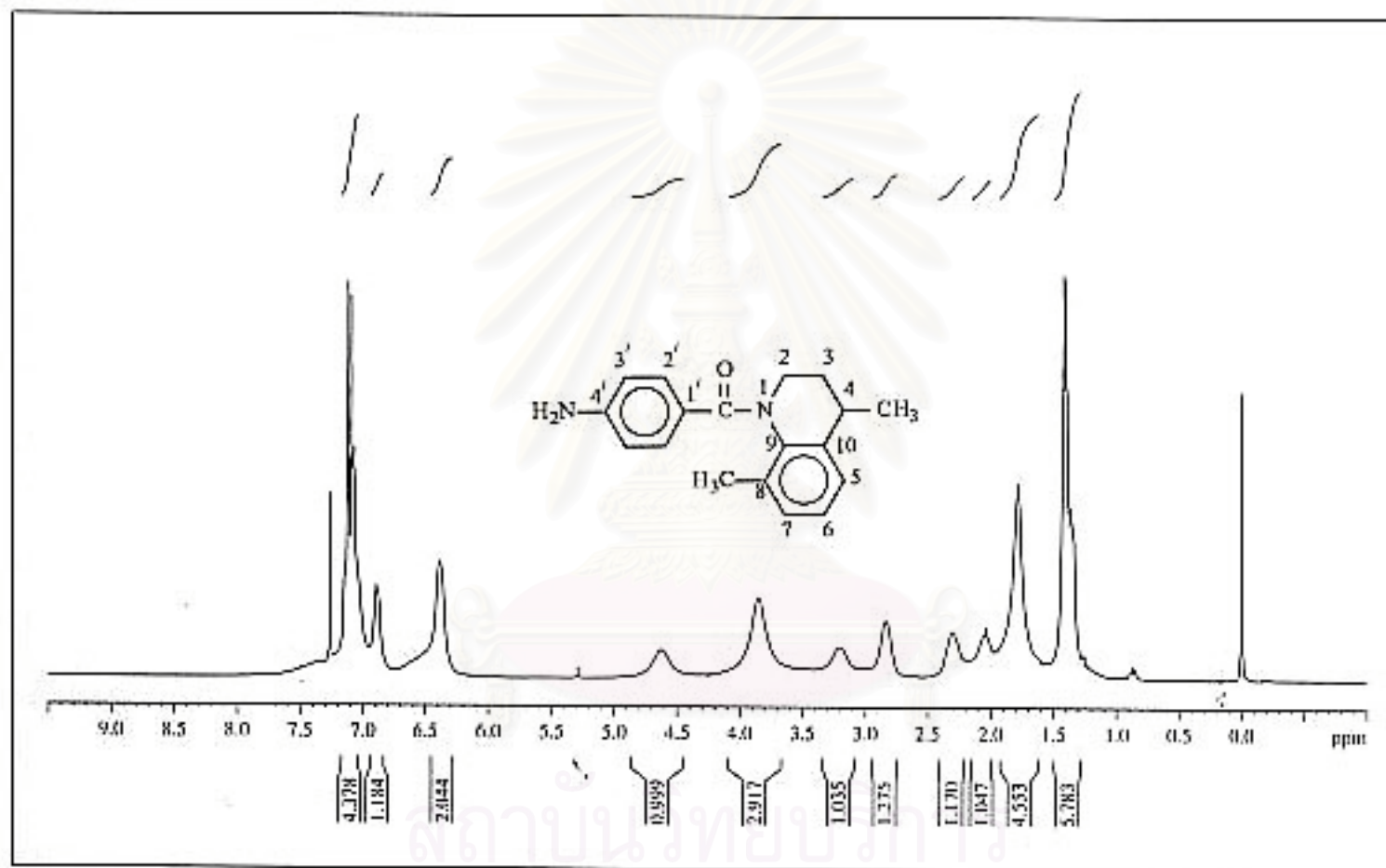
Figure 154. The 300 MHz ^{1}H-NMR spectrum of N-(*p*-aminobenzoyl)-1,2,3,4-tetrahydro-4,8-dimethylquinoline (4g, CU-17-14) in CDCl₃.
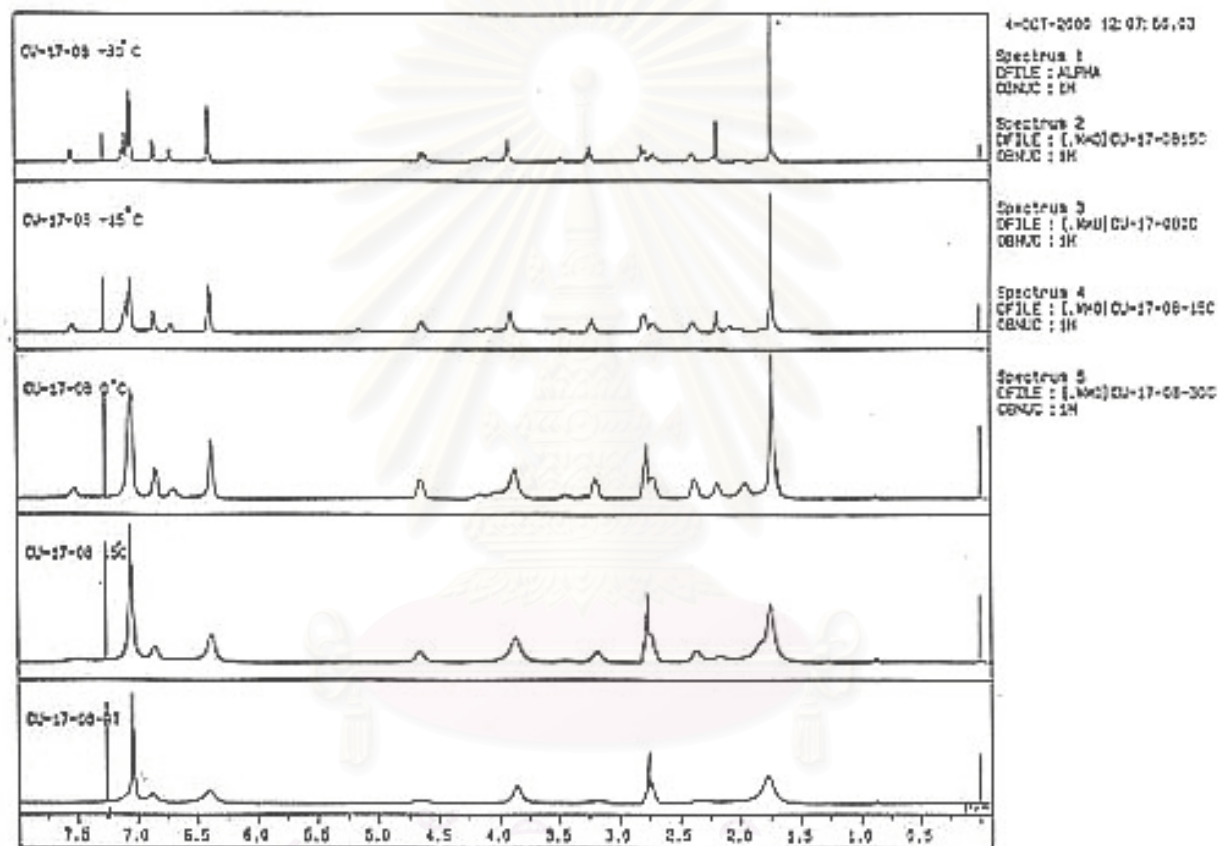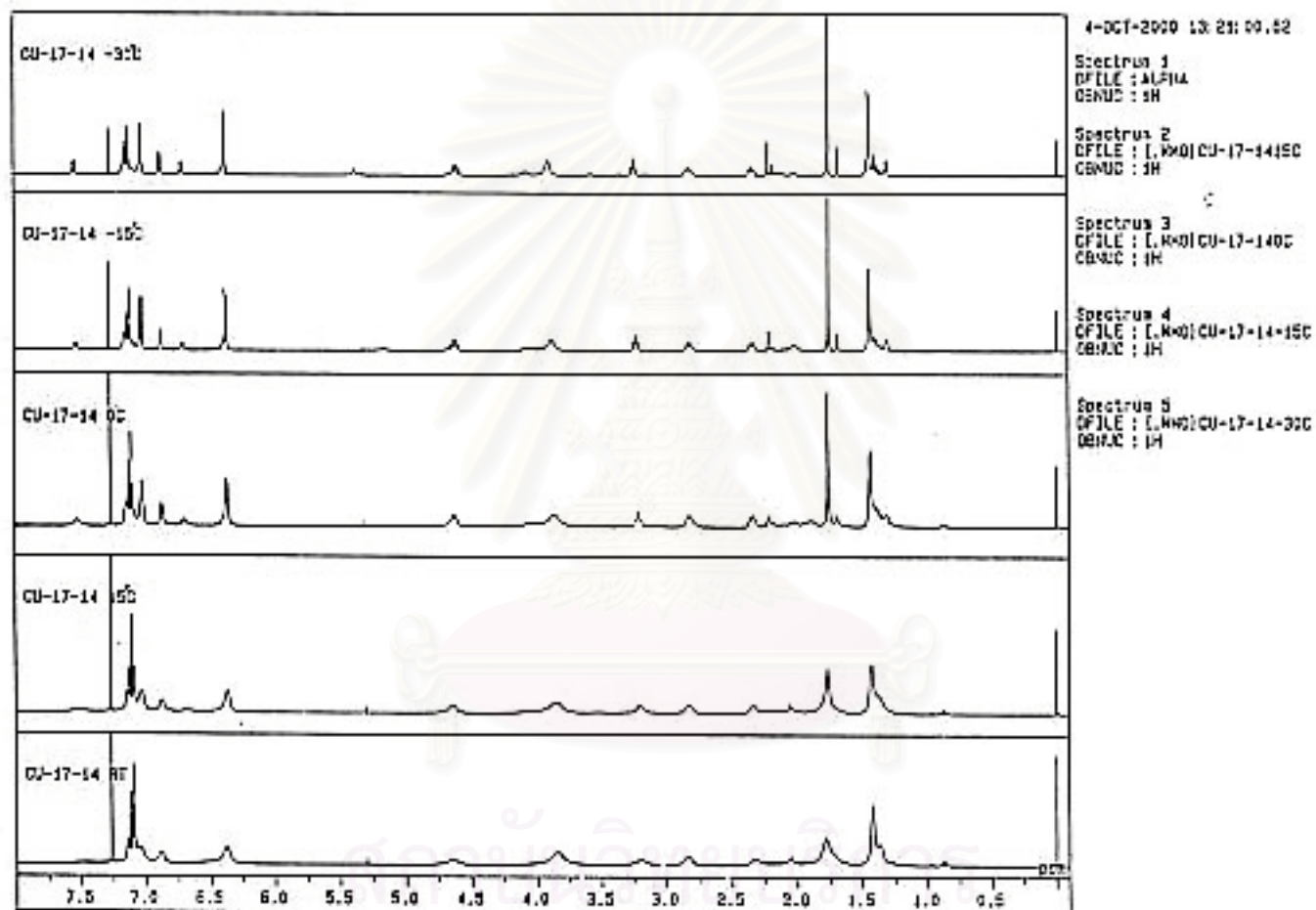
Figure 155. The 500 MHz 1H-NMR spectra of N-(*p*-aminobenzoyl)-1,2,3,4-tetrahydro-4,8-dimethylquinoline (4g, CU-17-14) in CDCl$_3$ at room

temperature (RT), 15 °C, 0 °C, -15 °C and -30 °C.
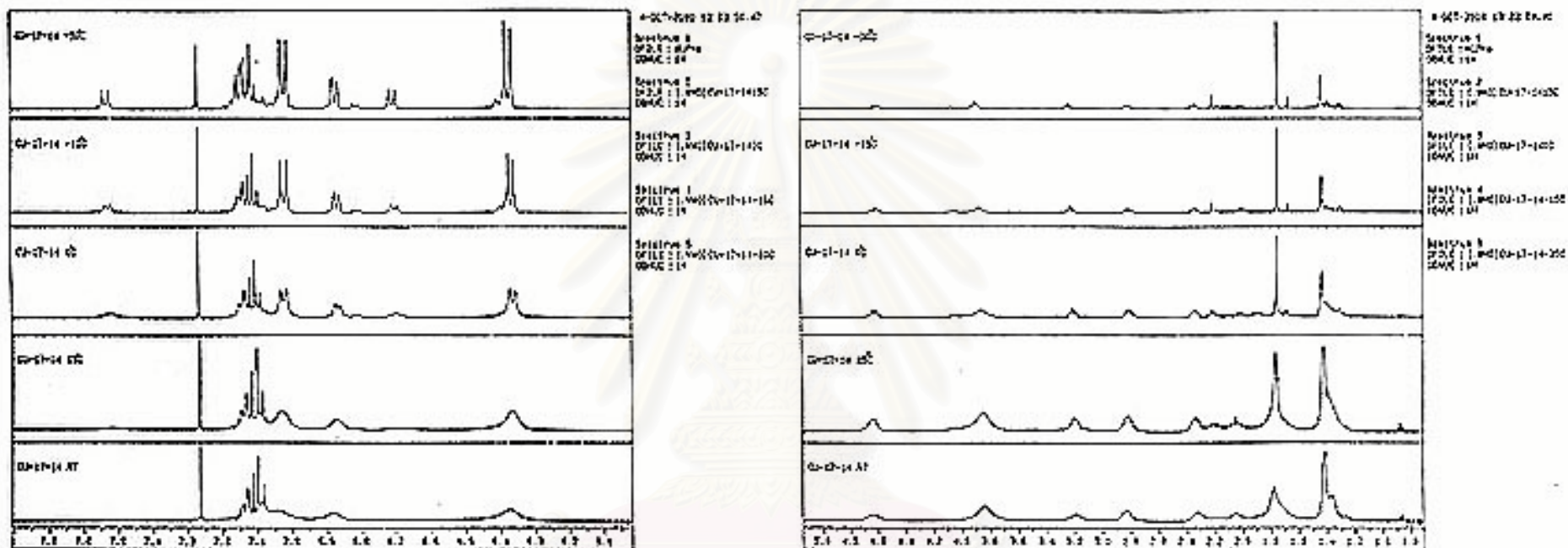
Figure 156. The 500 MHz 1H-NMR spectra of N-(*p*-aminobenzoyl)-1,2,3,4-tetrahydro-4,8-dimethylquinoline (4g, CU-17-14) in CDCl$_3$ at room

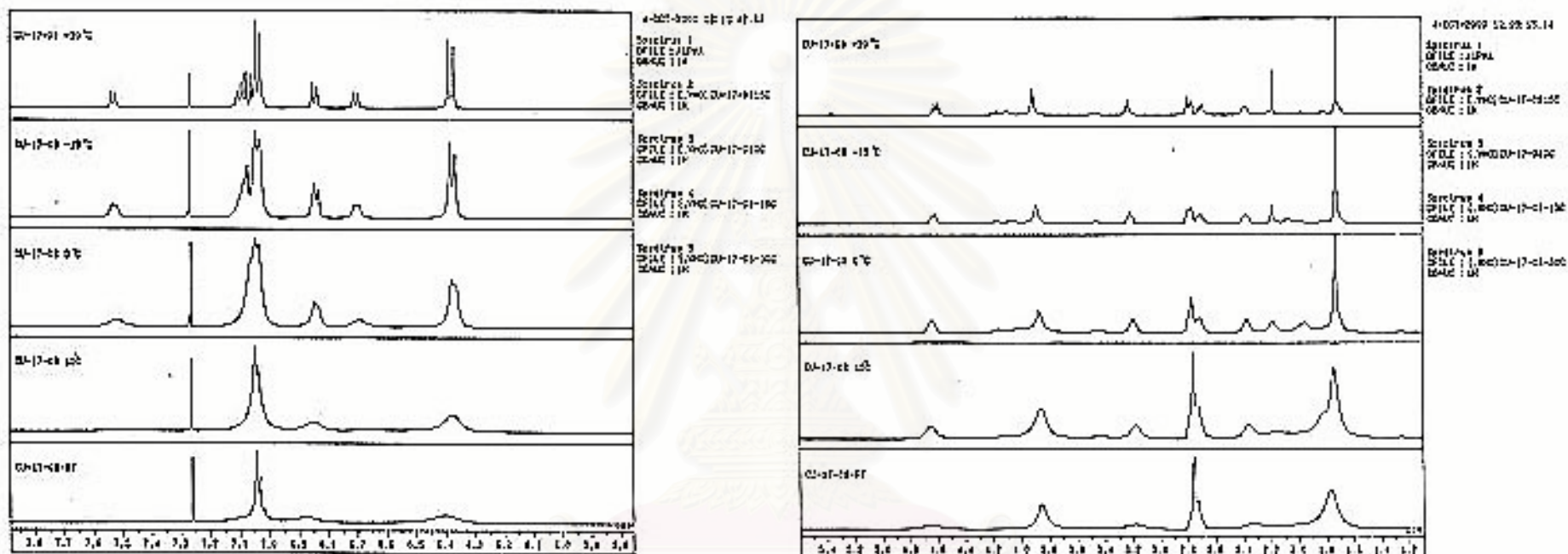temperature (RT), 15 °C, 0 °C, -15 °C and -30 °C. (Enlarged scale)
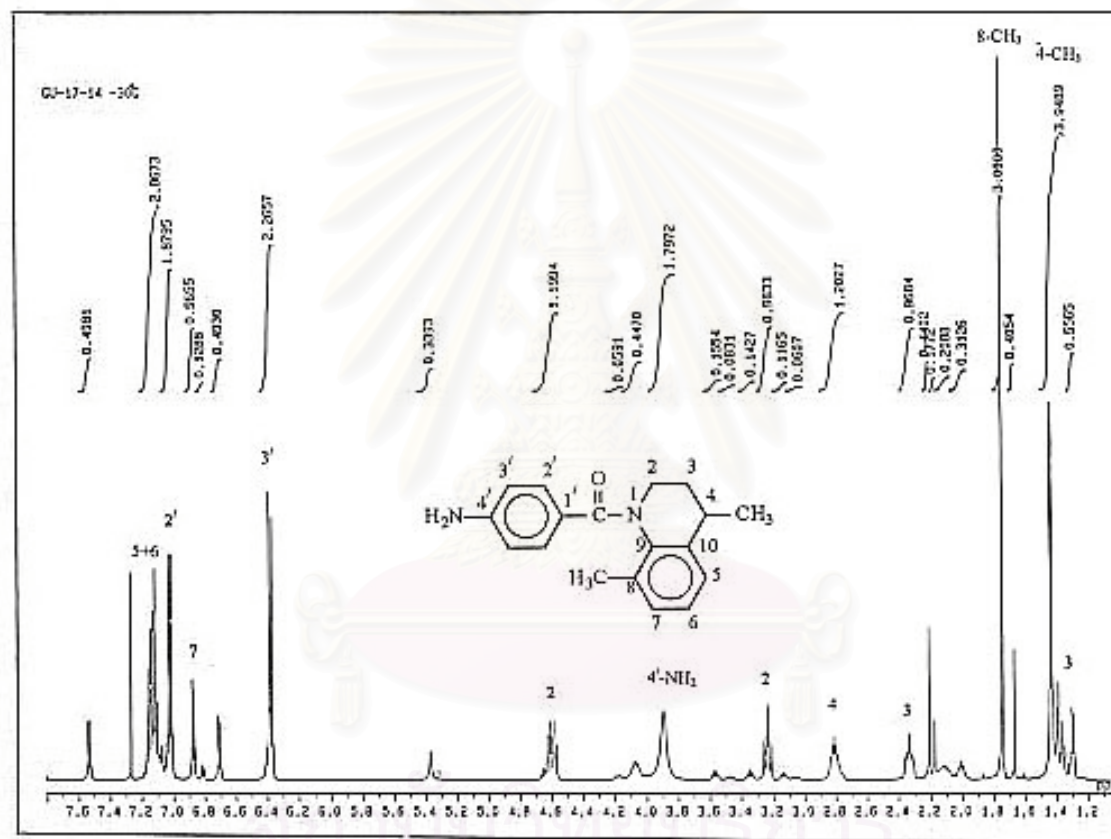
Figure 157. The 500 MHz 1H-NMR spectrum of N-(*p*-aminobenzoyl)-1,2,3,4-tetrahydro-4,8-dimethylquinoline (4g, CU-17-14) in CDCl₃ at
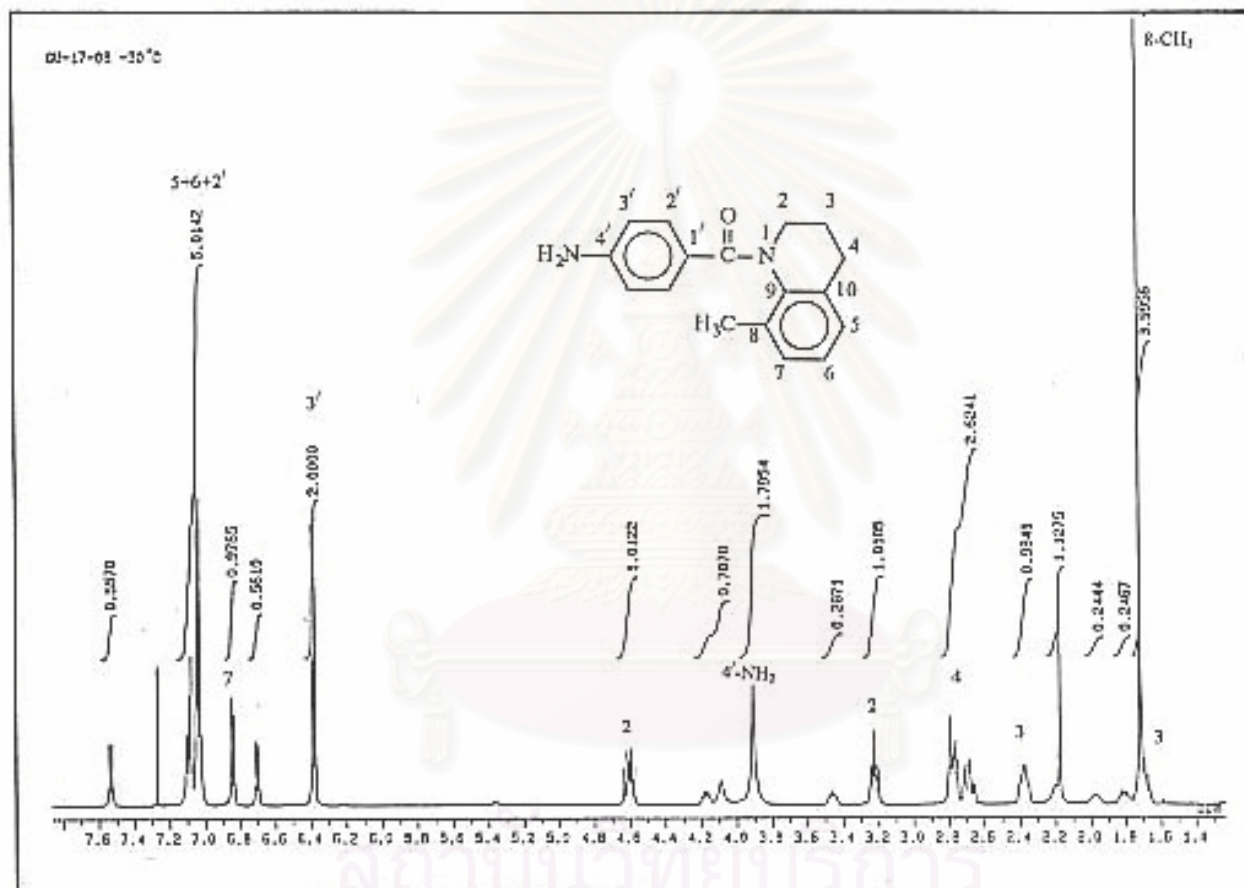-30 °C.

Figure 158. The 500 MHz 1H-NMR spectrum of N-(*p*-aminobenzoyl)-1,2,3,4-tetrahydro-4,8-dimethylquinoline (4g, CU-17-14) in CDCl₃ at

-30 °C. (Enlarged scale)
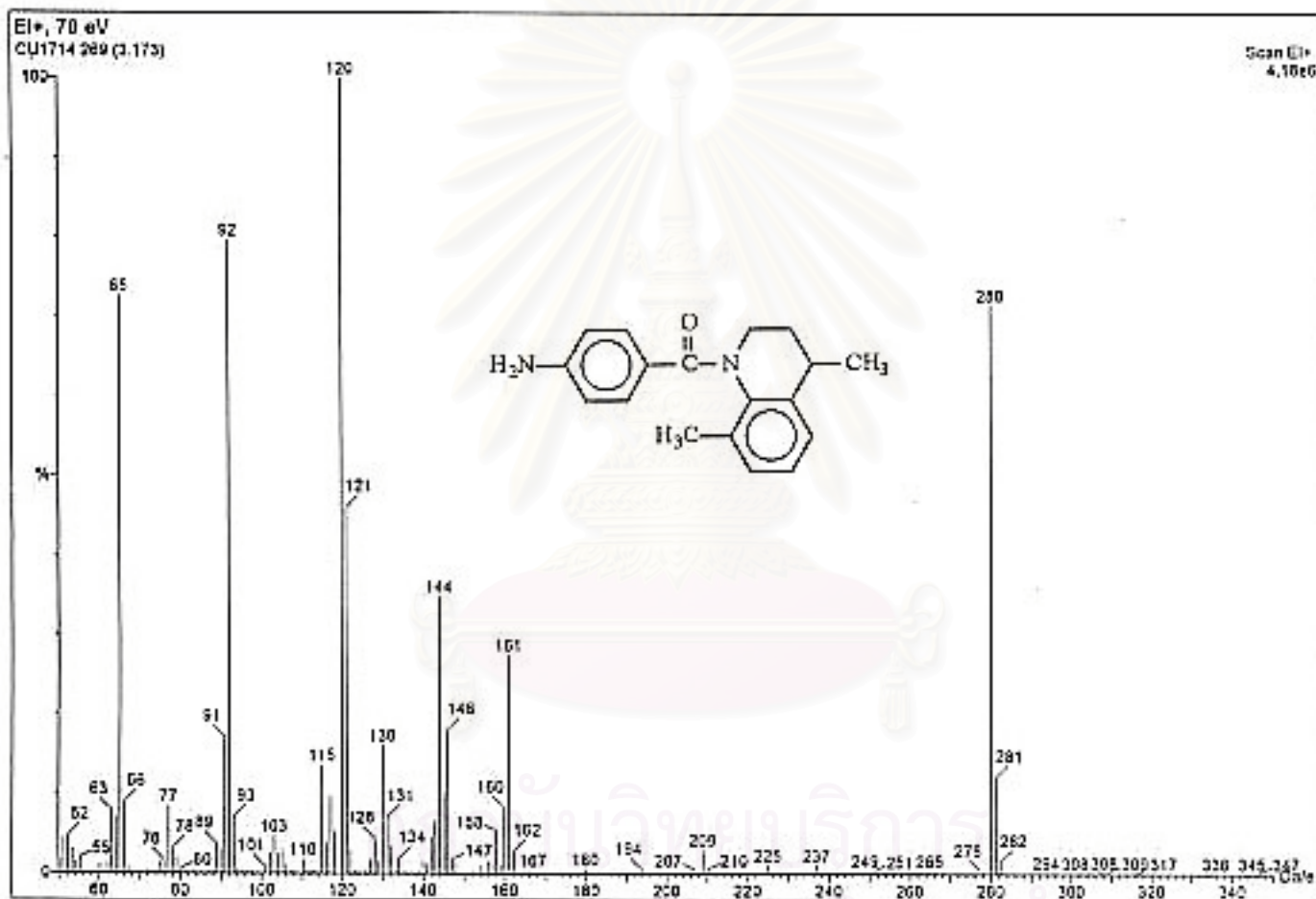
Figure 159. The electron impact mass spectrum of N-(*p*-aminobenzoyl)-1,2,3,4-tetrahydro-4,8-dimethylquinoline (4g, CU-17-14).
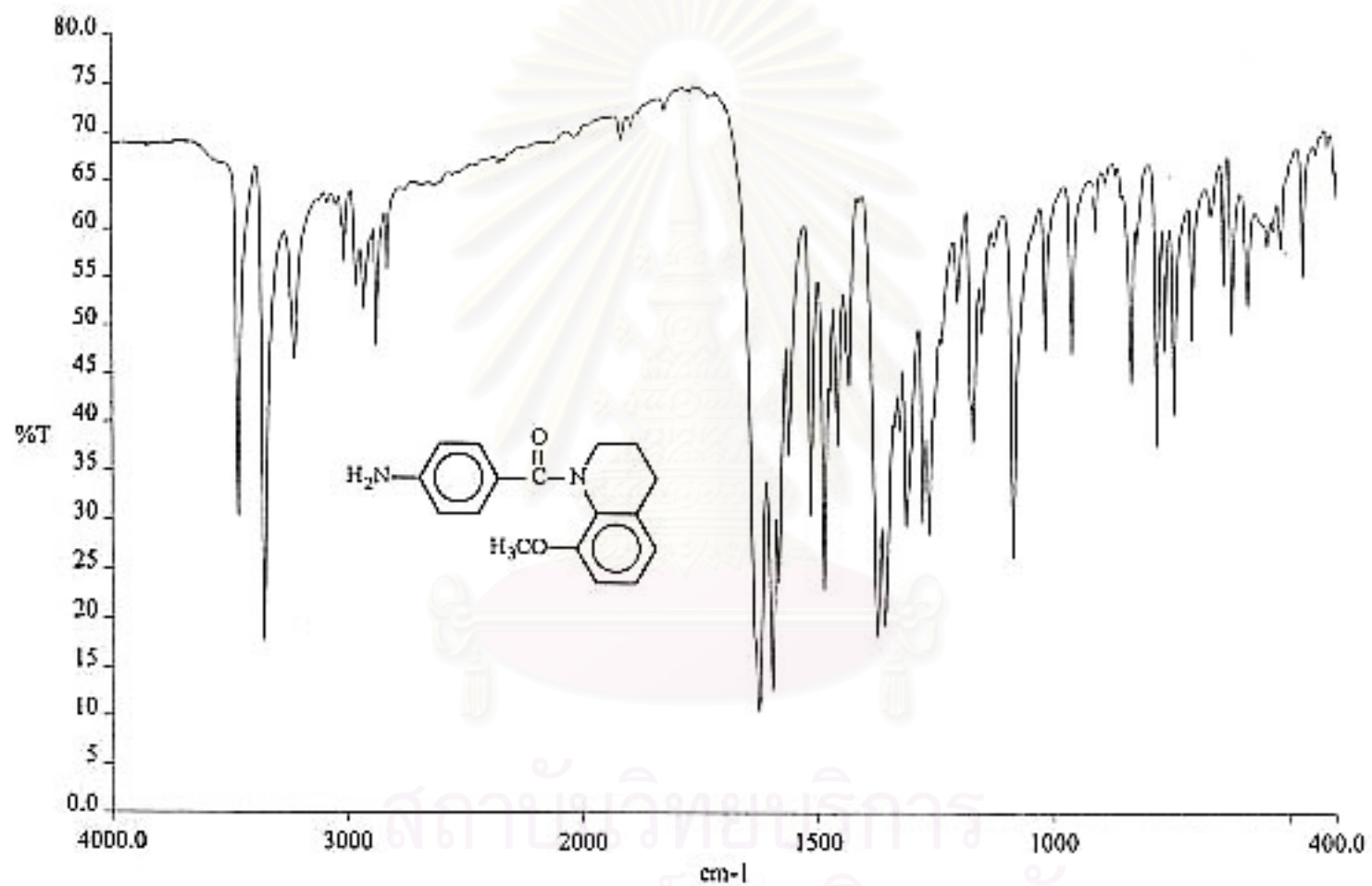
Figure 160. The IR spectrum (KBr) of N-(*p*-aminobenzoyl)-1,2,3,4-tetrahydro-8-methoxyquinoline (4h, CU-17-16).
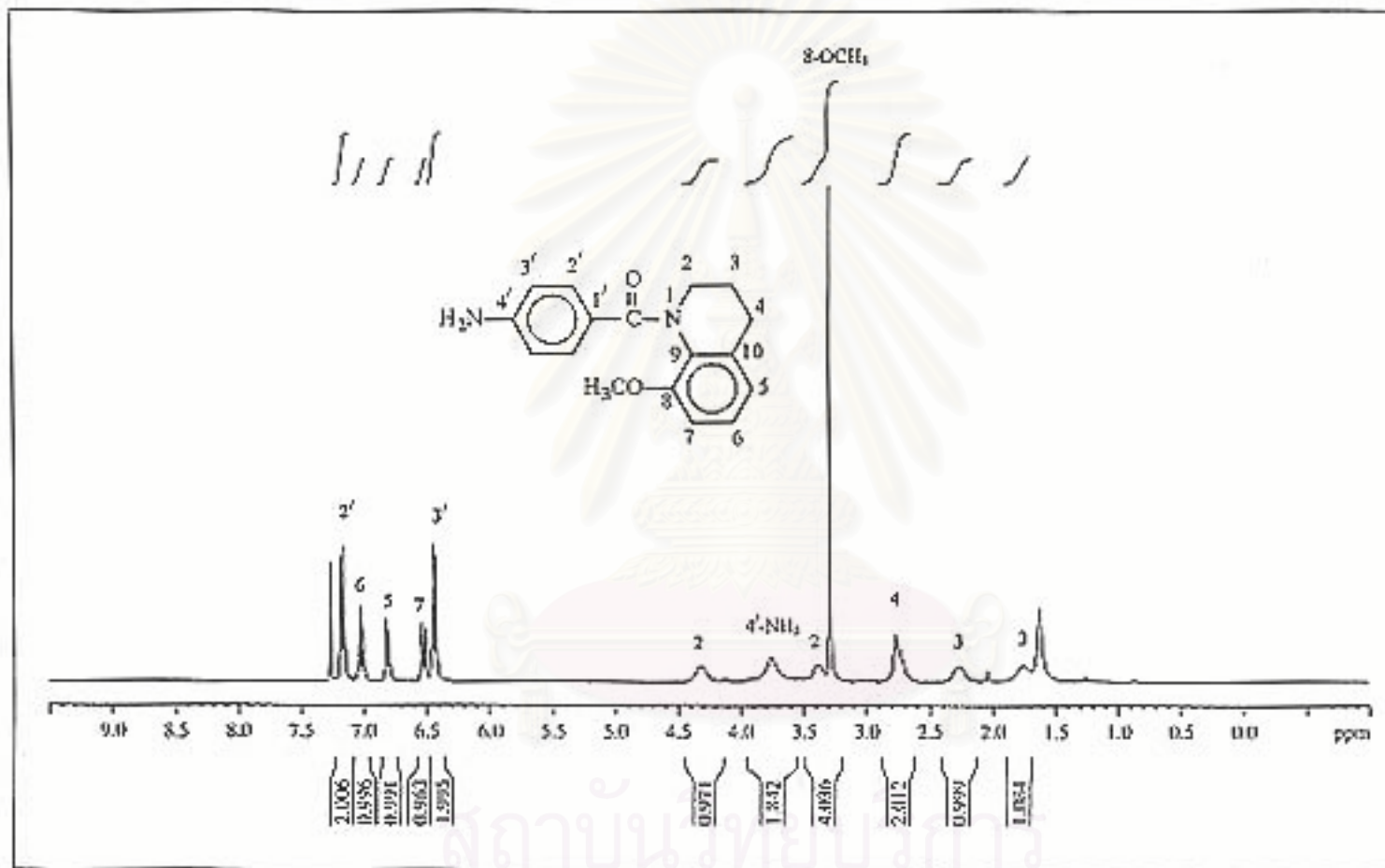
Figure 161. The 300 MHz 1H-NMR spectrum of N-(*p*-aminobenzoyl)-1,2,3,4-tetrahydro-8-methoxyquinoline (4h, CU-17-16) in CDCl₃.
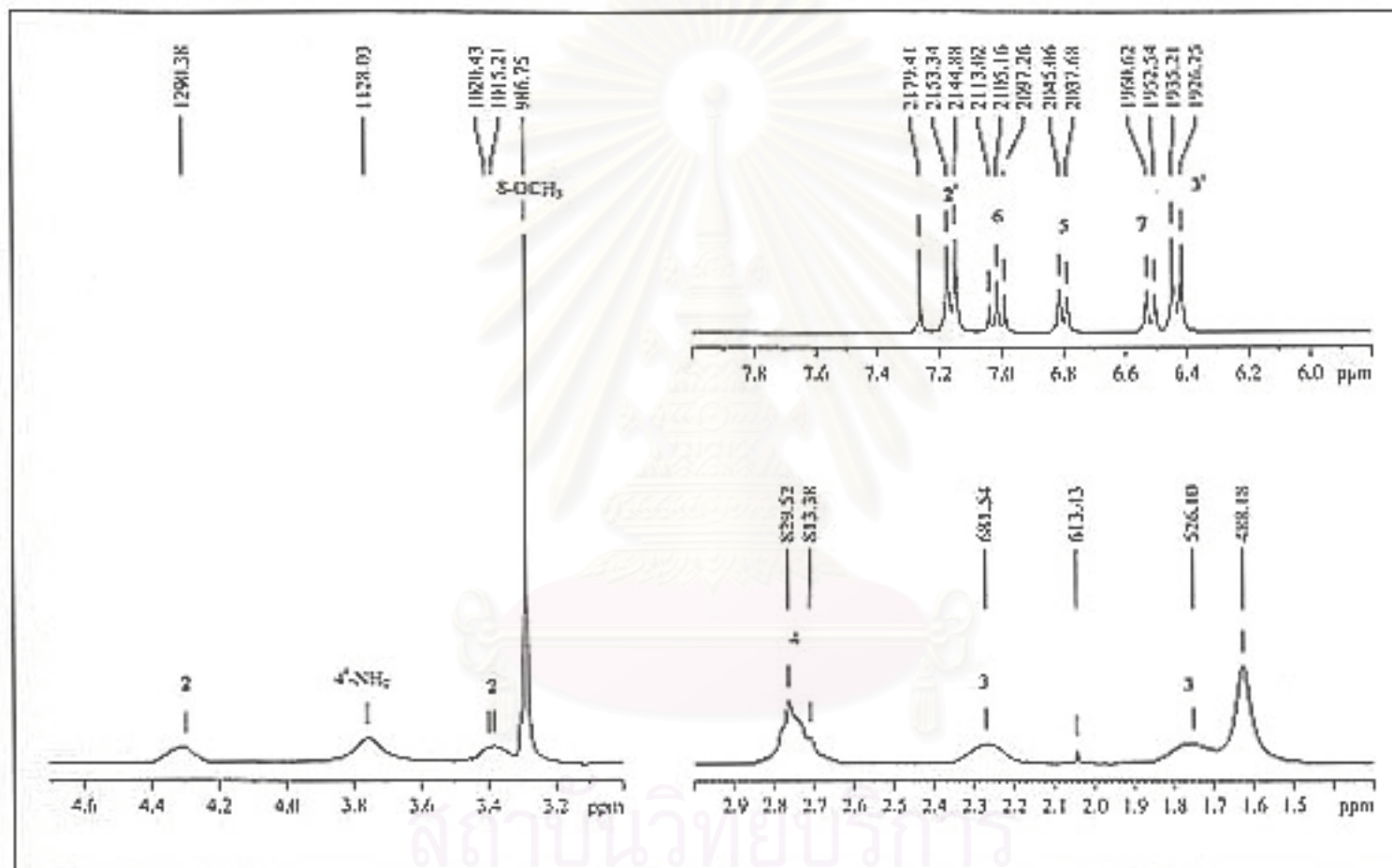
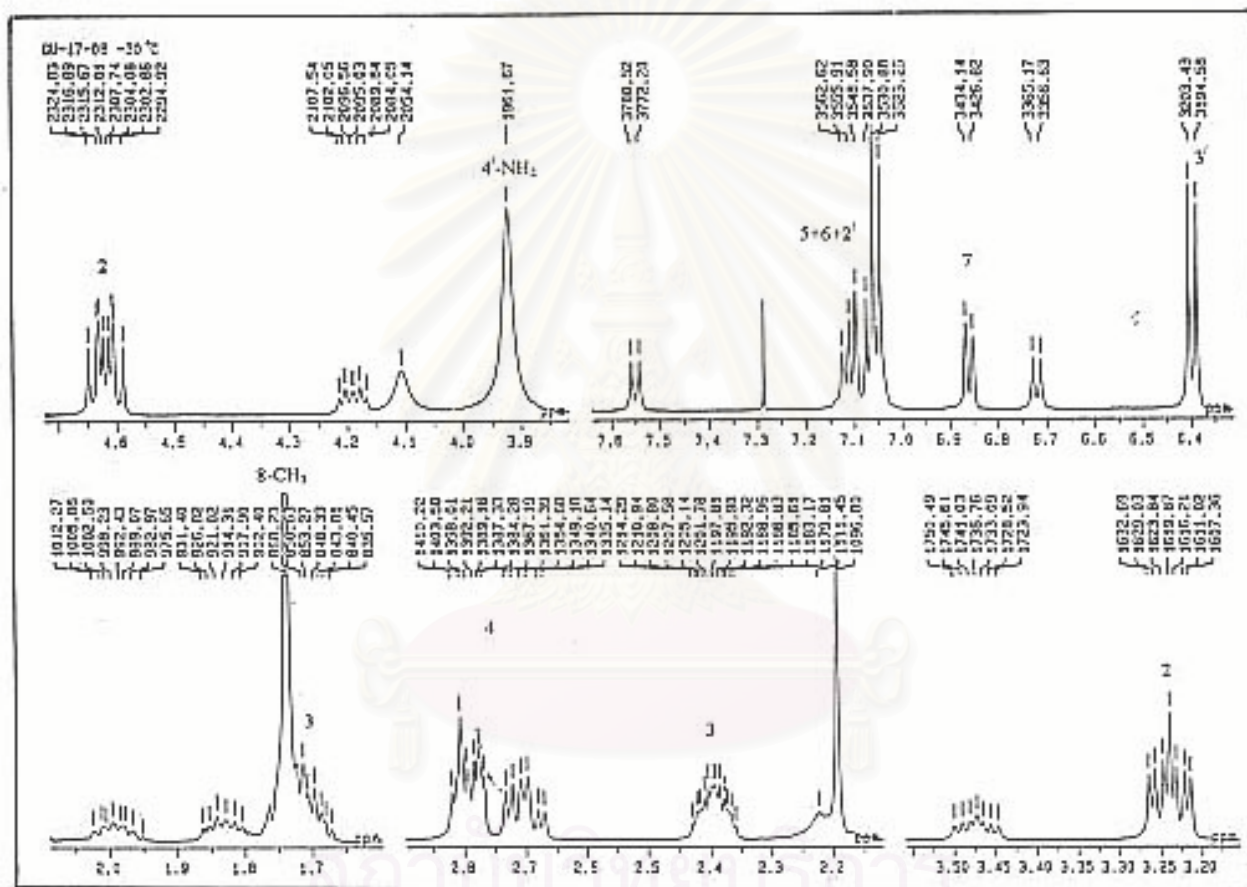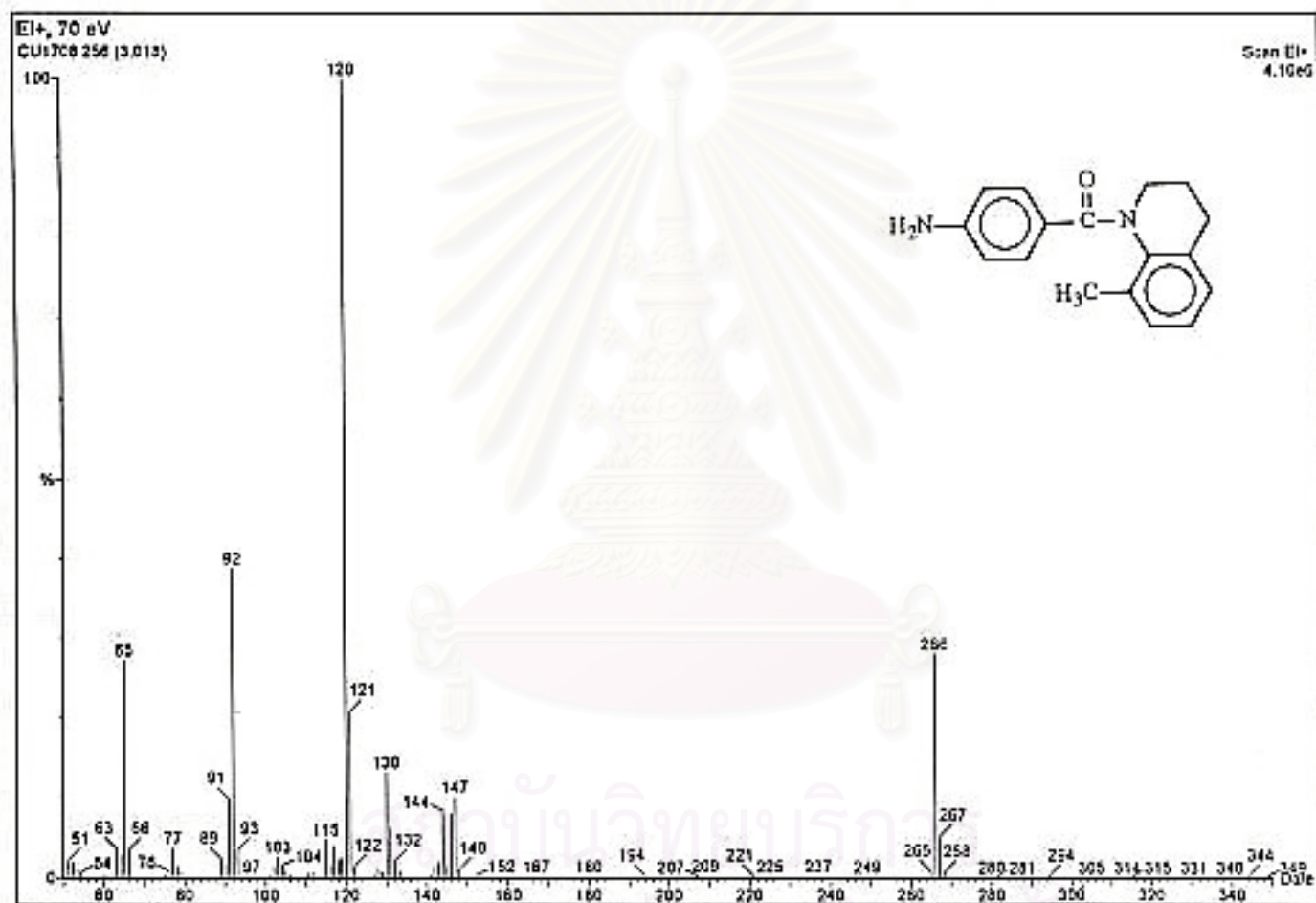Figure 162. The 300 MHz 1H-NMR spectrum of N-(*p*-aminobenzoyl)-1,2,3,4-tetrahydro-8-methoxyquinoline (4h, CU-17-16) in CDCl₃.

(Enlarged scale)
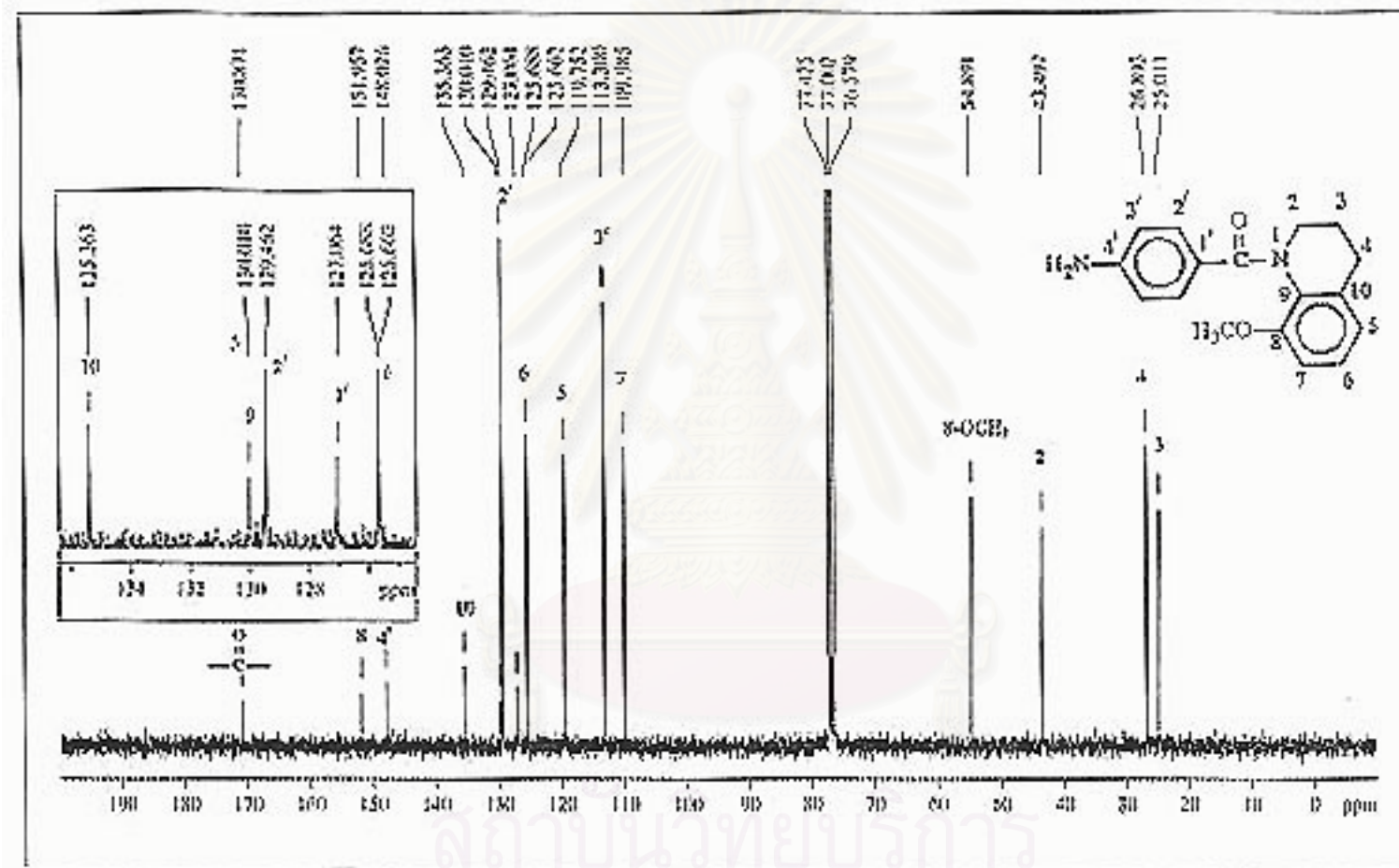
Figure 163. The 75 MHz 13C-NMR decoupled spectrum of N-(*p*-aminobenzoyl)-1,2,3,4-tetrahydro-8-methoxyquinoline (4h, CU-17-16) in CDCl₃.
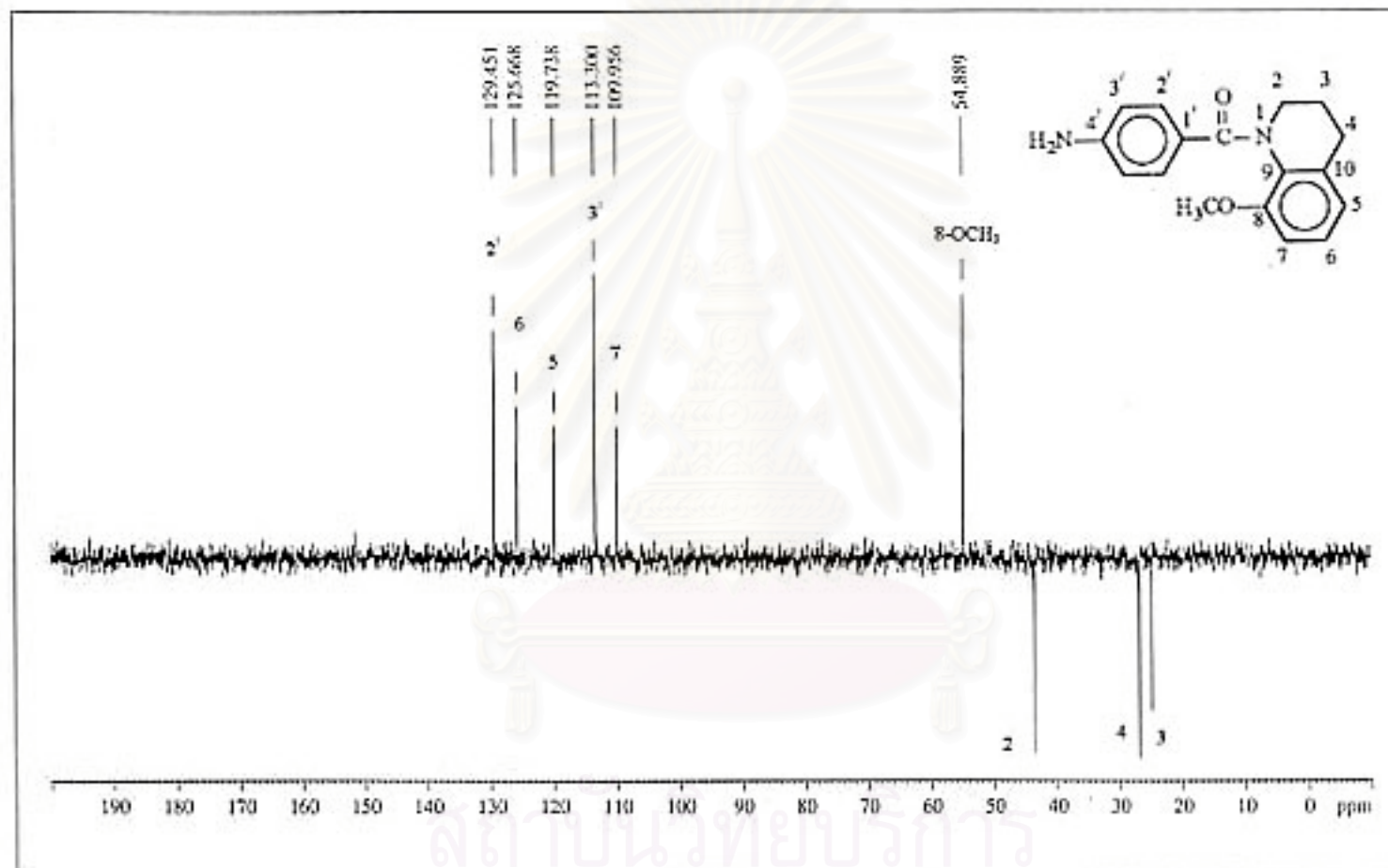
Figure 164. The 75 MHz DEPT-135 spectrum of N-(*p*-aminobenzoyl)-1,2,3,4-tetrahydro-8-methoxyquinoline (4h, CU-17-16) in CDCl$_3$.
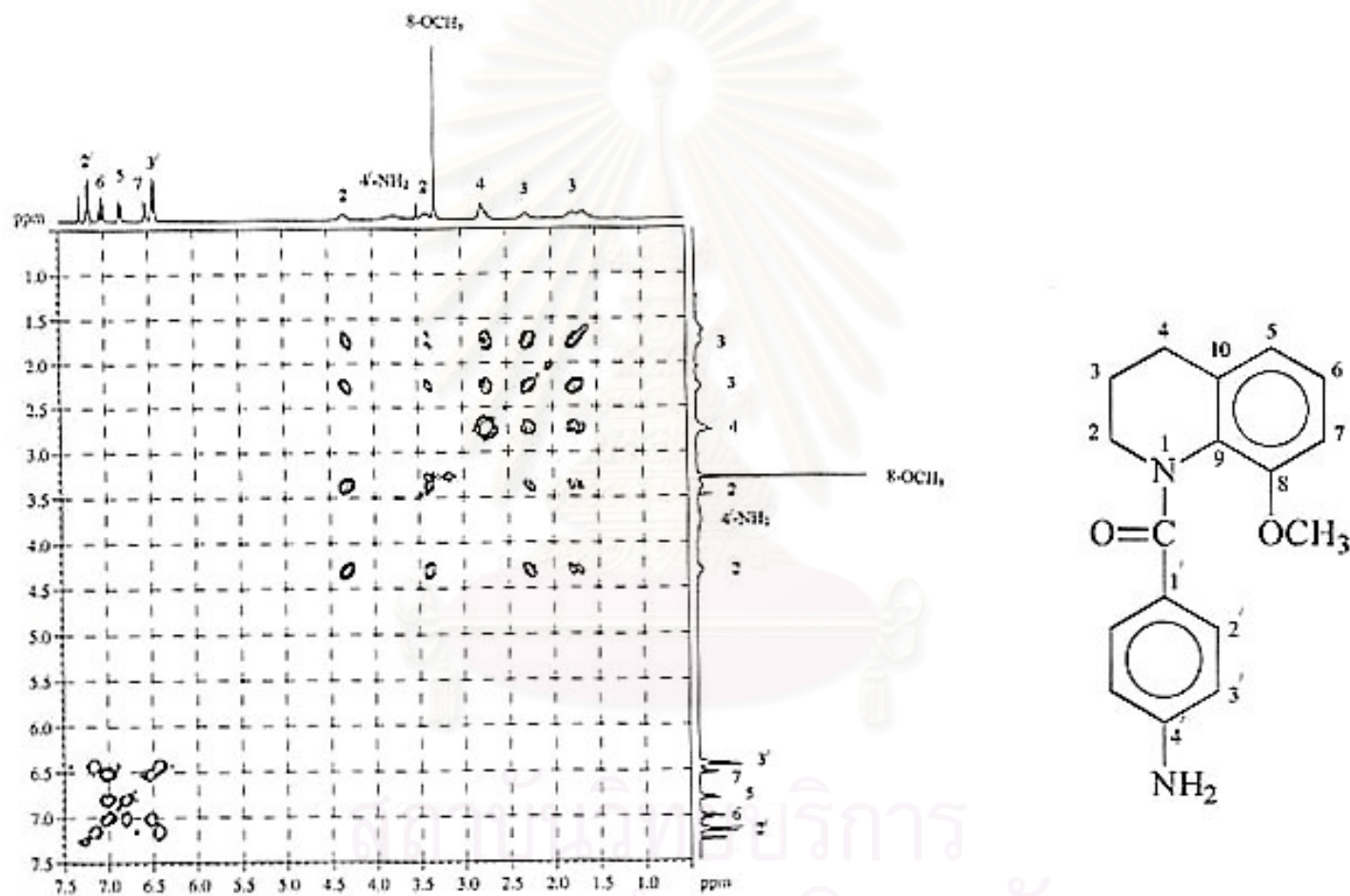
Figure 165. The 300 MHz HH COSY spectrum of N-(*p*-aminobenzoyl)-1,2,3,4-tetrahydro-8-methoxyquinoline (4h, CU-17-16) in CDCl₃.
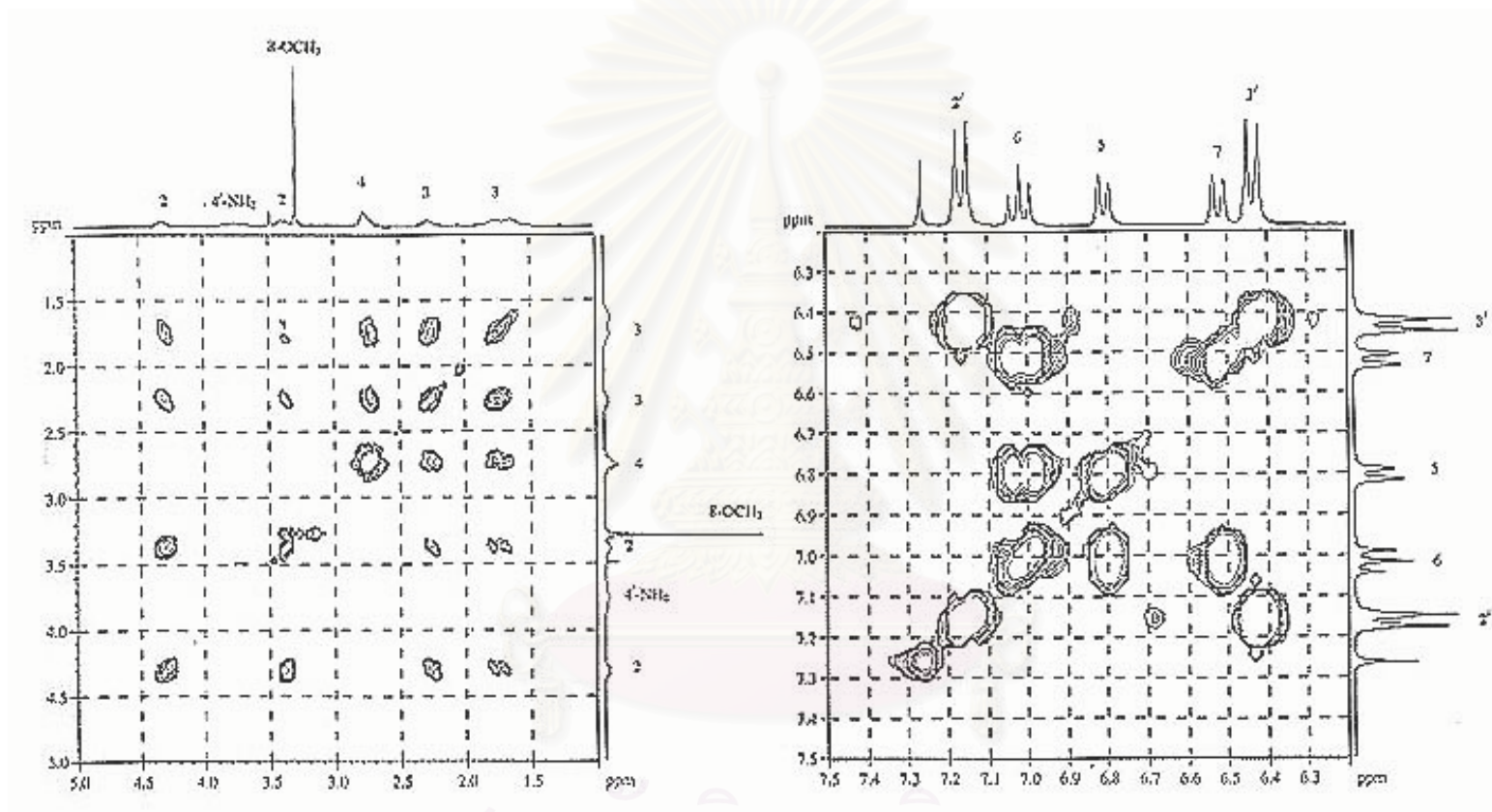
Figure 166. The 300 MHz HH COSY spectrum of N-(*p*-aminobenzoyl)-1,2,3,4-tetrahydro-8-methoxyquinoline (4h, CU-17-16) in CDCl₃.
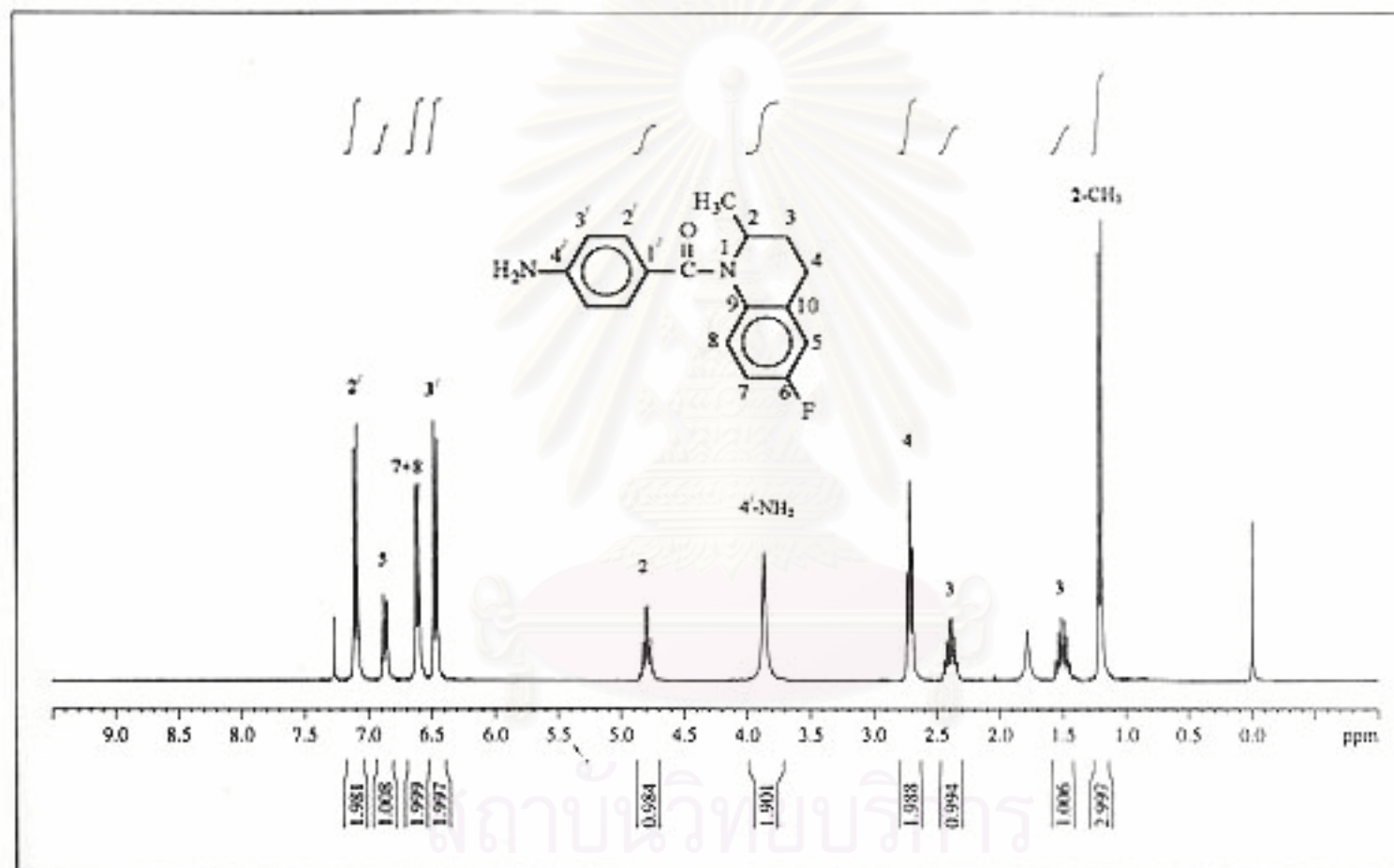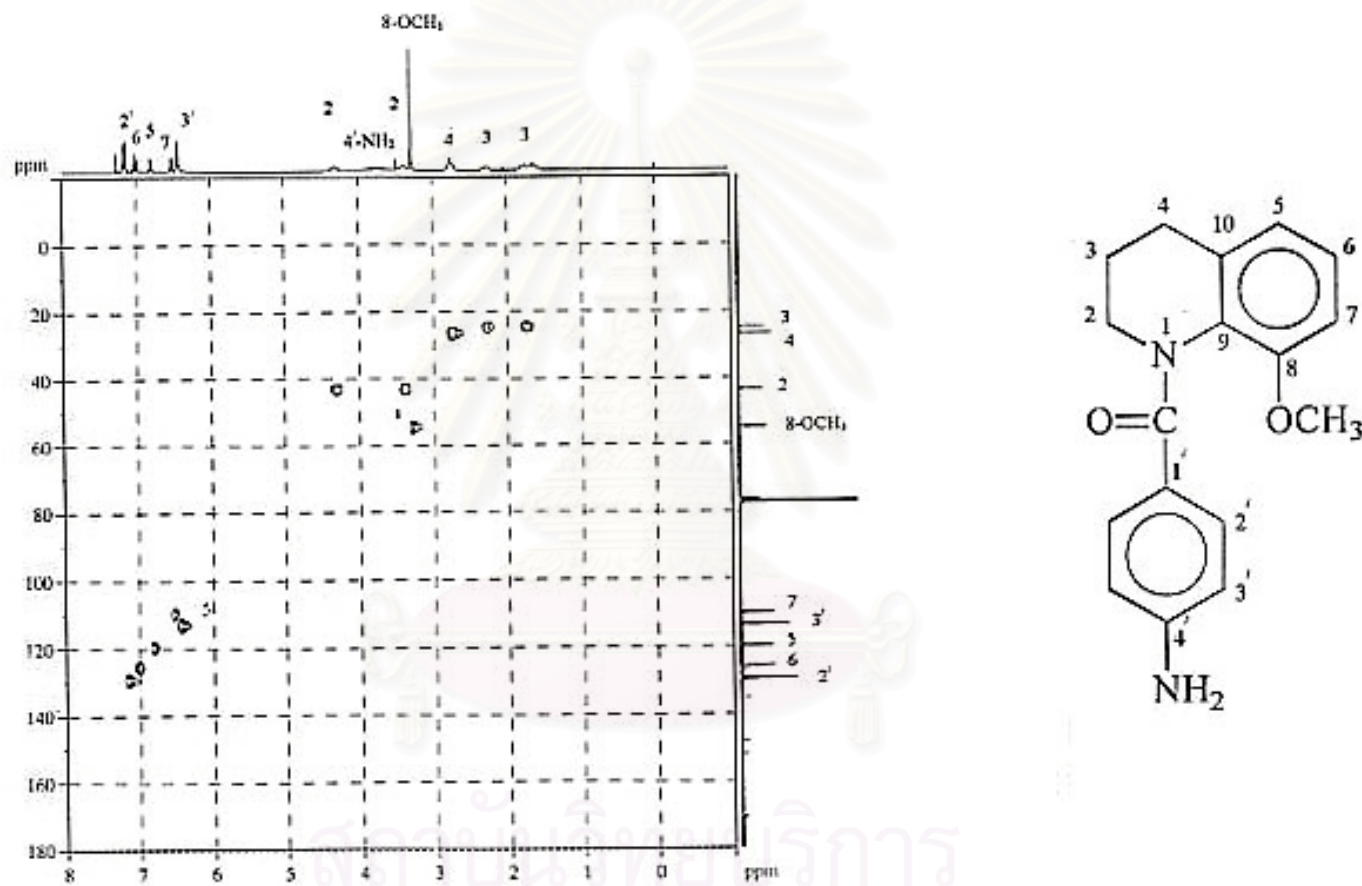
(Enlarged scale)

Figure 167. The 300 MHz HMQC spectrum of N-(*p*-aminobenzoyl)-1,2,3,4-tetrahydro-8-methoxyquinoline (4h, CU-17-16) in CDCl₃.
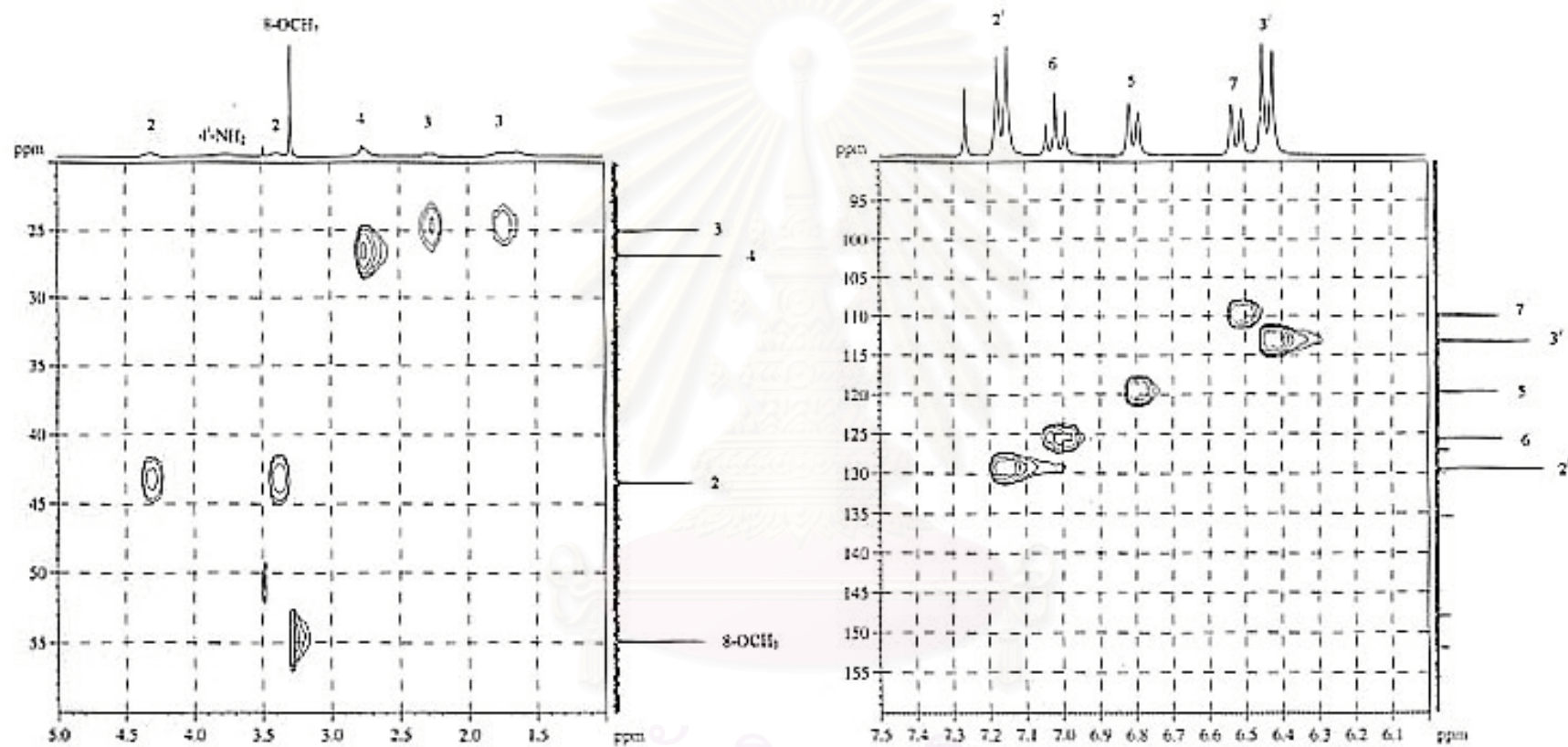
Figure 168. The 300 MHz HMQC spectrum of N-*(p*-aminobenzoyl)-1,2,3,4-tetrahydro-8-methoxyquinoline (4h, CU-17-16) in CDCl$_3$.

(Enlarged scale)
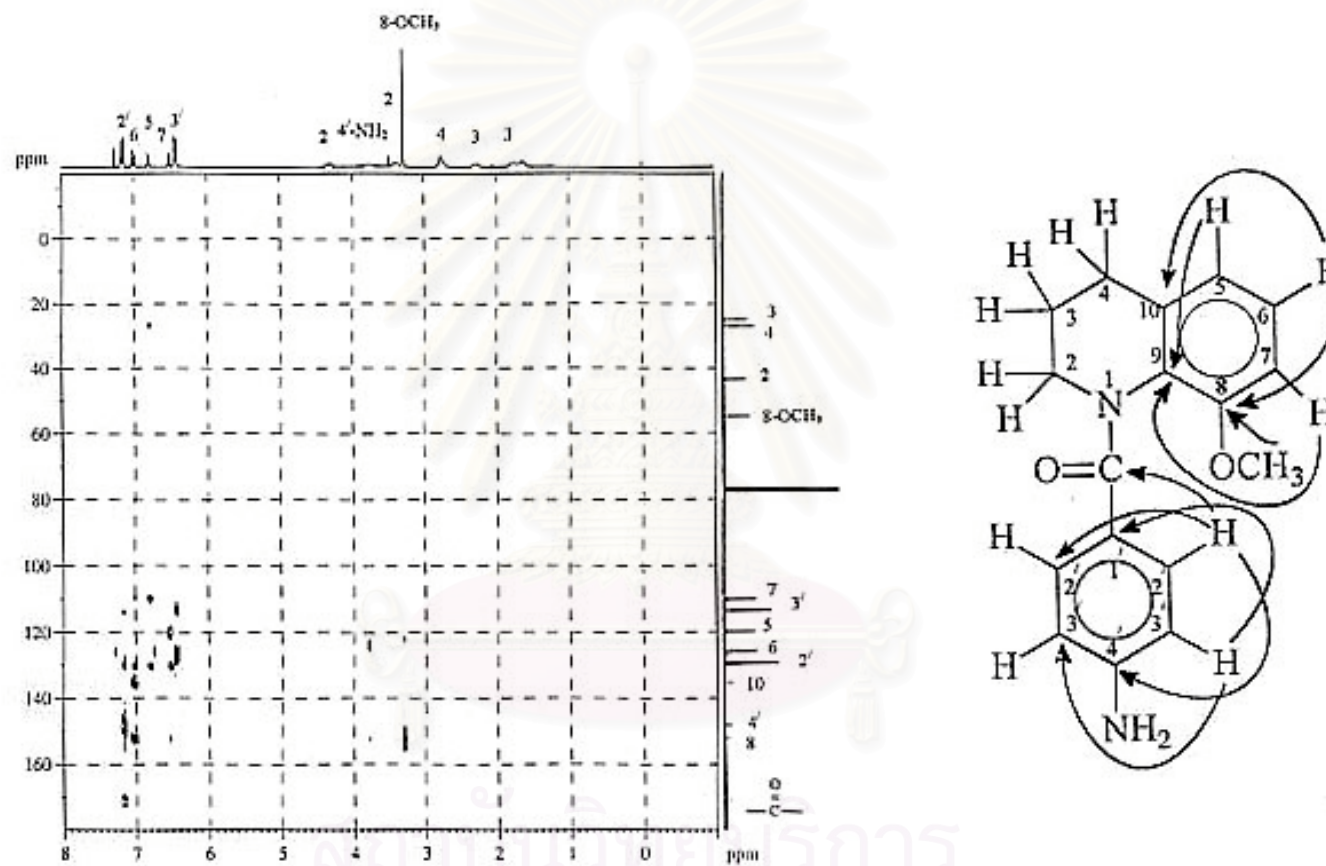
Figure 169. The 300 MHz HMBC spectrum (JHC = 8 Hz) of N-(*p*-aminobenzoyl)-1,2,3,4-tetrahydro-8-methoxyquinoline (4h, CU-17-16) in CDCl₃.
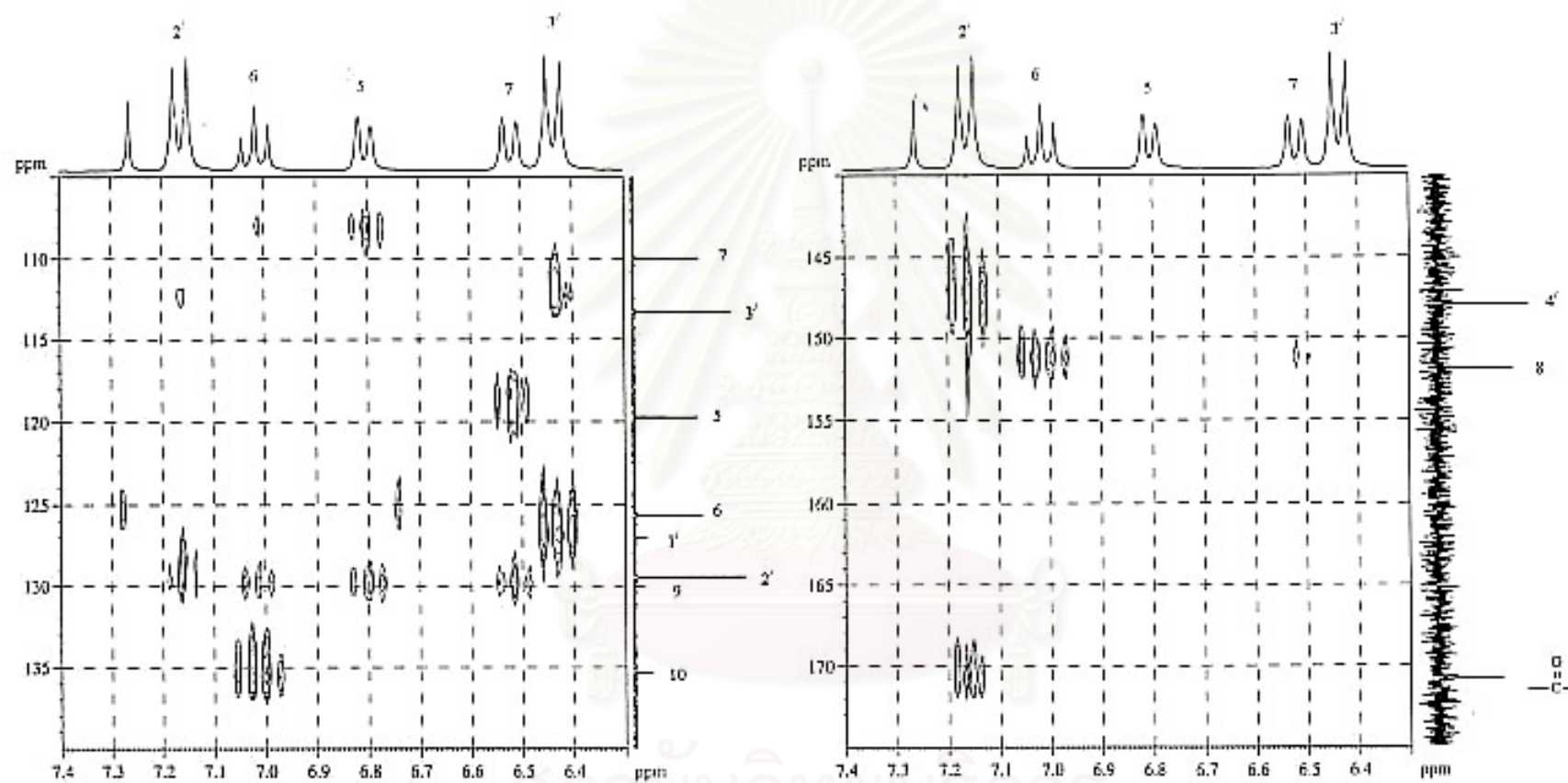
Figure 170. The 300 MHz HMBC spectrum (JHC = 8 Hz) of N-(*p*-aminobenzoyl)-1,2,3,4-tetrahydro-8-methoxyquinoline (4h, CU-17-16) in

CDCl₃. (Expanded: δH 6.3-7.4 ppm; δC 105-175 ppm)

CHAPTER IV

RESULTS AND DISCUSSION

Utilizing ameltolide, a very potent anticonvulsant, as a lead compound, N-(*p*-aminobenzoyl)-1,2,3,4-tetrahydroquinoline (CU-17-02) and seven derivatives (CU-17-04, CU-17-06, CU-17-08, CU-17-10, CU-17-12, CU-17-14 and CU-17-16), substituted at position 2, 4, 6 or/and 8 on 1,2,3,4-tetrahydroquinoline moiety, were designed and synthesized to be rigid analogues of ameltolide (Figure 171).

ameltolide
N-(*p*-aminobenzoyl)-1,2,3,4-tetrahydroquinolines
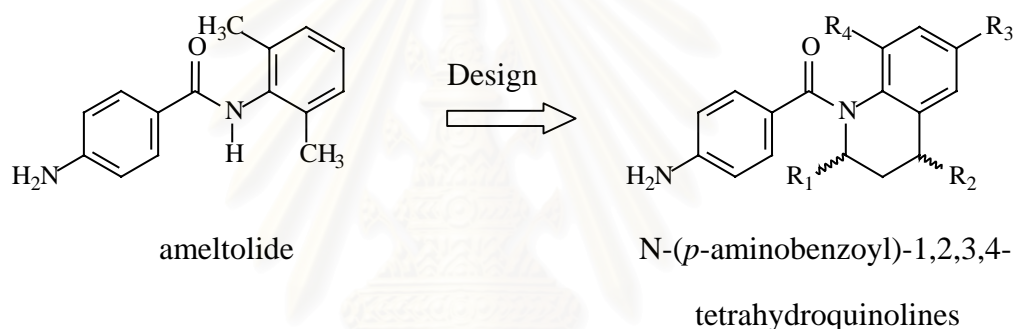
Figure 171. Design of a series of N-(*p*-aminobenzoyl)-1,2,3,4-tetrahydroquinolines

The general synthetic procedures could be outlined in four steps (Figure 7). Prepared by modified Skraup reaction, quinolines were reduced very cleanly to the required 1,2,3,4-tetrahydroquinolines by using sodium borohydride - nickelous chloride system. Then, N-acylation with *p*-nitrobenzoyl chloride followed by catalytic hydrogenation produced the desired products, N-(*p*-aminobenzoyl)-1,2,3,4-tetrahydroquinoline derivatives.

According to the preparative methods described above, the synthesis of compounds CU-17-12, CU-17-14 and CU-17-16 proceeded through the general four steps. Some target compounds (CU-17-04, CU-17-06, CU-17-08 and CU-17-10)

were prepared by the last three steps, i.e. reduction of quinolines followed by N-acylation and catalytic hydrogenation, respectively. The synthesis of CU-17-02 proceeded through only the last two steps, N-acylation and catalytic hydrogenation. The reason for designing synthetic approach depended on available reagents. Synthetic methods of each product were shown in Figure 172.
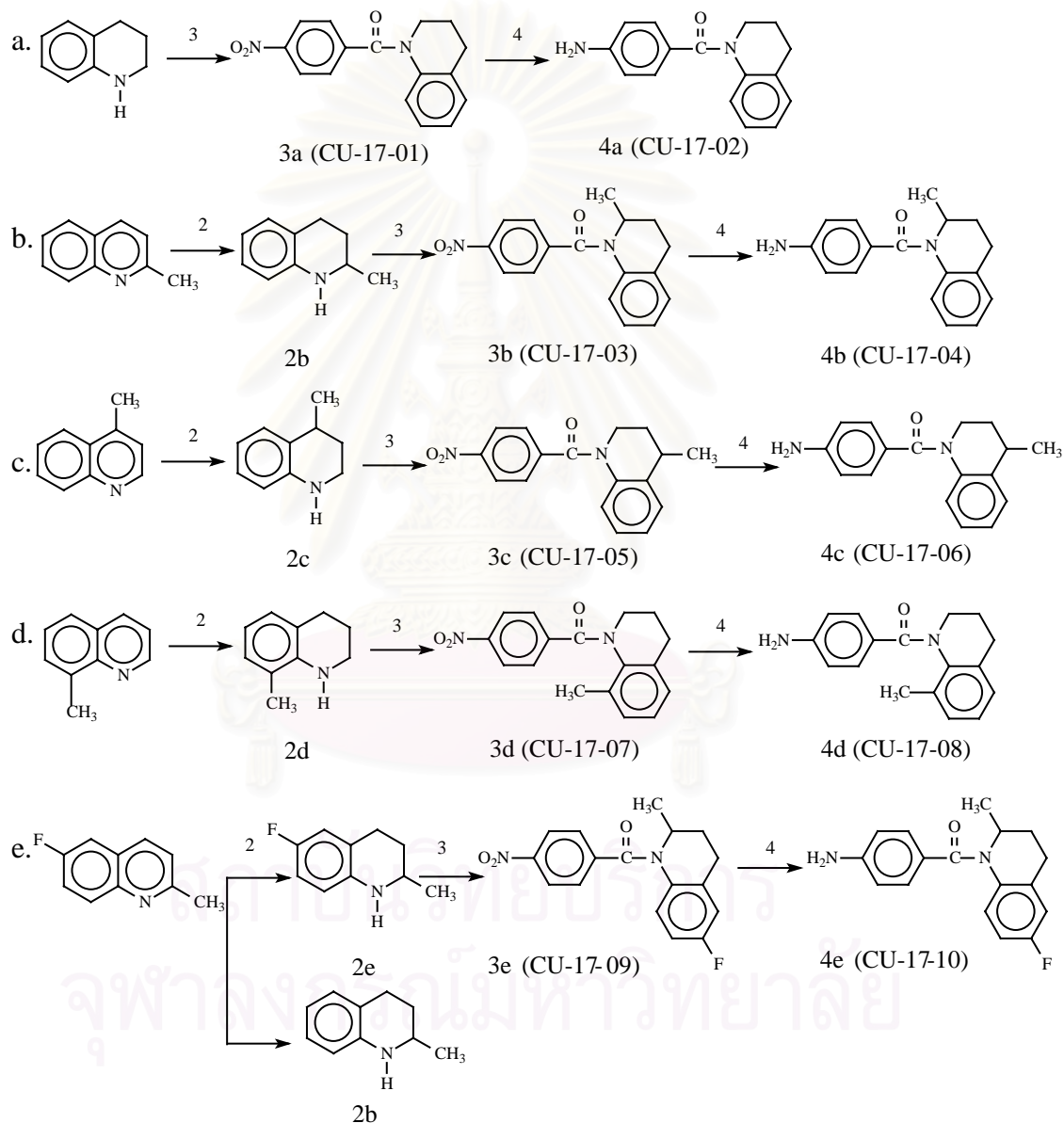
Figure 172. Synthesis routes of the synthesized N-(*p*-aminobenzoyl)-1,2,3,4-tetrahydroquinolines (4a - 4h). 1: conc. HCl, 2,3-dichloro-1,4-napthoquinone, EtOH, reflux; 2: NaBH$_4$, NiCl$_2$.6H$_2$O, MeOH; 3: *p*-nitrobenzoyl chloride, K$_2$CO$_3$, THF, reflux, 70°C; 4: H$_2$, 10% Pd/C, CH$_2$Cl$_2$
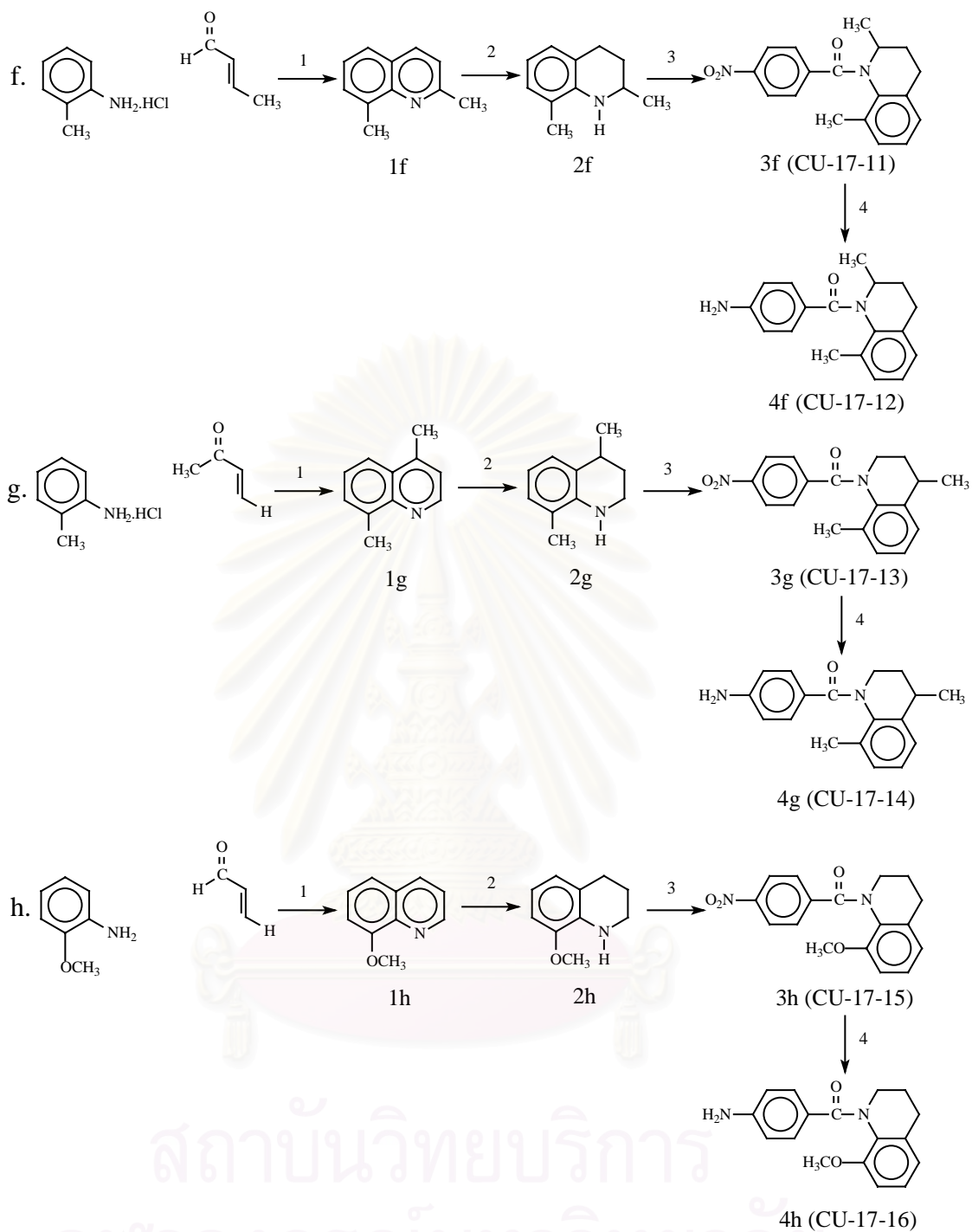
Figure 172. (continued) Synthesis routes of the synthesized N-(*p*-aminobenzoyl)-
1,2,3,4- tetrahydroquinolines (4a - 4h). 1: conc. HCl, 2,3-dichloro-1,4-
napthoquinone, EtOH, reflux; 2: NaBH$_4$, NiCl$_2$.6H$_2$O, MeOH; 3: *p*-
nitrobenzoyl chloride, K$_2$CO$_3$, THF, reflux, 70°C; 4: H$_2$, 10% Pd/C,
CH$_2$Cl$_2$

Quinolines (compounds 1f-1h)

Using the modified Skraup synthesis (Song, 1993), three quinolines (1f, 1g and 1h) were prepared by the reaction between the appropriate anilines and the α,β-unsaturated carbonyl compounds. 2,8-Dimethylquinoline (1f) was synthesized from *o*-toluidine and crotonaldehyde; 4,8-dimethylquinoline (1g) was synthesized from *o*-toluidine and methyl vinyl ketone; 8-methoxyquinoline (1h) was synthesized from *o*-anisidine and acrolein. 2,3-Dichloro-1,4-napthoquinone and absolute ethanol were used as the oxidant and solvent, respectively. The reactions were carried out by refluxing in hydrochloric acid (Figure 173). This method was proved to give a high yield of products. The condition was milder than that of the classical Skraup reaction in which nitro compounds were used as oxidants, or concentrated sulfuric acid was used instead of hydrochloric acid.

In the isolation step, zinc chloride dissolved in THF, was added at the end of the reaction. THF was used to dissolve the reduced quinone, and zinc chloride was used to form complex with quinolines and the excessive anilines. In general, bis-quinolinium tetrachlorozincates is insoluble in aqueous alcohol and crystallizes out, whilst under the same condition, bis-anilinium tetrachlorozincates remains in solution; therefore the zinc chloride complexes of quinolines could be collected by filtration. The quinolines (1f, 1g and 1h) obtained from their corresponding zinc chloride complex by acid-base extraction. Table 14 showed the structures, some physical properties and percent yield of the products.

Table 14. Structures, some physical properties and % yield of the synthesized quinolines (as the $ZnCl_2$ complex)
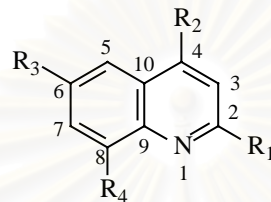
Quinoline.HCl. 1/2 $ZnCl_2$	Substituent				Description	Yield (%)	Quinoline	Description	m.p. (°C)
	R_1	R_2	R_3	R_4					
1f.HCl.1/2 $ZnCl_2$	CH_3	H	H	CH_3	brownish solid	77.6	1f	yellowish liquid	-
1g.HCl.1/2 $ZnCl_2$	H	CH_3	H	CH_3	brownish solid	65.6	1g	white solid	53-55
1h.HCl.1/2 $ZnCl_2$	H	H	H	OCH_3	brownish solid	50.0	1h	yellowish liquid	-

Figure 173. The formation of the synthesized quinolines (as the $ZnCl_2$ complex)

The mechanism of the Skraup reaction is still the subject of controversy. The simplest possible mechanism is shown in Figure 174. In this mechanism, the anilines add to α,β-unsaturated carbonyl compounds in a Michael addition reaction followed by condensation of the carbonyl with the aromatic. Elimination of water gives the dihydroquinoline which must be subsequently oxidized to form the quinoline products.

Figure 174. The proposed reaction mechanism of the synthesis of quinolines by Skraup reaction.

The structures of three quinolines could be distinguished by IR and ^{1}H-NMR spectrometry.

All of them showed the similar IR spectra patterns (1f, Figure 11; 1g, Figure 14; 1h, Figure 17). The most prominent bands occurred in the low frequency range between 845-713 cm^{-1}, resulted from the C-H out-of-plane bending of aromatic ring. For other aromatic parts, the C=C stretching and C=N stretching appeared in the same region of 1617-1426 cm^{-1}, and the aromatic C-H stretching bands occurred between 3074-3011 cm^{-1}. For aliphatic part, the aliphatic C-H stretching absorbed in the 2966-2839 cm^{-1} region.

The 300 MHz ^{1}H-NMR spectra of products showed the characteristic peaks of aromatic groups between 7.07-8.00 ppm (1f, Figure 12-13; 1g, Figure 15-16; 1h, Figure 18-19). The proton chemical shifts and assignment were exhibited in Table 15.

Table 15. The peak assignment for ^{1}H of quinoline derivatives.
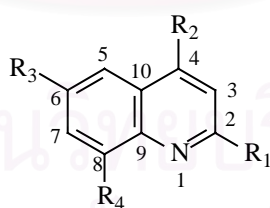
Position	δ ^{1}H (ppm)		
	1f	1g	1h
aliphatic	2.70, 2.83 (6H, 2-CH$_3$ + 8-CH$_3$)	2.62, 2.90 (6H, 4-CH$_3$ + 8-CH$_3$)	4.10 (s, 3H, 8-OCH$_3$)
aromatic	7.20-8.00 (5H)	7.17-8.80 (5H)	7.07-8.98 (6H)

1,2,3,4-Tetrahydroquinolines (compounds 2b-2h)

Seven 1,2,3,4-tetrahydroquinoline derivatives (2b-2h) were synthesized by selective reduction of pyridine ring in quinolines with sodium borohydride in the presence of nickel (II) chloride (Figure 175).
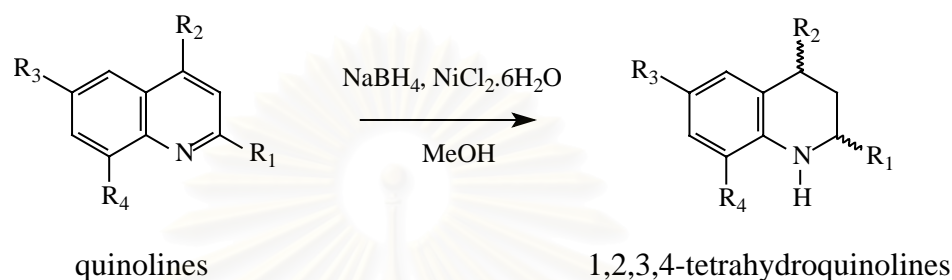
Figure 175. The formation of the synthesized 1,2,3,4-tetrahydroquinolines.

The reduction proceeds via the complex of the quinolines and $NiCl_2$, and then this complex is reduced by $NaBH_4$. Therefore, the order of mixing is essential; reduction does not occur when quinolines are added after $NaBH_4$ to a methanol solution of $NiCl_2$.

Since $NaBH_4$ reacted vigorously with $NiCl_2$, the reaction was kept under cooling until the addition of $NaBH_4$ was completed. To collect the products, the black precipitate occurred in the reaction, was eliminated by filtration, followed by removal of methanol from the reaction mixture. 10% HCl was added in order to decompose the remainder of $NaBH_4$. The acidic solution was then basified by using conc. ammonium hydroxide, then extracted with $CHCl_3$. The excess $NiCl_2$ was removed concurrently with the aqueous part. On the other hand, the products were soluble in the organic part; after solvent was removed, the residual 1,2,3,4-tetrahydroquinolines was pure enough to use without further purification. The structures and some physical properties including percent yield of these products were illustrated in Table 16.

Table 16. Structures, some physical properties and % yield of the synthesized 1,2,3,4-tetrahydroquinolines**.**
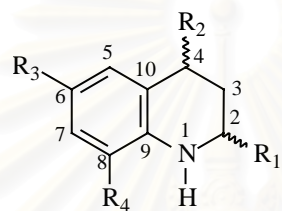
Compounds	Substituent				Description	Yield (%)
	R_1	R_2	R_3	R_4		
2b	CH_3	H	H	H	yellowish liquid	89.4
2c	H	CH_3	H	H	yellowish liquid	89.2
2d	H	H	H	CH_3	yellowish liquid	97.8
2e	CH_3	H	F	H	yellowish liquid	59.1
2f	CH_3	H	H	CH_3	yellowish liquid	89.2
2g	H	CH_3	H	CH_3	yellowish liquid	83.1
2h	H	H	H	OCH_3	yellowish liquid	87.5

All reactions proceeded very smoothly, and each of them produced a high yield of one product except the reduction of 6-fluoro-2-methylquinoline. This reaction gave a moderate yield of the desired product, 1,2,3,4-tetrahydro-6-fluoro-2-methylquinoline (2e), combined with by product, 1,2,3,4-tetrahydro-2-methylquinoline (2b). The side reaction may result from nucleophilic aromatic substitution to form 2-methylquinoline followed by reduction to form 2b.

The structures of these 1,2,3,4-tetrahydroquinolines were confirmed by IR and ^{1}H-NMR spectrometry.

The characteristic bands observed in the spectra of 1,2,3,4-tetrahydroquinoline derivatives were similar (2b, Figure 20; 2c, Figure 23; 2d, Figure 26; 2e, Figure 29; 2f, Figure 32; 2g, Figure 35; 2h, Figure 38). These spectra showed characteristic absorption bands of secondary amine and aromatic ring. The former resulted from N-H stretching in the 3429-3394 cm^{-1} region as a single band, and the latter showed prominent bands of C-H out-of-plane bending between 895-711 cm^{-1}. The other bands presented in the spectra were the aromatic C-H stretching bands at 3069-3010 cm^{-1}, the aromatic C=C stretching bands mixed with the N-H bending bands between 1611-1583 cm^{-1}, and the aliphatic C-H stretching bands in the region of 2998-2835 cm^{-1}.

The 300 MHz ^{1}H-NMR spectra of 1,2,3,4-tetrahydroquinoline derivatives could prove the structure of each product (2b, Figure 21-22; 2c, Figure 24-25; 2d, Figure 27-28; 2e, Figure 30-31; 2f, Figure 33-34; 2g, Figure 36-37; 2h, Figure 39-40). The spectral assignment is summarized in Table 17.

Table 17. The peak assignment for ^{1}H of the synthesized 1,2,3,4-tetrahydroquinoline derivatives.
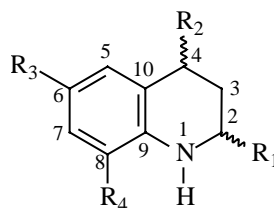
Position	$\delta\ ^1$H (ppm)			
	2b	2c	2d	2e
NH	-	3.64 (s, broad, 1H)	3.45 (s, broad, 1H)	2.60-2.90 (m, 3H, NH + H-4)
2-Me	1.20 (d, J = 6.3 Hz, 3H)	-	-	1.20 (d, J = 6.3 Hz, 3H)
4-Me	-	1.27 (dd, J = 7.0, 2.7 Hz, 3H)	-	-
8-Me	-	-	2.04 (s, 3H)	-
2	3.40 (m, 1H)	3.25 (m, 2H)	3.33 (t, J = 5.4 Hz, 2H)	3.35 (m, 1H)
3	1.60 (m, 1H) 1.90 (m, 1H)	1.65 (m, 1H) 1.95 (m, 1H)	1.91 (m, 2H)	1.57 (m, 1H) 1.92 (m, 1H)
4	2.78 (m, 2H)	2.89 (m, 1H)	2.76 (t, J = 6.3 Hz, 2H)	2.60-2.90 (combined with NH)
aromatic	6.43-7.02 (4H)	6.40-7.07 (4H)	6.49-6.89 (3H)	6.35-6.75 (3H)

Table 17. (continued) The peak assignment for ^{1}H of the synthesized 1,2,3,4-
tetrahydroquinoline derivatives.
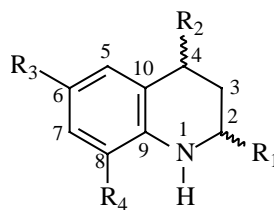
Position	δ ^{1}H (ppm)		
	2f	2g	2h
NH	3.35-3.50 (m, 2H, NH +H-2)	-	-
2-Me	1.25 (d, J = 6.2 Hz, 2H)	-	-
4-Me	-	1.29 (d, J = 7.1 Hz, 3H)	-
8-Me	2.08 (s, 3H)	2.08 (s, 3H)	-
8-OMe	-	-	3.84 (s, 3H)
2	3.35-3.50 (combined with NH)	3.37 (m, 2H)	3.33 (dd, J = 5.5, 5.4 Hz, 2H)
3	1.58 (m, 1H) 1.92 (m, 1H)	1.70 (m, 1H) 1.98 (m, 1H)	1.95 (m, 2H)
4	2.80 (m, 2H)	2.94 (m, 1H)	2.77 (t, J = 6.4 Hz, 2H)
aromatic	6.54 (t, J = 7.4 Hz, 1H, H-6) 6.80-6.92 (2H, H-5 + H-7)	6.58 (dd, J = 7.4, 7.5 Hz, 1H, H-6) 6.85-7.00 (2H, H-5 + H-7)	6.52-6.68 (m, 3H)

N-(*p*-Nitrobenzoyl)-1,2,3,4-tetrahydroquinolines (compounds CU-17-01, CU-17-03, CU-17-05, CU-17-07, CU-17-09, CU-17-11, CU-17-13, CU-17-15).

A series of N-(*p*-nitrobenzoyl)-1,2,3,4-tetrahydroquinolines were prepared from *p*-nitrobenzoyl chloride and the appropriate 1,2,3,4-tetrahydroquinolines under refluxing in the presence of potassium carbonate (Figure 176).

p-Nitrobenzoyl chloride is a reactive acylating reagent because of the inductive effect of the chloride group which substitutes on the carbonyl group. In addition, the tetrahedral intermediate can expel such relatively good leaving group.

Added in the reaction, potassium carbonate served two proposes. It neutralized hydrochloric acid generated in the reaction and prevented the development of high acid concentrations.
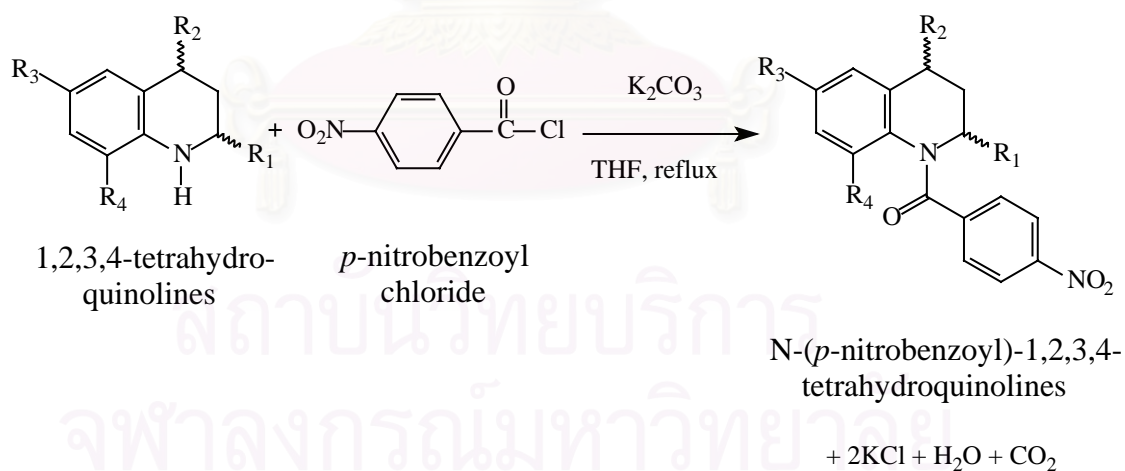
Figure 176. The formation of the synthesized N-(*p*-nitrobenzoyl)-1,2,3,4-tetrahydroquinolines.

The general mechanisms are well known. 1,2,3,4-Tetrahydroquinolines, the nucleophilic species, undergo addition at the carbonyl group, followed by elimination of chloride group. The reactions proceed through the tetrahedral intermediate (Figure 177).
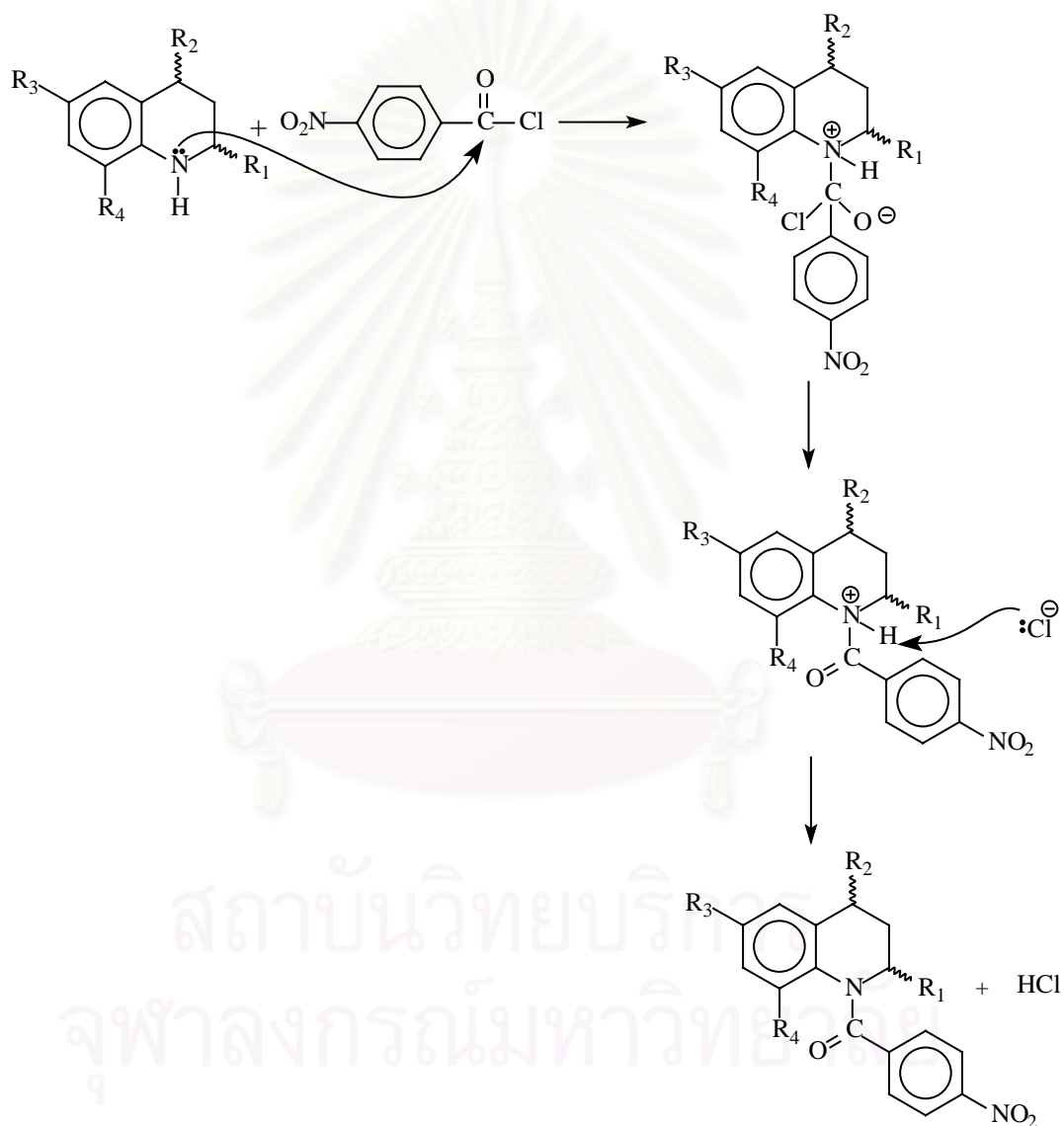
Figure 177. The reaction mechanism of the synthesis of N-(*p*-nitrobenzoyl)-1,2,3,4-tetrahydroquinoline derivatives.

The purity and the structures of N-(*p*-nitrobenzoyl)-1,2,3,4-tetrahydroquinolines were proven by the results of some physical properties and spectroscopic data. Table 18 showed the structures and some physical properties including percent yield of these products. All of them are yellowish solid with a narrow range of melting point. The component of carbon, hydrogen and nitrogen in each molecule, detected by elemental analyses, were within $\pm$ 0.4 % of the corresponding calculated percentage.

The results of spectroscopic data were obtained from IR, ^{1}H-NMR and ^{13}C-NMR decoupled techniques.

Similar IR absorption patterns were observed in a series of N-(*p*-nitrobenzoyl)-1,2,3,4-tetrahydroquinolines (CU-17-01, Figure 41; CU-17-03, Figure 46; CU-17-05, Figure 51; CU-17-07, Figure 56; CU-17-09, Figure 61; CU-17-11, Figure 66; CU-17-13, Figure 71; CU-17-15, Figure 76). The absorption bands of amide, nitro and aromatic groups were presented as characteristic parts.

Tertiary amide had a strong band of C=O stretching in the region of 1649-1639 cm^{-1} occurring at lower frequencies than "normal" carbonyl absorption due to the resonance effect. Each asymmetrical and symmetrical stretching of NO$_2$ group displayed a strong band in the 1525-1517 cm^{-1} and 1348-1342 cm^{-1} region, respectively. The C-N stretching band of *p*-nitrophenyl part was incorporated with the eminent bands of aromatic C-H out-of-plane bending in the region between 871-706 cm^{-1}. Other bands, presented in the spectra, were assigned as followed. The aromatic C-H stretching bands occurred in the 3113-3026 cm^{-1} region. The aliphatic C-H stretching absorbed in the 2983-2481 cm^{-1} region. The bands between 1605-1599 cm^{-1} exhibited the aromatic C=C stretching vibration, and the bands in the

region of 1493-1380 cm^{-1} represented aliphatic C-H bending combined with aromatic C=C stretching vibration.

The 300 MHz ^{1}H-NMR and ^{13}C-NMR decoupled spectra were used to prove the structure of each nitro compound (CU-17-01, Figure 42-44; CU-17-03, Figure 47-49; CU-17-05, Figure 52-54; CU-17-07, Figure 57-59; CU-17-09, Figure 62-64; CU-17-11, Figure 67-69; CU-17-13, Figure 72-74; CU-17-15, Figure 77-79).

The results from these spectra indicated that substitution of methyl group on 1,2,3,4-tetrahydroquinoline ring at position 2,4 or/and 8 did effect the conformation of synthesized products. This effect can be illustrated by ^{1}H-NMR and ^{13}C-NMR spectra of compounds CU-17-07, CU-17-11 and CU-17-13 that exhibited many small peculiar signals excluding the expected signals. These phenomena explained different conformers existing in the solution due to rotation around the (C=O)-N, C(aromatic)-(C=O) bonds, and also inversion of the piperiding ring. However, in other compounds (CU-17-01, CU-17-03, CU-17-05, CU-17-09, and CU-17-15), these phenomena were not observed.

The interpretation of ^{1}H and ^{13}C, shown in table 19-26, were clarified by using ^{1}H-NMR and ^{13}C-NMR assignment of their corresponding amino target compounds, discussed later, as models. For CU-17-07, CU-17-11 and CU-17-13, only major conformers were assigned.

Table 18. Structures, some physical properties and % yield of the synthesized N-(*p*-nitrobenzoyl)-1,2,3,4-tetrahydroquinolines

Compounds	Substituent				Description	m.p. (°C)	Yield (%)	Formula	CHN Analysis
	R_1	R_2	R_3	R_4					
CU-17-01	H	H	H	H	yellowish solid	99-100	88.2	$C_{16}H_{14}N_2O_3$	Calcd. C:68.075;H:4.998;N:9.923 Found. C:68.062;H:5.102;N:9.933
CU-17-03	CH_3	H	H	H	yellowish solid	140-141	79.0	$C_{17}H_{16}N_2O_3$	Calcd. C:68.906;H:5.442;N:9.454 Found. C:68.925;H:5.500:N:9.505
CU-17-05	H	CH_3	H	H	yellowish solid	132-134	82.9	$C_{17}H_{16}N_2O_3$	Calcd. C:68.906;H:5.442;N:9.454 Found. C:69.047;H:5.414;N:9.446
CU-17-07	H	H	H	CH_3	yellowish solid	113-114	77.0	$C_{17}H_{16}N_2O_3$	Calcd. C:68.906;H:5.442;N:9.454 Found. C:68.979;H:5.406;N:9.496
CU-17-09	CH_3	H	F	H	yellowish solid	139-140	85.6	$C_{17}H_{15}N_2O_3F$	Calcd. C:64.962;H:4.810;N:8.912 Found. C:64.994;H:4.784;N:8.929
CU-17-11	CH_3	H	H	CH_3	yellowish solid	134-135	76.2	$C_{18}H_{18}N_2O_3$	Calcd. C:69.662;H:5.846;N:9.026 Found. C:69.723;H:5.831;N:9.037
CU-17-13	H	CH_3	H	CH_3	yellowish solid	141-142	83.1	$C_{18}H_{18}N_2O_3$	Calcd. C:69.662;H:5.846;N:9.026 Found. C:69.702;H:5.576;N:9.010
CU-17-15	H	H	H	OCH_3	yellowish solid	156-157	79.2	$C_{17}H_{16}N_2O_4$	Calcd. C:65.376;H:5.163;N:8.969 Found. C:65.460;H:5.128;N:8.979

Table 19. The peak assignment for ^{1}H and ^{13}C of N-(*p*-nitrobenzoyl)-1,2,3,4-
tetrahydroquinoline (CU-17-01).
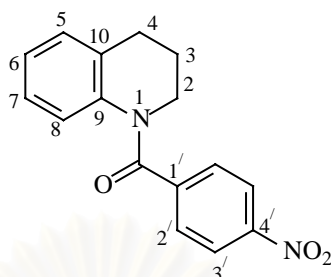
Position	δ ^{13}C (ppm)	δ ^{1}H (ppm)
2	44.33	3.93 (t, J = 6.6 Hz, 2H)
3	24.00	2.09 (m, 2H)
4	26.88	2.86 (dd, J = 6.6, 6.5 Hz, 2H)
5	123.31-148.45 (aromatic C)	7.18 (d, J = 7.4 Hz, 1H)
6		7.04 (dd, J = 7.2, 7.3 Hz, 1H)
7		6.86 (t, J = 7.5 Hz, 1H)
8		6.57 (d, J = 5.9 Hz, 1H)
9		-
10		-
1$^/$		-
2$^/$		7.48 (d, J = 8.7 Hz, 2H)
3$^/$		8.11 (d, J = 8.6 Hz, 2H)
4$^/$		-
C = 0	167.72	-

Table 20. The peak assignment for ^{1}H and ^{13}C of N-(*p*-nitrobenzoyl)-1,2,3,4-tetrahydro-2-methylquinoline (CU-17-03).
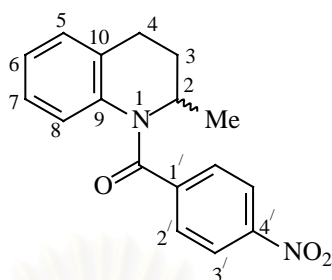
Position	δ [13]C (ppm)	δ [1]H (ppm)
2-Me	19.82	1.27 (d, J = 6.5 Hz, 3H)
2	49.81	4.86 (m, 1H)
3	32.28	1.52 (m, 1H)
		2.49 (m, 1H)
4	25.84	2.77 (m, 2H)
5	123.15-148.28 (aromatic C)	7.20 (d, J = 7.4 Hz, 1H)
6		7.06 (dd, J = 7.4, 7.5 Hz, 1H)
7		6.86 (dd, J = 7.5, 7.6 Hz, 1H)
8		6.48 (d, J = 6.2 Hz, 1H)
9		-
10		-
1$^{/}$		-
2$^{/}$		7.40 (d, J = 8.6 Hz, 2H)
3$^{/}$		8.07 (d, J = 8.6 Hz, 2H)
4$^{/}$		-
C = 0	167.30	-

Table 21. The peak assignment for ^{1}H and ^{13}C of N-(p-nitrobenzoyl)-1,2,3,4-
tetrahydro-4-methylquinoline (CU-17-05).
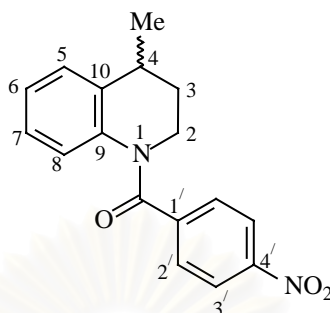
Position	δ ^{13}C (ppm)	δ ^{1}H (ppm)
4-Me	19.45	1.44 (d, J = 6.9 Hz, 3H)
2	43.23	3.87 (m, 1H)
		4.03 (m, 1H)
3	32.07	1.70 (m, 1H)
		2.25 (m, 1H)
4	30.98	2.98 (m, 1H)
5	123.32-148.36 (aromatic C)	7.27 (d, J = 7.5 Hz, 1H)
6		7.09 (dd, J = 7.5, 7.7 Hz, 1H)
7		6.86 (dd, J = 7.5, 7.6 Hz, 1H)
8		6.54 (s, broad, 1H)
9		-
10		-
1$^/$		-
2$^/$		7.48 (d, J = 8.6 Hz, 2H)
3$^/$		8.11 (d, J = 8.6 Hz, 2H)
4$^/$		-
C = 0	167.64	-

Table 22. The peak assignment for ^{1}H and ^{13}C of N-(*p*-nitrobenzoyl)-1,2,3,4-
tetrahydro-8-methylquinoline (CU-17-07).

.
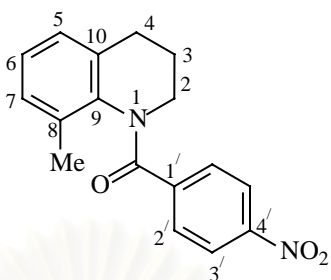
Position	δ ^{13}C (ppm)	δ ^{1}H (ppm)
8-Me	18.51-48.25 (aliphatic C)	1.72 (s, 3H)
2		3.22 (m, 1H)
		4.75 (m, 1H)
3		1.79 (m, 1H)
		2.42 (m, 1H)
4		2.80 (m, 2H)
5	123.05-148.64 (aromatic C)	7.02-7.18 (m, 2H, H-5 + H-6)
6		
7		6.83 (d, J = 6.8 Hz, 1H)
8		-
9		-
10		-
1$^/$		-
2$^/$		7.37 (d, J = 8.6 Hz, 2H)
3$^/$		8.00 (d, J = 8.6 Hz, 2H)
4$^/$		-
C = O	167.42	-

Table 23. The peak assignment for ^{1}H and ^{13}C of N-(*p*-nitrobenzoyl)-1,2,3,4-
tetrahydro-6-fluoro-2-methylquinoline (CU-17-09).
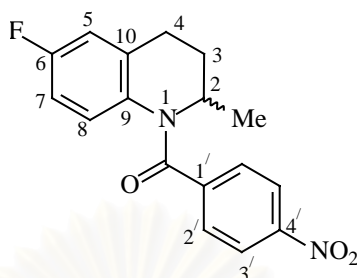
Position	δ ^{13}C (ppm)	δ ^{1}H (ppm)
2-Me	19.65	1.25 (d, J = 6.4 Hz, 3H)
2	49.74	4.83 (broad, 1H)
3	31.85	1.52 (m, 1H)
		2.48 (m, 1H)
4	25.95	2.76 (m, 2H)
5	113.06-161.88 (aromatic C)	6.93 (dd, J = 8.4, 2.2 Hz, 1H)
6		-
7		6.59 (dd, J = 6.6, 7.7 Hz, 1H)
8		6.49 (s, broad, 1H)
9		-
10		-
1$^/$		-
2$^/$		7.41 (d, J = 8.4 Hz, 2H)
3$^/$		8.11 (d, J = 8.5 Hz, 2H)
4$^/$		-
C = 0	167.18	-

Table 24. The peak assignment for ^{1}H and ^{13}C of N-(*p*-nitrobenzoyl)-1,2,3,4-tetrahydro-2,8-dimethylquinoline (CU-17-11).
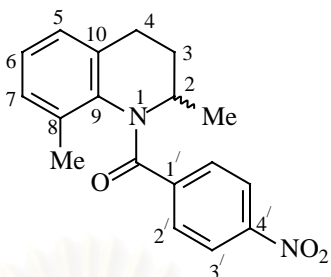
Position	δ [13]C (ppm)	δ [1]H (ppm)
2-Me	20.93	1.21 (d, J = 6.5 Hz, 3H)
8-Me	17.61	1.74 (s, 3H)
2	50.32	5.00 (m, 1H)
3	33.79	1.23 (m, 1H) 2.64 (m, 3H, H-3 + H-4)
4	27.52	2.64 (combined with one proton of H-3)
5	122.55-148.34 (aromatic C)	7.04-7.19 (m, 2H, H-5 + H-6)
6		
7		6.82 (1H)
8		-
9		-
10		-
1′		-
2′		7.34 (d, J = 8.7 Hz, 2H)
3′		7.98 (d, J = 8.7 Hz, 2H)
4′		-
C = O	166.76	-

Table 25. The peak assignment for ^{1}H and ^{13}C of N-(*p*-nitrobenzoyl)-1,2,3,4-
tetrahydro-4,8-dimethylquinoline (CU-17-13).
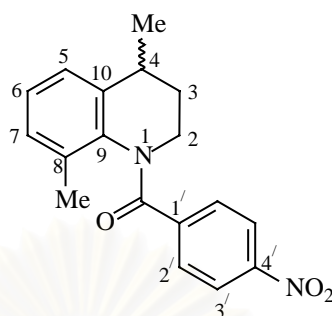
Position	δ ^{13}C (ppm)	δ ^{1}H (ppm)
4-Me	17.02-42.43 (aliphatic C)	1.45 (d, J = 6.8 Hz, 3H)
8-Me		1.75 (s, 3H)
2		3.24 (m, 1H)
		4.74 (m, 1H)
3		2.07 (m, 1H)
		2.39 (m, 1H)
4		2.84 (m, 1H)
5	121.75-148.40 (aromatic C)	7.10-7.23 (m, 2H, H-5 + H-6)
6		
7		6.85 (d, J = 6.8 Hz, 1H)
8		-
9		-
10		-
1$^/$		-
2$^/$		7.35 (d, J = 8.7 Hz, 2H)
3$^/$		7.99 (d, J = 8.5 Hz, 2H)
4$^/$		-
C = 0	167.15	-

Table 26. The peak assignment for ^{1}H and ^{13}C of N-(*p*-nitrobenzoyl)-1,2,3,4-
tetrahydro-8-methoxyquinoline (CU-17-15).
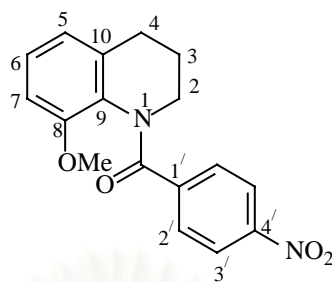
Position	$\delta\ ^{13}$C (ppm)	$\delta\ ^1$H (ppm)
8-OMe	54.40	3.24 (s, 3H)
2	43.19	3.36 (m, 1H)
		4.47 (m, 1H)
3	24.55	1.80 (m, 1H)
		2.36 (m, 1H)
4	26.85	2.79 (m, 2H)
5	109.77-151.20 (aromatic C)	6.85 (d, J = 7.5 Hz, 1H)
6		7.06 (dd, J = 8.0, 7.9 Hz, 1H)
7		6.46 (d, J = 8.2 Hz, 1H)
8		-
9		-
10		-
1$^/$		-
2$^/$		7.44 (d, J = 8.6 Hz, 2H)
3$^/$		8.03 (d, J = 8.7 Hz, 2H)
4$^/$		-
C = O	168.42	-

Electron impact mass spectra of N-(*p*-nitrobenzoyl)-1,2,3,4-tetrahydro-quinolines (CU-17-01, figure 45; CU-17-03, figure 50; CU-17-05, figure 55; CU-17-07, figure 60; CU-17-09, figure 65; CU-17-11, figure 70; CU-17-13, figure 75) presented similar principal peaks at m/z M$^+$, 150, 104 and 76. All spectra showed a strong molecular ion peak (M$^+$). Cleavage of amide bond gave a prominent peak of a resonance-stabilized *p*-nitrobenzoyl ion (m/z 150). Then, elimination of NO$_2$ radical and CO accounted for other intense peak at m/z 104 and 76, respectively. Cleavage of amide bond also gave a moderate or weak peak of 1,2,3,4-tetrahydroquinolines ion (m/z M-150). This fragmentation pattern was illustrated in Figure 178.

In the case of methyl substituted compounds, (CU-17-03, CU-17-05, CU-17-07, CU-17-09, CU-17-11, and CU-17-13), moderate or weak peaks at M-CH$_3$ (M-15) were also detected.
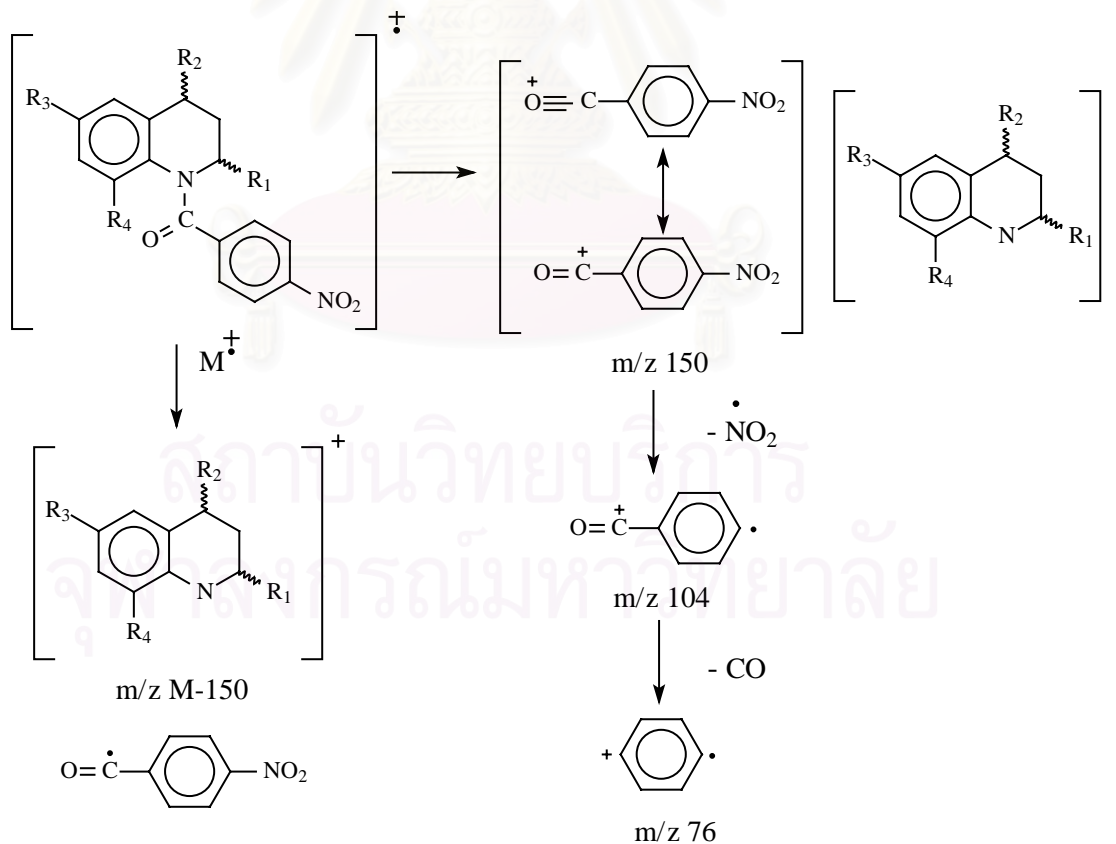
Figure 178. The mass fragmentation pattern of the synthesized N-(*p*-nitrobenzoyl)-1,2,3,4-tetrahydroquinoline derivatives.

N-(*p*-Aminobenzoyl)-1,2,3,4-tetrahydroquinolines (compounds CU-17-02, CU-17-04, CU-17-06, CU-17-08, CU-17-10, CU-17-12, CU-17-14 and CU-17-16)

Eight final products in a series of N-(*p*-aminobenzoyl)-1,2,3,4-tetrahydroquinoline derivatives were synthesized by catalytic hydrogenation of their nitro intermediates to amines; 10 % palladium on activated charcoal (10 % Pd/C) was added as a catalyst (Figure 179). The reaction proceeded rapidly and cleanly, giving a high yield of products.

N-(*p*-nitrobenzoyl)-1,2,3,4-
tetrahydroquinolines

N-(*p*-aminobenzoyl)-1,2,3,4-
tetrahydroquinolines
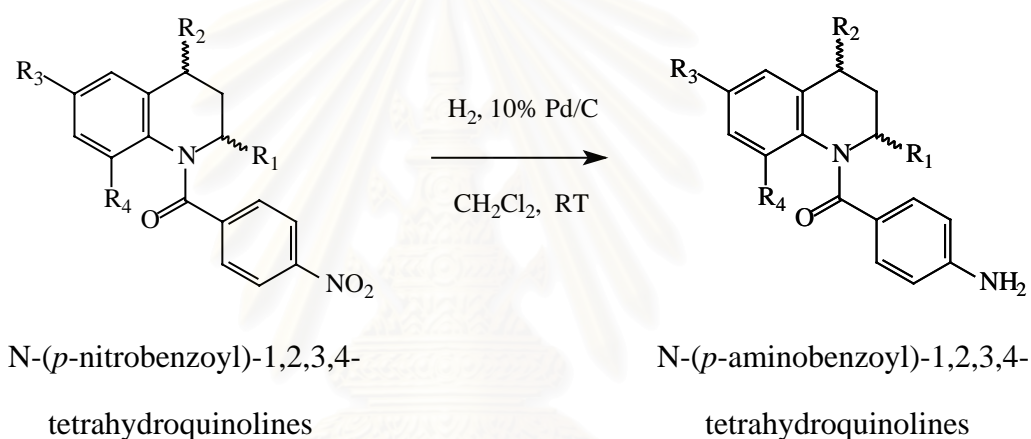
Figure 179. The formation of the synthesized N-(*p*-aminobenzoyl)-1,2,3,4-
tetrahydroquinolines.

The mechanism of reaction is proposed as followed. First, a reactant molecule, an aromatic nitro compound, is adsorbed on the catalyst surface. Next, the adsorption is thought to be followed by the simultaneous transfer of two or more hydrogen atoms from the catalyst to the adsorbed molecule and subsequent desorption of the reduced molecule, an aromatic amine (House, 1972).

The purity and chemical structures of these target compounds were confirmed by the results of some physical properties and spectroscopic data. All of them are

white solid, having a sharp melting point. Their molecular formulas were proven by the elemental analyses. The component of carbon, hydrogen and nitrogen in each molecule was within ± 0.4 % of each corresponding calculated percentage. The structures and some physical properties including percent yield of products were listed in table 27.

The spectroscopic data obtained from IR, NMR and mass spectrometry.

In general, The IR spectrum of N-(*p*-aminobenzoyl)-1,2,3,4-tetrahydroquinoline derivatives had similar absorption patterns (CU-17-02, Figure 80; CU-17-04, Figure 93; CU-17-06, Figure 106; CU-17-08, Figure 119; CU-17-10, Figure 126; CU-17-12, Figure 140; CU-17-14, Figure 153; CU-17-16, Figure 160). The amine, amide and aromatic groups were detected as major bands in all spectra. Primary amines displayed two absorption bands: one in the 3469-3437 cm^{-1} region and the other in the 3355-3331 cm^{-1} region. These bands represent, respectively, the "free" asymmetrical and symmetrical N-H stretching modes. One band at 3227-3210 cm^{-1} arose from the overtone of the N-H bending band intensified by Fermi resonance. The strong bands in the region of 1637-1589 cm^{-1} showed the C=O stretching vibration of the amide group combined with the N-H bending vibration of the primary amino group and the aromatic C=C stretching vibration. For aromatic part, the characteristic C-H out-of-plane bending bands appeared at 842-707 cm^{-1}, and the aromatic C-H stretching bands appeared at 3084-3011 cm^{-1}. The bands between 2982-2832 cm^{-1} represented the aliphatic C-H stretching vibration.

NMR spectra from several NMR experiments were also used to prove the structure of each amino compound (CU-17-02, Figure 81-91; CU-17-04, Figure 94-104; CU-17-06, Figure 107-117; CU-17-08, Figure 120-124; CU-17-10, Figure 127-

138; CU-17-12, Figure 141-151; CU-17-14, Figure 154-158; CU-17-16, Figure 161-170).

The ^{1}H-NMR spectra indicated that substitution of methyl group on 1,2,3,4-tetrahydroquinoline ring at position 2,4 or/and 8 also did effect the conformation of products similar to the phenomena observed in their corresponding nitro compounds. Only ^{1}H-NMR spectra of CU-17-08, CU-17-12 and CU-17-14 showed many small signals excluding the expected signals because of different conformers existing in the solution. However, unlike ^{1}H-NMR spectra of CU-17-12, isolated sharp signals of CU-17-08 and CU-17-14 could not be detected at room temperature; in this condition, they showed several broad signals that could be change to several isolated sharp signals at low temperature. These observations indicated rapid inversion of their existed conformers in solution at room temperature.

The peak assignment for ^{1}H and ^{13}C decoupled spectra were accomplished by supporting of DEPT 135, HH COSY, HMQC and HMBC spectra. In the case of CU-17-08, CU-17-12 and CU-17-14, only major conformers were assigned. In addition, for CU-17-08 and CU-17-14, only ^{1}H-NMR spectra were performed, and their proton assignment used ^{1}H-NMR spectra of other amino compounds as models. (Table 28-35)

By the 75 MHz DEPT 135 (Distortionless Enhancement by Polarization Transfer) procedure, CH_2 peaks were identified as negative, but CH and CH_3 peaks were identified as positive. In this technique, quaternary carbon atoms gave no signals.

By the 300 MHz HH COSY (Correlated Spectroscopy: HH coupling) procedure, the ^{1}H-^{1}H connectivity could be determined.

The 300 MHz HMQC (Heteronuclear Multiple Quantum Correlation Spectroscopy) spectrum correlated the peaks between ^{1}H spectrum and the peak of ^{13}C spectrum attached together. Since the quaternary carbon atoms are not attached with protons, their peaks could not be assigned by this technique.

Almost complete carbon assignment were achieved by the analysis of the HMBC (^{1}H-detected Heteronuclear Multiple Bond Connectivity) technique ($J_{HC} = 8$ Hz) that provided the correlation between ^{1}H and ^{13}C through long-range coupling. The correlation via 3 bonds was detected as prominent signals while correlation via 2 bonds was detected as moderate or weak signals; correlation signals via 4 bonds were sometime detected.

According to electron impact mass fragmentation of N-(*p*-aminobenzoyl)-1,2,3,4-tetrahydroquinoline derivatives (CU-17-02, Figure 92; CU-17-04, Figure 105; CU-17-06, Figure 118; CU-17-08, Figure 125; CU-17-10, Figure 139; CU-17-12, Figure 152; CU-17-14, Figure 159), the dominant modes of their cleavage were similar (Figure 180). The molecular ion peak (M$^+$) was discernible. Primary cleavage at amide bond gave the base peak of a resonance-stabilized *p*-aminobenzoyl cation (m/z 120) that in turn underwent cleavage to an aniline cation (m/z 92). Loss of a neutral molecule of HCN gave a moderate peak at m/z 65.

Table 27. Structures, some physical properties and % yield of the synthesized N-(*p*-aminobenzoyl)-1,2,3,4-tetrahydroquinolines

Compounds	Substituent				Description	m.p. (°C)	Yield (%)	Formula	CHN Analysis
	R_1	R_2	R_3	R_4					
CU-17-02	H	H	H	H	white solid	211-212	87.4	$C_{16}H_{16}N_2O$	Calcd. C:76.165;H:6.391;N:11.103 Found. C:76.150;H:6.312;N:11.040
CU-17-04	CH_3	H	H	H	white solid	214-216	73.6	$C_{17}H_{18}N_2O$	Calcd. C:76.663;H:6.812;N:10.518 Found. C:76.560;H:6.806:N:10.445
CU-17-06	H	CH_3	H	H	white solid	192-193	70.0	$C_{17}H_{18}N_2O$	Calcd. C:76.663;H:6.812;N:10.518 Found. C:76.299;H:6.913;N:10.488
CU-17-08	H	H	H	CH_3	white solid	172-173	71.9	$C_{17}H_{18}N_2O$	Calcd. C:76.663;H:6.812;N:10.518 Found. C:76.640;H:6.796;N:10.541
CU-17-10	CH_3	H	F	H	white solid	210-211	70.6	$C_{17}H_{17}N_2OF$	Calcd. C:71.813;H:6.026;N:9.852 Found. C:71.833;H:6.027;N:9.847
CU-17-12	CH_3	H	H	CH_3	white solid	184-185	67.8	$C_{18}H_{20}N_2O$	Calcd. C:77.112;H:7.190;N:9.992 Found. C:77.119;H:7.019;N:9.967
CU-17-14	H	CH_3	H	CH_3	white solid	170-171	72.9	$C_{18}H_{20}N_2O$	Calcd. C:77.112;H:7.190;N:9.992 Found. C:77.185;H:7.221;N:9.999
CU-17-16	H	H	H	OCH_3	white solid	199-200	79.0	$C_{17}H_{18}N_2O_2$	Calcd. C:72.319;H:6.426;N:9.922 Found. C:72.313;H:6.528;N:9.921

Table 28. The peak assignment for ^1H and ^{13}C of N-(*p*-aminobenzoyl)-1,2,3,4-
tetrahydroquinoline (CU-17-02), and long-range correlation between
carbons and protons.
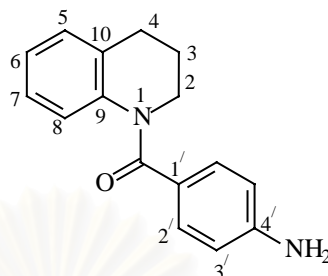
Position	δ ^{13}C (ppm)	δ ^{1}H (ppm)	Long-range correlation from ^{13}C to ^{1}H in HMBC spectrum
$4'$ – NH$_2$	-	3.88 (4H, $4'$-NH$_2$ + H-2)	-
1	-	-	-
2	44.44	3.88 (combined with $4'$-NH$_2$)	H-3, H-4
3	24.25	2.03 (m, 2H)	H-2, H-4
4	26.99	2.82 (t, J = 6.6 Hz, 2H)	H-2, H-3
5	128.22	7.13 (d, J = 7.4 Hz, 1H)	H-4, H-7
6	124.01	6.97 (dd, J = 7.3, 7.2 Hz, 1H)	H-8
7	125.35	6.88 (dd, J = 7.3, 7.8 Hz, 1H)	H-5, H-6
8	or 125.69	6.74 (d, J = 8.0 Hz, 1H)	H-6
9	140.23	-	H-2, H-4, H-5, H-6, H-7, H-8
10	131.29	-	H-3, H-6, H-7, H-8
$1'$	125.61	-	H-3$'$
$2'$	130.86	7.20 (d, J = 8.4 Hz, 2H)	H-2$'$ (connected to the other C-2$'$)
$3'$	113.81	6.50 (d, J = 8.4 Hz, 2H)	H-2$'$, H-3$'$ (connected to the other C-3$'$)
$4'$	148.54	-	H-2$'$
C = 0	170.36	-	H-2, H-2$'$

Table 29. The peak assignment for ^{1}H and ^{13}C of N-(*p*-aminobenzoyl)-1,2,3,4-
tetrahydro-2-methylquinoline (CU-17-04), and long-range correlation
between carbons and protons.
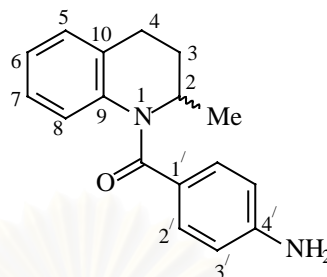
Position	δ ^{13}C (ppm)	δ ^{1}H (ppm)	Long-range correlation from ^{13}C to ^{1}H in HMBC spectrum
2-Me	19.71	1.22 (d, J = 6.5 Hz, 3H)	H-3a, H-3b
4$^{/}$ – NH$_2$	-	3.82 (s, broad, 2H)	-
1	-	-	-
2	49.16	4.81 (m, 1H)	2-Me, H-3a, H-3b, H-4
3	32.11	1.52 (m, 1H) 2.41 (m, 1H)	2-Me, H-2, H-4
4	25.49	2.74 (dd, J = 6.8 , 6.4 Hz, 2H)	H-2, H-3a, H-3b
5	127.47	7.14 (1H)	H-4, H-7
6	124.37	6.99 (dd, J = 7.4, 7.3 Hz, 1H)	H-8
7	125.84	6.88 (dd, J = 7.2, 7.6 Hz, 1H)	H-5
8	126.74	6.63 (d, J = 7.9 Hz, 1H)	H-6
9	138.70	-	H-2, H-4, H-5, H-6, H-7, H-8
10	132.78	-	H-3a, H-3b, H-4, H-6, H-7, H-8
1$^{/}$	125.89	-	H-3$^{/}$
2$^{/}$	130.77	7.11 (d, J = 8.6 Hz, 2H)	H-2$^{/}$ (connected to the other C-2$^{/}$)
3$^{/}$	113.72	6.46 (d, J = 8.5 Hz, 2H)	H-2$^{/}$, H-3$^{/}$ (connected to the other C-3$^{/}$)
4$^{/}$	148.22	-	H-2$^{/}$
C = 0	169.83	-	H-2, H-2$^{/}$

H-3a and H-3b represented the methylene protons at position 3 that are not equivalent.

Table 30. The peak assignment for ^{1}H and ^{13}C of N-(*p*-aminobenzoyl)-1,2,3,4-
tetrahydro-4-methylquinoline (CU-17-06), and long-range correlation
between carbons and protons.

Position	δ ^{13}C (ppm)	δ ^{1}H (ppm)	Long-range correlation from ^{13}C to ^{1}H in HMBC spectrum
4-Me	19.80	1.40 (d, J = 6.9 Hz, 3H)	H-3a
4$^{/}$- NH$_2$	-	3.92 (4H, 4$^{/}$- NH$_2$ + H-2)	-
1	-	-	-
2	43.26	3.92 (combined with 4$^{/}$- NH$_2$)	-
3	32.46	1.64 (m, 1H) 2.18 (m, 1H)	4-Me
4	31.01	2.94 (m, 1H)	4-Me, H-2
5	126.08	7.21 (1H)	H-7
6	124.14	7.02 (dd, J = 7.3, 7.2 Hz, 1H)	H-8
7	125.45	6.89 (dd, J = 7.4, 7.5 Hz, 1H)	H-5
8	or 125.72	6.71 (d, J = 7.9 Hz, 1H)	H-6
9	139.59	-	H-5, H-6, H-7, H-8
10	136.12	-	4-Me, H-3b, H-6, H-7, H-8
1$^{/}$	125.60	-	H-3$^{/}$
2$^{/}$	130.97	7.18 (d, J = 8.6 Hz, 2H)	H-2$^{/}$ (connected to the other C-2$^{/}$)
3$^{/}$	113.78	6.48 (d, J = 8.4 Hz, 2H)	H-2$^{/}$, H-3$^{/}$ (connected to the other C-3$^{/}$)
4$^{/}$	148.46	-	H-2$^{/}$
C = 0	170.27	-	H-2$^{/}$

H-3a and H-3b represented the methylene protons at position 3 that are not equivalent.

Table 31. The peak assignment for ^{1}H of N-(*p*-aminobenzoyl)-1,2,3,4 tetrahydro-
8-methylquinoline (CU-17-08). (The experiment was detected at -30° C.)
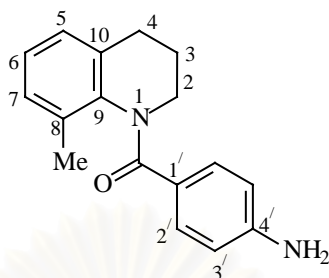
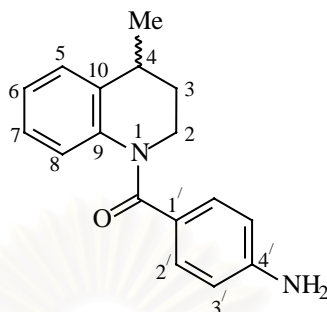| Position	δ ^{1}H (ppm)
8-Me	1.74 (s, 3H)
4$^/$ - NH$_2$	3.93 (s, broad, 2H)
1	-
2	3.24 (m, 1H) 4.62 (m, 1H)
3	1.71 (m, 1H) 2.38 (m, 1H)
4	2.78 (m, 2H)
5	7.05 – 7.15 (m, 4H, H-2$^/$ + H-6 + H-5)
6	7.05 – 7.15 (combined with H-2$^/$ and H-5)
7	6.86 (d, J = 7.3 Hz)
8	-
9	-
10	-
1$^/$	-
2$^/$	7.05 – 7.15 (combined with H-5 and H-6)
3$^/$	6.40 (d, J = 8.8 Hz, 2H)
4$^/$	-
C=0	-

Table 32. The peak assignment for ^{1}H and ^{13}C of N-(*p*-aminobenzoyl)-1,2,3,4-
tetrahydro-6-fluoro-2-methylquinoline (CU-17-10), and long-range
correlation between carbons and protons.

Position	δ [13]C (ppm)	δ [1]H (ppm)	Long-range correlation from ^{13}C to ^{1}H in HMBC spectrum
2-Me	19.55	1.21 (d, J = 6.5 Hz, 3H)	H-2, H-3a, H-3b
4$'$ - NH$_2$	-	3.87 (s, broad, 2H)	-
1	-	-	-
2	49.10	4.80 (m, 1H)	2-Me, H-3a, H-3b, H-4
3	31.76	1.51 (m, 1H) 2.39 (m, 1H)	2-Me, H-2, H-4
4	25.62	2.72 (dd, J = 6.7, 6.5 Hz, 2H)	H-2, H-3a, H-3b, H-5
5	113.87, 114.16 (d, J = 22.4 Hz)	6.87 (d, J = 8.5 Hz, 1H)	H-4, H-7
6	157.93, 161.16 (d, J = 244.1Hz)	-	H-5, H-8
7	112.66, 112.96 (d, J = 22.6 Hz)	6.58–6.65 (m, 2H, H-7 + H-8)	H-5
8	127.91, 128.02 (d, J = 8.4 Hz)		-
9	134.60	-	H-2, H-4, H-5, H-7
10	(C-9 + C-10)	-	H-3a, H-3b, H-5, H-8
1$'$	125.52	-	H-3$'$
2$'$	130.65	7.10 (d, J = 8.4 Hz, 2H)	H-2$'$ (connected to the other C-2$'$)
3$'$	113.76	6.47 (d, J = 8.4 Hz, 2H)	H-2$'$, H-3$'$ (connected to the other C-3$'$)
4$'$	148.34	-	H-2$'$
C = 0	169.73	-	H-2, H-2$'$

H-3a and H-3b represented the methylene protons at position 3 that are not equivalent.

Table 33. The peak assignment for ^1H and ^{13}C of N-(p-aminobenzoyl)-1,2,3,4-
tetrahydro-2,8-dimethylquinoline (CU-17-12), and long-range correlation
between carbons and protons.

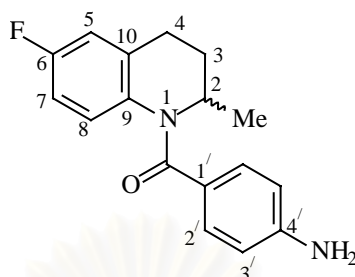| Position	δ ^{13}C (ppm)	δ ^1H (ppm)	Long-range correlation from ^{13}C to ^1H in HMBC spectrum
2-Me	21.25	1.17 (d, J = 6.4 Hz, 3H)	H-3a
8-Me	17.74	1.74 (s, 3H)	-
4$^/$ - NH$_2$	-	3.81 (s, broad, 2H)	-
1	-	-	-
2	49.76	4.92 (m, 1H)	2-Me, H-4
3	34.31	1.22 (m, 1H) 2.48-2.65 (m, 3H, H-3+H-4)	2-Me, H-4
4	27.48	2.48–2.65 (combined with H-3)	H-3a, H-3b
5	124.17	6.95-7.10 (m, 4H, H-5 + H-6 + H-2$^/$)	H-4, H-7
6	125.75	6.95-7.10 (combined with H-5 and H-2$^/$)	-
7	129.01	6.84 (d, J = 6.5 Hz)	8-Me
8	133.68	-	8-Me, H-6
9	138.16	-	8-Me, H-5, H-7
10	137.36	-	H-3b, H-6
1$^/$	126.05	-	H-3$^/$
2$^/$	130.34	6.95-7.10 (combined with H-5 and H-6)	H-2$^/$ (connected to the other C-2$^/$)
3$^/$	113.27	6.34 (d, J = 8.4 Hz, 2H)	H-2$^/$, H-3$^/$ (connected to the other C-3$^/$)
4$^/$	148.25	-	H-2$^/$
C = 0	169.01	-	H-2$^/$

H-3a and H-3b represented the methylene protons at position 3 that are not equivalent.

Table 34. The peak assignment for ^{1}H of N-(*p*-aminobenzoyl)-1,2,3,4 tetrahydro-
4,8-dimethylquinoline (CU-17-14). (The experiment was detected at
-30° C.)

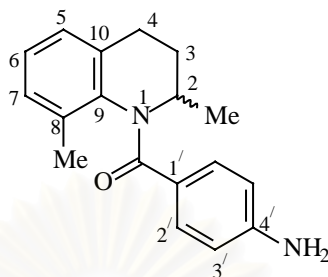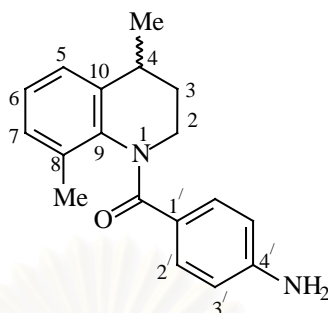| Position	δ ^{1}H (ppm)
4-Me	1.45 (d, J = 6.7 Hz, 3H)
8-Me	1.74 (s, 3H)
$4^/$ – NH$_2$	3.93 (s, broad, 2H)
1	-
2	3.24 (m, 1H)
	4.62 (m, 1H)
3	1.38 (m, 1H)
	2.35 (m, 1H)
4	2.82 (m, 1H)
5	7.10 – 7.20 (m, 2H, H-6 + H-5)
6	7.10 – 7.20 (combined with H-5)
7	6.89 (d, J = 7.0 Hz, 1H)
8	-
9	-
10	-
$1^/$	-
$2^/$	7.05 (d, J = 8.5 Hz, 2H)
$3^/$	6.40 (d, J = 8.5 Hz, 2H)
$4^/$	-
C=0	-

Table 35. The peak assignment for ^{1}H and ^{13}C of N-(*p*-aminobenzoyl)-1,2,3,4-
tetrahydro-8-methoxyquinoline (CU-17-16), and long-range correlation
between carbons and protons.
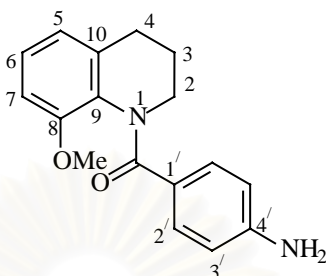
Position	δ [13]C (ppm)	δ [1]H (ppm)	Long-range correlation from ^{13}C to ^{1}H in HMBC spectrum
8-OMe	54.89	3.29 (s, 3H)	-
$4'$ – NH$_2$	-	3.76 (s, broad, 2H)	-
1	-	-	-
2	43.50	3.39 (s, broad, 1H) 4.30 (s, broad, 1H)	-
3	25.01	1.75 (s, broad, 1H) 2.27 (s, broad, 1H)	-
4	26.89	2.74 (broad, 2H)	-
5	119.75	6.80 (d, J = 7.4 Hz, 1H)	H-7
6	125.69	7.01 (t, J = 7.9 Hz, 1H)	-
7	109.98	6.52 (d, J = 8.1 Hz, 1H)	H-5, H-6
8	151.96	-	8-OMe, H-6, H-7
9	130.01	-	H-5, H-6, H-7
10	135.36	-	H-6
$1'$	127.06	-	H-$3'$
$2'$	129.46	7.16 (d, J = 8.5 Hz, 2H)	H-$2'$ (connected to the other C-$2'$)
$3'$	113.30	6.43 (d, J = 8.5 Hz, 2H)	H-$2'$, H-$3'$ (connected to the other C-$3'$)
$4'$	148.03	-	H-$2'$
C = 0	170.87	-	H-$2'$
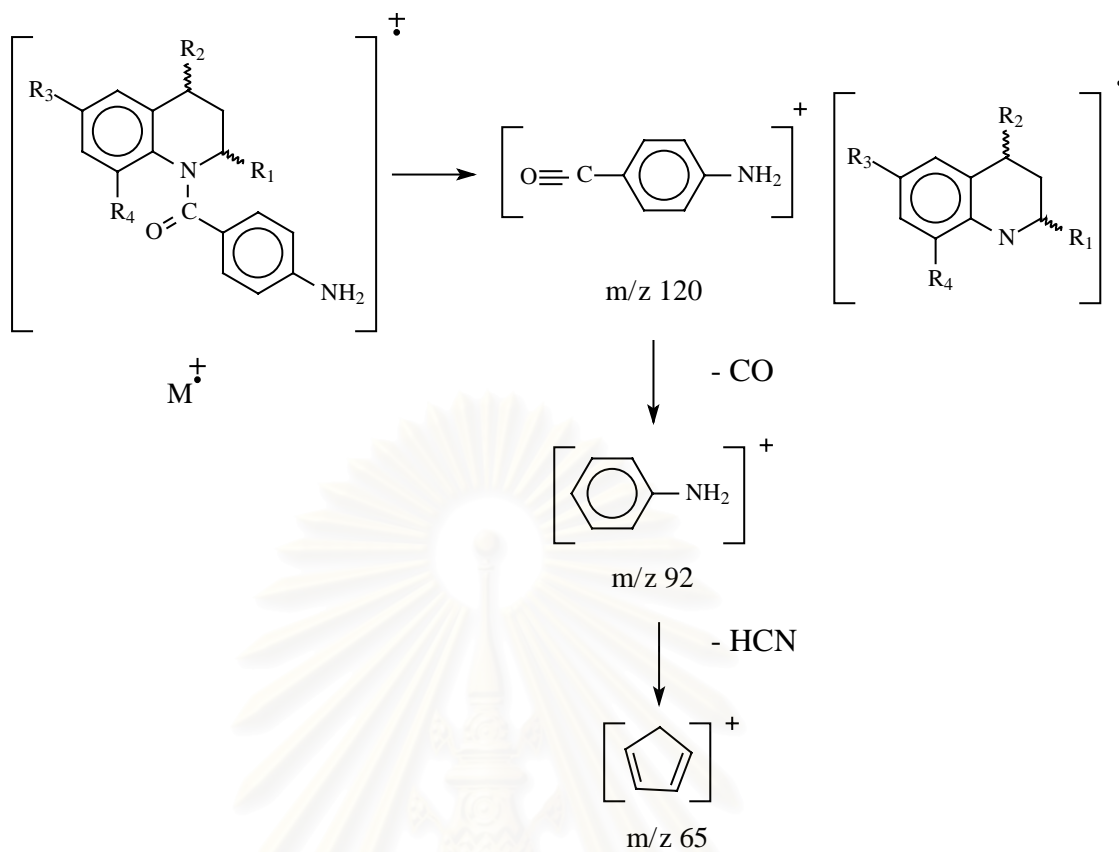
Figure 180. The mass fragmentation pattern of the synthesized N-(*p*-aminobenzoyl)-

1,2,3,4-tetrahydroquinoline derivatives.

CHAPTER V

CONCLUSION

The previous discovery of ameltolide, a potent and specific anticonvulsant, has stimulated considerable interest in the synthesis of novel analogues of this compound. An effort reported herein resulted in the design and synthesis of eight compounds (CU-17-02, CU-17-04, CU-17-06, CU-17-08, CU-17-10, CU-17-12, CU-17-14 and CU-17-16) in a series of N-(*p*-aminobenzoyl)-1,2,3,4-tetrahydroquinolines as rigid analogues of ameltolide.

This investigation could successfully prepare N-(*p*-aminobenzoyl)-1,2,3,4-tetrahydroquinoline and its derivatives with various substitutions on the 1,2,3,4-tetrahydroquinoline nucleus, by the four-step procedure that could be summarized as followed.

1. By modified Skraup reaction, quinolines were prepared by the reaction between the appropriate amines and the α,β-unsaturated carbonyl compounds in the presence of 2,3-dichloro-1,4-napthoquinone.

2. By chemical reduction, quinolines were reduced very cleanly to their corresponding 1,2,3,4-tetrahydroquinolines by using sodium borohydride and nickel chloride.

3. By N-acylation, 1,2,3,4-tetrahydroquinolines were acylated by *p*-nitrobenzoyl chloride to the corresponding N-(*p*-nitrobenzoyl)-1,2,3,4-tetrahydroquinolines.

4. By catalytic hydrogenation, reduction of N-(*p*-nitrobenzoyl)-1,2,3,4-tetrahydroquinolines in the presence of palladium on activated charcoal afforded the final products, N-(*p*-aminobenzoyl)-1,2,3,4-tetrahydroquinolines.

The structures of all synthesized compounds were identified by infrared spectrometry, nuclear magnetic resonance spectrometry, mass spectrometry and elemental analysis techniques.

The preliminary pharmacological data which are not reported here indicated that most of target compounds exhibited anticonvulsant activity at moderate to high levels against maximal electroshock induced seizures; therefore a series of N-(*p*-aminobenzoyl)-1,2,3,4-tetrahydroquinolines represent an important new class of anticonvulsant candidates that is waiting for further study and development.

Modification of methyl substituents on the 1,2,3,4-tetrahydroquinoline moiety does affect the conformation of some products (CU-17-08, CU-17-12 and CU-17-14) that could be demonstrated by many NMR experiments. The insight study in these phenomena will be the challenging work since their stereochemistry could certainly affect their activity as anticonvulsants. By the same reason, the study of configuration in some products (CU-17-04, CU-17-06, CU-17-10, CU-17-12 and CU-17-14), having methyl substituent on position 2 or 4, will also be an interesting topic. In addition, the study of structure and anticonvulsant activity relationship (SAR) involving extension of their SAR may lead to conclusion of the best structure in this series for optimal anticonvulsant activity.

REFERENCES

Adams, R. D., Victor, M., and Ropper, A. H. 1997. Epilepsy and other seizure disorder. In R. D. Adams, M. Victor, and A. H. Ropper (eds.), Principles of neurology. 6th ed., pp. 313-343. New York: McGraw-Hill.

Bailleux, V., et. al. 1994. Synthesis and anticonvulsant activity of some *N*-phenylphthalimides. Chem. Pharm. Bull. 42 (9): 1817-1821.

Bailleux, V., et. al. 1995. Comparative anticonvulsant activity and neurotoxicity of 4-amino-*N*-(2,6-dimethylphenyl)phthalimide and prototype antiepileptic drugs in mice and rats. Epilepsia 36 (6): 559-565.

Bruice, P. Y. 1995. Organic chemistry. New Jersey: Prentice-Hall.

Carey, F. A., and Sunberg, R. J. 1993. Advanced organic chemistry: Part B, reaction and synthesis. 3rd ed. New York: Plenum Press.

Clark, C. R., Wells, M. J. M., Sansom, R. T., Norris, G. N., Dockens, R. C., and Ravis W. R. 1984. Anticonvulsant activity of some 4-aminobenzamides. J. Med. Chem. 27: 779-782.

Clark, C. R., Sansom, R. T., Lin, C., and Norris, G. N. 1985. Anticonvulsant activity of some 4-aminobenzanilides. J. Med. Chem. 28: 1259-1262.

Clark, C. R., Lin, C., and Sansom, R. T. 1986. Anticonvulsant activity of 2- and 3-aminobenzanilides. J. Med. Chem. 29: 1534-1537.

Clark, C. R., and Davenport, T. W. 1987. Anticonvulsant activity of some 4-aminophenylacetamides. J. Pharm. Sci. 76 (1): 18-20.

Clark, C. R. 1988. Comparative anticonvulsant activity and neurotoxicity of 4-amino-*N*-(2,6-dimethylphenyl)benzamide and prototype antiepileptic drugs in mice and rat. Epilepsia 29 (2): 198-203.

Cosford, N. D. P., McDonald, I. A., and Schweiger, E. J. 1998. Chapter 7 Recent progress in antiepileptic drug research. Annual Reports in Medicinal

Chemistry 33: 61-70.

Dhillon, S., and Sander, J. W. A. S. 1999. Epilepsy. In R. Walker, and C. Edwards (eds.), <u>Clinical pharmacy and therapeutics</u>. 2nd ed., pp. 435-451. Edinburgh: Churchill Livingstone.

Duke, N.E.C., and Codding P. W. 1992. Molecular modeling and crystallographic studies of 4-amino-*N*-phenylbenzamide anticonvulsants. J.Med.Chem. 35: 1806-1812.

Edafiogho, I. O., and Scott, K. R. 1996. Chapter thirty-nine: Anticonvulsants. In M. E. Wolff (ed.), <u>Burger's medicinal chemistry and drug discovery.</u> vol. 3. 5th ed., pp. 175-260. New York: John Wiley & Sons.

Furniss, B. S., Hannaford, A. J., Smith, P. W. G., and Tatchell, A. R. 1991. <u>Vogel's textbook of practical organic chemistry.</u> 5th ed., pp. 1188. England: Bath Press.

Graves, N. M., and Garnett, W. R. 1999. Epilepsy. In J. T. Dipiro, R. L. Talbert, G. C. Yee, G. R. Matzke, B. G. Wells, and L. M. Posey (eds.), <u>Pharmacotherapy: A pathophysiologic approach</u>. 4th ed., pp.952-975. Stamford: Appleton & Lange.

House, H. O. 1972. <u>Modern synthetic reaction</u>. California: W.A. Benjamin.

Joule, J. A., Mills, K., and Smith G. F. 1995. <u>Heterocyclic chemistry</u>. 3rd ed. London: Chapman & Hall.

Kadir, Z. A., and Chadwick, D. W. 1999. Principles of treatment of epilepsy. <u>Drugs on Today</u> 35 (1): 35-41.

Kanyonyo, M. R., Poupaert, J. H., and Lambert, D. M. 1998. Anticonvulsant profile of 4-amino-(2-methyl-4-aminophenyl)benzamide in mice and rats. <u>Pharmacology & Toxicology</u> 82: 47-50.

Leander, J. D. 1992. Interaction of the anticonvulsant ameltolide with standard anticonvulsants. <u>Epilepsia</u> 33 (4) : 705-711.

Leander, J. D., Parli, C. J., Potts, B., and Lodge, D. 1992. Relation of plasma and brain concentrations of the anticonvulsant ameltolide to its pharmacologic

effects. Epilepsia 33(4): 696-704.

March, J. 1968. Advanced organic chemistry: Reaction, mechanisms, and structure. International student ed. New York: McGraw-Hill.

McNamara, J. O. 1996. Chapter 20: Drugs effective in the therapy of the epilepsies. In J. G. Hardman, and L. E. Limbird (eds.), Goodman & Gilman's: The pharmacological basis of therapeutics. 9th ed., pp. 461-486. New York: McGraw-Hill.

Meldrum, B. S. 1996. Update on the mechanism of action of antiepileptic drugs. Epilepsia 37 (Suppl. 6): s4-s11.

Morrison, R. T., and Boyd, R. N. 1987. Organic chemistry. 5th ed. Boston: Allyn and Bacon.

Nose, A., and Kudo, T. 1984. Reduction of heterocyclic compounds. II. Reduction of heterocyclic compounds with sodium borohydride-transition metal salt systems. Chem. Pharm. Bull. 32 (6): 2421-2425.

Potts, B. D., Gabriel, S., and Parli, C. J. 1989. Metabolism, disposition and pharmacokinetics of a potent anticonvulsant 4-amino-*N*-(2,6-dimethylphenyl)-benzamide (LY201116) in rats. Drug Metab. Dispos 17 (6): 656-661.

Poupaert, J. H., Hamoir, G., Barbeaux, P., Lambert, D., and Henichart, J. 1995. Letter to the editor: Anticonvulsant activity of some *N*-phenylphthalimide derivatives in rats and mice. J. Pharm. Pharmacol. 47: 89-91.

Robertson, D. W., et. al. 1987. Discovery and anticonvulsant activity of the potent metabolic inhibitor 4-amino-*N*-(2,6-dimethylphenyl)-3,5-dimethylbenzamide. J. Med. Chem. 30: 1742-1746.

Robertson, D. W., Lawson, R. R., Rathbun, R. C., and Leander, J. D. 1988. Pharmacology of LY201409, a potent benzamide anticonvulsant. Epilepsia 29 (6): 760-769.

Robertson, D. W., et. al. 1991. Synthesis and pharmacological evaluation of a major

metabolite of ameltolide, a potent anticonvulsant. J. Med. Chem. 34: 1253-1257.

Sabers, A., and Gram, L. 1996. Drug treatment of epilepsy in the 1990s. Drugs 52 (4): 483-493.

Sathit Niratisai. 1994. Synthesis of N-(*p*-aminobenzoyl)-1,2,3,4-tetrahydro-4,8-dimethylquinoline. Master's Thesis, Department of Pharmaceutical Chemistry, The Faculty of Pharmaceutical Science, Graduate School, Chulalongkorn University.

Song, Z., Mertzman, M., and Hughes, D. L. 1993. Improved synthesis of quinaldines by the skraup reaction. J. Heterocyclic Chem. 30: 17-21.

Vamecq, J., Lambert, D., Poupaert, J. H., Masereel, B., and Stables, J. P. 1998. Anticonvulsant activity and interactions with neuronal voltage-dependent sodium channel of analogues of ameltolide. J. Med. Chem. 41: 3307-3313.

Vamecq, J., Bac, P., Herrenknecht, C., Maurois, P., Delcourt, P., and Stables, J. P. 2000. Synthesis and anticonvulsant and neurotoxic properties of substituted *N*-phenyl derivatives of the phthalimide pharmacophore. J. Med. Chem. 43: 1311-1319.

Vierhapper, F. W., and Eliel, E. L. 1975. Selective hydrogenation of quinoline and its homologs, isoquinoline, and phenyl-substituted pyridines in the benzene ring. J. Org. Chem. 40 (19): 2723-2742.

White, H. S. 1997. Clinical significance of animal seizure models and mechanism of action studies of potential antiepileptic drugs. Epilepsia 38 (Suppl. 1): s9-s17.

VITA

Miss Tanarat Kietsakorn was born on July, 1974 in Sakonnakorn, Thailand. She received her Bachelor of Science in Pharmacy with second class honors in 1998 from the Faculty of Pharmaceutical Sciences, Khon Kaen University, Khon Kaen, Thailand. Since her graduation, she has become a member of the Faculty of Pharmacy and Health Sciences, Mahasarakharm University, Mahasarakharm, Thailand.